

#4521

REPORT FOR ENERGY, MINES AND RESOURCES

**TO IMPROVE THE PREDICTION OF WIND VELOCITIES ACTING ON
BUILDINGS**

FILE: 9327-1/93270897

Prepared By:

**G. K. YUILL AND ASSOCIATES LTD.
200-1200 Pembina Highway
Winnipeg, Manitoba
R3T 2A7**

July 31, 1990

TABLE OF CONTENTS

1.0 INTRODUCTION	1
2.0 WIND CORRECTION MODELS	3
2.1 Introduction	3
2.2 Sherman's Model (LBL)	3
2.3 The Alberta Infiltration Model (AIM-2)	5
2.4 ASHRAE Model	6
2.5 Log Profile Model	7
3.0 PROCEDURE	10
3.1 The Approach	10
3.2 Wind Speed Data	10
3.3 Estimating the Terrain Class	12
3.4 Wind Data Comparison Algorithm	15
4.0 RESULTS AND DISCUSSION	17
5.0 CONCLUSIONS AND RECOMMENDATIONS	22
REFERENCES	
APPENDIX A	
APPENDIX B	

1.0 INTRODUCTION

The transformation of wind speed data from station measurements to a building site of interest has been made difficult by the lack of a systematic method to account for small scale terrain effects. Studies have shown that the presence of nearby buildings or trees even at distances of 10 obstacle heights or more can decrease local wind speed by 10% to 25%, depending on the situation. There are a number of models available that take into account the terrain effects and perform the wind speed data transformation from one site to another. However, the reliability of the results from these models cannot be completely trusted. The objective of this project, therefore, is to: analyze the wind speed predictions from these models by comparing them with the actual measured wind speed data, and as a first step in the development of a method to most correctly predict the wind velocities at building sites under consideration, from the wind data measured at nearby meteorological stations.

Four wind correction models were reviewed and tested by using the wind data available from five nearby meteorological stations. The four models used were: LBL model, AIM-2 model, ASHRAE model and the Log Profile model. The experimental site was the Alberta Home Heating Research Facility (AHHRF) and the five nearby wind measuring stations were: Edmonton International Airport, Edmonton Municipal Airport, Namao Airport, Eilerslie Climate Station and Stony Plain Climate Station. Each wind correction model estimated the wind speed at the AHHRF (experimental site) from the wind speed data measured at each of the five nearby wind measuring sites mentioned. All the measuring stations, including the AHHRF can be classified as being situated in a rural terrain. Therefore, any conclusions drawn from this study can only be applied to wind comparison of two sites in rural areas. In order to predict the wind speed of an urban site from that of a rural site, another study must be carried out, which will have the experimental site located in an urban terrain.

The most important element in applying the wind correction models was the proper assignment of terrain factors to each station and site. Each model has its own system of defining the terrain classes and parameters. The terrain coefficients were assigned according to the upwind obstruction. All the four models were first run by assigning the terrain coefficients in 22.5° direction bins

(called the first iteration). The terrain classes for each station were estimated by examining the upwind terrain based on site visits. Aerial photographs were used to establish distances between measurement point and upwind roughness for all sites. During the second iteration, the terrain classes and therefore, the respective terrain coefficients were modified based on the results from the first iteration. It should be noted that the terrain classification system and the corresponding terrain coefficients for the models were not changed. During the second iteration, however, the terrain classes in some cases were reconsidered and reassigned.

The four wind models were programmed into the computer and runs were made using the data from the five wind measuring stations and the Alberta Home Heating Research Facility (AHHRF). The wind velocity at the AHHRF site was estimated from the wind speed at the other five measuring stations. The estimated wind speed was compared with the actual measured wind speed at the AHHRF site and the percent error and its standard deviation was calculated. The output data was binned into day, night and day+night based on the solar altitude for the station. The output data was also binned into twelve one meter per second wind speed bins and four 90° direction quadrant bins. The output data was also analyzed on the basis of monthly averages in order to determine if there are any seasonal effects on the wind speed estimates.

2.0 WIND CORRECTION MODELS

2.1 Introduction

This chapter describes the four wind velocity correction models tested in this project. These are the LBL model, the AIM-2 model, the ASHRAE model and the Log Profile model. The first three of these are power law models and are essentially the same except for the coefficients used. The fourth has a logarithmic form, as its name implies, but its profile shape is not greatly different from the other three models. The following sections describe the four models in detail.

2.2 Sherman's Model (LBL) [1]

Terrain effects result from the fact that the measurement of wind speed may not occur at the same height or in the same general geographical terrain as the building site under consideration. To calculate the wind speed at one site from measured data at another, the standard wind speed at measurement site is first calculated by using the following standard wind engineering formula:

$$U_2 = U_0 \alpha_2 (H_2/10)^{\gamma_2} \quad (2.2.1)$$

$$\text{or } U_0 = U_2 / [\alpha_2 (H_2/10)^{\gamma_2}] \quad (2.2.2)$$

where

- U_2 = actual wind speed at the measurement site,
- U_0 = wind speed at standard conditions,
- H_2 = height of the measurement site,
- α_2, γ_2 = constants that depend upon terrain class of the measurement site.

Then the standard wind speed is used to calculate the wind speed at the desired site. Standard conditions are defined to be a height of 10 m and a terrain of Class II. The following formulae are used to estimate the wind speed (U_e) at desired site of height H_1 :

$$U_e = U_0 \alpha_1 (H_1/10)^{\gamma_1} \quad (2.2.3)$$

From equation (2.2.2) and (2.2.3)

$$U_e = U_2 [\alpha_1 (H_1/10)^{\gamma_1}] / [\alpha_2 (H_2/10)^{\gamma_2}] \quad (2.2.4)$$

$$U_e = C_T U_2 \quad (2.2.5)$$

where

U_e = estimated wind speed at the desired site,
 α_1, γ_1 = constants that depend upon the terrain class of the site where the wind speed is to be estimated.

and C_T = terrain coefficient = $[\alpha_1 (H_1/10)^{\gamma_1}] / [\alpha_2 (H_2/10)^{\gamma_2}]$

This model (LBL) classifies the terrain into five classes depending on the relative surface roughness at the ground level. The terrain parameters α and γ for each class are listed in Table 2.1.

Table 2.1 Terrain Parameters for Standard Terrain Classes (LBL model)

Class	α	γ	Description
I	1.30	0.10	Ocean or other body of water with at least 5 km of unrestricted expanse
II	1.00	0.15	Flat terrain with some isolated obstacles (e.g., buildings or trees well separated from each other)
III	0.85	0.20	Rural areas with low buildings, trees, etc.
IV	0.67	0.25	Urban, industrial or forest areas
V	0.47	0.35	Large city centre

2.3 The Alberta Infiltration Model (AIM-2) [2]

The shape of the wind velocity acting on a building depends highly upon the overall terrain roughness that extends several kilometers upwind of the building. Once the wind speed at a meteorological station is measured at a height H_2 , usually in open flat terrain, some adjustment is required to estimate the wind speed at height H_1 in the local building terrain. One simple method for accounting for these differences in measuring heights (H_2 and H_1) and in terrain roughness is to use a power law profile $U \propto H^p$ for the mean wind speed with height H above the ground. Table 2.2 gives values of the exponent p for varying terrain roughnesses and atmospheric stability classes. Then, if it is assumed that the wind speed at the surface influenced boundary layer height $H = 600$ m is the same above the meteorological (met) station and the building site, the wind speed at the building at height H_1 is

$$U_e = C_T U_{\text{met}}$$

where

C_T	=	$[600/H_2]^{p_2} [H_1/600]^{p_1}$
H_2	=	height at which met station wind speed is measured, m,
H_1	=	height of the building site, m,
p_2	=	wind speed exponents at the met station,
p_1	=	wind speed exponent at the building site,
U_e	=	estimated wind speed at building site at height H_1 ,
U_{met}	=	wind speed measured at the met station.

Table 2.2 gives values of p for four different levels of terrain roughness, defined quantitatively by their roughness scaling lengths. (The roughness scaling length is derived from the log-law velocity variation, and is typically about 3% of the largest roughness element height). For airport met locations the "mixed woods and fields" terrain class II is often a reasonable approximation. Met tower wind speeds greater than 3 m/s occur in neutral stability and less than 3 m/s are in stable conditions.

Table 2.2 Wind Speed Power Law Exponent p for Adjusting Meteorological Tower Wind speeds to Local Building Sites (AIM-2 model)

Terrain Class	Terrain Roughness	$U_{met} > 3$ m/s neutral stability Class D	$U_{met} < 3$ m/s stable Class E
I	Open Flat Terrain Rural Grassland $z_0 = 1$ cm	0.12	0.34
II	Suburban Detached Housing Mixed Woods and Fields $z_0 = 10$ cm	0.16	0.32
III	Dense Urban Housing with Multi Story Buildings Heavy Forests $z_0 = 100$ cm	0.27	0.38
IV	High Rise Urban Centers $z_0 = 300$ cm	0.37	0.47

2.4 ASHRAE Model [3]

The local wind speed, U_e is estimated by applying terrain and height corrections to the wind speed, U_{met} from a nearby meteorological station. The wind speed, U_{met} at airport meteorological stations is measured at height H_2 , usually about 10 m, in open flat terrain. U_{met} is related to the reference wind speed U_{ref} at the same height in the local building terrain by

$$U_{ref} = A_0 U_{met}$$

where, the constant A_0 depends on the local terrain roughness. The height correction to the approach wind velocity profile is made by using the following relationship:

$$U_e = U_{ref} (H_1/H_2)^a$$

or $U_e = A_0 (H_1/H_2)^a U_{met}$

or $U_e = C_T U_{met}$

where

$$C_T = A_0(H_1/H_2)^a$$

a = the velocity profile exponent,

This model has defined only three general terrain classes: Airport, Suburban and Urban. The values of terrain roughness factor A_0 , velocity profile exponent, a , and the scaling length Z_0 are shown in Figure 1.

2.5 Log Profile Model [4]

It is assumed in this model that at heights 60 m above ground level, the wind velocity profile does not vary with surface terrain roughness. The wind speed at heights of 60 m is referred to as mesowind, U_{60} .

The mesowind can be determined from station measured wind speed U_{met} , observed at a height H_2 , by way of applying the logarithmic wind profile between H_2 and 60 m as follows:

$$U_{60} = U_{met} \ln(60/Z_{met}) [\ln(H_2/Z_{met})]^{-1} \quad (2.5.1)$$

where

Z_{met} = surface roughness length (Z_0) for the met station,

Now assuming that mesowind is same at the met station and at the building site, equations (2.5.1) can be applied to estimate the wind speed at the building site, U_e as follows:

$$U_{60} = U_e \ln(60/Z_{site}) [\ln(H_1/Z_{site})]^{-1} \quad (2.5.2)$$

$$U_e = U_{60} \ln(H_1/Z_{site}) [\ln(60/Z_{site})]^{-1} \quad (2.5.3)$$

$$\text{or } U_e = \ln(60/Z_{met}) \ln(H_1/Z_{site}) [\ln(H_2/Z_{met})]^{-1} [\ln(60/Z_{site})]^{-1} U_{met}$$

$$\text{or } U_e = C_T U_{met}$$

where

$$C_T = \ln(60/Z_{met}) \ln(H_1/Z_{site}) [\ln(H_2/Z_{met})]^{-1} [\ln(60/Z_{site})]^{-1}$$

Z_{site} = surface roughness length (Z_0) for the building site

and H_1 = height of the building site at which the wind speed is estimated.

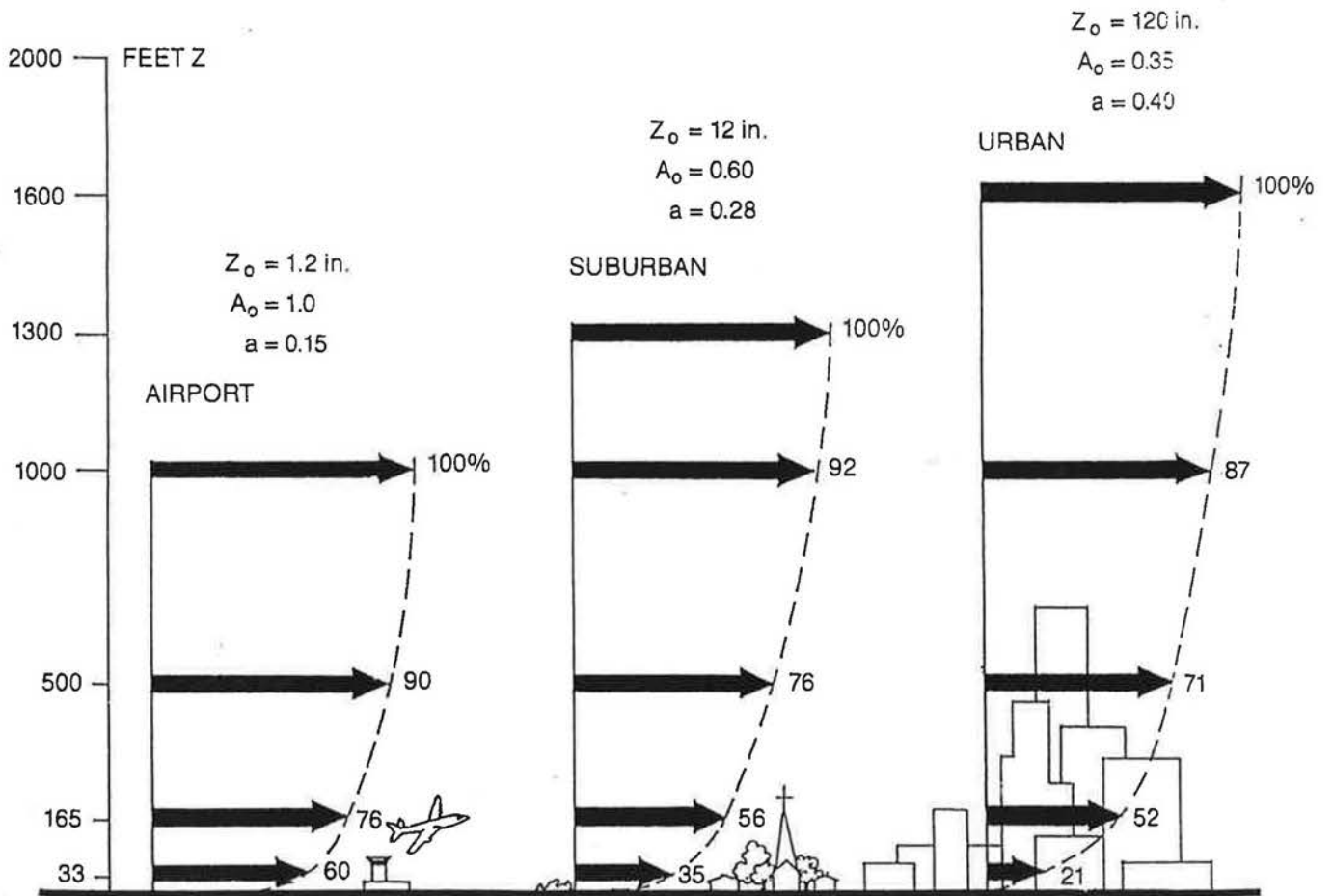


Fig. 1 Typical Mean Wind Speed Profiles Over Different Terrain Roughness

The description of terrain classes and the corresponding roughness lengths (Z_0) are listed in Table 2.3.

TABLE 2.3 Davenport Roughness Classification (Log Profile model)

Class	Terrain Description	Z_0 (m)
1	Open sea, fetch at least 5 km	0.0002
2	Mud flats, snow; no vegetation, no obstacles	0.005
3	Open flat terrain; grass, few isolated obstacles	0.03
4	Low crops; occasional large obstacles, $x/H > 20$	0.10
5	High crops; scattered obstacles, $15 < x/H < 20$	0.25
6	Parkland, bushes; numerous obstacles, $x/H \approx 10$	0.5
7	Regular large obstacle coverage (suburb, forest)	1.0
8	City centre with high- and low-rise buildings	?

Note: Here x is a typical upwind obstacle distance and H the height of the corresponding major obstacles. Class 8 is analytically intractable and can better be modelled in a wind-tunnel.

3.0 PROCEDURE

3.1 The Approach

The approach taken was to first make a preliminary estimate of the terrain coefficients of the two sites whose wind speed data were to be compared. Then these preliminary terrain coefficients were used in the model to predict the wind speed of site 1 (experimental site) from the wind speed of site 2 (met station). This predicted wind speed of site 1 was compared with the actual measured wind speed of site 1 in order to assess the validity of the terrain coefficients used. A re-evaluation of the terrain class was carried out and the terrain class descriptors were modified. The re-evaluation of terrain class was based on a close re-examination of the terrain belonging to the two sites whose wind data was to be compared. A second set of runs, called the second iteration was then carried out and the results were studied to more correctly predict the terrain class descriptors.

3.2 Wind Speed Data

The Alberta Home Heating Research Facility (AHHRF) was selected as the experimental site for which the wind speed predictions were to be made from the wind speed data of the neighboring wind measurement sites. The wind speed data from the following five neighboring wind measurement sites was used in the analysis:

- 1) Edmonton International Airport
- 2) Edmonton Municipal Airport
- 3) Namao Airport
- 4) Ellerslie Climate Station
- 5) Stony Plain Climate Station.

All the wind measuring sites including the AHHRF site are located in rural terrain. The first three stations listed above report 2 minute averages around the hour while the last two report wind run. The wind speed data from all the five stations was compared with the hour average data measured at the Alberta Home Heating Research Facility (AHHRF).

The wind speed data at the Alberta Home Heating Research Facility (AHHRF) was gathered by Dr. Wilson of the University of Alberta. Dr. Wilson employed extremely strict quality control measures to minimize the human and experimental errors. He used two pairs of anemometers; one pair was used to record the wind speed while the other pair was being calibrated in the wind tunnel. The two pairs were periodically switched with each other so that the calibration of the anemometers could be checked on a regular basis. It is believed that the wind data recorded at the AHHRF site was more accurate than that from any of the nearby meteorological stations. Wilson's low wind speed data is especially more accurate than the data from other meteorological stations. The wind speed data at met stations is manually estimated from continuous analog recordings (for example a strip chart). After talking to a number of officials who perform these estimates, it was realized that the officials at the wind measuring stations tend to over estimate the low wind speeds. Also the wind speed is recorded in steps of one km/hr, that is in whole numbers only. Therefore, the instrumentation error involved in the wind speed measurements made at met stations, is much higher at lower wind speeds. Dr. Wilson's wind speed data, on the other hand, is recorded nearest to one decimal place and therefore more accurate than that from met stations.

3.3 Estimating the Terrain Class

Since the wind speed at a site is definitely affected by the upwind obstruction, the terrain classes and terrain descriptors were assigned in 22.5 degree direction bins. Each site, therefore, had 16 terrain classes associated with it. The terrain class for each of the 16 direction bins varies with respect to the magnitude of the obstruction in that direction bin. The upwind terrain classes were assigned based on the visits to the sites. Aerial photographs were used to establish the distances between the measurement point and the upwind obstruction. As discussed in chapter 2, each wind correction model has its own way of describing the terrain class. Some models have very coarse description while others have relatively fine terrain class description. For example, the ASHRAE model uses a very coarse three class terrain description while the Log Profile model uses a relatively fine description of eight terrain classes. Since the terrain class description of each model is different, there is a different terrain class descriptor for each model for the same site and for the same direction bin. Table 3.1 lists the terrain descriptors used by the four models in comparing the wind speed data from the five wind measuring stations with that from the Alberta Home Heating Research Facility (AHHRF). Each number represents an approximate class description of the terrain in 22.5 degree bins for several hundred meters upwind of the measuring tower. Directions are taken clockwise from north with the first number in each row indicating terrain class for the bin range 0 - 22.5 degrees.

The terrain descriptors in Table 3.1 are based on the preliminary estimates of terrain surrounding each site. These terrain descriptors were used in the analysis to perform the first iteration. After making the first iteration runs, the terrain descriptors were re-evaluated by examining the detailed information on the terrain belonging to the two sites being compared and by studying the results of the first iteration. A second set of runs called the second iteration, were then carried out with the new terrain descriptors. Table 3.2 lists the terrain descriptors for the second iteration runs. Once the terrain descriptor for a particular location and direction was estimated, the terrain coefficient was calculated with the help of terrain class parameters table provided with each model as explained in chapter 2.

It is important to note that this second assessment of the terrain descriptors was not an iterative process in which numbers were juggled to make answers fit. It was a realistic attempt to assign terrain classes as an experienced terrain class assessor would do it. It was necessary because Mr. Ackerman, in spite of his experience with wind data measurement and analysis, was not an experienced terrain class assessor at the start of the project. The first iteration gave him the experience to assign terrain classes more exactly.

3.4 Wind Data Comparison Algorithm

The following algorithm was used during the analysis of comparing the wind speed data of the two neighboring wind measuring stations:

- 1) Estimated the terrain class of the two measuring stations whose wind speed data were to be compared. The terrain class was estimated based on the upwind direction for each hour.
- 2) The above estimates of terrain class were used to calculate the terrain coefficients for each model and location.
- 3) Estimated the wind speed (U_e) of site 1 from the wind speed (U_2) of site 2 (met) by using the following relationship:

$$U_e = C_T U_2$$

- 4) Calculated the percentage error in estimating the wind speed of site 1 as following:

$$e = (U_e - U_1) \times 100 / U_1$$

where

$$U_1 = \text{measured wind speed of site 1.}$$

- 5) Averaged this error for the following data sets:
 - a) all the data in each velocity bin and in the whole year (velocity bins were 0-1, 1-2, 2-3, 3-4,9-10 m/s),

- b) all the daytime data in each velocity bin and in the whole year,
 - c) all the nighttime data in each velocity bin and in the whole year,
 - d) calculated the standard deviation of each set and its 10th and 90th percentile.
- 6) Repeated steps 2 and 3 for wind speed data sorted into four directional quadrant bins based on the direction of wind at site 2. In those cases when the wind direction data of site 2 was missing, the wind direction data of site 1 was used.
- 7) Calculate the monthly average values of U_1 , U_e and the ratio r_k for each month, k:

$$r_k = U_e/U_1$$

Repeated this for the daytime, nighttime and day+night time data sets separately.

- 8) Repeated steps 1 to 7 for the direct comparison method and for each of the four models: LBL, AIM-2, ASHRAE and Log Profile model.
- 9) Repeated steps 1 to 8 for each of the five pairs of wind speed data.
- 10) Re-evaluated the terrain class and terrain coefficients for each model and location in order to perform the second iteration.
- 11) Repeated steps 1 to 9 by using the second iteration terrain coefficients as evaluated above in step 10. The runs made during this step are referred to as the second iteration runs.

4.0 RESULTS AND DISCUSSION

The Alberta Home Heating Research Facility (AHHRF) whose wind speed was predicted from nearby meteorological stations, was classified as being located in rural terrain. The nearby wind measuring stations used for the wind comparison also belonged to rural terrain. Therefore, any conclusions that can be drawn from the present study can be applied only to situations where the wind speed of a rural site is to be predicted from the wind speed of a nearby meteorological station. A separate study will need to be carried out in order to develop a method for predicting the wind speed of a site located in an urban terrain.

In the present analysis, the height of the wind measuring instrument at each of the six stations was the same (10 meters). Therefore, the effect of the height of wind measuring instrument on the terrain coefficient could not be modelled in the analysis.

The computer runs during the first iteration, using the terrain descriptors listed in Table 3.1, were carried out and the output data was plotted as shown in Appendix A. The plots show the percent error in predicting the wind velocity of site 1 (AHHRF) from that of site 2 (met station), and the monthly ratio of the measured wind velocity to the predicted wind velocity of site 1 (AHHRF). As mentioned earlier, five different measuring stations were used for the wind data at site 2. The plots for each station were grouped into four 90 degree direction quadrant bins. The comparison of 24 hour (day + night) data in each quadrant bin was performed by using the direct comparison method and by using the four wind correction models: LBL, AIM-2, ASHRAE, and the Log Profile model. The percent error was plotted for the direct comparison method and for the four wind correction models, while the monthly ratio was plotted for only two models: LBL and AIM-2. The percent error and the monthly ratio are expressed as following:

$$\% \text{ error} = (U_{\text{predicted}} - U_{\text{measured}}) \times 100 / U_{\text{measured}}$$

$$\text{Ratio} = U_{\text{measured}} / U_{\text{predicted}}$$

The analysis of wind data (1984) comparison between the Alberta Home Heating Research Facility (AHHRF) and Edmonton International Airport is shown in Figures A1 to A35. Figures A1 to A7 belong to the analysis of data sorted into the

first quadrant (0-90 degrees) bin. These figures show the percent error of day+night predictions for the direct method, LBL, AIM-2, ASHRAE and the Log Profile models in Figure A1 to A5 respectively. Figures A6 and A7 show the monthly ratios for the day, night and day+night separately. Similarly, Figures A8 to A14 show these plots for the second quadrant direction bin (90-180 degrees) and so on for the remaining quadrants. Figures A29 to A35 show similar plots for a single bin (0-360 degrees) containing all the data from the four quadrants. Similarly, the comparison of AHHRF wind data with that of Edmonton Municipal Airport is shown in Figures A36 to A70, with Namao Airport in Figures A71 to A105, with Ellerslie Climate Station in Figures A106 to A140 and with Stony Plain Climate Station in Figures A141 to A175. The error in these graphs is plotted as the average percent error in each velocity bin.

An inspection of the computer program output data sorted into day, night and day+night revealed that there was no significant difference in the results of separate day and night analysis. Therefore, it was decided that only the day+night data be plotted for the percent error graphs. However, the results of the measured to predicted wind speed ratio were analyzed on a separate day, night and day+night basis.

It can be observed from all the percent error graphs that in predicting the wind velocity of AHHRF site (first iteration), the average errors resulting from the direct comparison were most often smaller than the errors produced by LBL, AIM-2 and ASHRAE models. However, the standard deviation of the error from the direct comparison method was found to be larger than that from the other models.

It was noted from all the error graphs that the error in predicting the wind speed was generally higher for the lower velocity bins. There are two possible reasons for this occurrence. The first reason could be that the wind correction models are not as sensitive to the lower wind velocities as they are to the higher wind velocities. The second probable reason is the involvement of human error and instrumentation error in estimating the lower wind speeds from inspecting the strip chart recordings at the meteorological stations. The standard deviation of the error in lower wind velocity bins is generally higher, possibly due to the same two reasons mentioned above, and also discussed in Section 3.2.

The error plots from the first iteration indicate that the error bias is in the same general direction for the most cases. For the velocity bins greater than 3 m/s, the bias is mostly in the negative direction. In other words the predicted wind velocity of the experimental site (AHHRF) is lower than the measured wind velocity at the experimental site. This implies that the terrain coefficient is most often underestimated. This also suggests that the terrain class descriptors were incorrectly estimated in the same direction. Since the bias is in the same direction, the terrain descriptors can be easily re-evaluated to minimize the error involved in predicting the wind speeds. In fact, this approach was tried and the terrain class descriptors were modified by closely examining the site terrain and by studying the error plots from the first iteration runs. The results of the second iteration will be discussed later in this section.

When comparing the percent error associated with each of the four models, it was found that the Log Profile model predicted the wind velocity of the experimental site most closely to the measured wind velocity than any of the other models (for example, see Figures A30, A31, A32 & A33 for the Edmonton International Airport). This observation, however does not imply that the Log Profile model is superior to the other models. The main reason that the Log Profile model predicted the wind speed of the experimental site with the lowest error is that the terrain class for this model is more finely defined than that of the other models studied. For similar reasons the ASHRAE model showed the highest errors because it uses the most coarse graduation between terrain classes.

As mentioned earlier, the wind data recorded at Edmonton International Airport, Namao Airport and Edmonton Municipal Airport was based on two minute averages around the hour whereas, the wind data recorded at Ellerslie Climate Station and Stony Plain Climate station was based on the wind run. The error plots of the wind predictions obtained by using the wind data from the two methods (see Figures A29 and A134 for example) indicate that the use of data from stations which report wind run can reduce the amount of scatter when transferring wind data to similar terrains. When the terrain classification of the two stations being compared is different, data bias is likely to be introduced. The magnitude of the bias may depend on the difference in the terrain classes of the two sites.

It should be noted that wind speeds less than 2 m/s were not included in the analysis when calculating the monthly ratios of the measured to predicted wind speeds. The reason for doing so was the unreliability of the wind data under 2 m/s recorded at the met stations. Also, monthly ratios were only calculated for the LBL and AIM-2 models. The analysis of the monthly ratios was carried out separately for the day, night and day+night. Figures A6 and A7 show the monthly ratio profiles for 0-90 degree direction quadrant bin for the Edmonton International Airport using the LBL and AIM-2 models respectively. It can be seen from the ratio plots (for example Figures A34 & A35) of all the sites that the LBL and AIM-2 ratios have the same general shape over the entire year with AIM-2 slightly lower, possibly due to the different power law for the wind speeds below and above 3 m/s. Since the predicted wind speed was generally less than the measured wind speed, the ratio of the measured to predicted wind speed plotted was generally greater than one. This trend can be seen quite consistently in all the monthly ratio plots from the first iteration.

The terrain surrounding all the sites was re-examined and the effect of trees was re-assessed. The terrain class descriptors were re-evaluated. The re-evaluation of terrain descriptors for the second iteration was not based on the juggling of numbers but was based on a logical review of terrain classes for the site. Mark Ackerman, a research engineer with the University of Alberta, who did not have any past experience in the classification of terrain made all terrain class assessments himself. He had a better understanding of classifying the terrain for each model and site during the second iteration. Computer runs during the second iteration were carried out by using a set of revised terrain class descriptors. The output data from these runs was plotted as in the first iteration for the percent error and monthly ratios. The plots for the second iteration runs are shown in Figures B1 to B21 in Appendix B. The terrain class descriptors as during the first iteration were assigned in 16 direction bins 22.5 degrees apart. Since the results of the first iteration were not affected by the directional quadrants, the analysis for the second iteration was based only on the single direction bin 0 - 360 degrees.

The results from the second iteration were encouraging. The percent error in predicting the wind speed of the experimental site was reduced for LBL, AIM-2 and Log Profile models, as can be seen by comparing Figures A30, A31, A33 with

Figures B2, B3 and B5 respectively. The ASHRAE model results did not change much because of the coarse terrain classification which could not be adjusted in smaller steps. The monthly ratios for the three pairs of site data also showed great improvement. The monthly ratios for all the cases appeared to have moved closer to the best possible value of one, as evident from Figures B6, B7, B13, B14, B20 and B21.

It appears from the results of this study that simple methods are available for accurately predicting the wind speed at a building site in a rural terrain from the wind speed data of a nearby meteorological station. However, this conclusion cannot yet be made concerning the prediction of wind speed of an urban site from a nearby rural meteorological station. It is recommended that further study should be carried out including both urban and rural sites in order to ensure that the present results are not site specific and to develop a method that could be used to predict the wind speed at any site from a nearby meteorological station.

It is probable that a simple standard method can be developed to estimate the terrain class descriptors more accurately and quickly. The approach will be to take photographs of the site surroundings to estimate the height of the obstructions in each direction. Then estimate the distance of that obstruction from the measuring tower and calculate the distance to height ratio (X/H) for the obstruction. This ratio could then be used to determine the terrain class descriptors for each direction bin separately. A first element of the second study should be to develop such an objective method of defining terrain classes (or of defining a continuously variable terrain descriptor). This method should be tested first on the data from the present project, then applied in the extended study.

An important observation, which Dr. Wilson and Mark Ackerman made from the field measurements, was that the terrain effect doesn't travel down wind too far ($\approx 500\text{m}$). This observation should be reconfirmed in the second study and should also be considered in determining the terrain descriptors. Once the terrain descriptors have been determined, each of the models should be used to estimate the wind speed at each of the test sites from the wind speed of nearby meteorological stations, to select and further develop the best model.

5.0 CONCLUSIONS AND RECOMMENDATIONS

The present study was carried out in order to test the available methods for predicting the wind speed of an experimental site from the wind speed data measured at nearby meteorological stations. The height of the wind measuring device at each of the wind measuring stations, including the Alberta Home Heating Research Facility (AHHRF) was the same (10 meters). The five nearby meteorological stations were: Edmonton International, Edmonton Municipal Airport, Namao Airport, Ellerslie Climate Station and Stony Plain Climate Station. A direct comparison between the wind speeds of AHHRF and those from the five nearby meteorological stations was performed first. Then the wind speed of AHHRF was predicted from the nearby meteorological station with the help of the four wind correction models: LBL, AIM-2, ASHRAE and the Log Profile model. The wind comparison using these models was carried out in two iterations. The first iteration runs used the terrain descriptors that were based on a preliminary assessment of the site terrains. The percent error between the predicted and the measured wind speed of the experimental site was significant for all the models. The terrain descriptors were modified and the second iteration runs were carried out. The percent error was significantly reduced.

The other conclusions that were drawn from this study are as follows:

- 1) All of the terrain models adequately predicted the wind speed at a rural site from wind data measured at a nearby meteorological station. The log profile model predicted wind speeds with the lowest percentage error, but it is likely that this was due to the model's larger number of terrain classes, not to the fundamental nature of the model.
- 2) This project is a study of a single case. The results are encouraging, but cannot be generalised. It is necessary to extend the study to other rural sites as well as to urban sites. It is likely that there are several other sets of sites for which existing data is available, so that the same approach used in the present study could be repeated.
- 3) The difference in the data binned into day, night and day+night was insignificant. If this observation is confirmed by further study, it means

that the final wind model developed can avoid the complication of dealing with the thermal environment.

- 4) The standard deviation of the velocity bins lower than 3 m/s was found to be higher than those from other velocity bins.

Based on the conclusions of this study it is recommended that a further project be carried out to generalise the results of this study to other sites and other terrains. The first step should be to develop an objective method of defining terrain classes or a continuously variable terrain descriptor. This method should be developed using the existing data set from the present project. Then a thorough search should be made for all the available data sets from other sites. This data should be used to assess the power law and log law models using the same terrain class descriptor system in each case.

REFERENCES:

1. Sherman M.H., AIR INFILTRATION IN BUILDINGS, Applied Science Division, Lawrence Berkeley Laboratory, University of California, LBL-10712, Oct. 1980.
2. Walker I.S., Wilson D.J., THE ALBERTA AIR INFILTRATION MODEL (AIM-2), Department of Mechanical Engineering, The University of Alberta, Report 71, January 1990.
3. 1989 Ashrae Handbook Fundamentals (I-P Edition), American Society of Heating, Refrigeration and Air Conditioning Engineering, Inc., Atlanta, GA, pp. 14.4A.
4. Wieringa J., ROUGHNESS-DEPENDENT GEOGRAPHICAL INTERPOLATION OF SURFACE WIND SPEED AVERAGES, Quart J.R. Met. Soc. (1986), 112, pp. 867-889

APPENDIX A

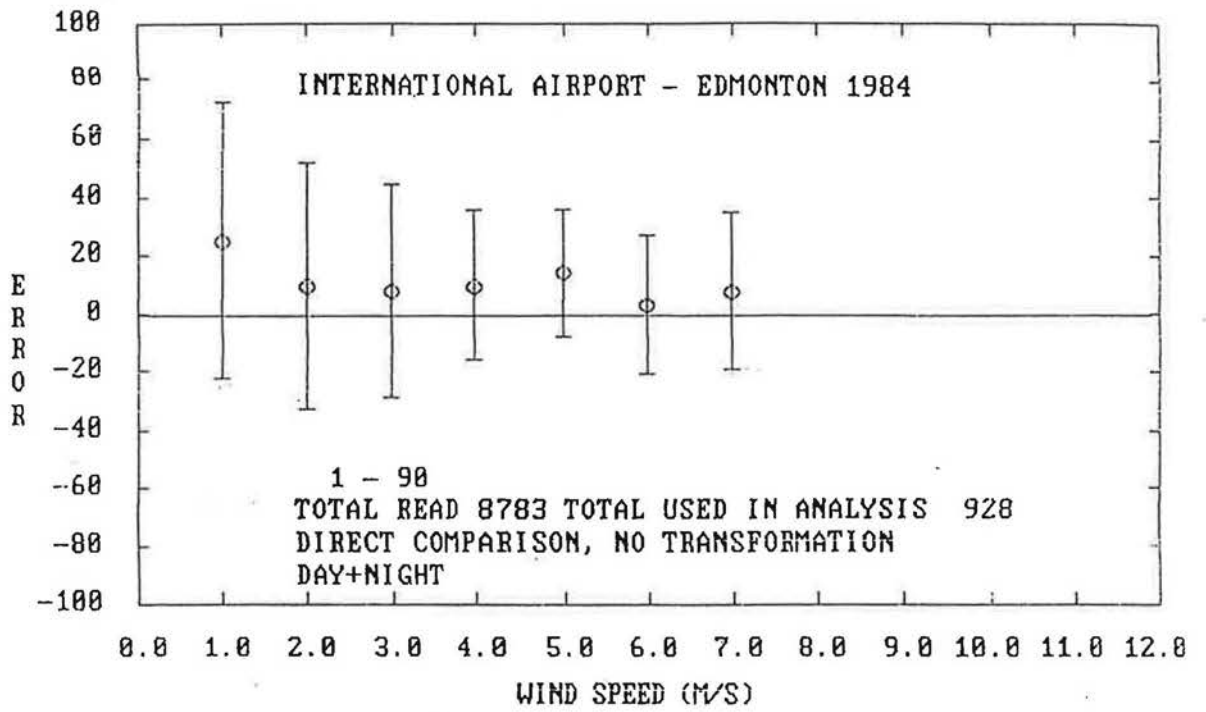


Figure A1

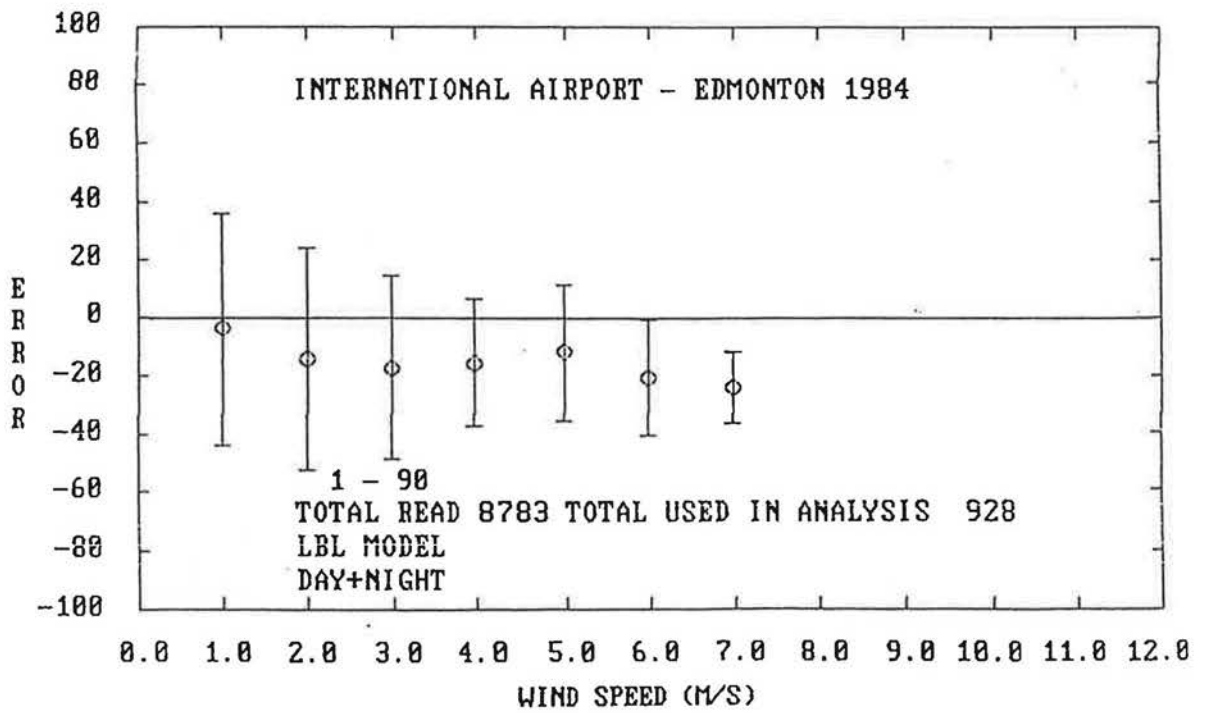


Figure A2

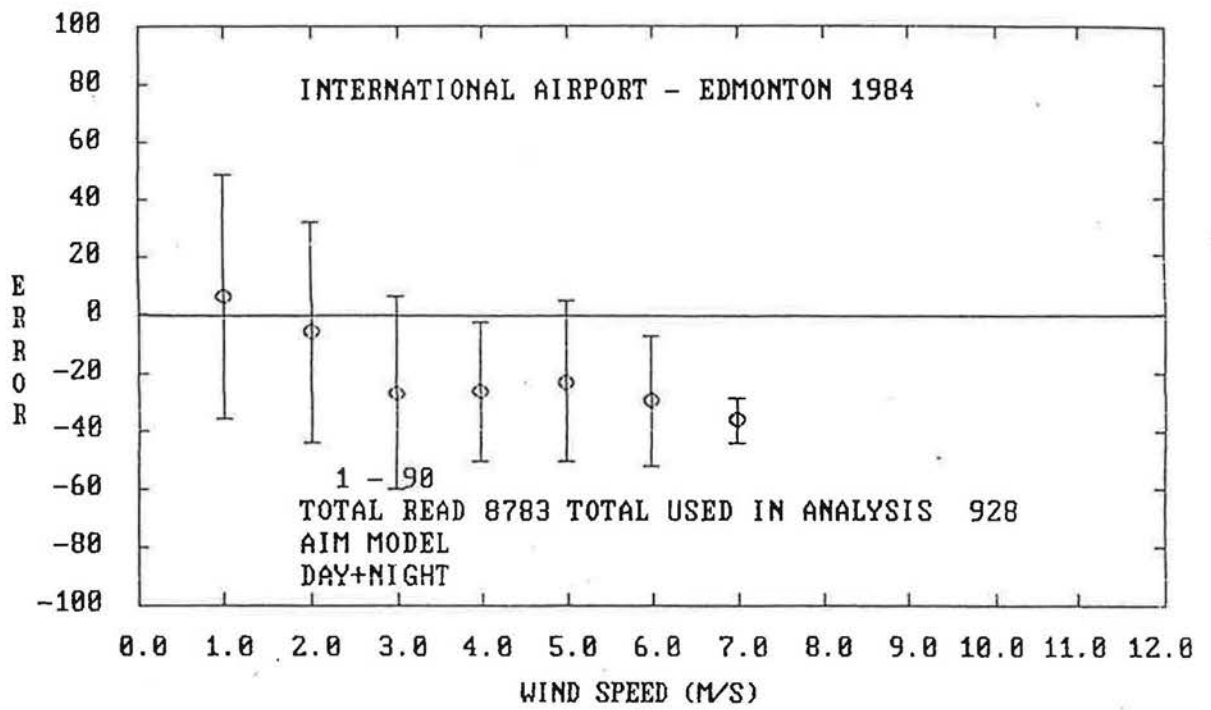


Figure A3

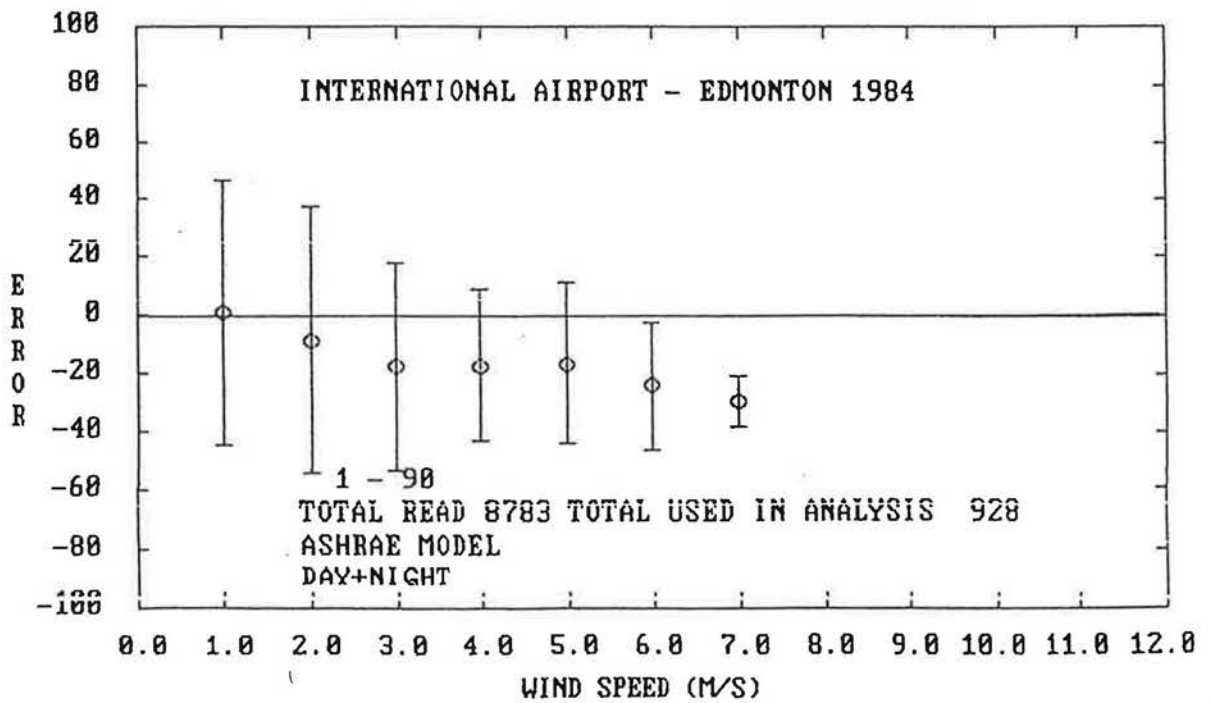


Figure A4

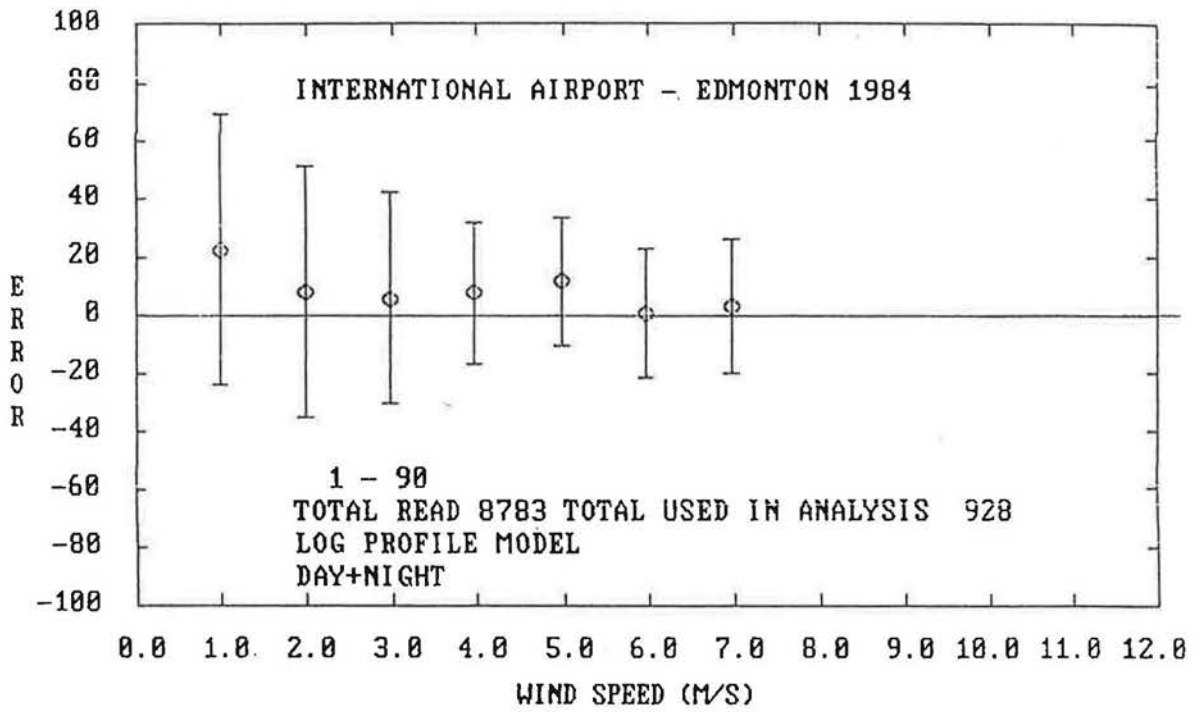


Figure A5

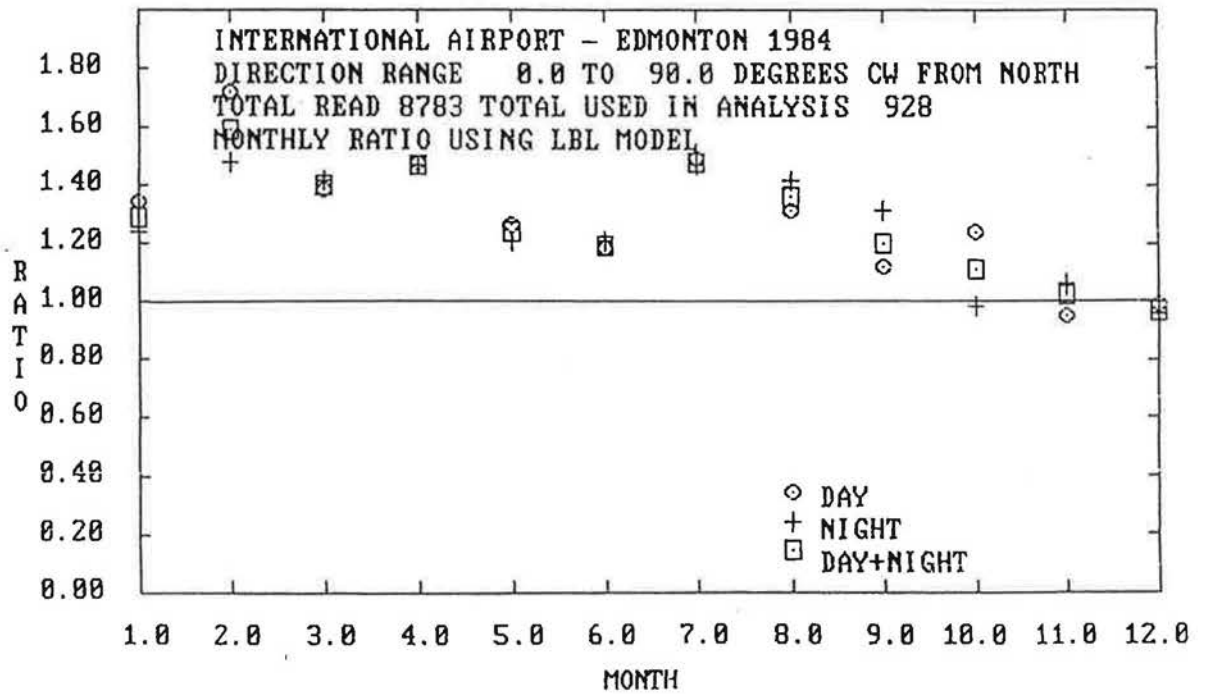


Figure A6

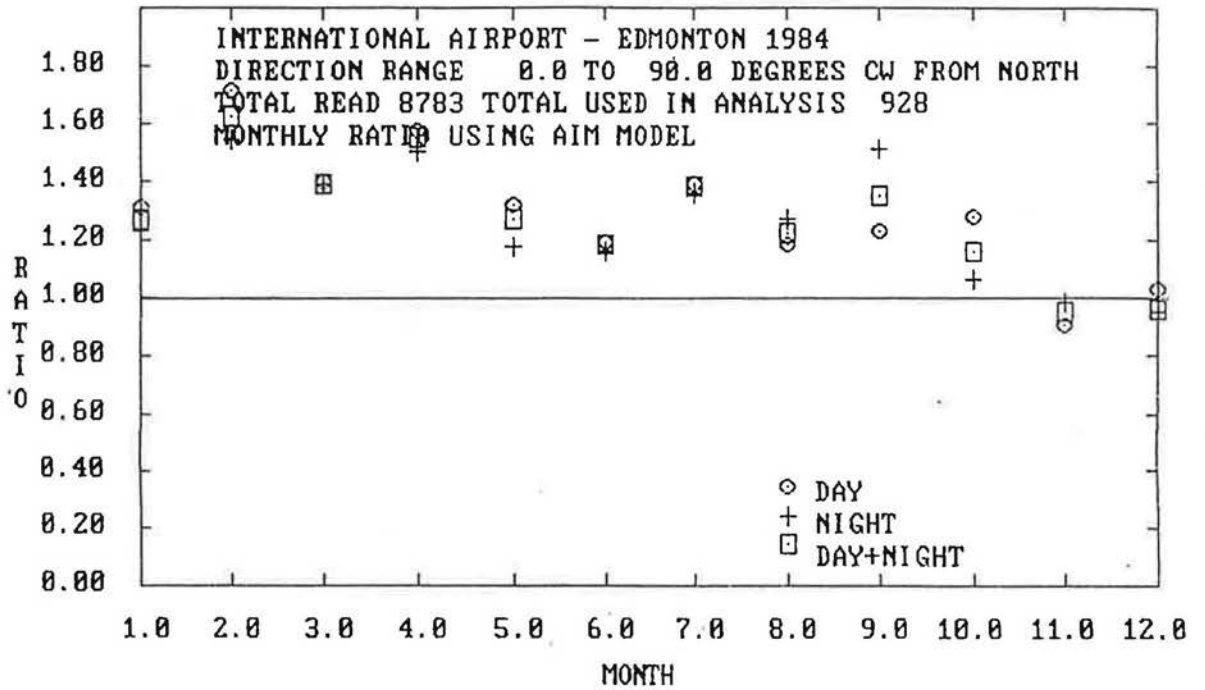


Figure A7

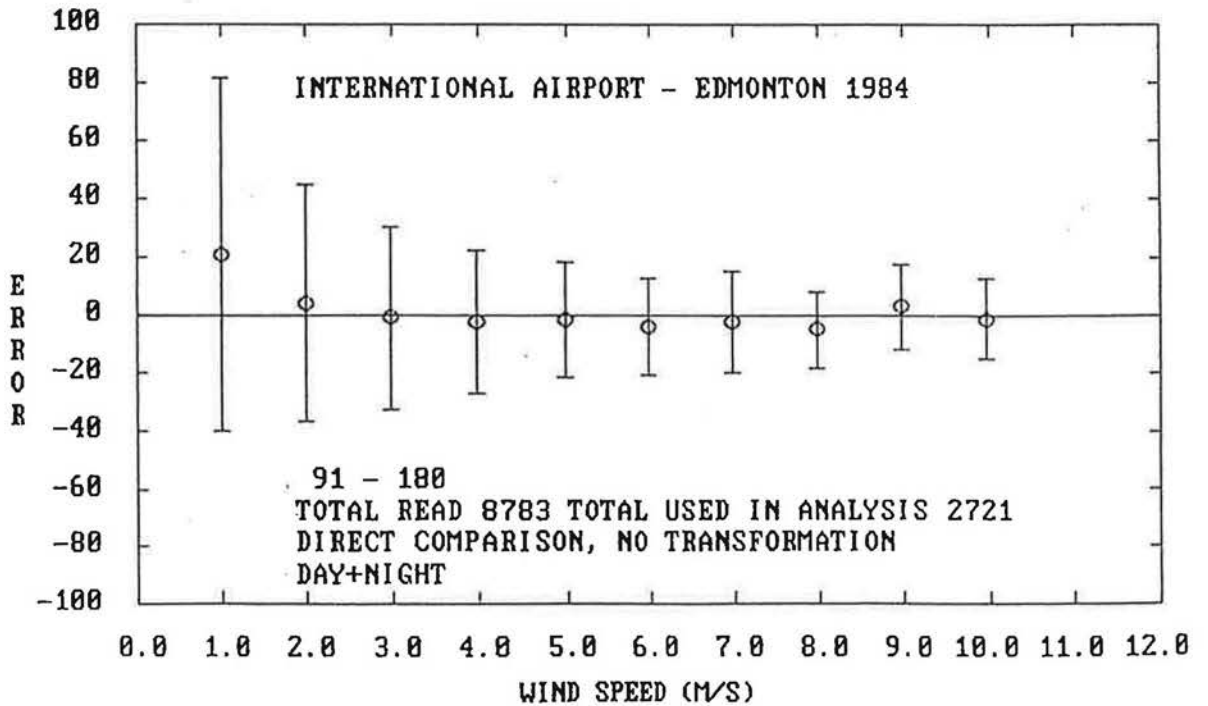


Figure A8

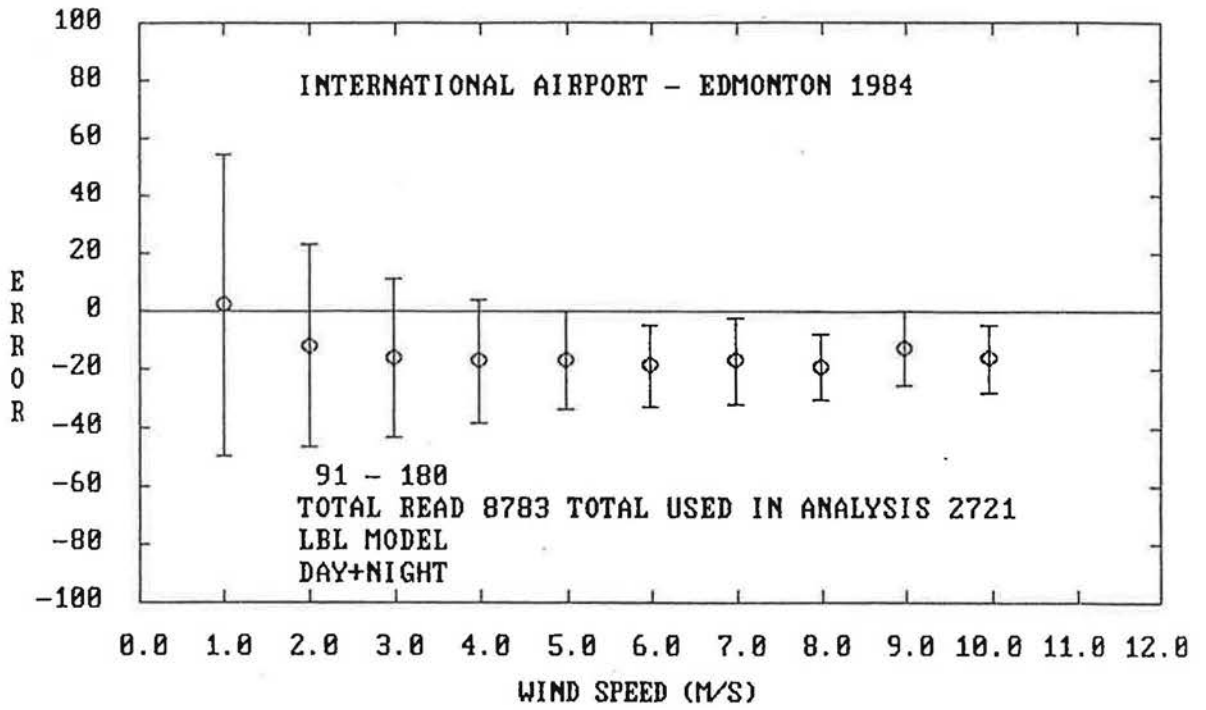


Figure A9

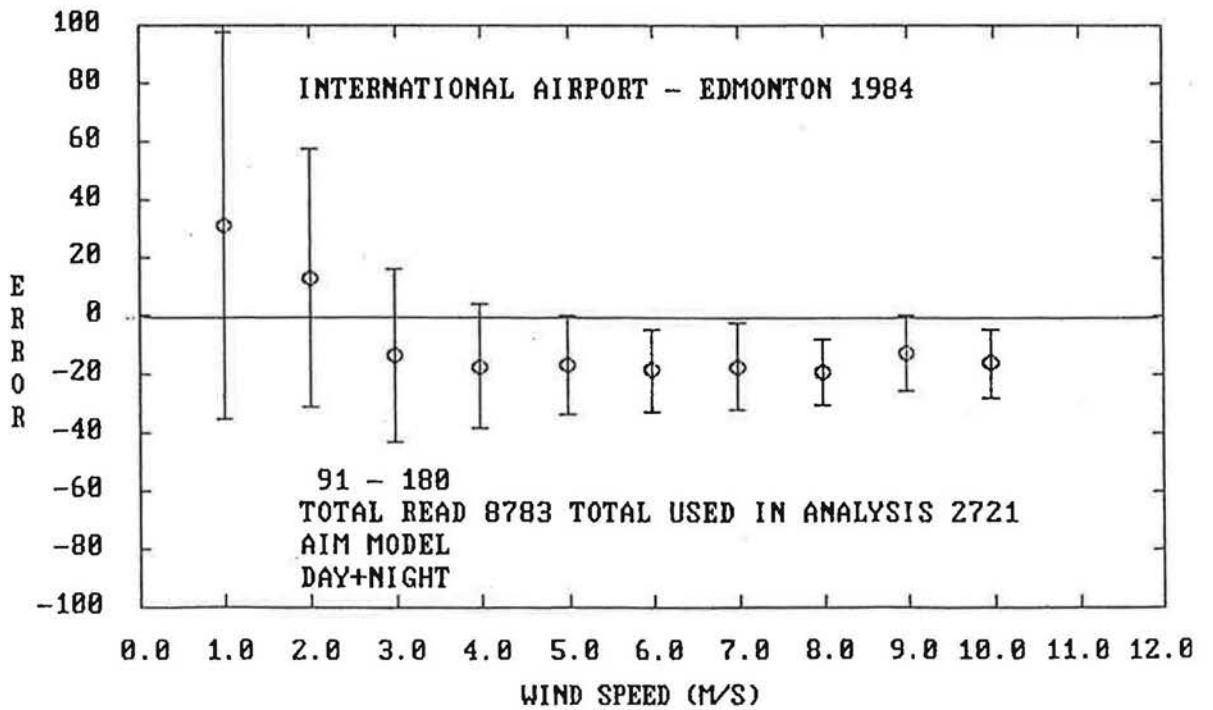


Figure A10

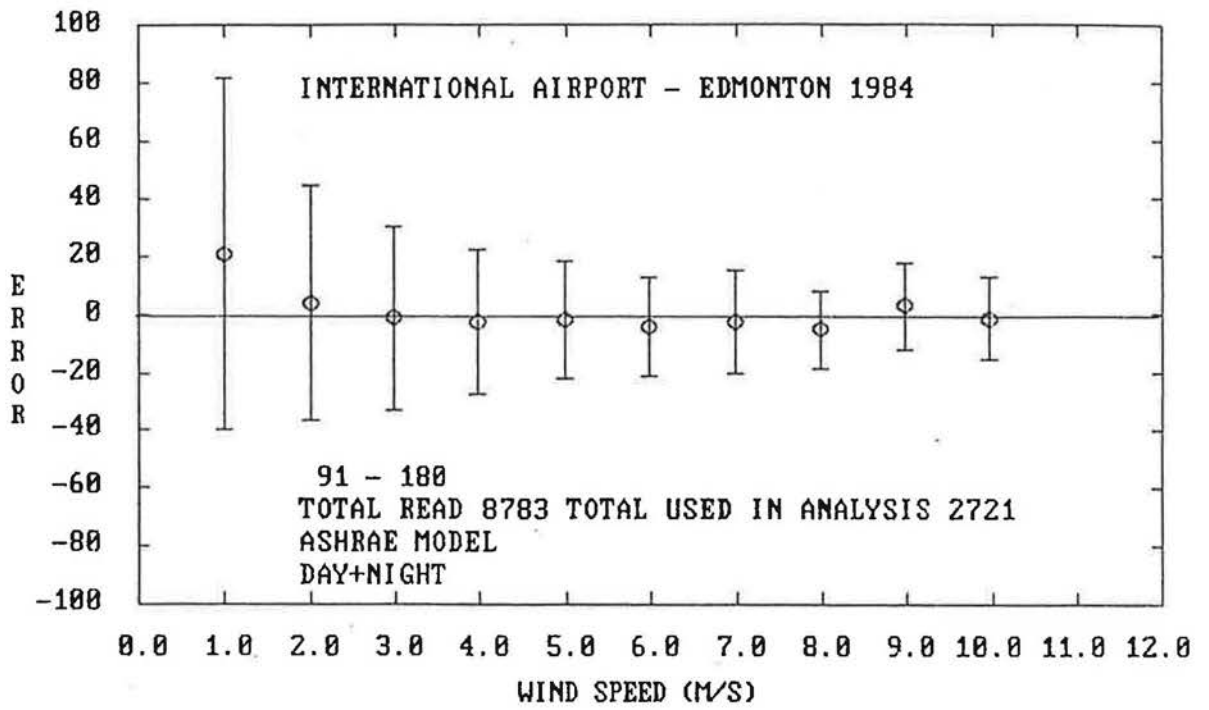


Figure A11

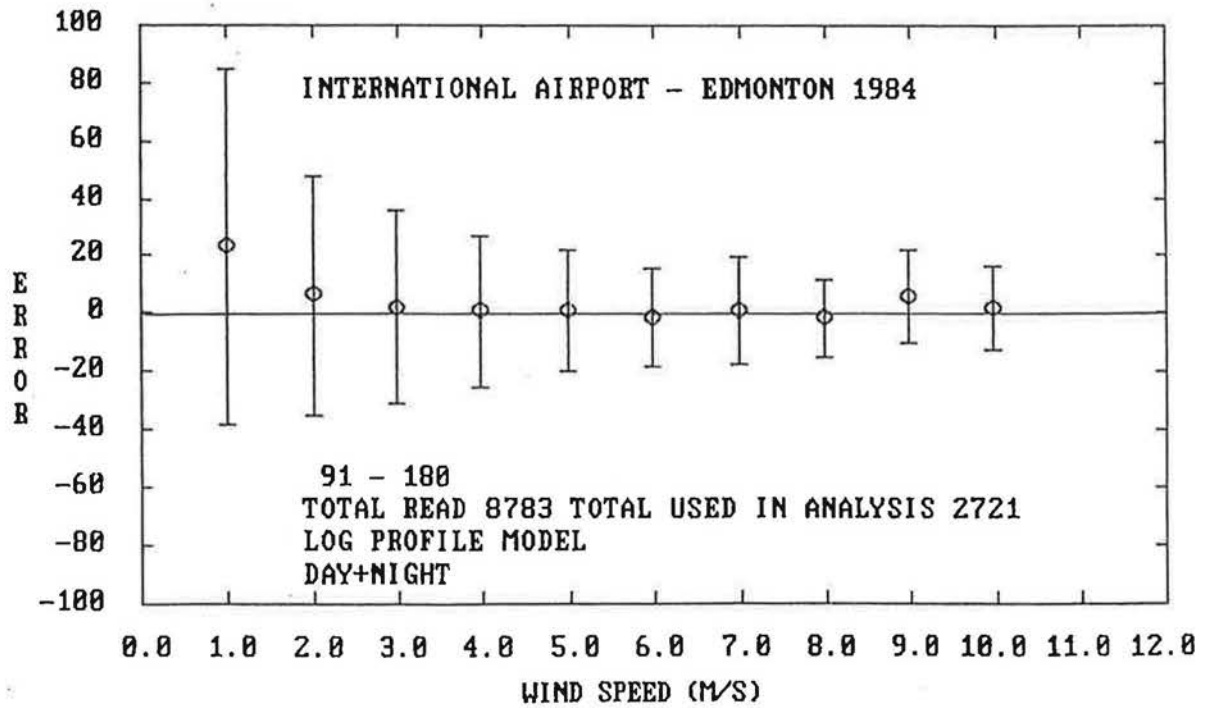


Figure A12

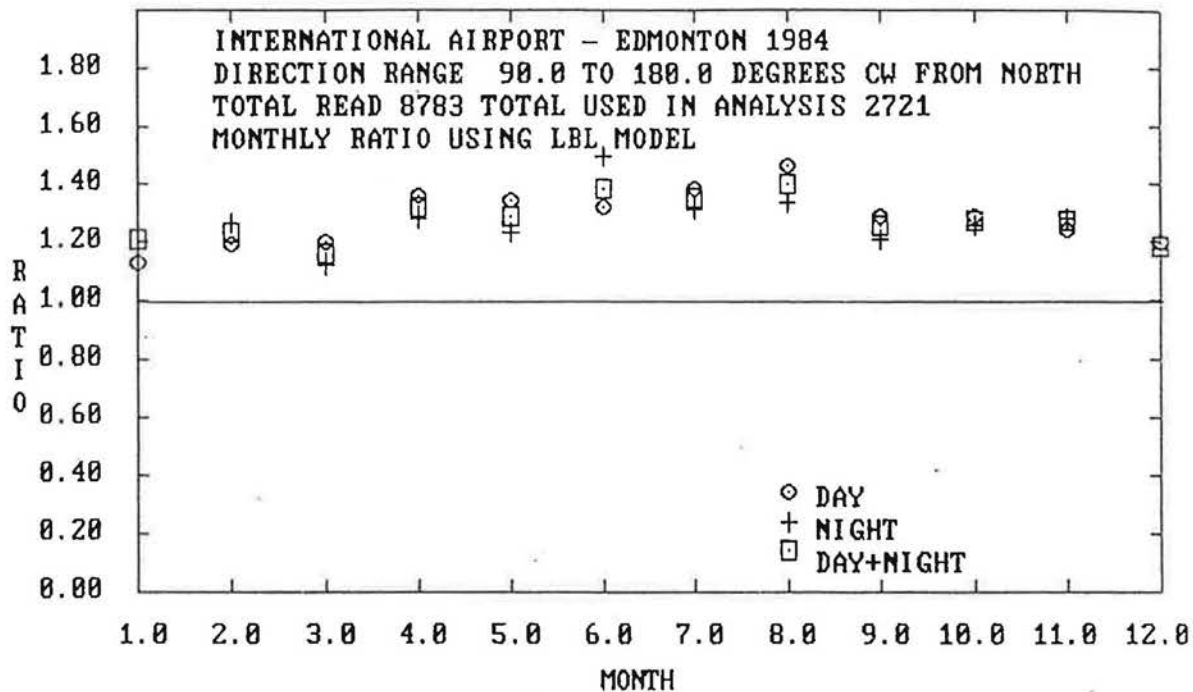


Figure A13

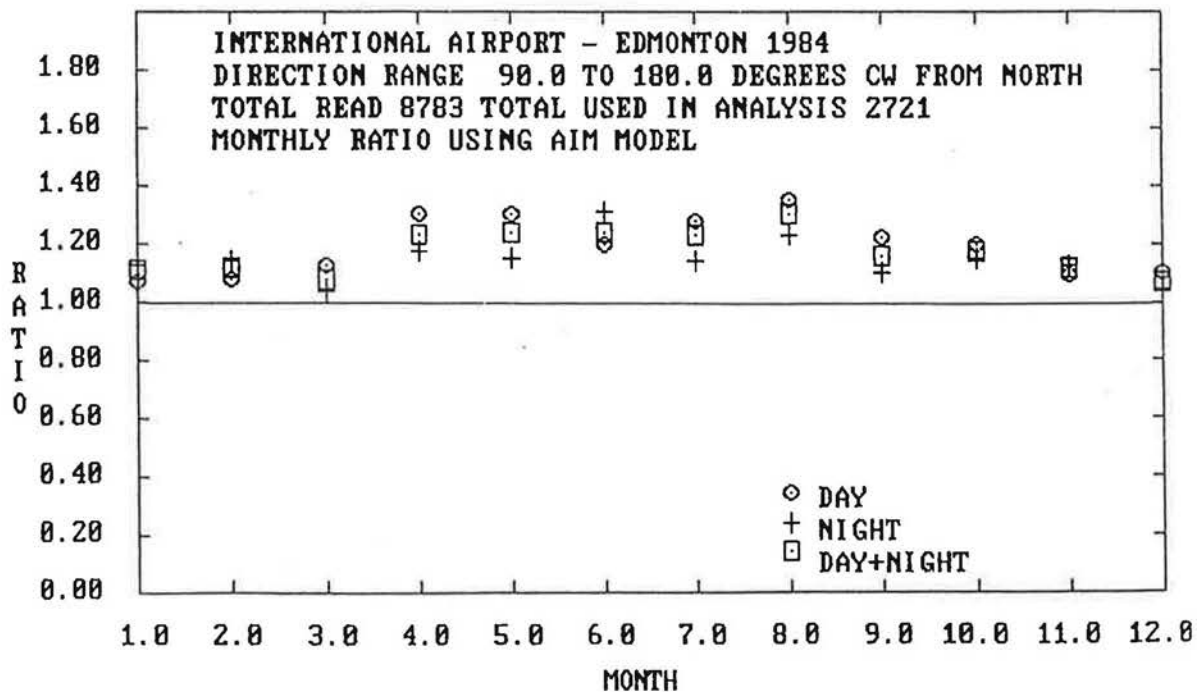


Figure A14

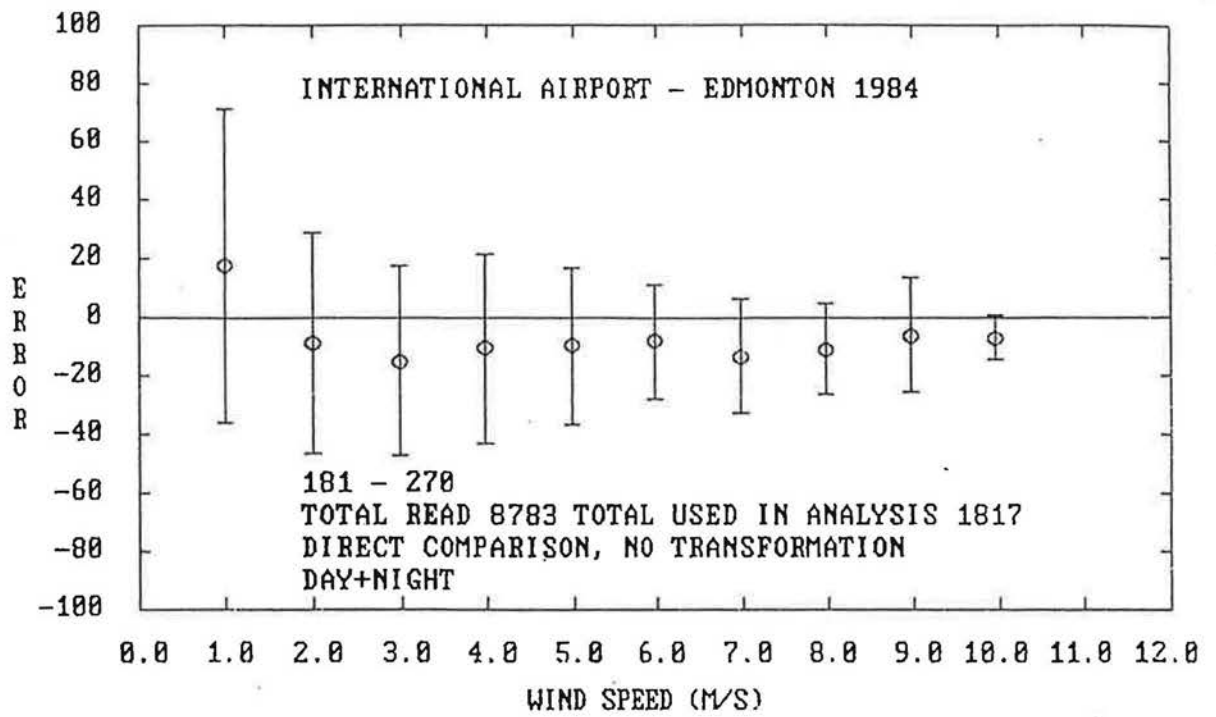


Figure A15

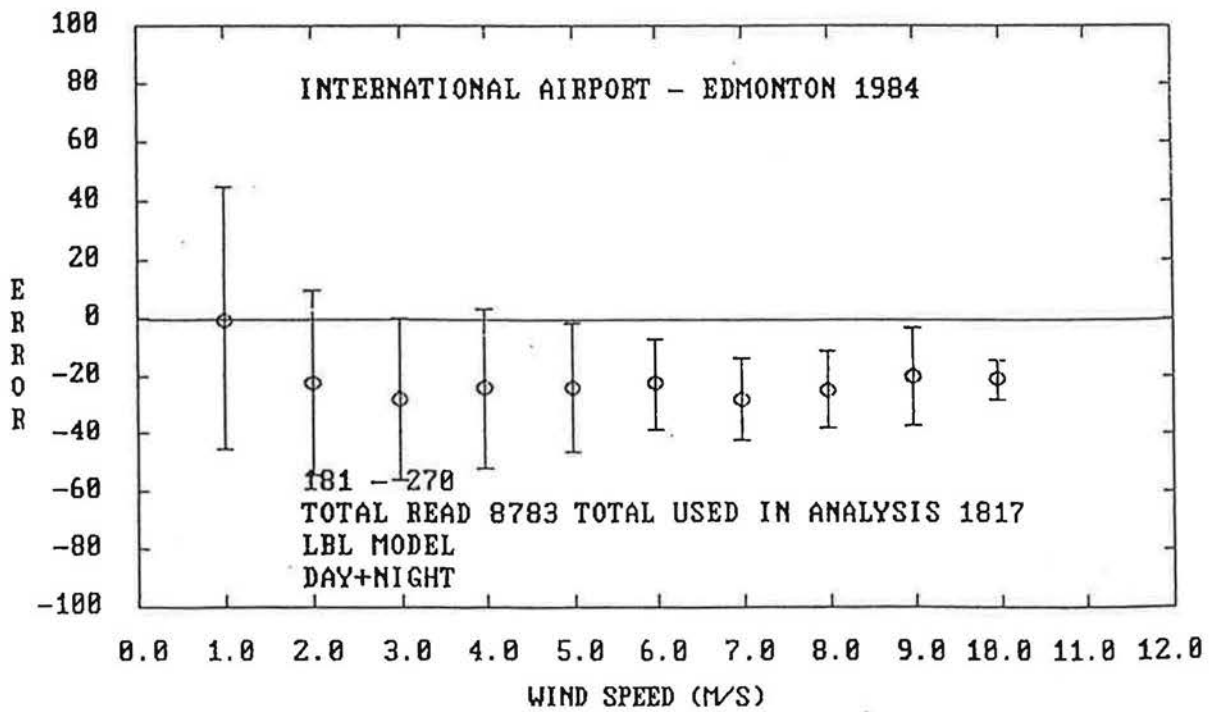


Figure A16

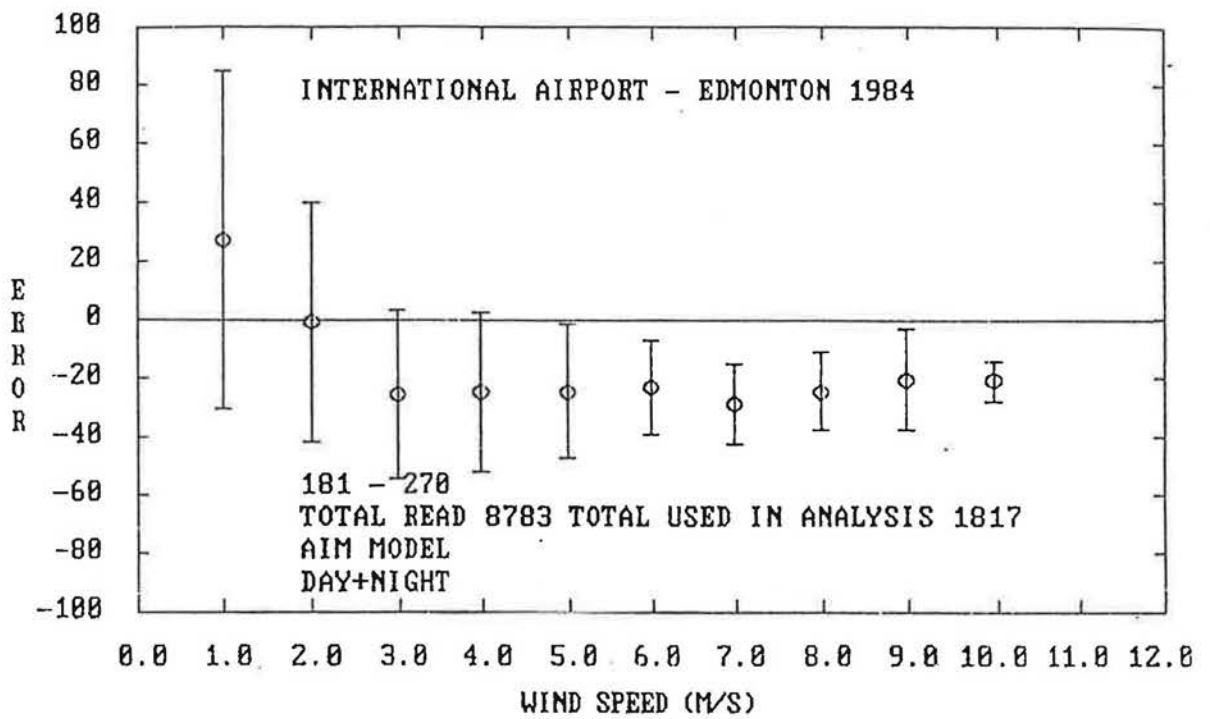


Figure A17

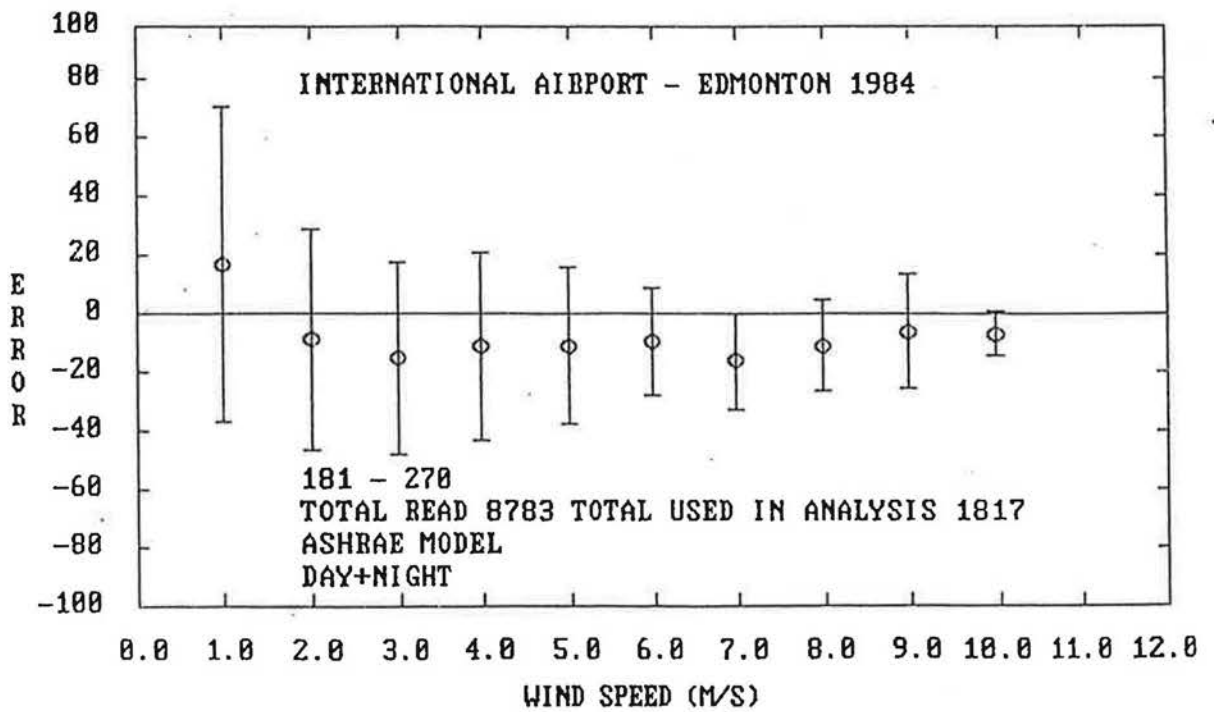


Figure A18

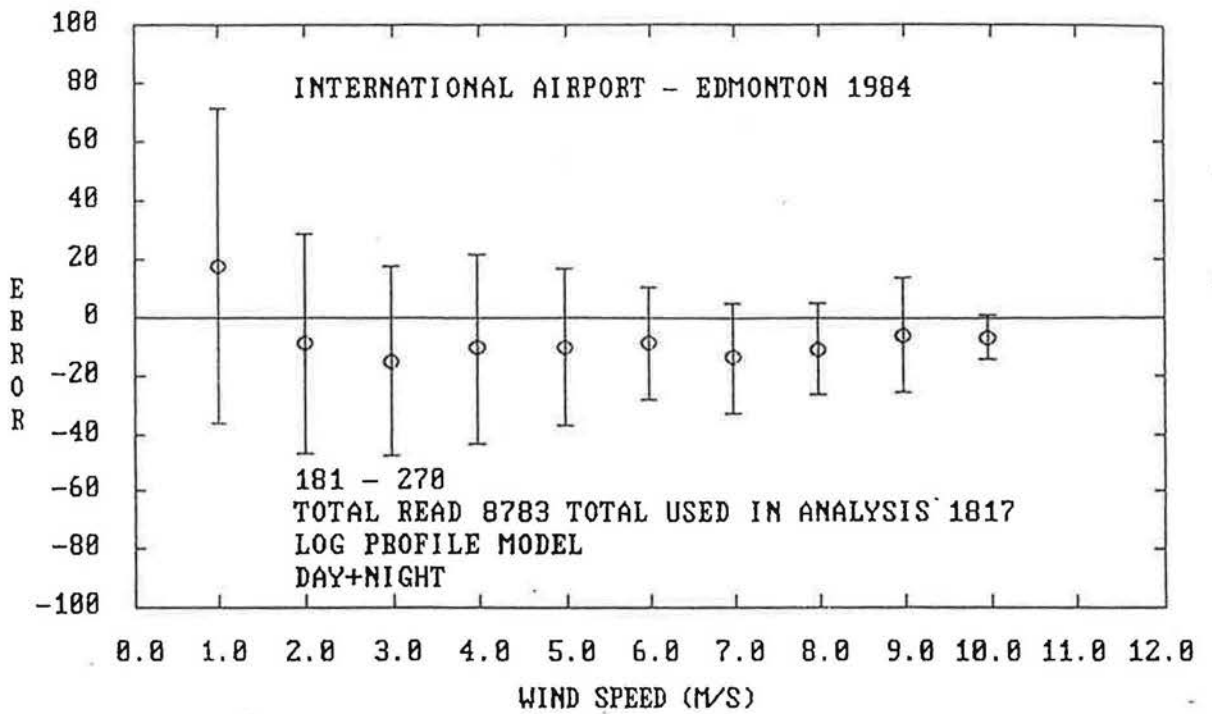


Figure A19

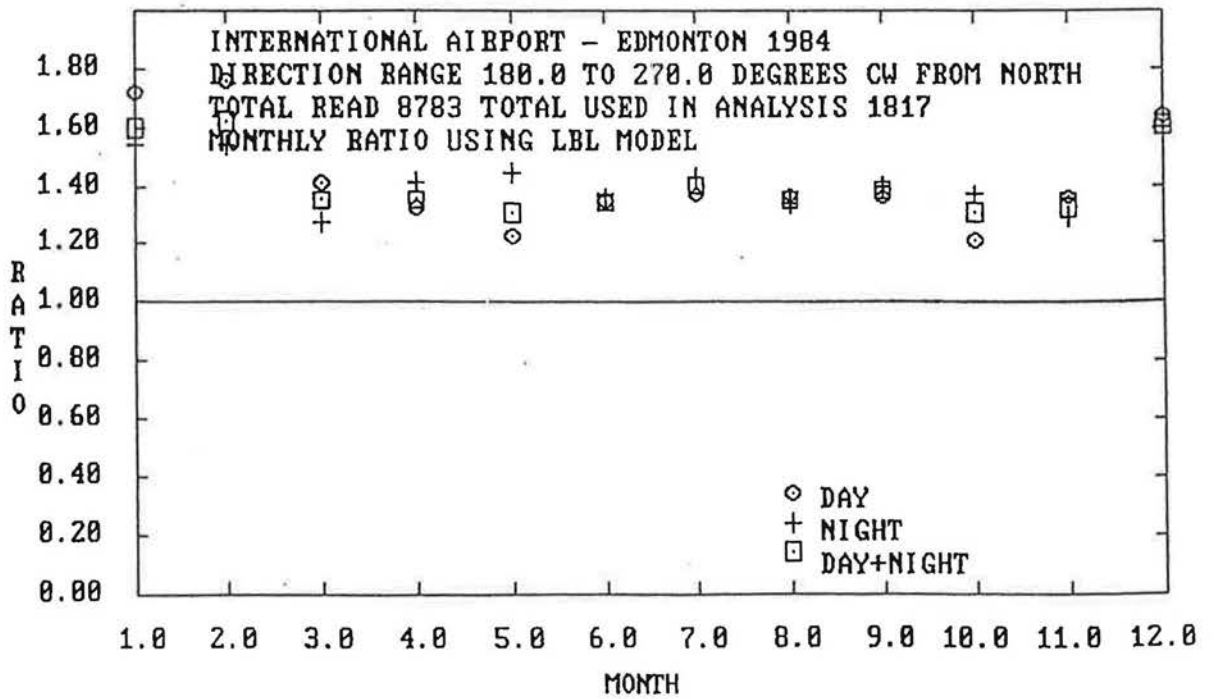


Figure A20

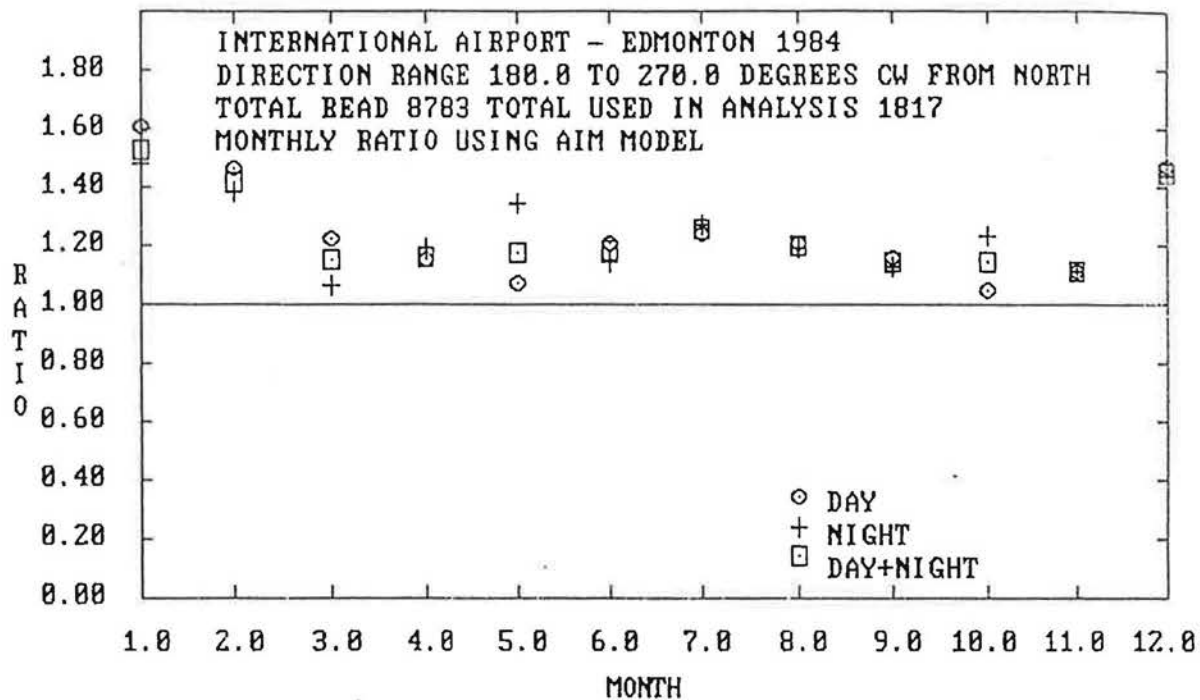


Figure A21

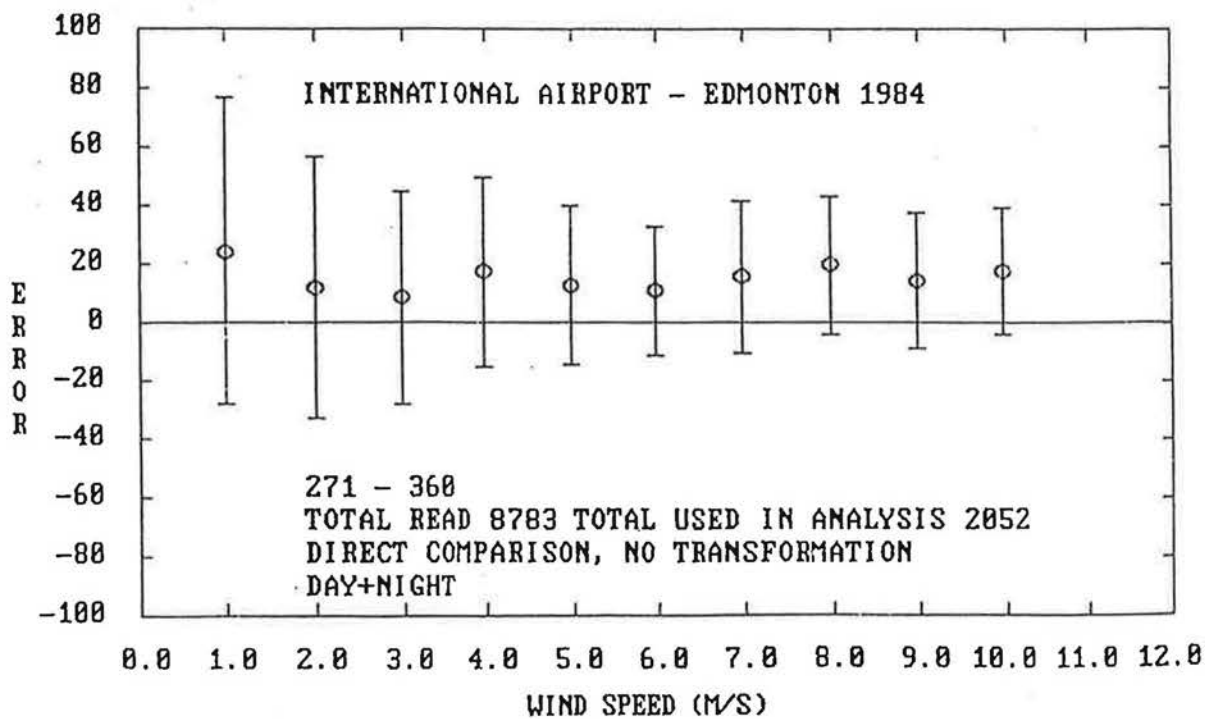


Figure A22

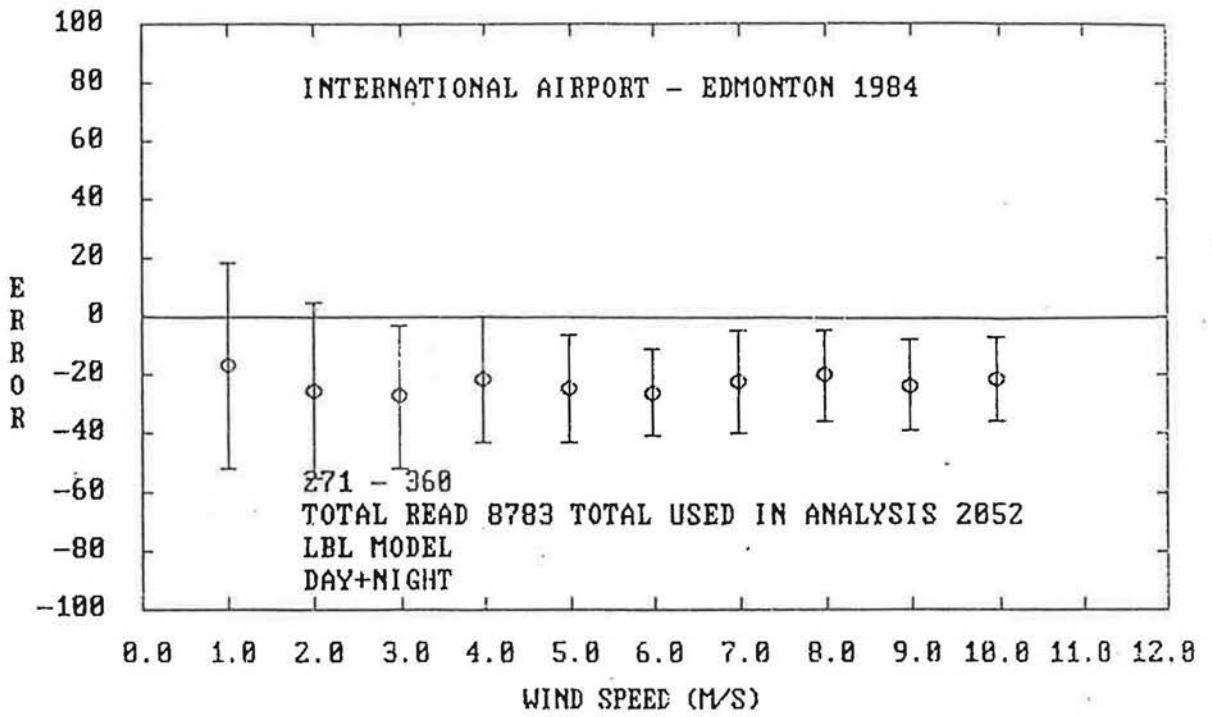


Figure A23

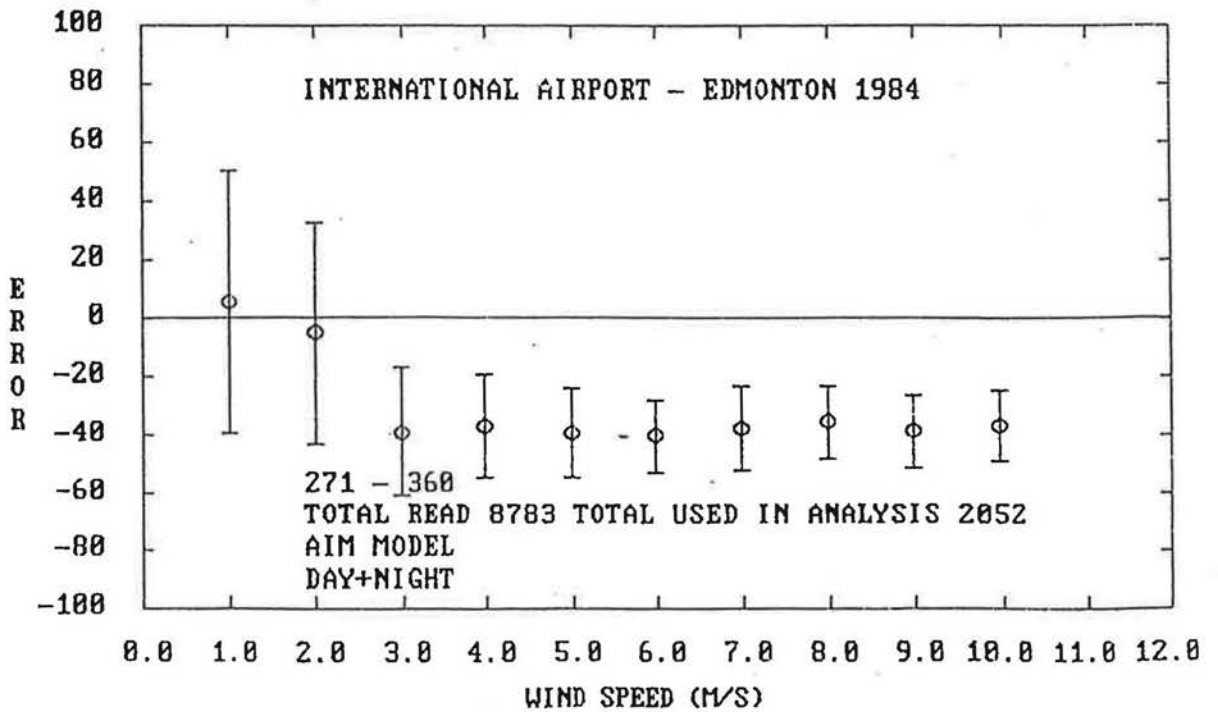


Figure A24

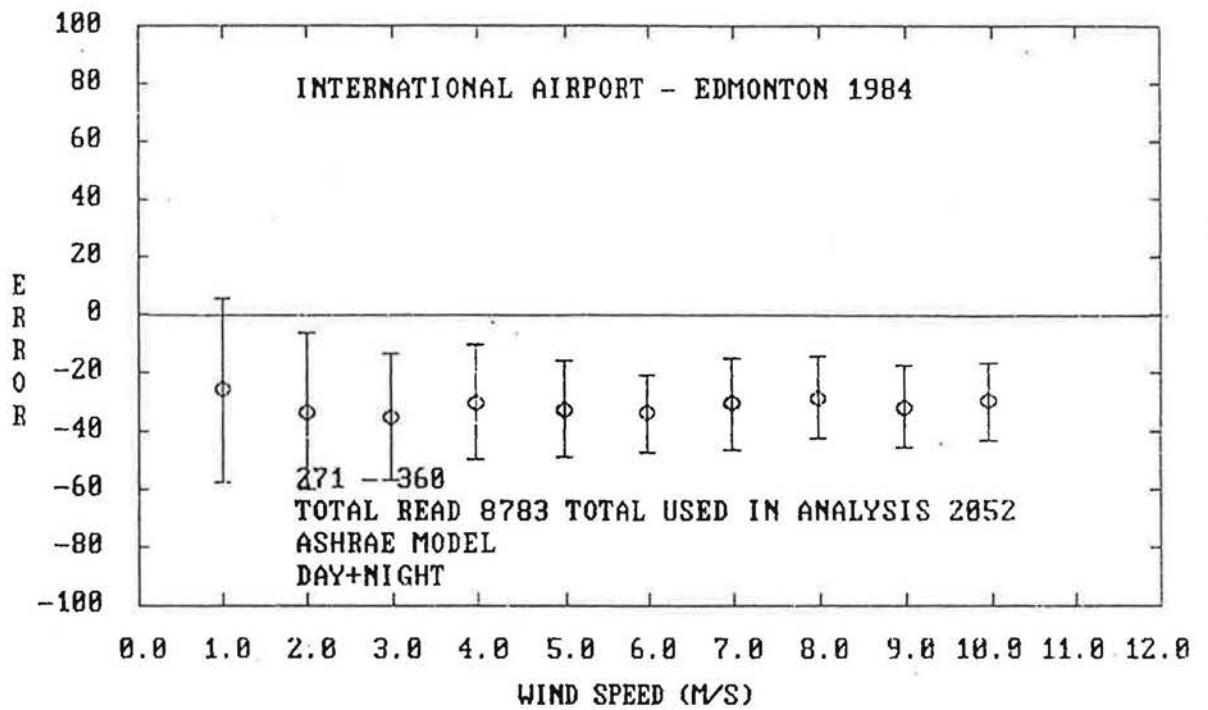


Figure A25

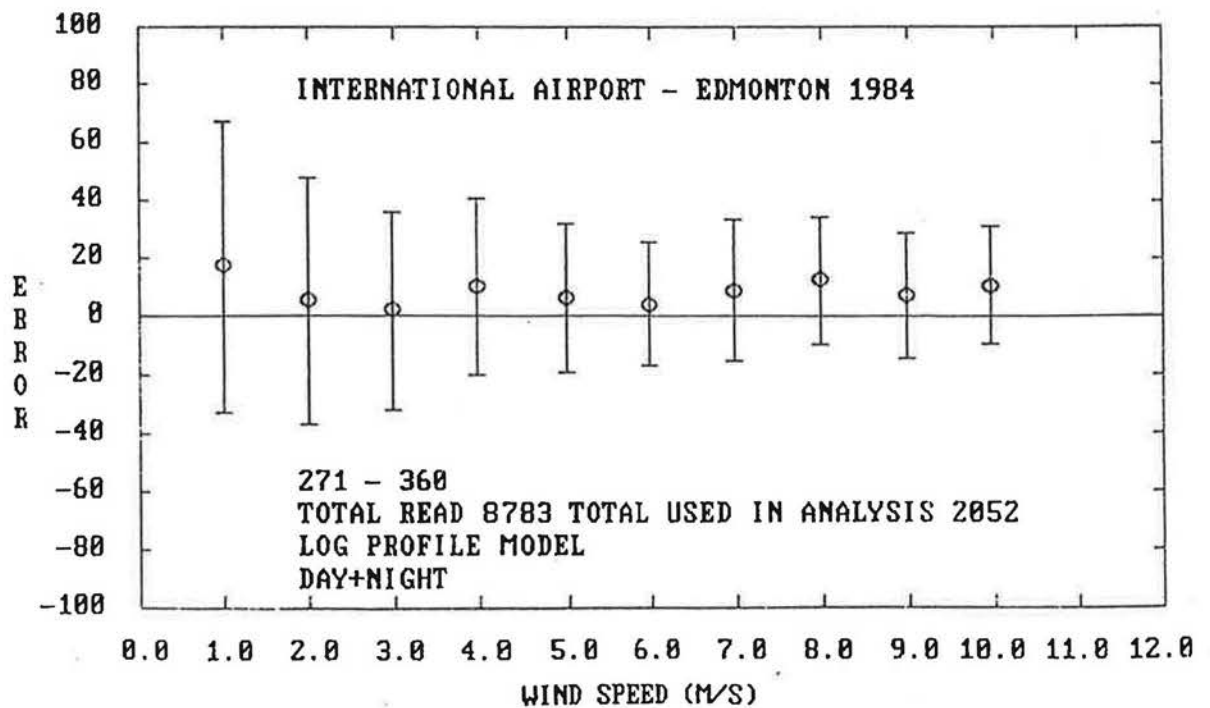


Figure A26

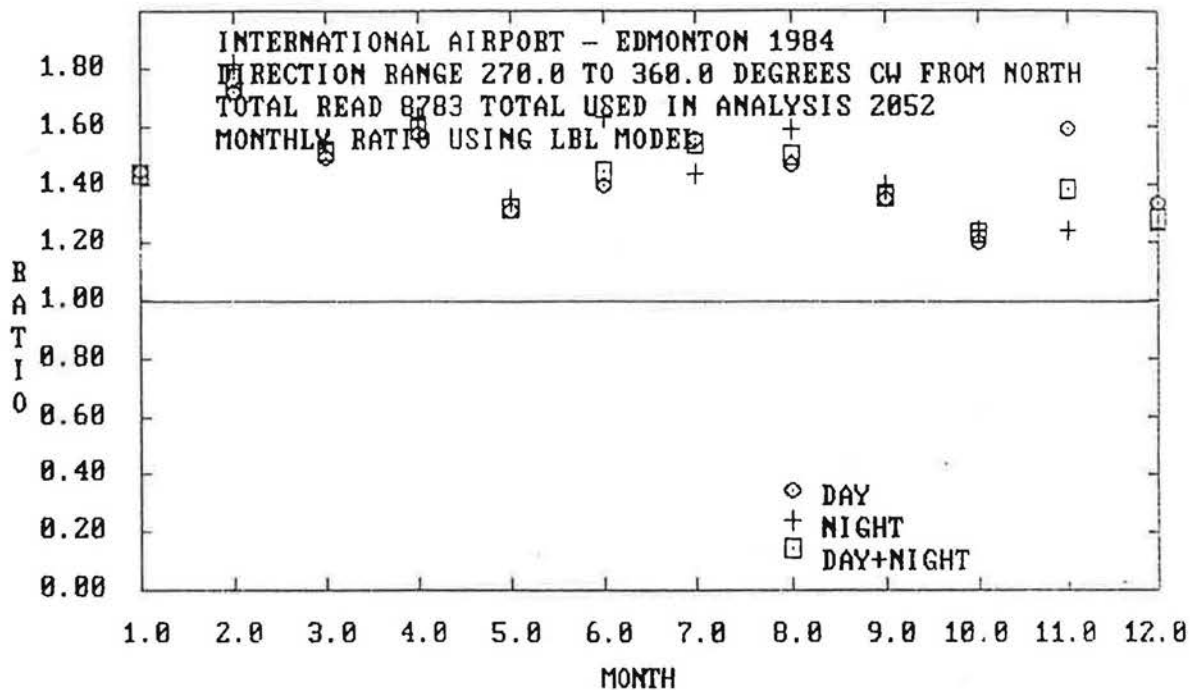


Figure A27

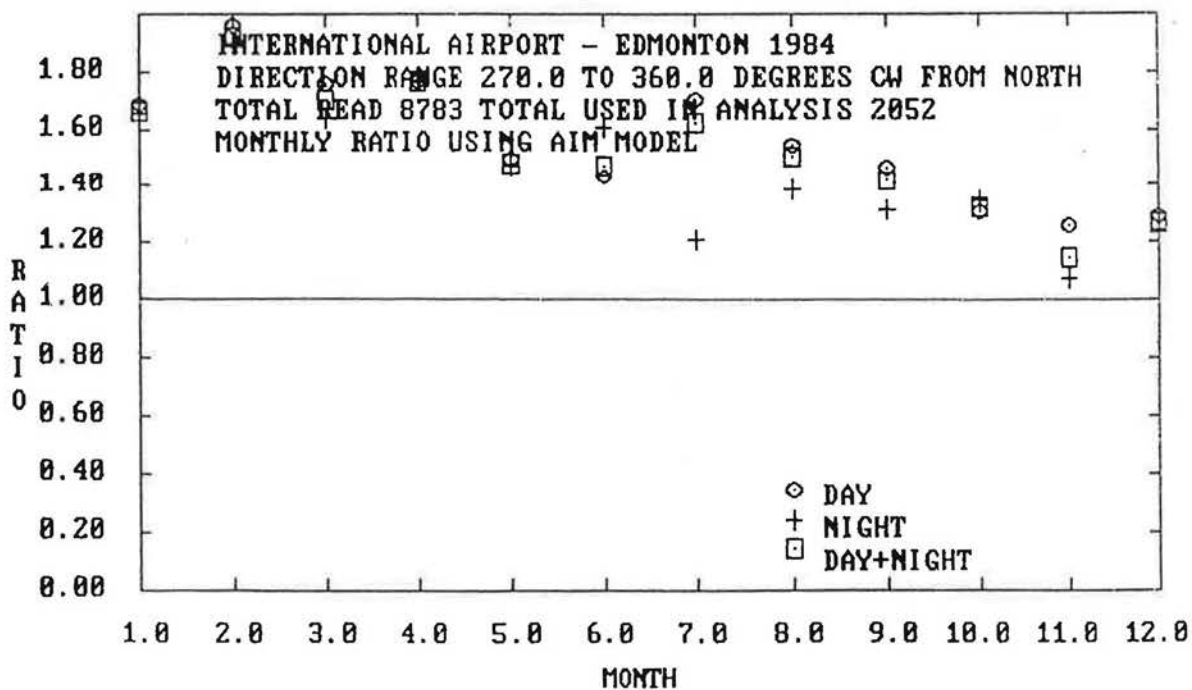


Figure A28

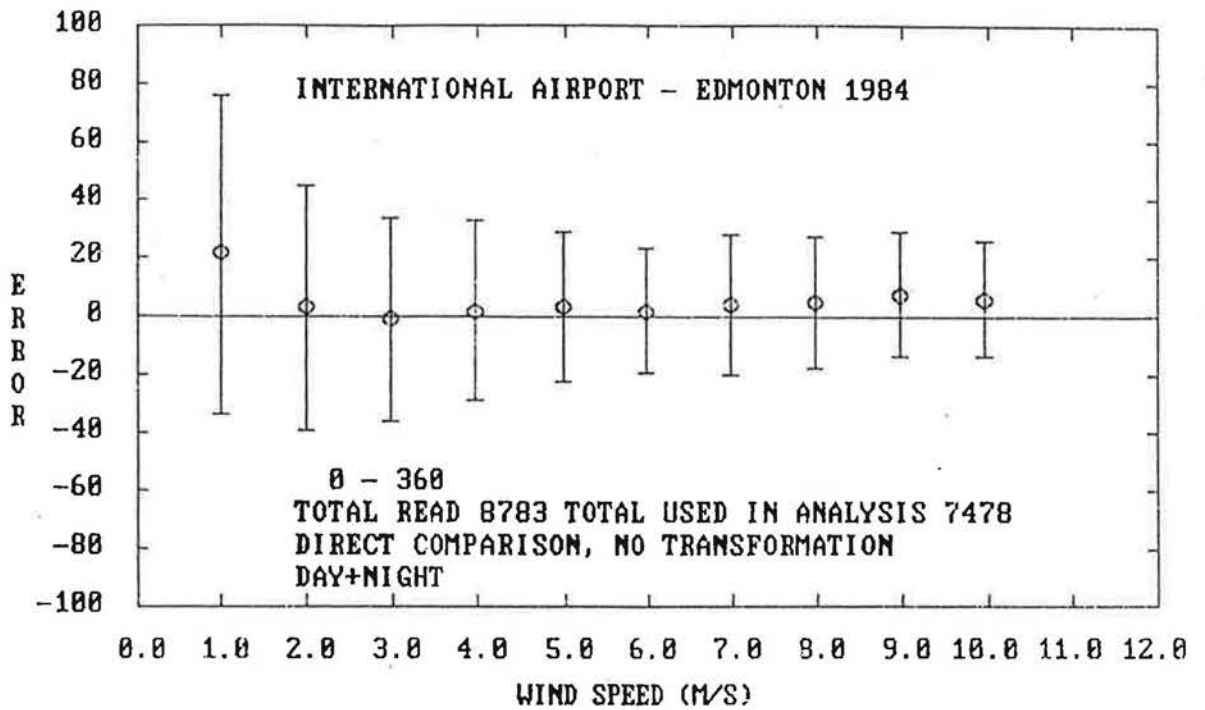


Figure A29

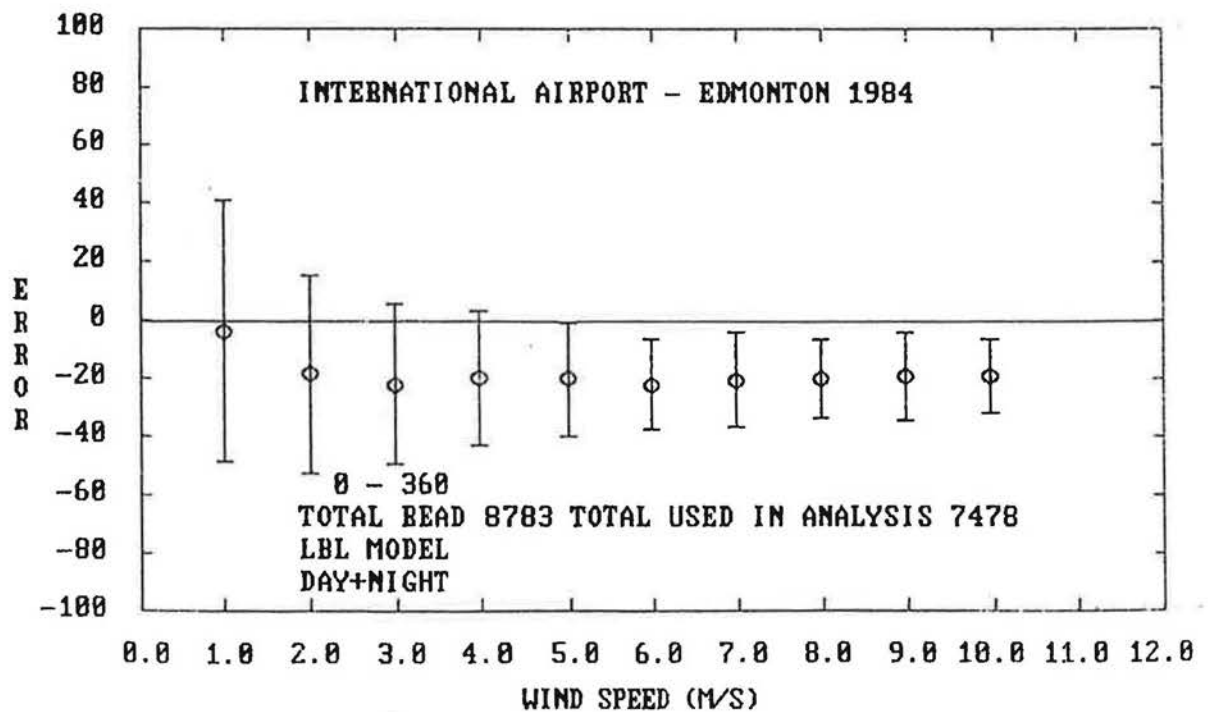


Figure A30

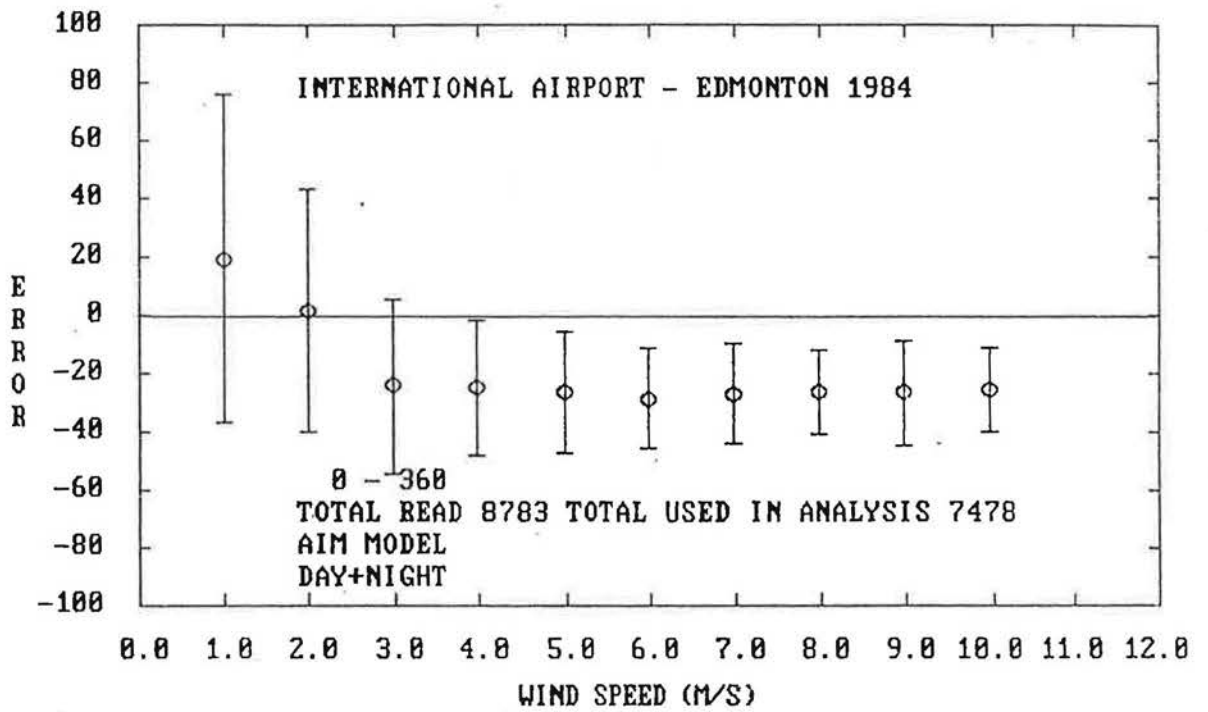


Figure A31

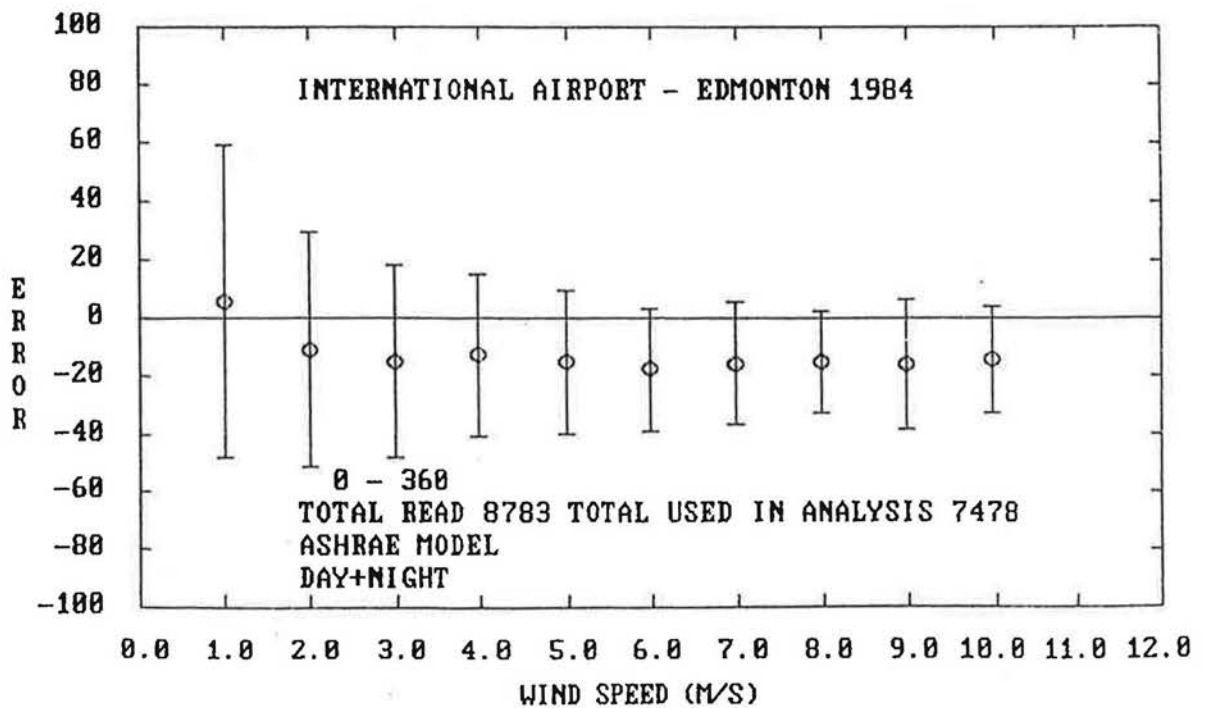


Figure A32

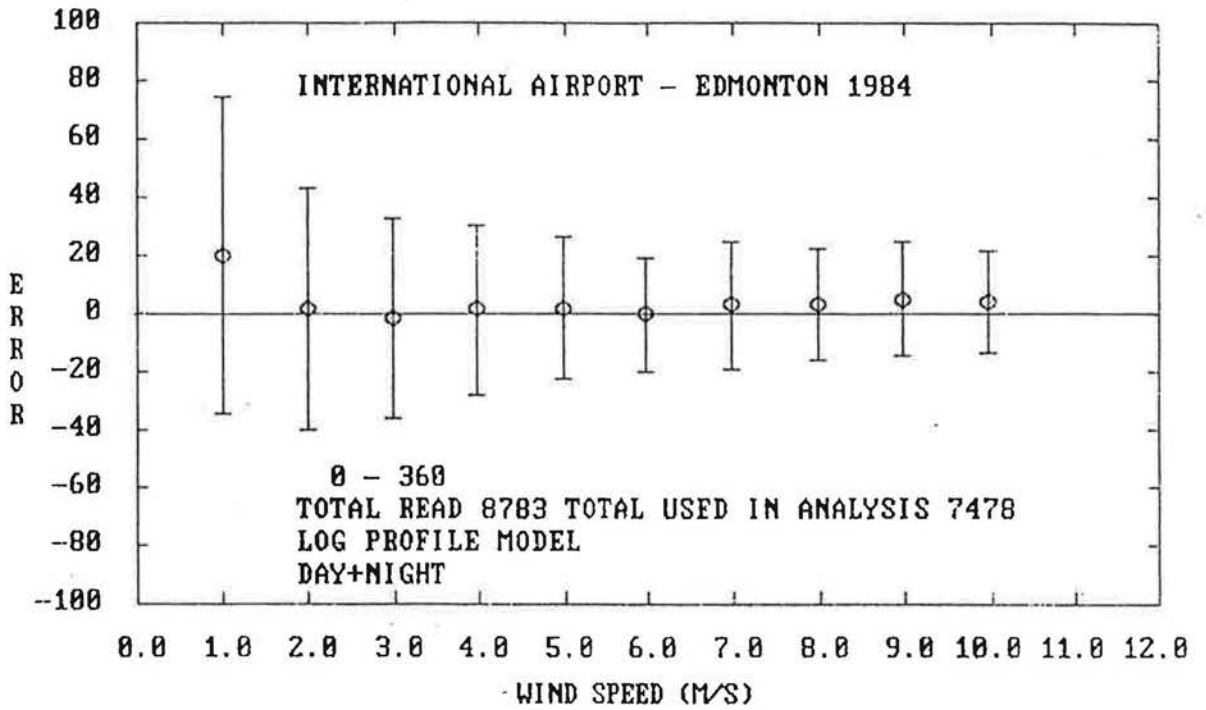


Figure A33

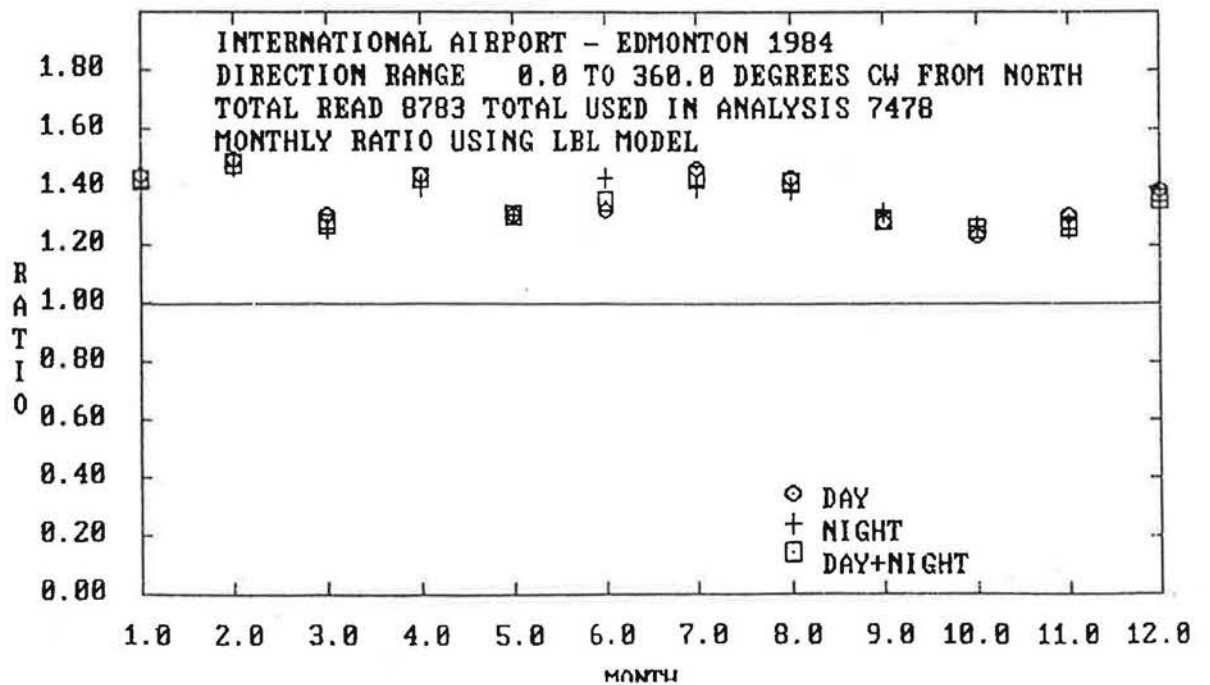


Figure A34

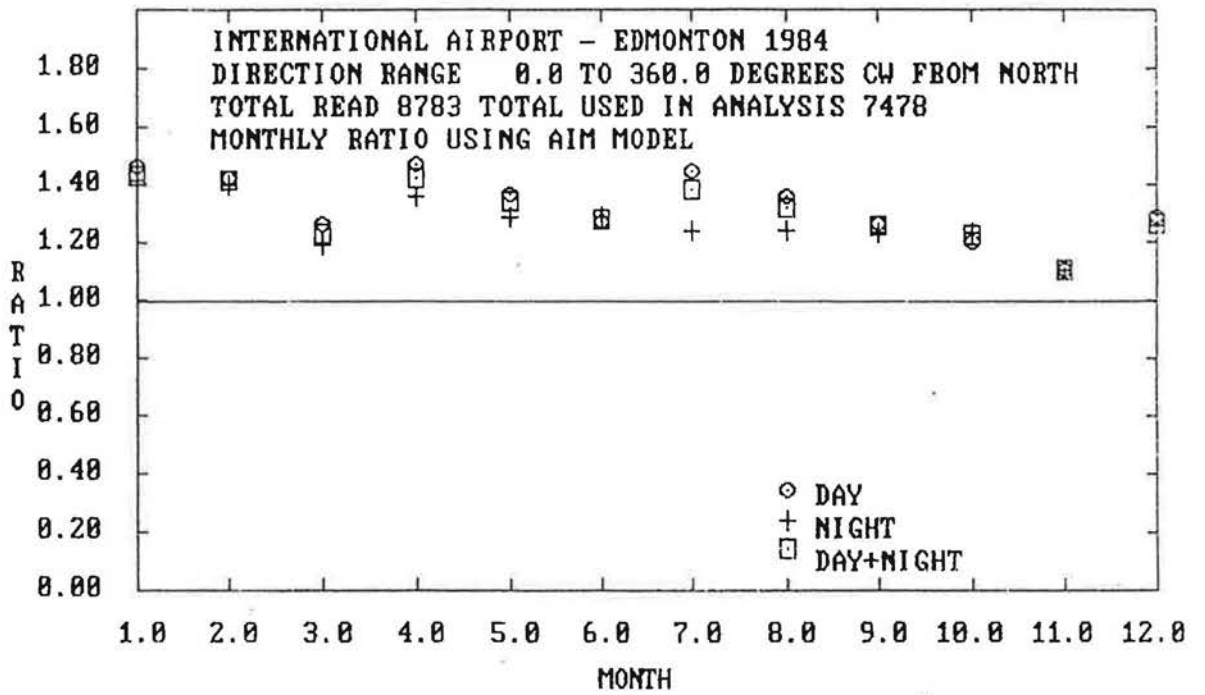


Figure A35

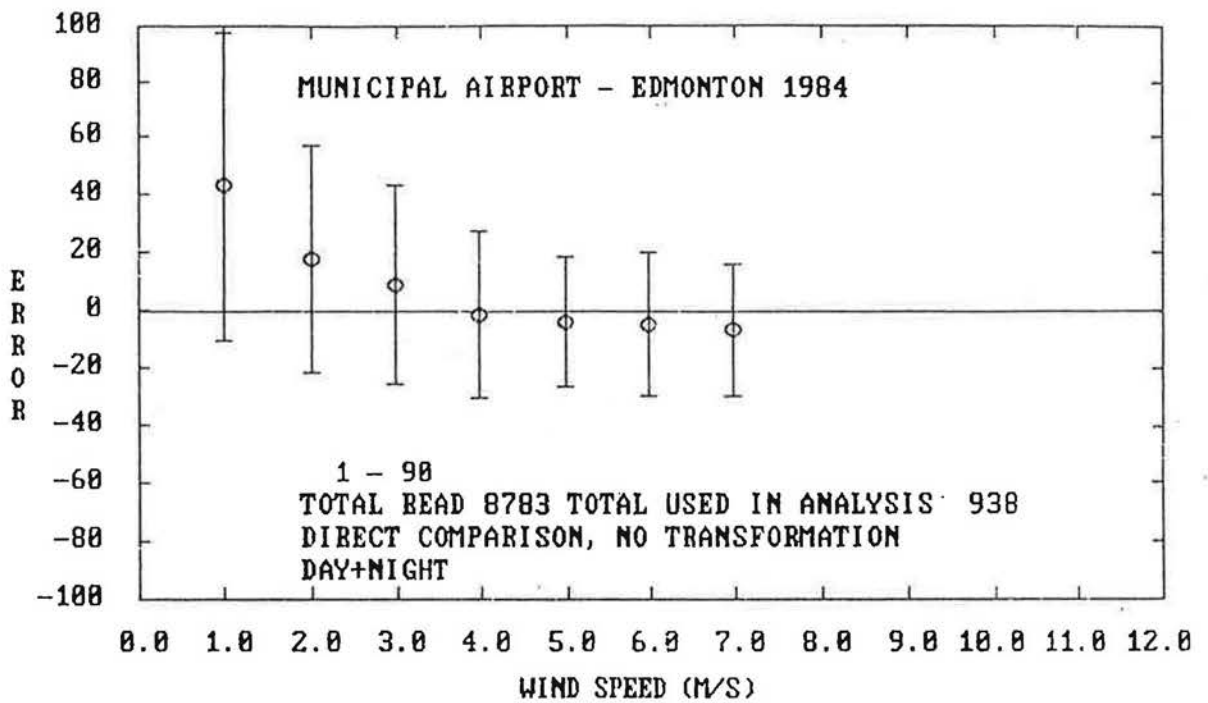


Figure A36

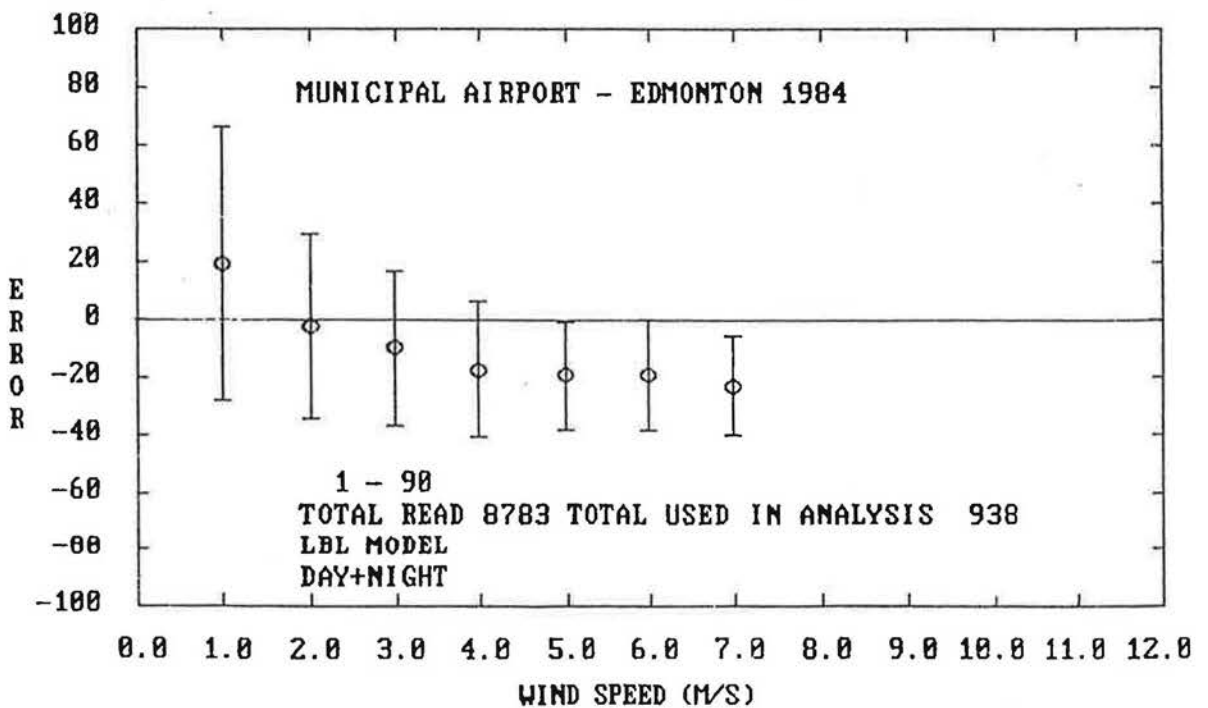


Figure A37

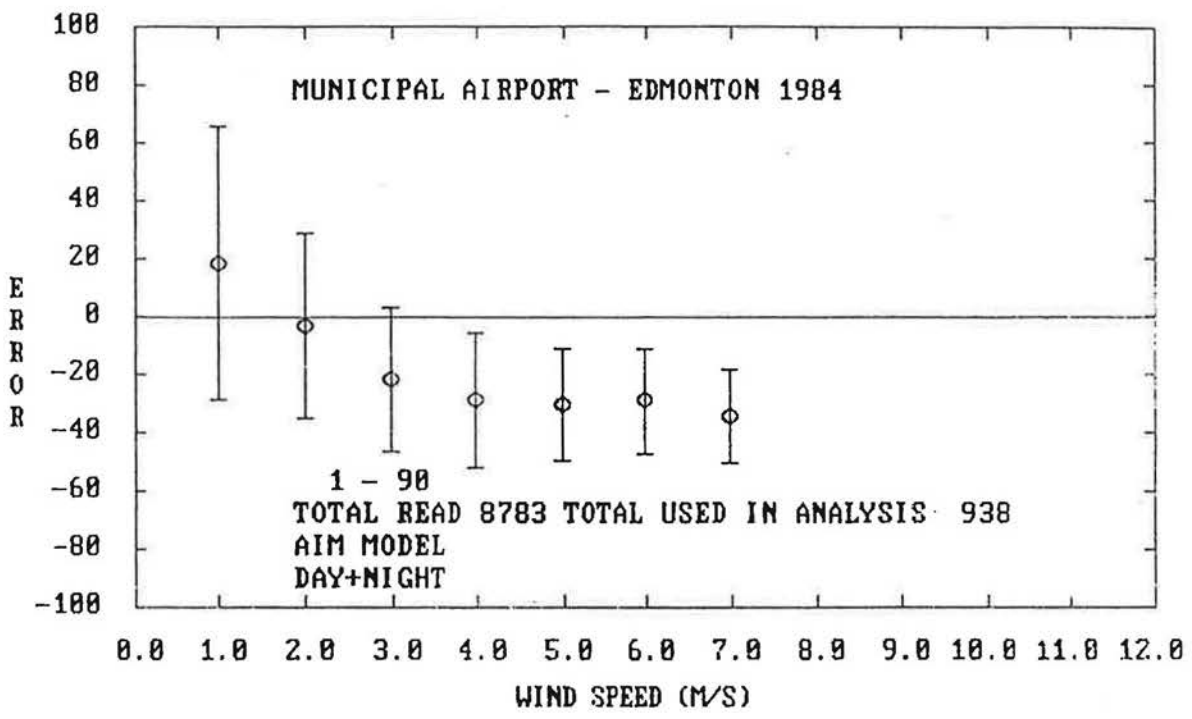


Figure A38

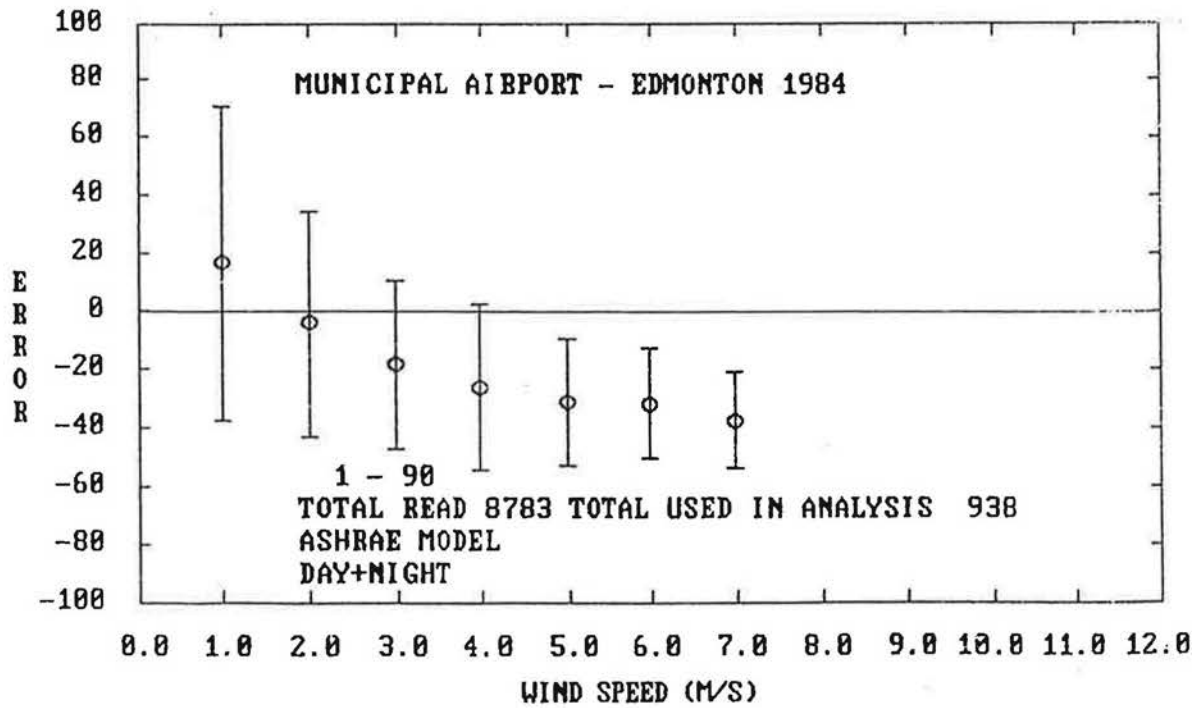


Figure A39

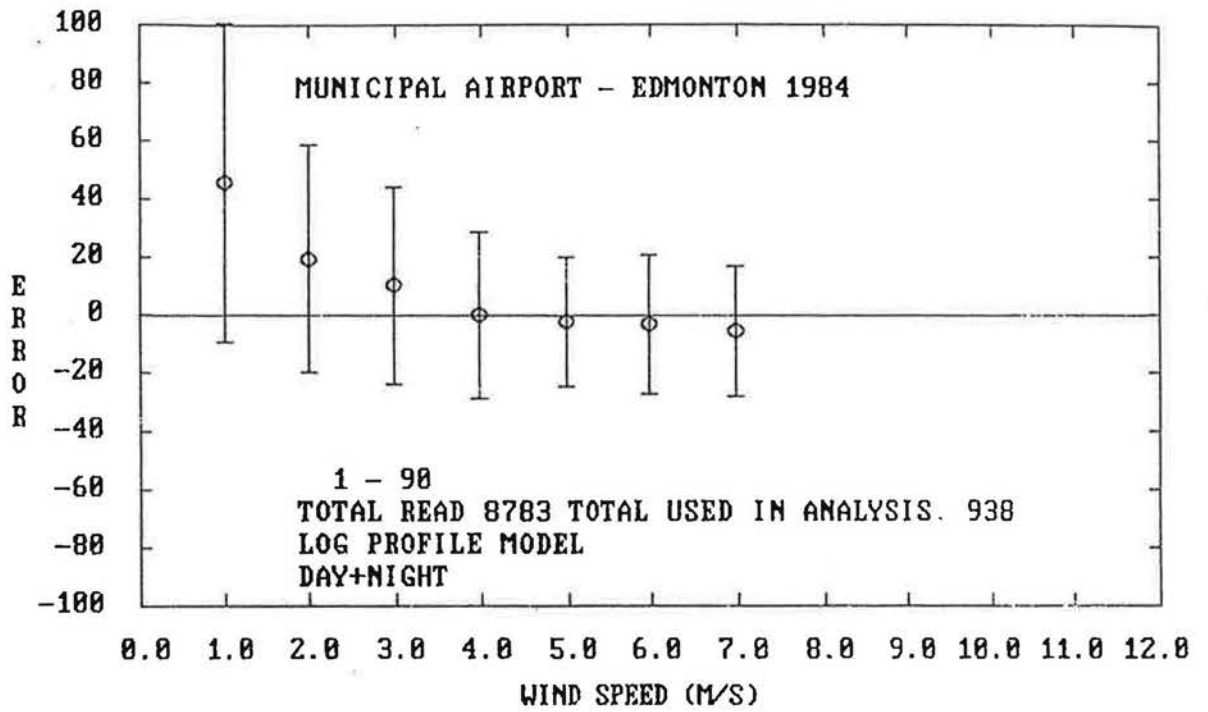


Figure A40

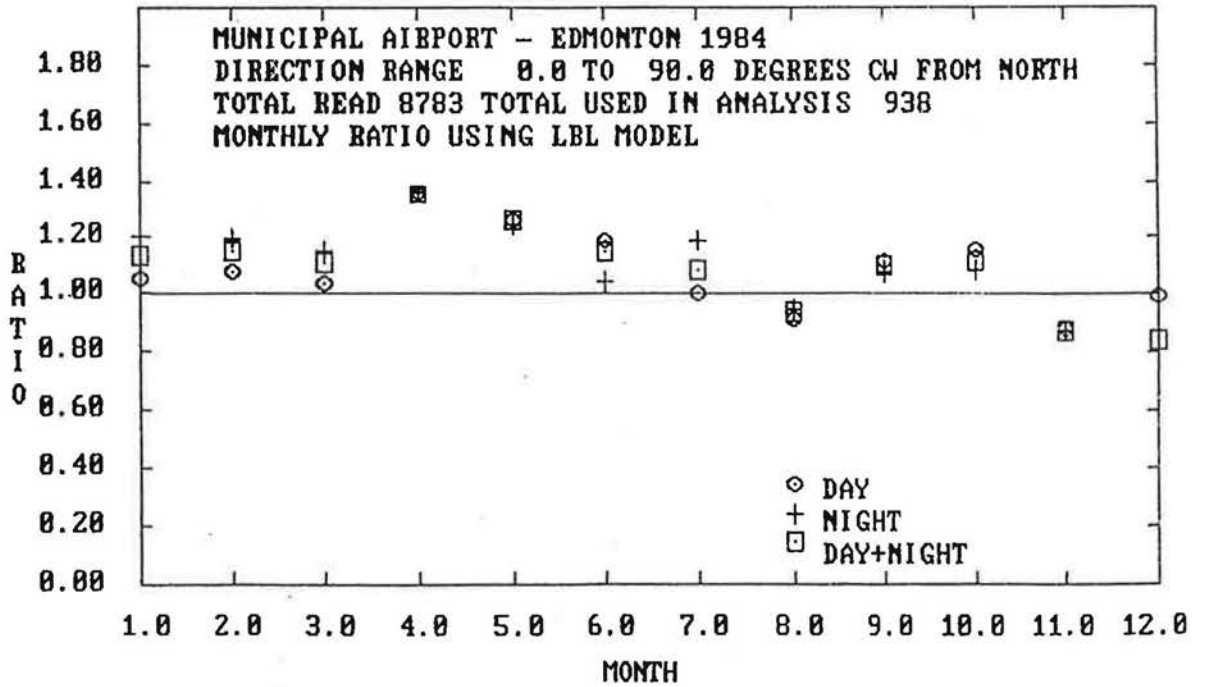


Figure A41

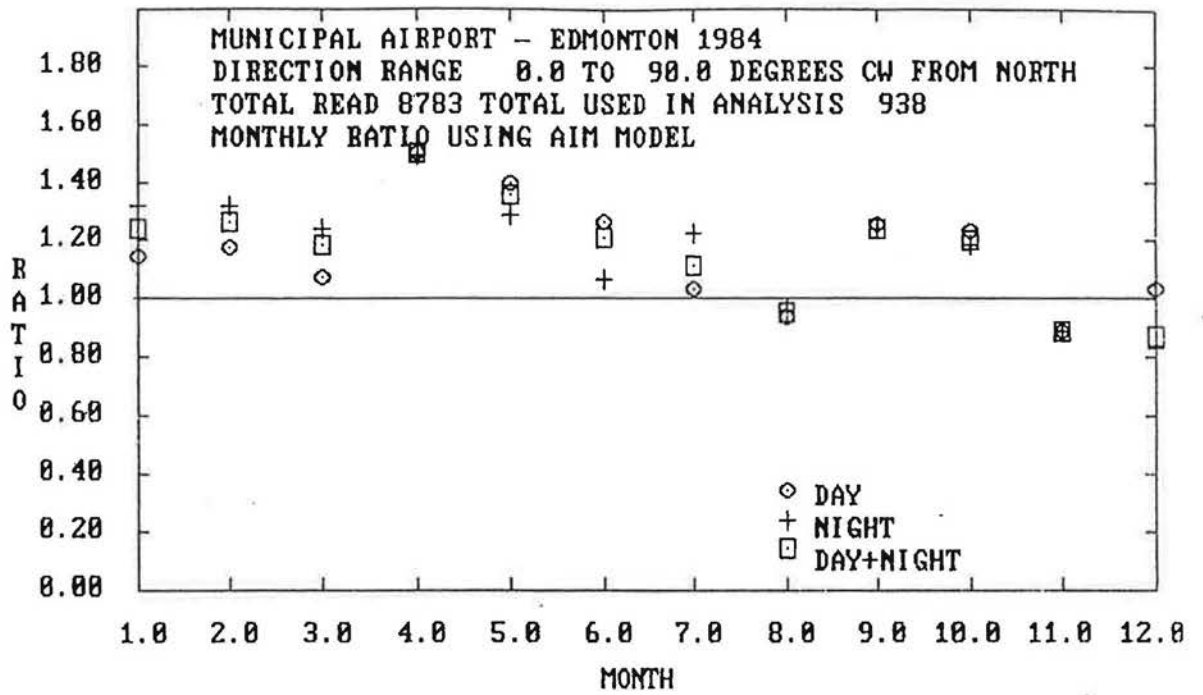


Figure A42

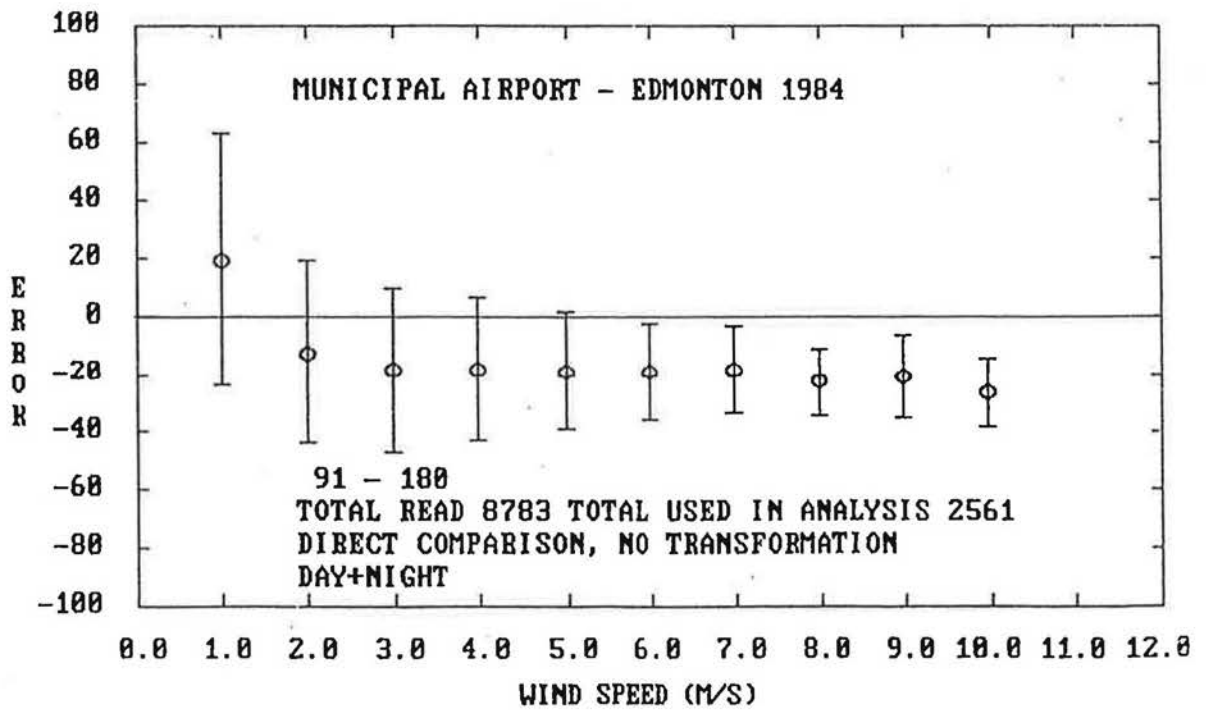


Figure A43

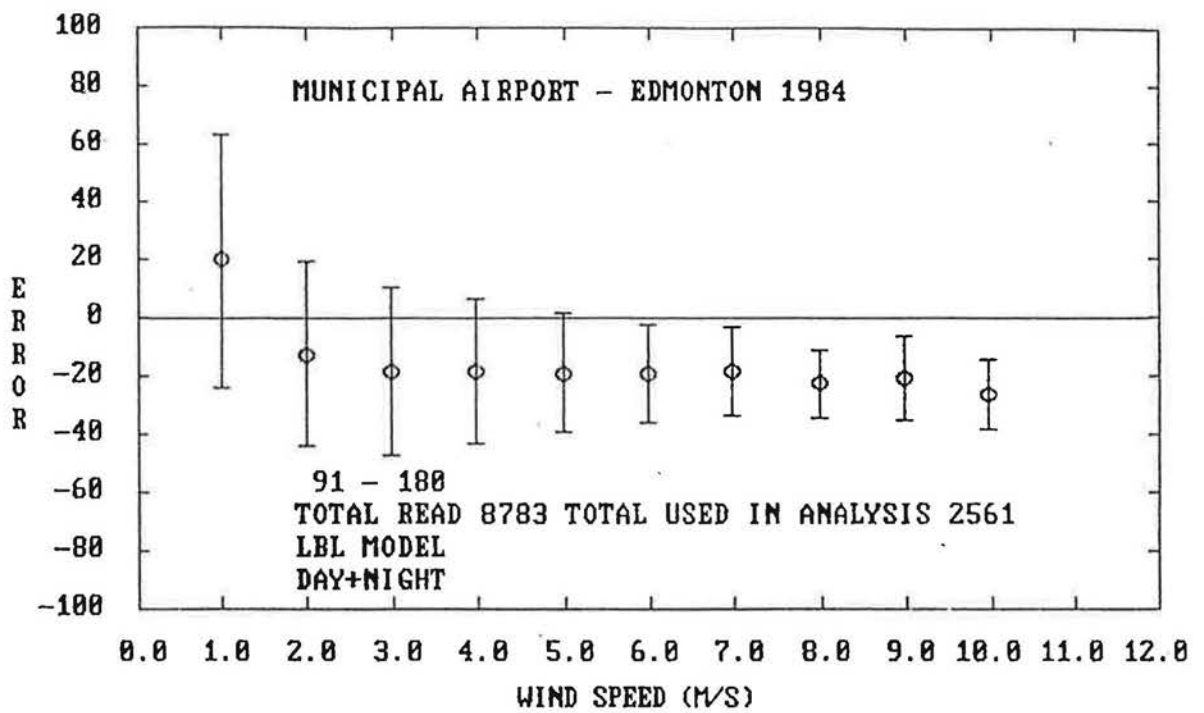


Figure A44

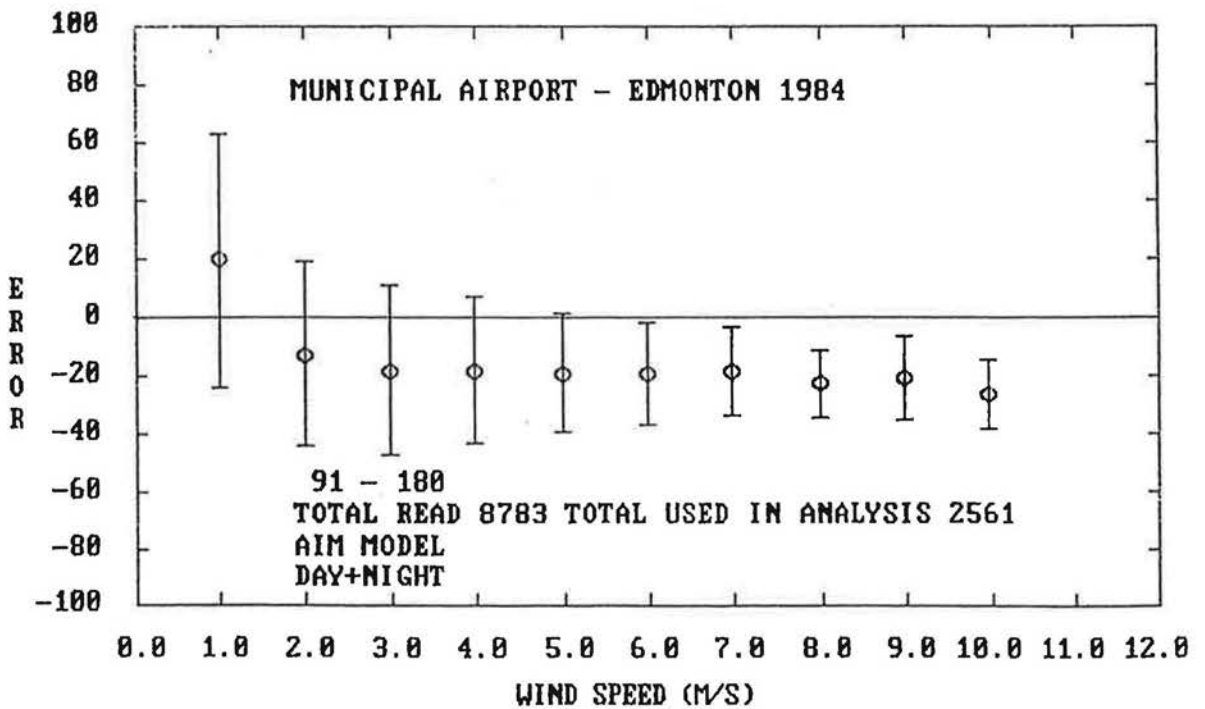


Figure A45

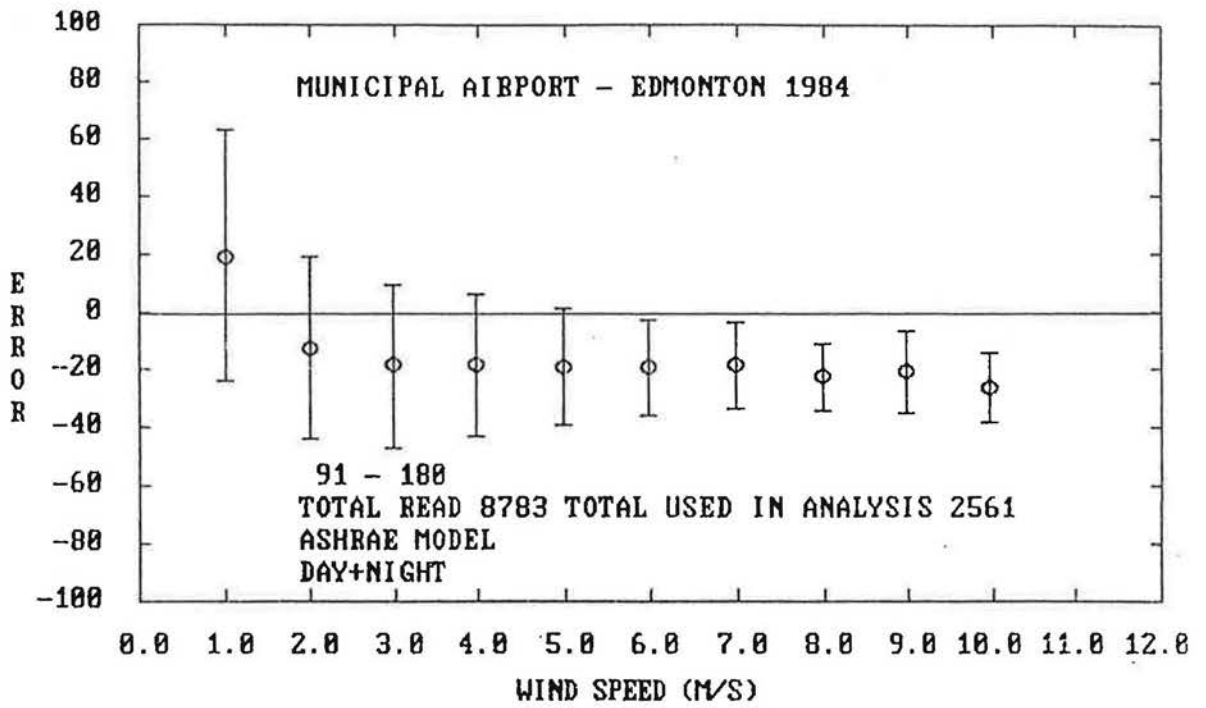


Figure A46

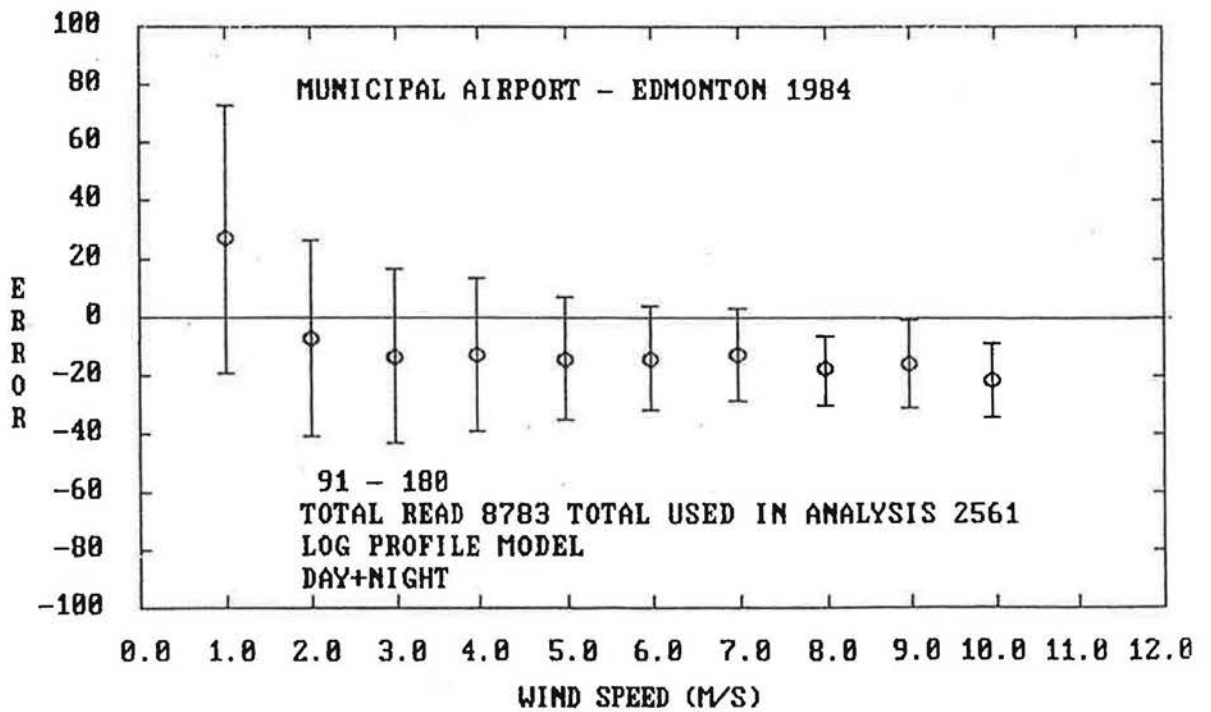


Figure A47

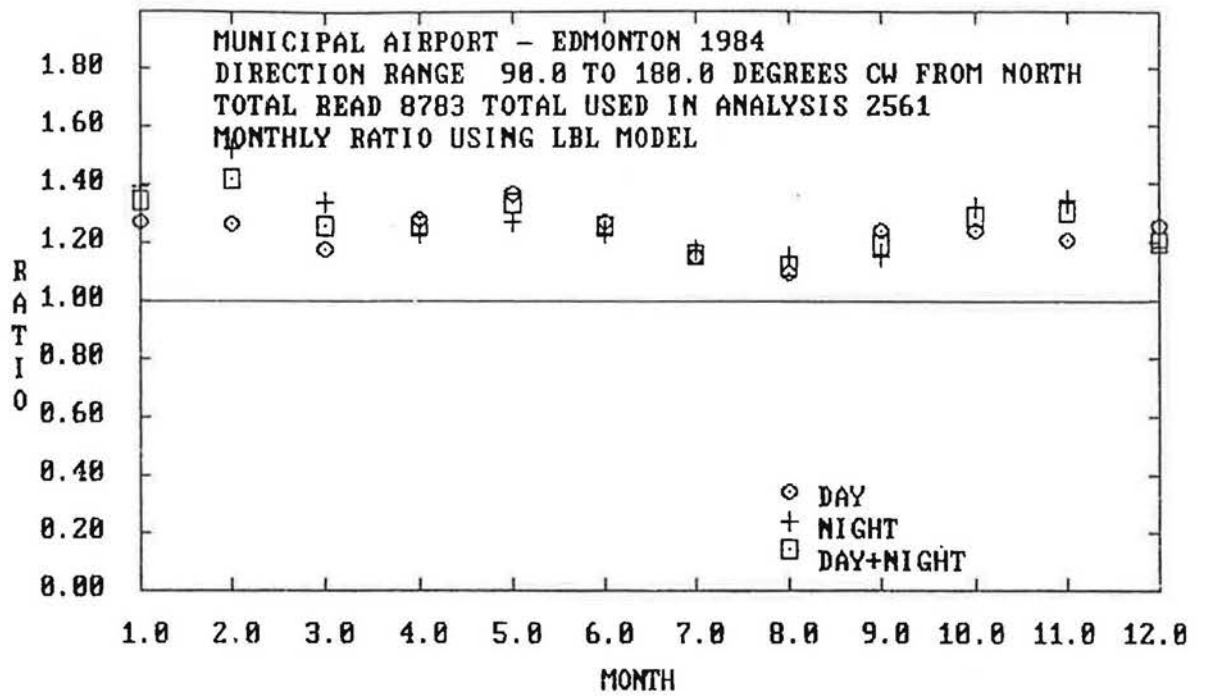


Figure A48

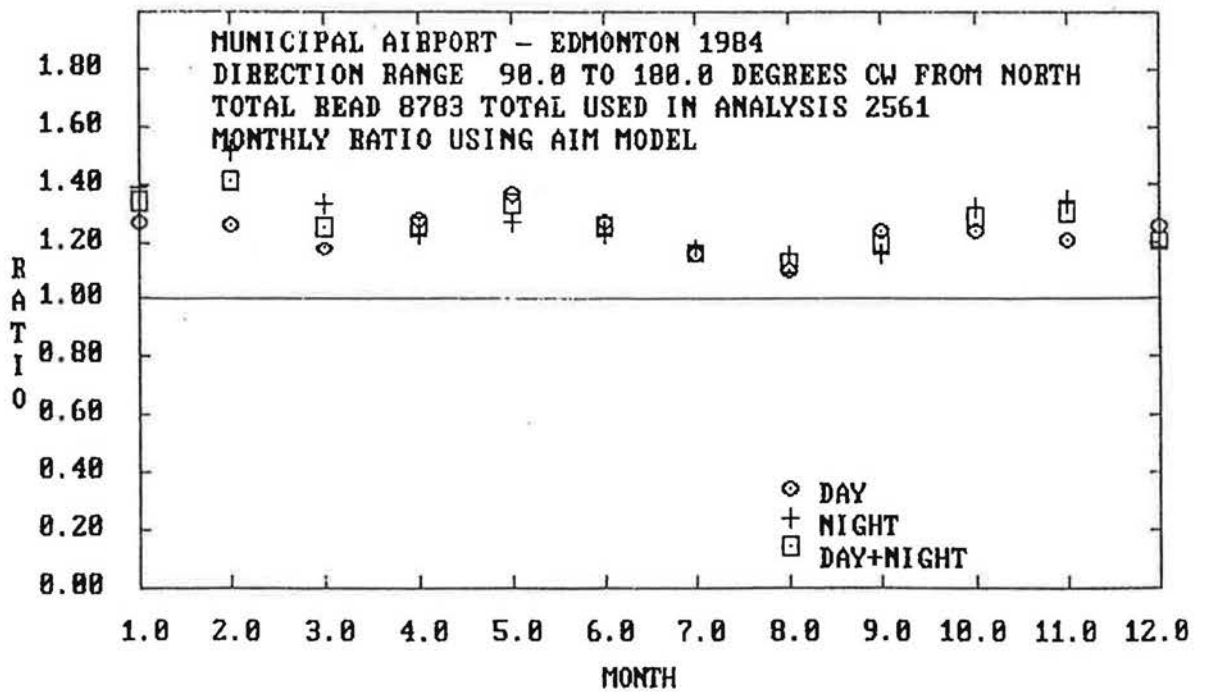


Figure A49

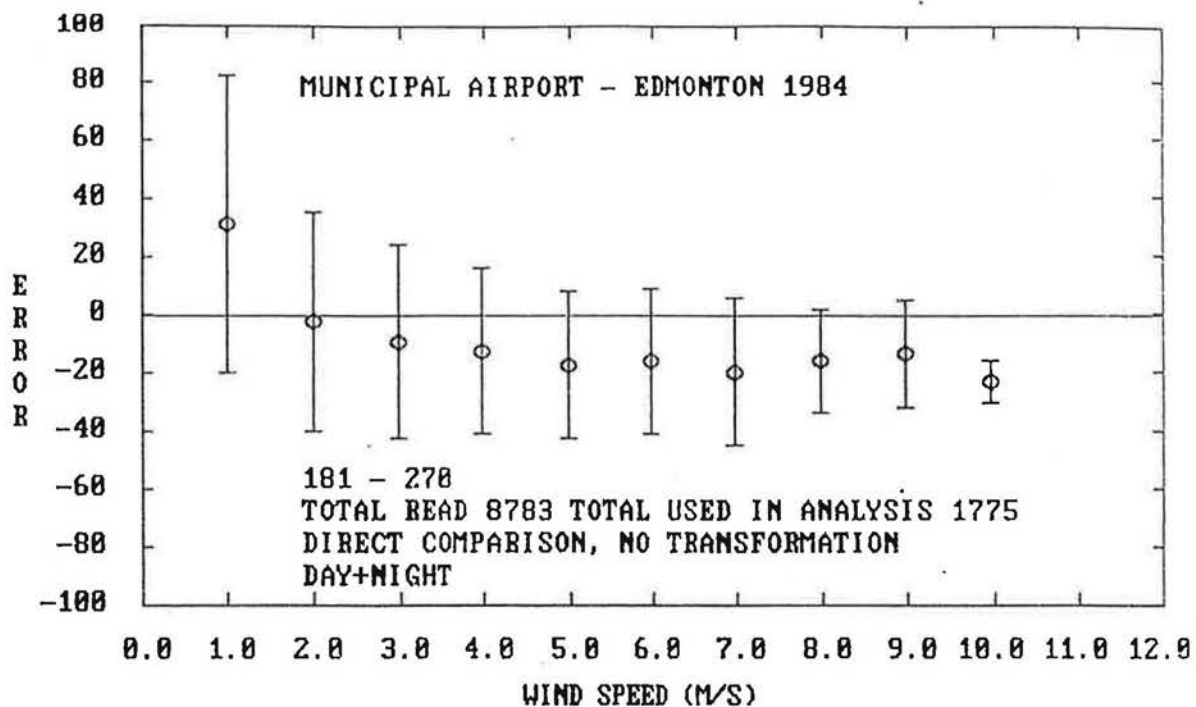


Figure A50

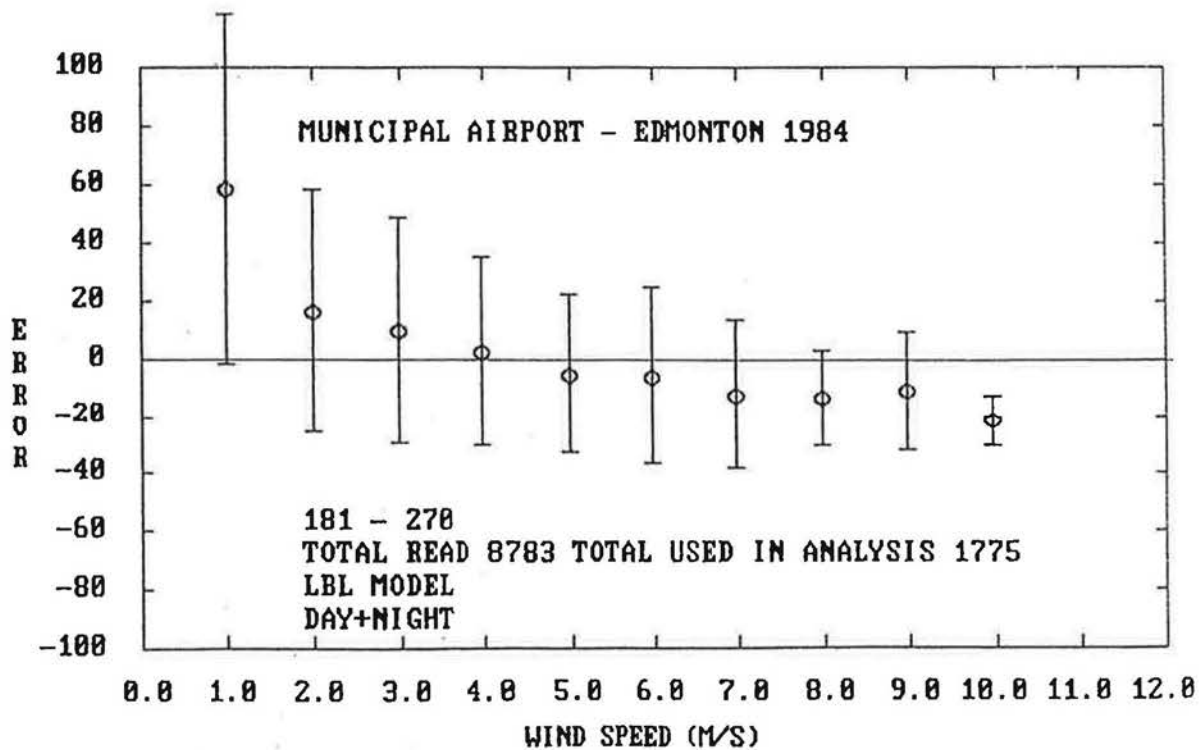


Figure A51

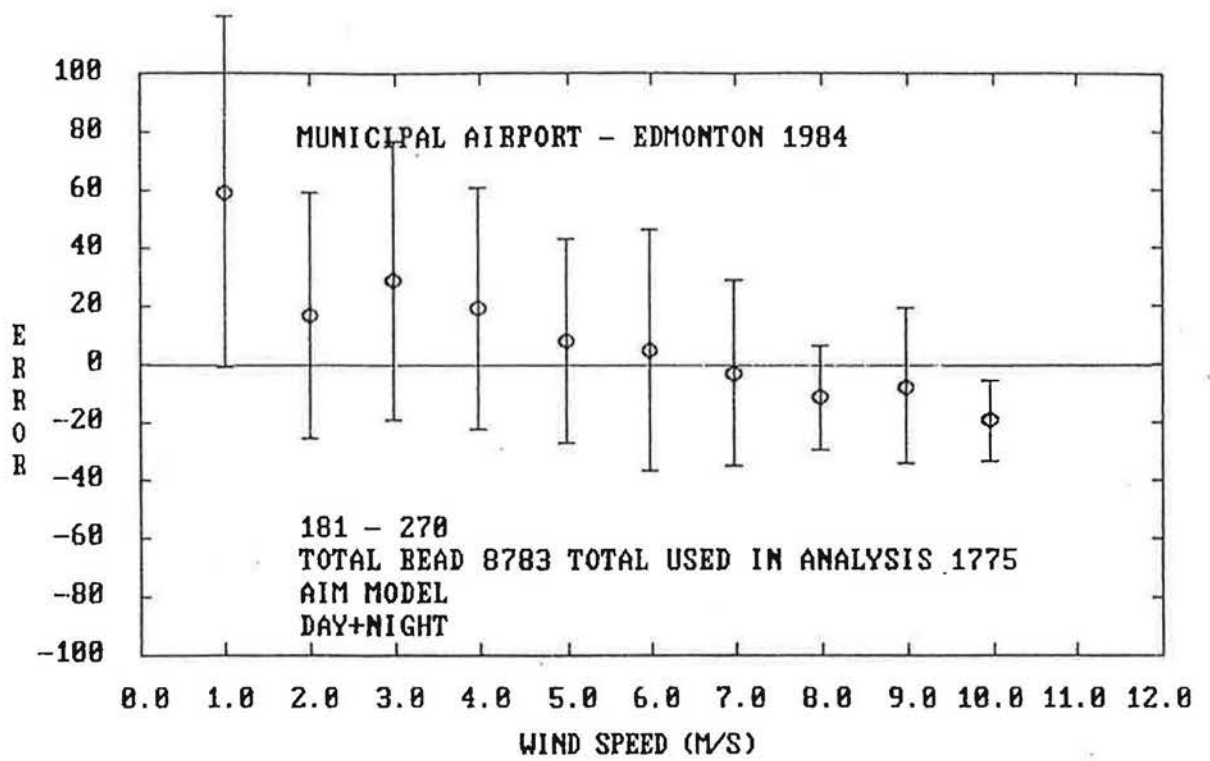


Figure A52

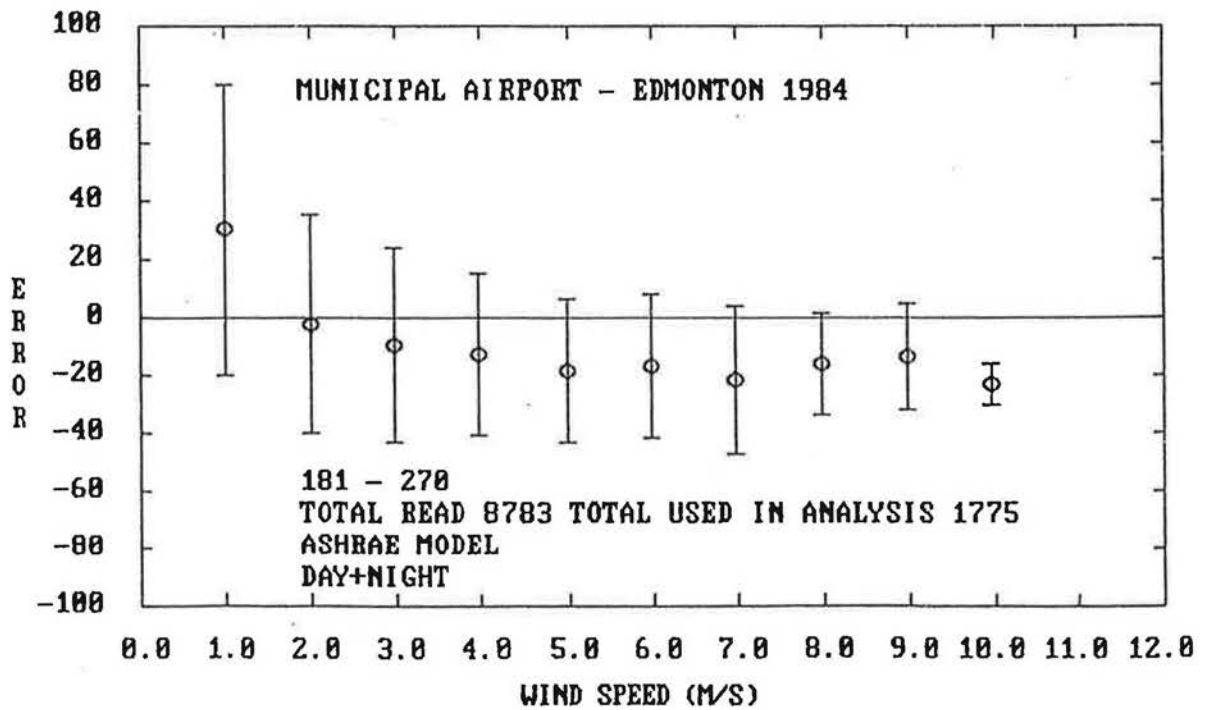


Figure A53

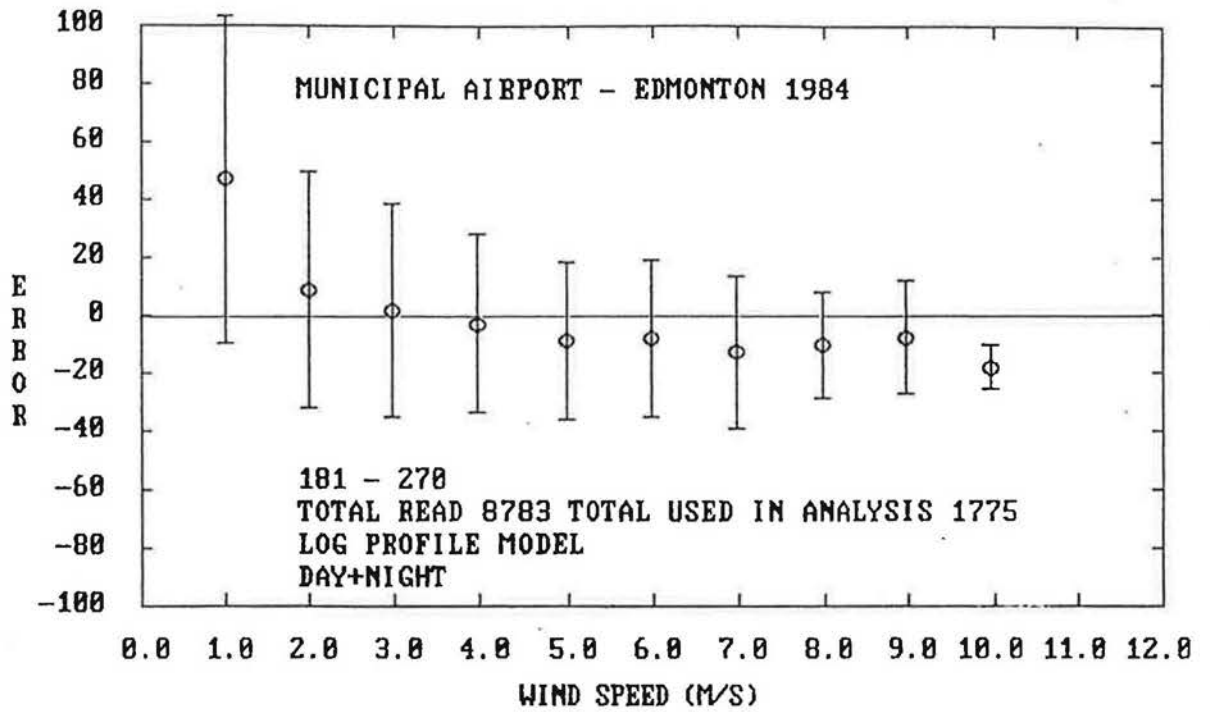


Figure A54

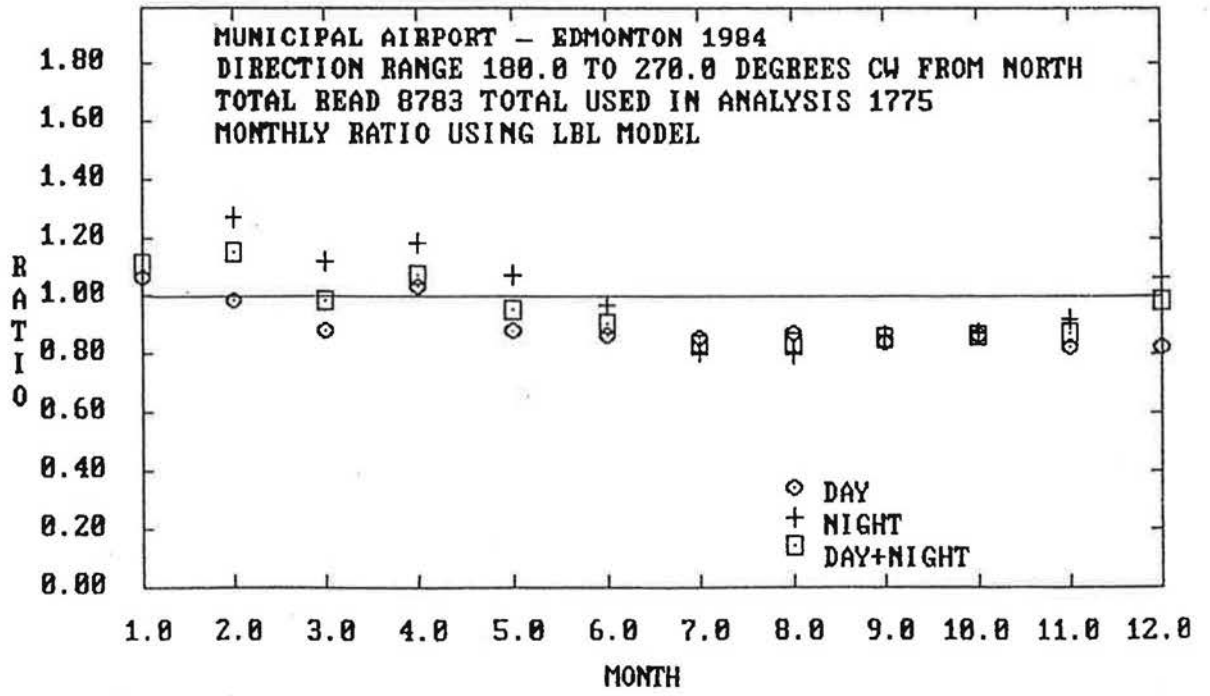


Figure A55

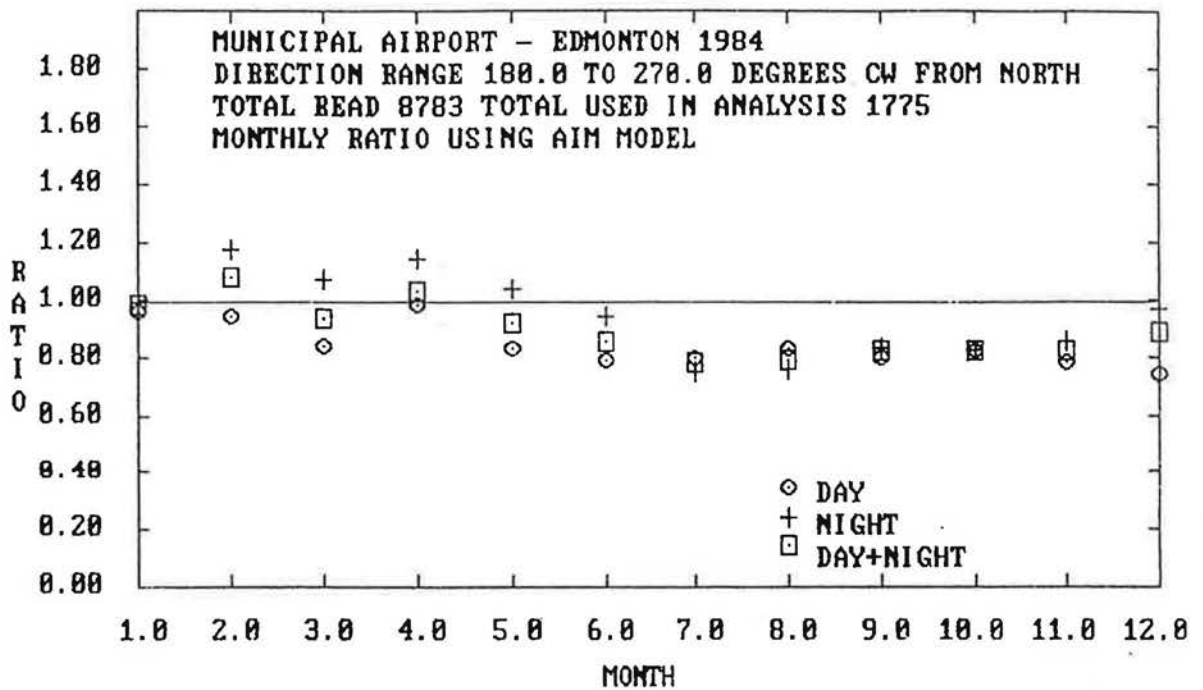


Figure A56

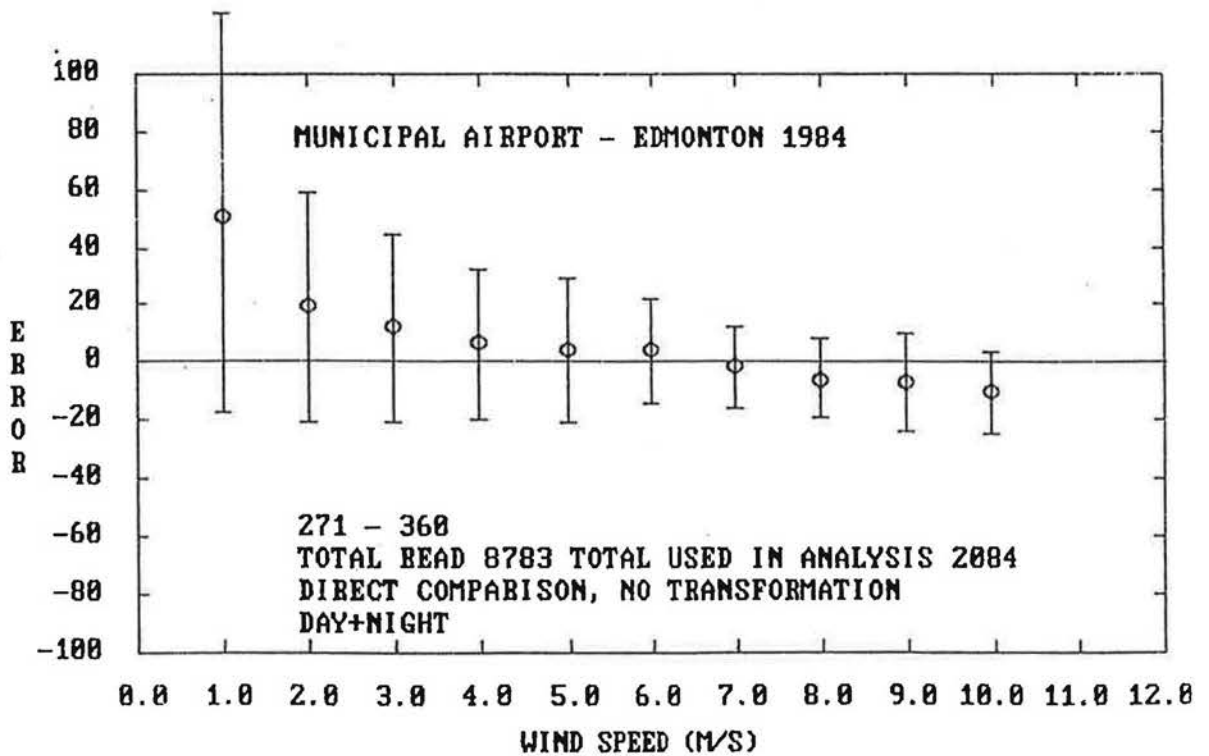


Figure A57

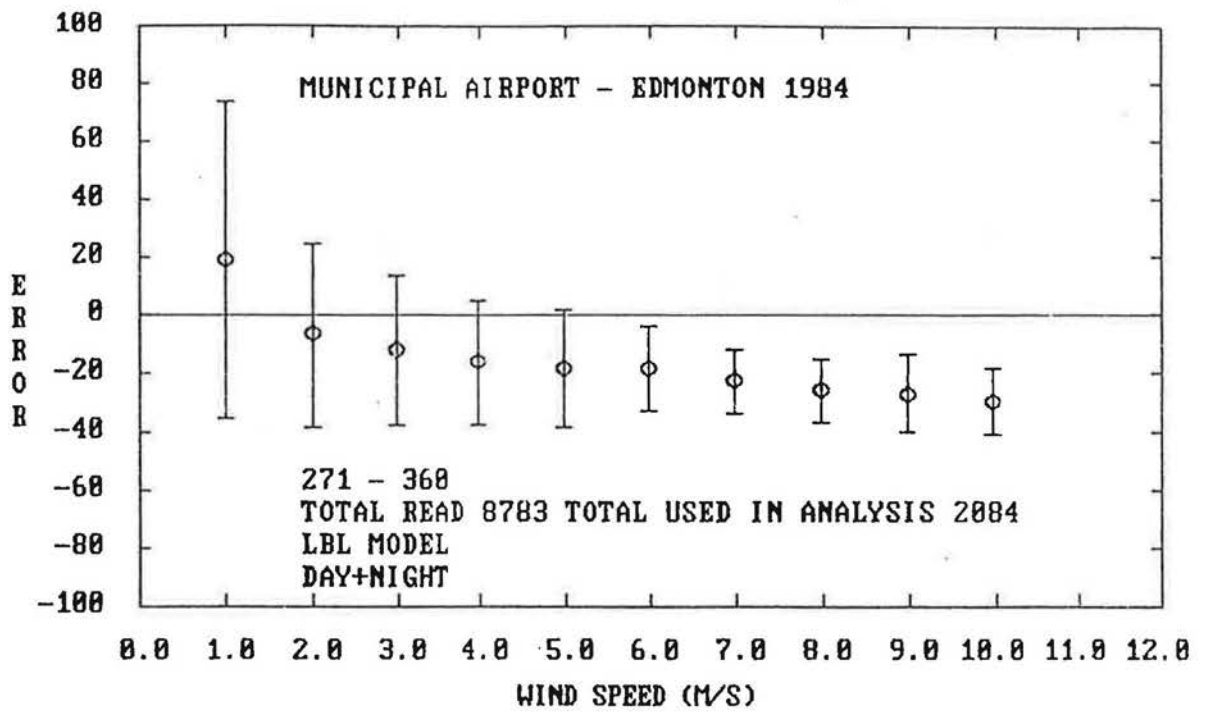


Figure A58

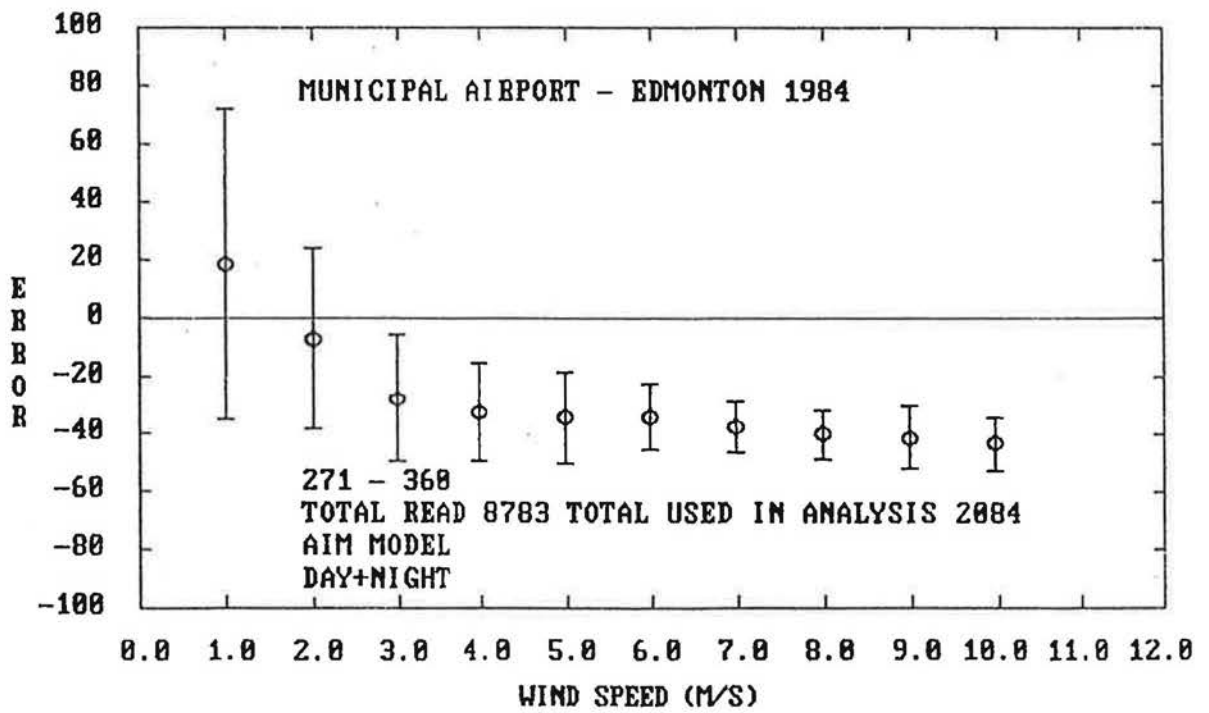


Figure A59

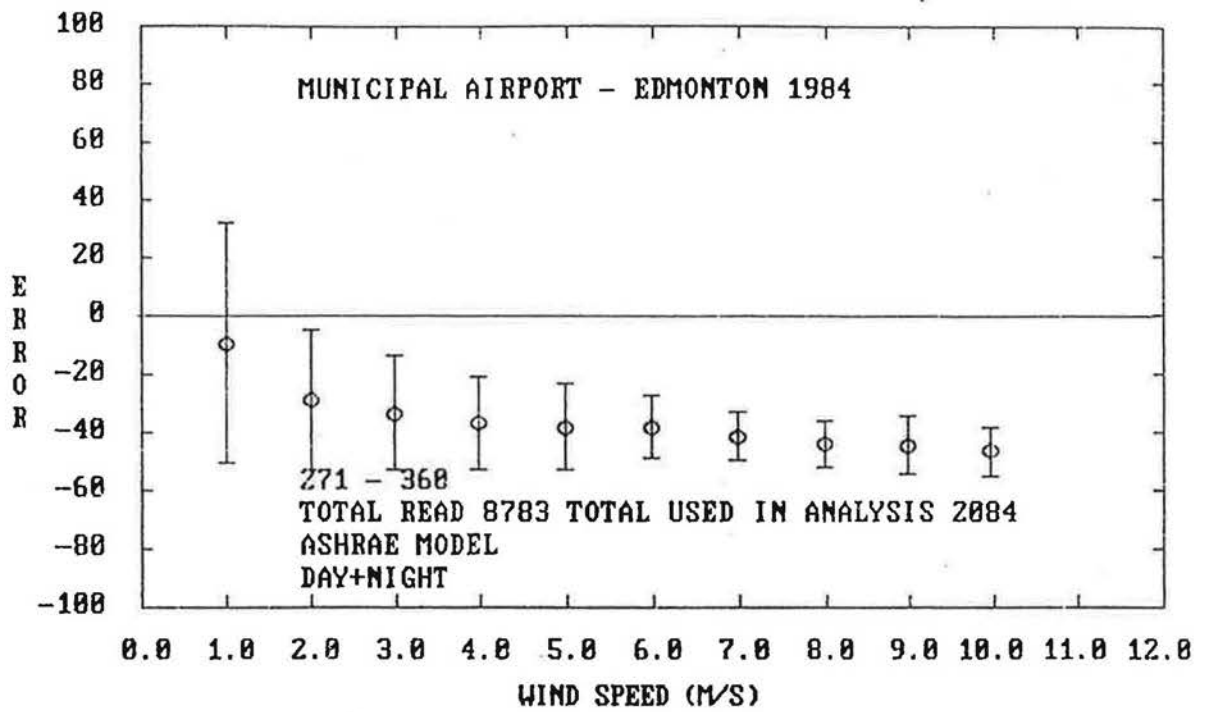


Figure A60

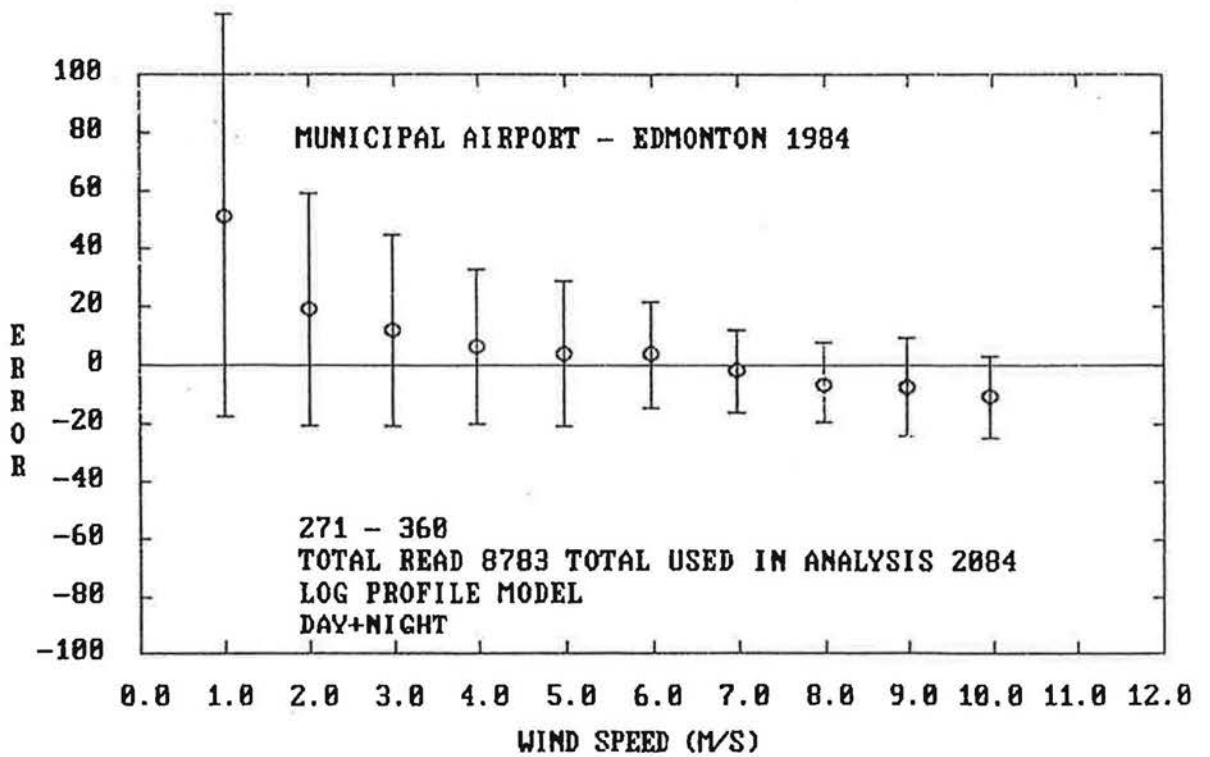


Figure A61

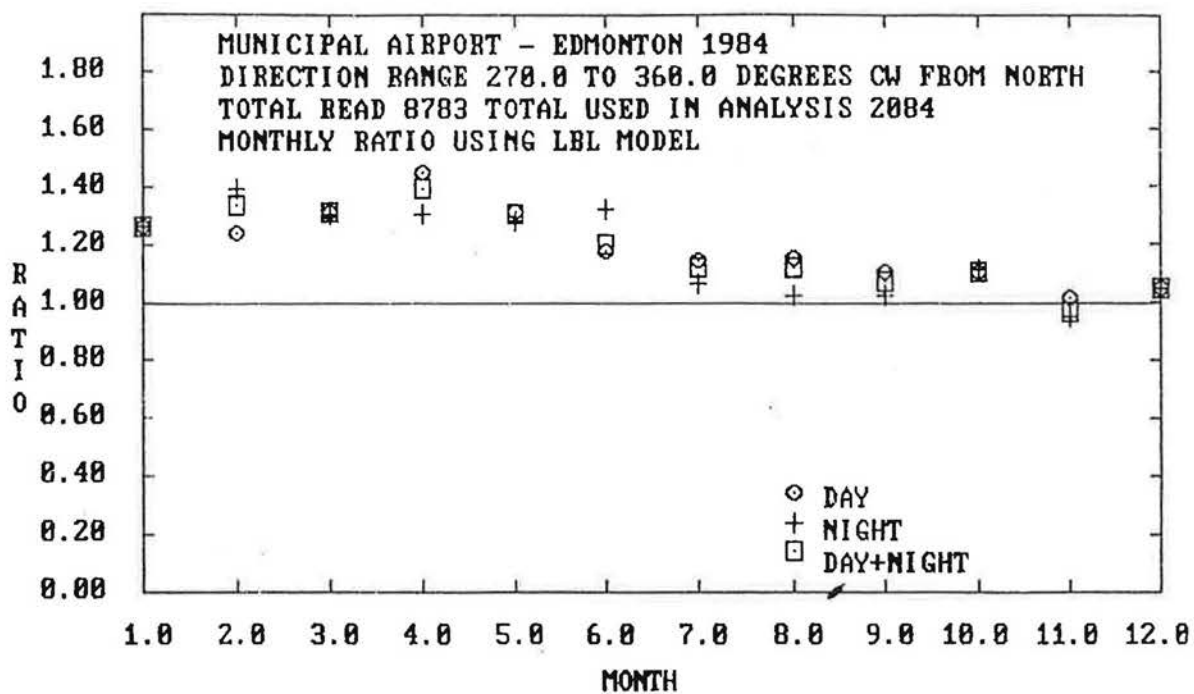


Figure A62

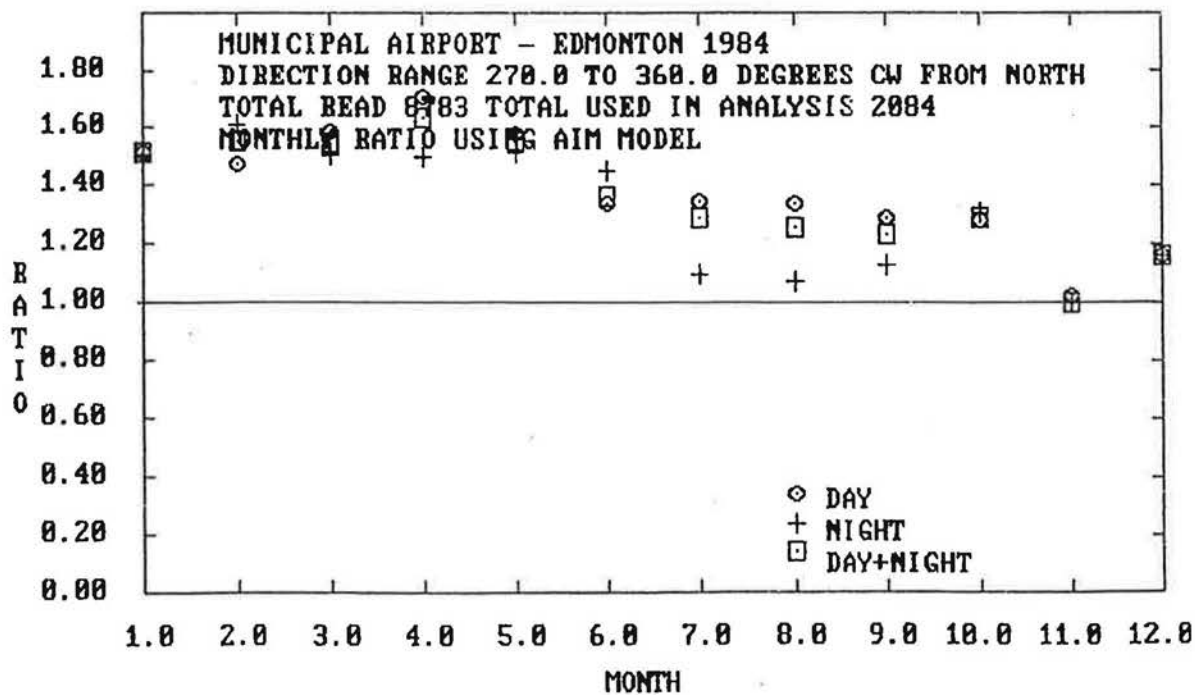


Figure A63

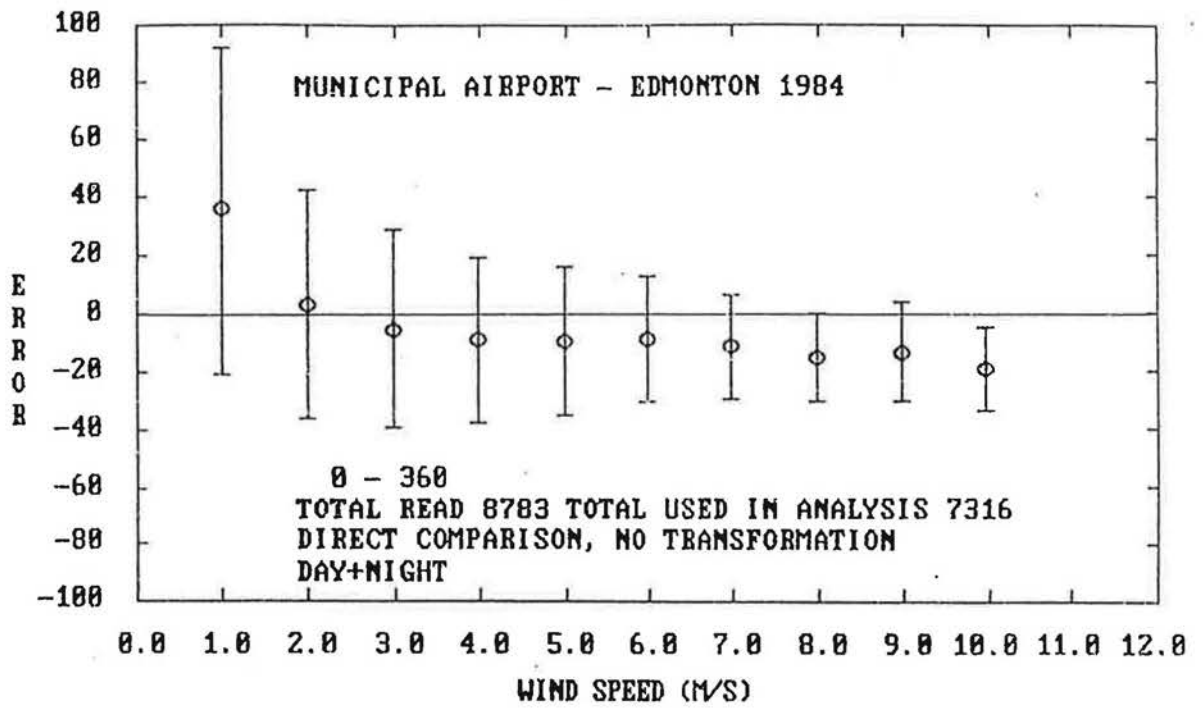


Figure A64

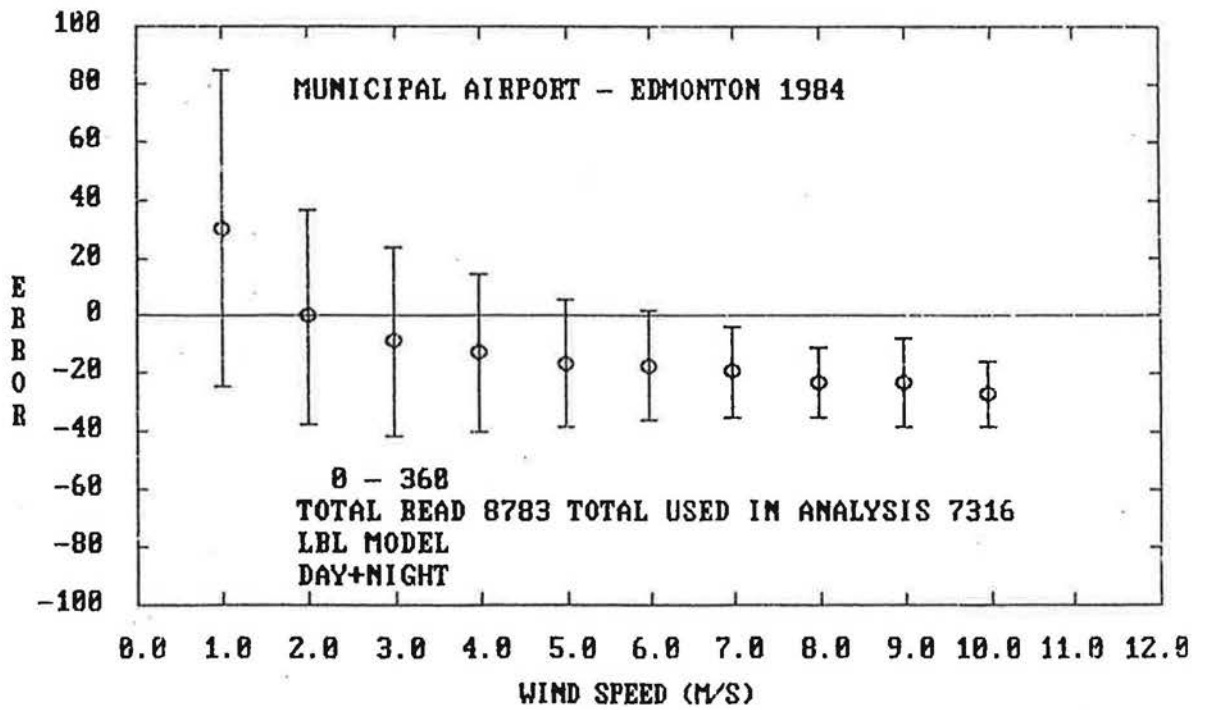


Figure A65

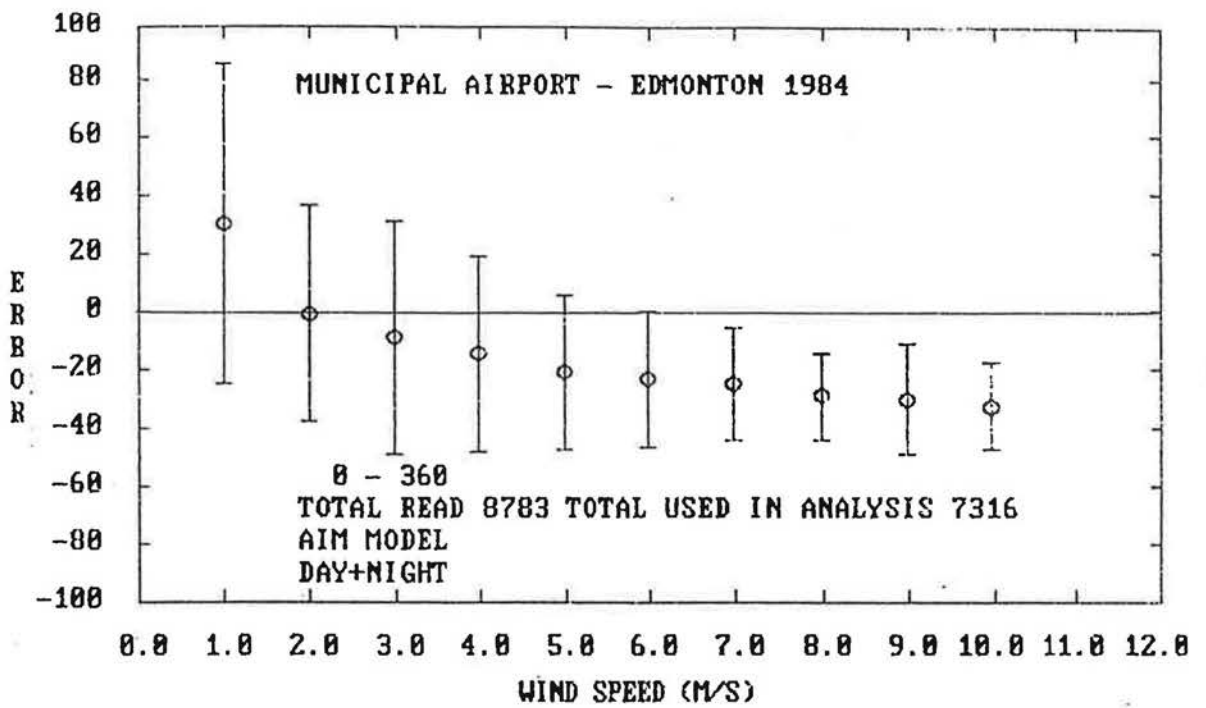


Figure A66

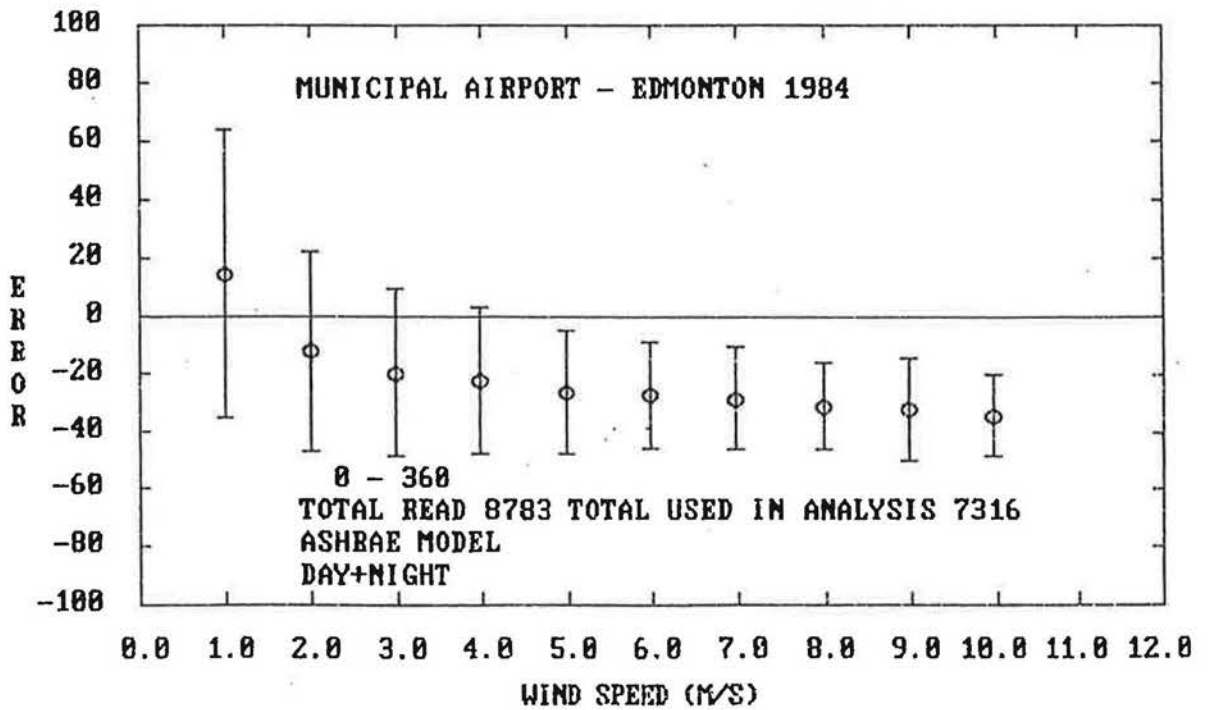


Figure A67

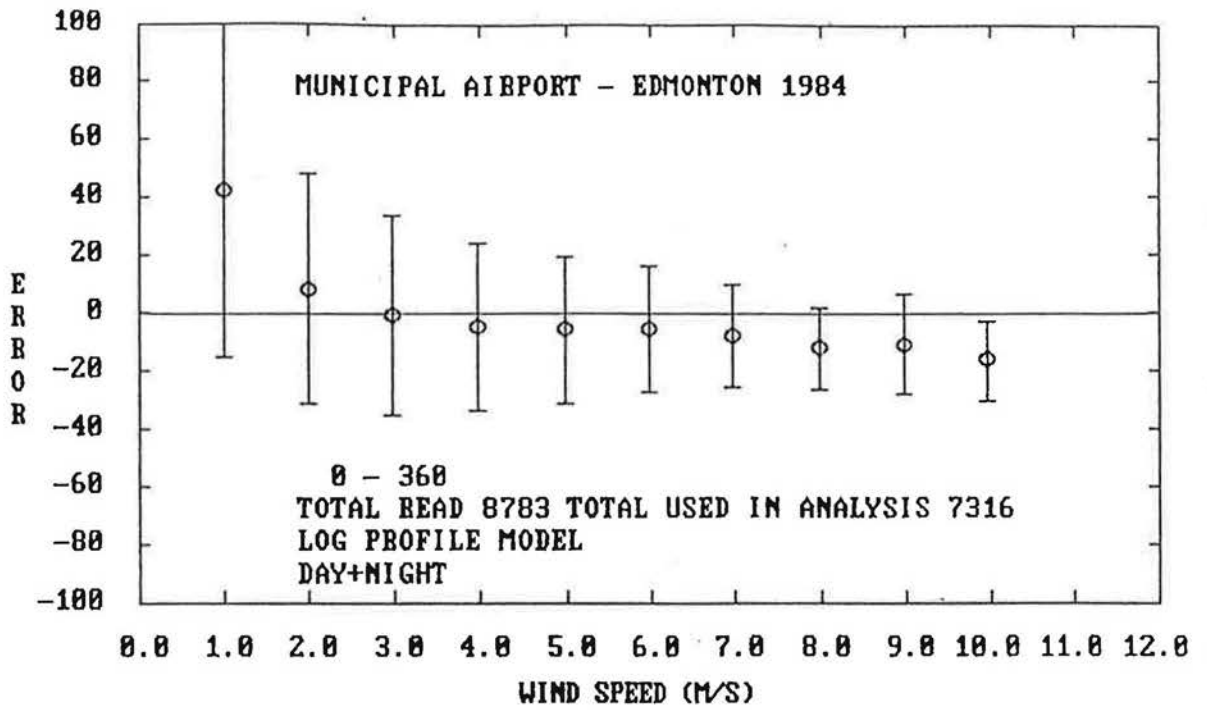


Figure A68

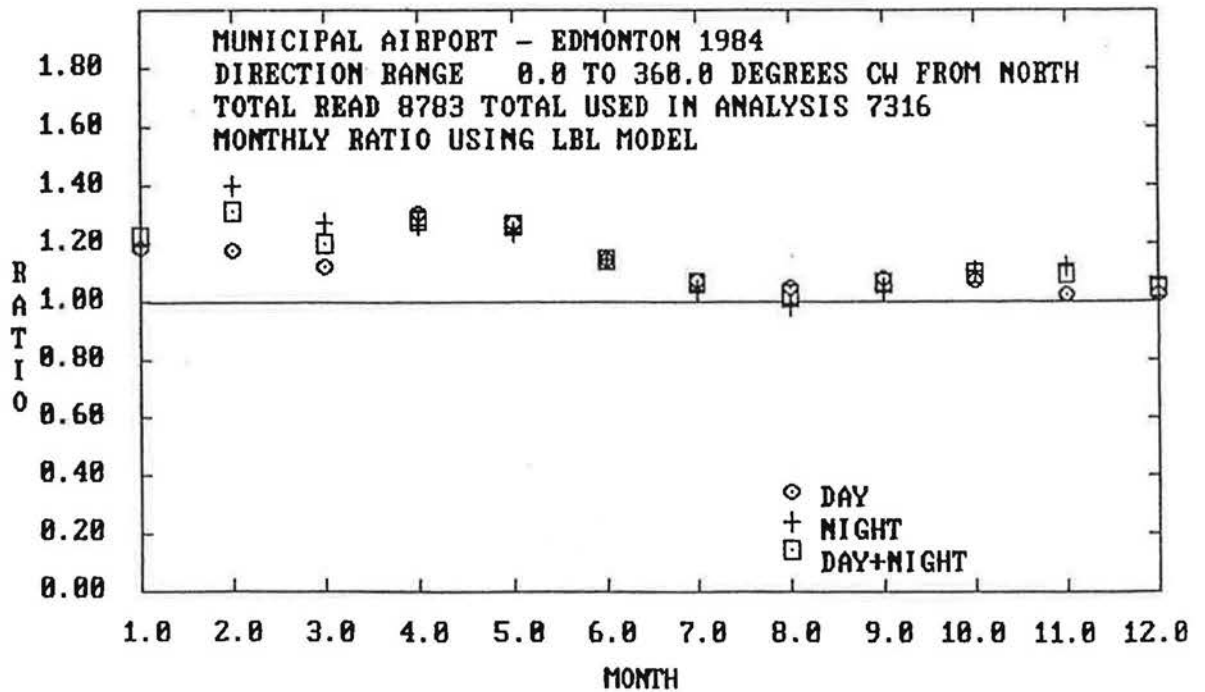


Figure A69

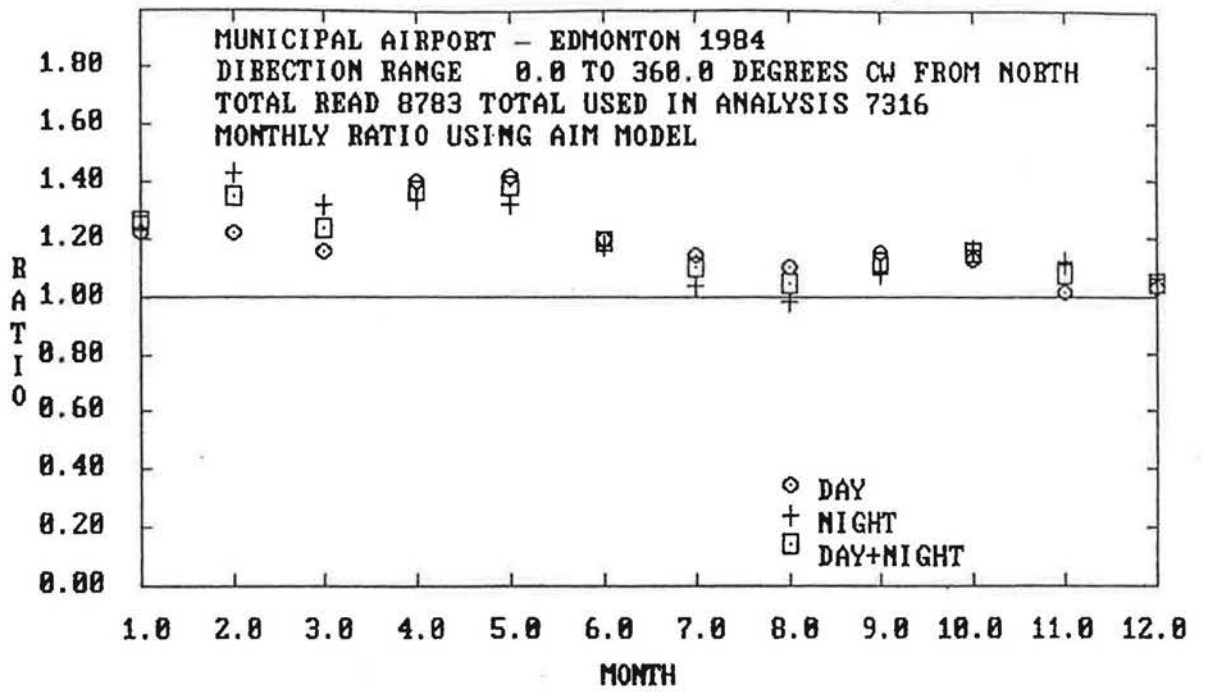


Figure A70

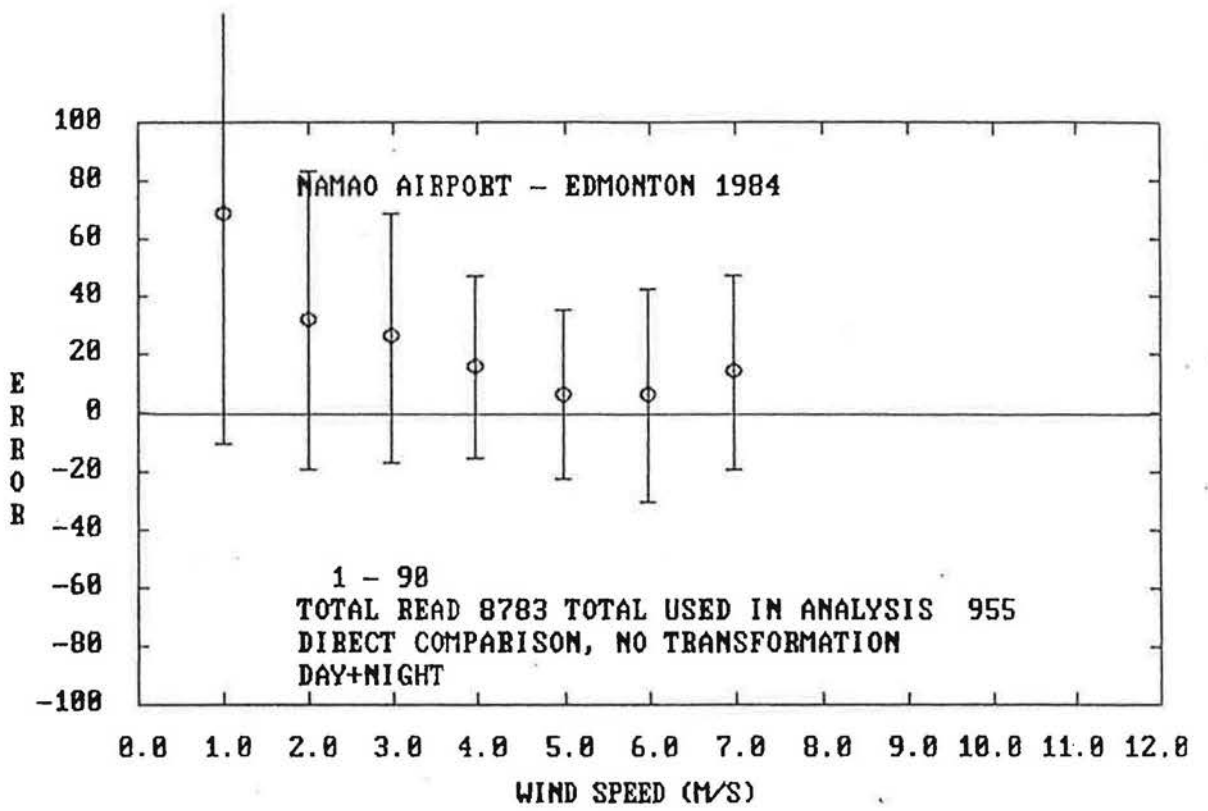


Figure A71

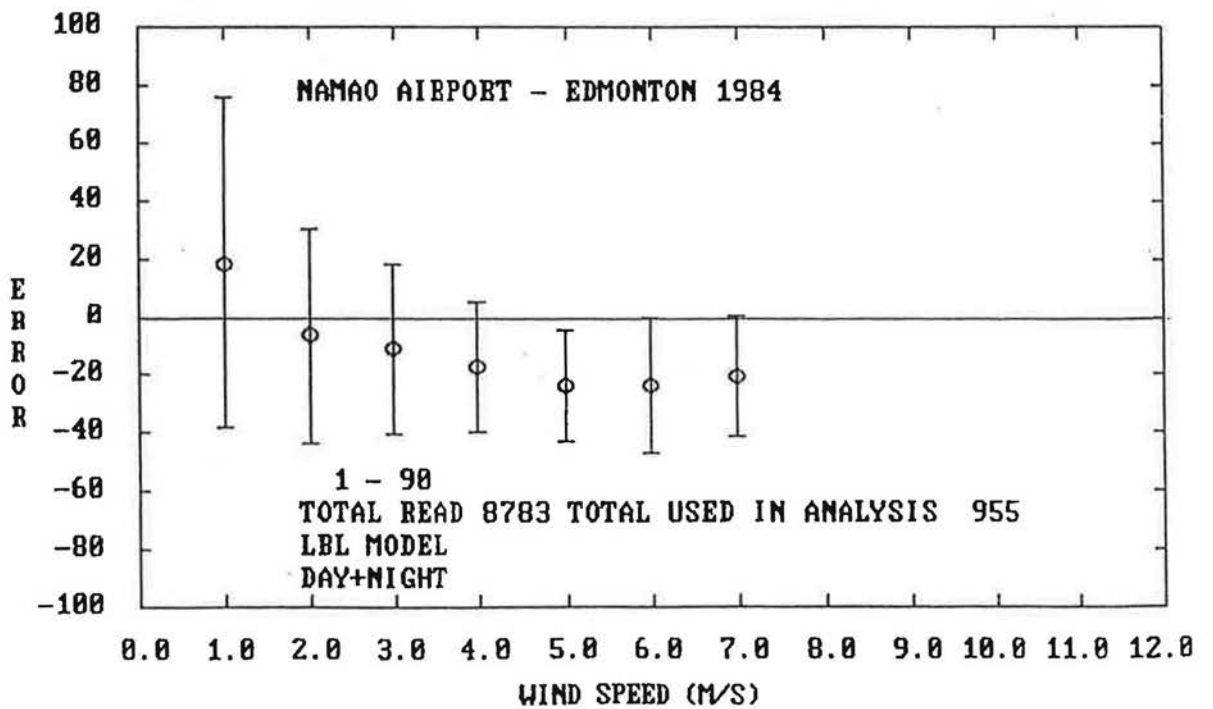


Figure A72

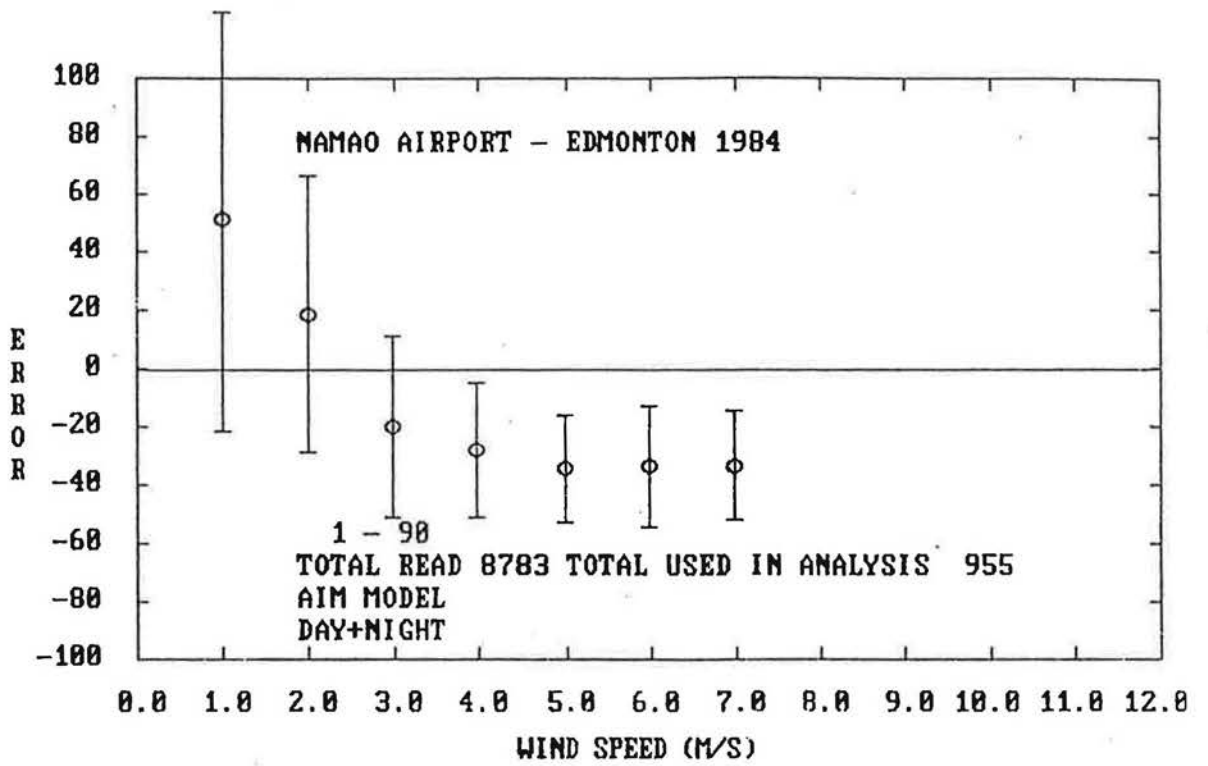


Figure A73

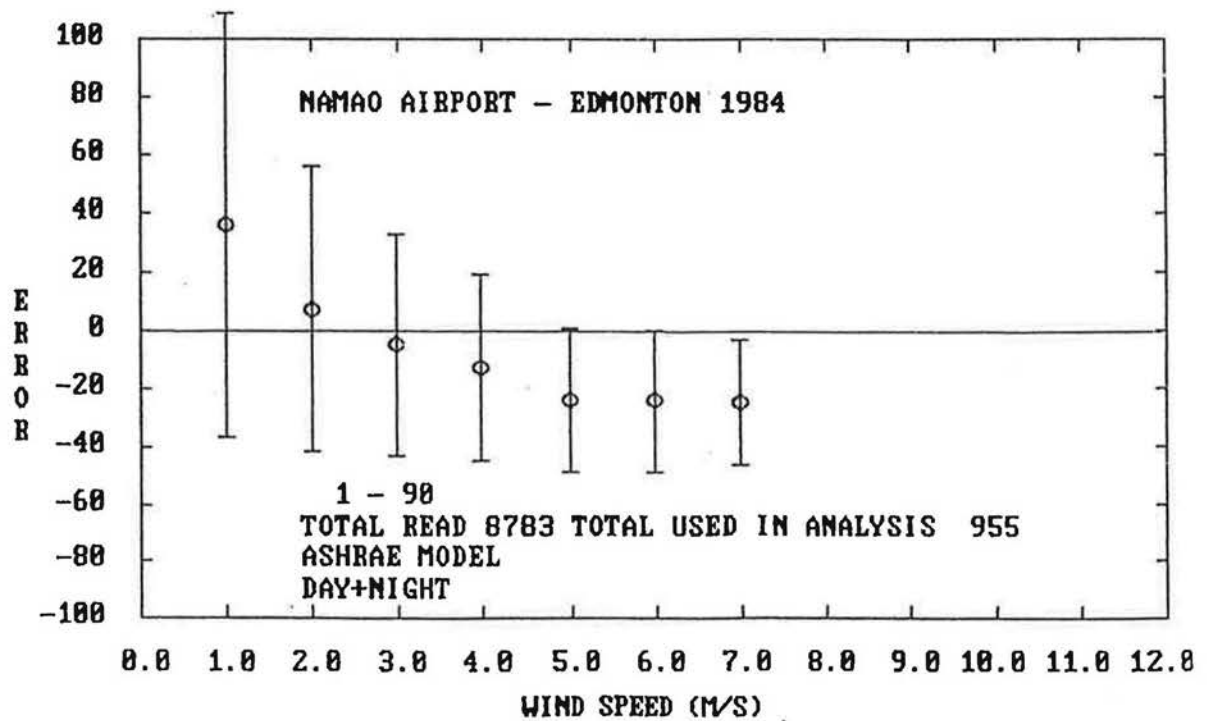


Figure A74

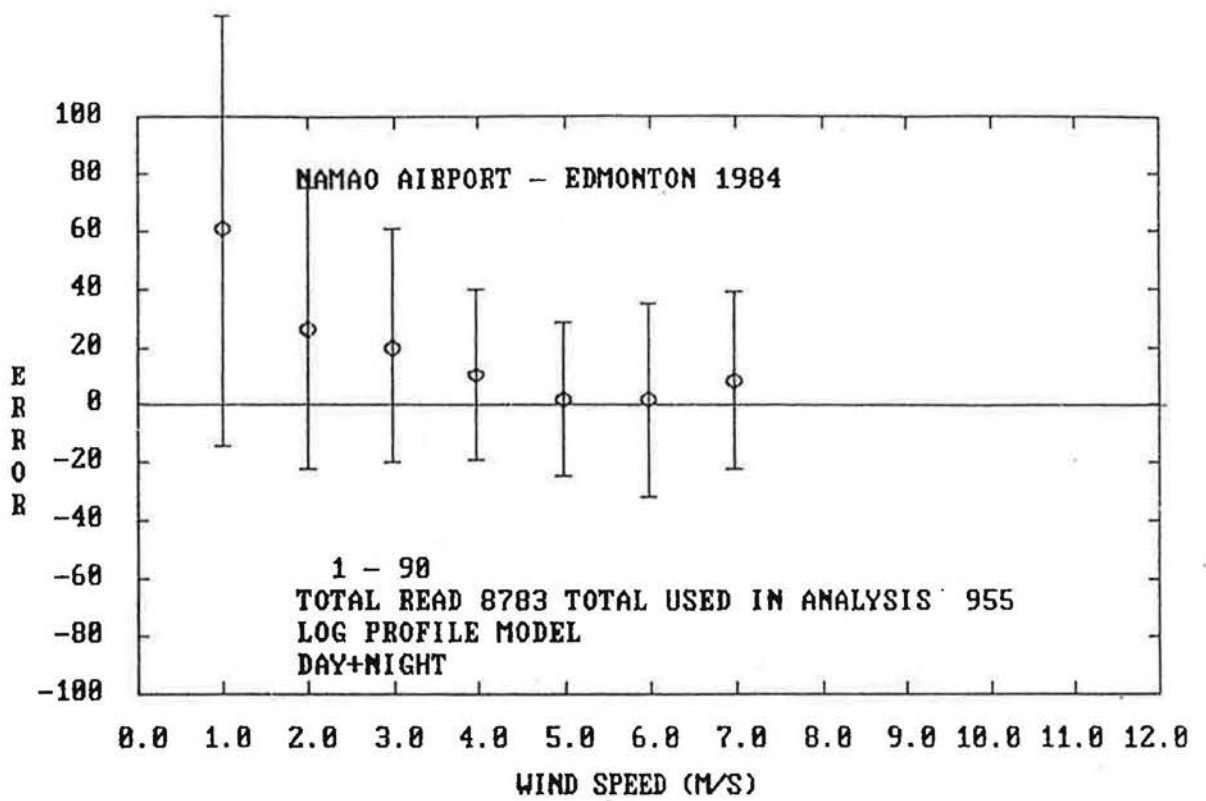


Figure A75

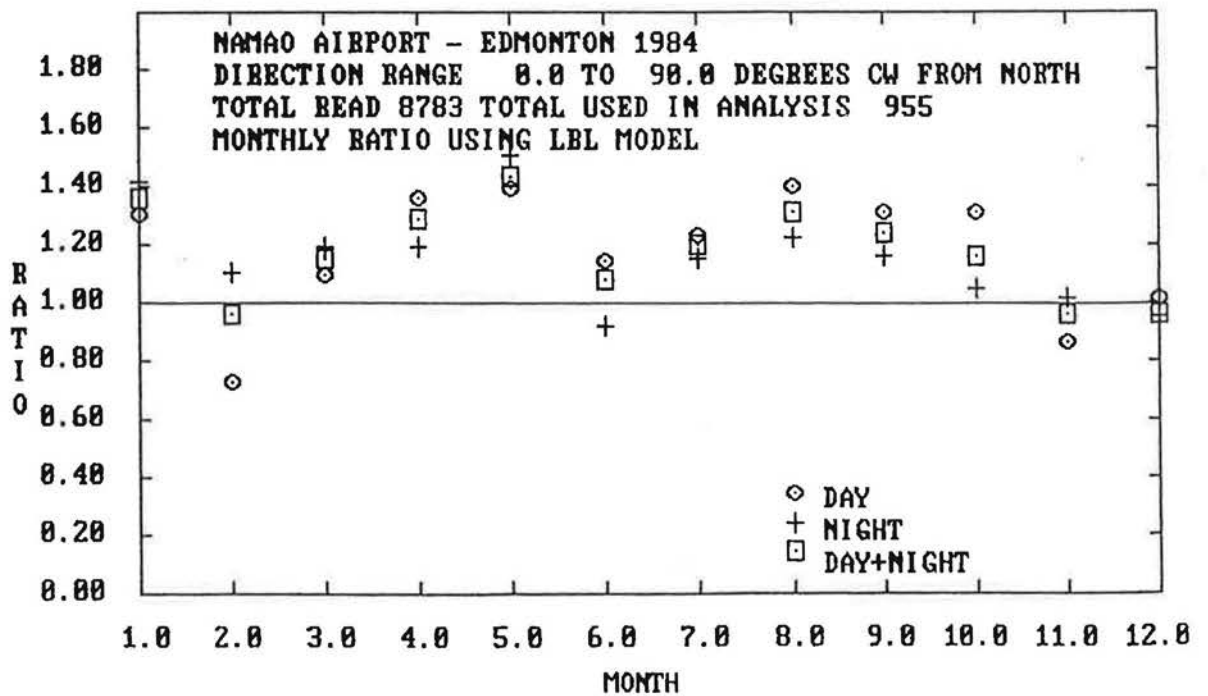


Figure A76

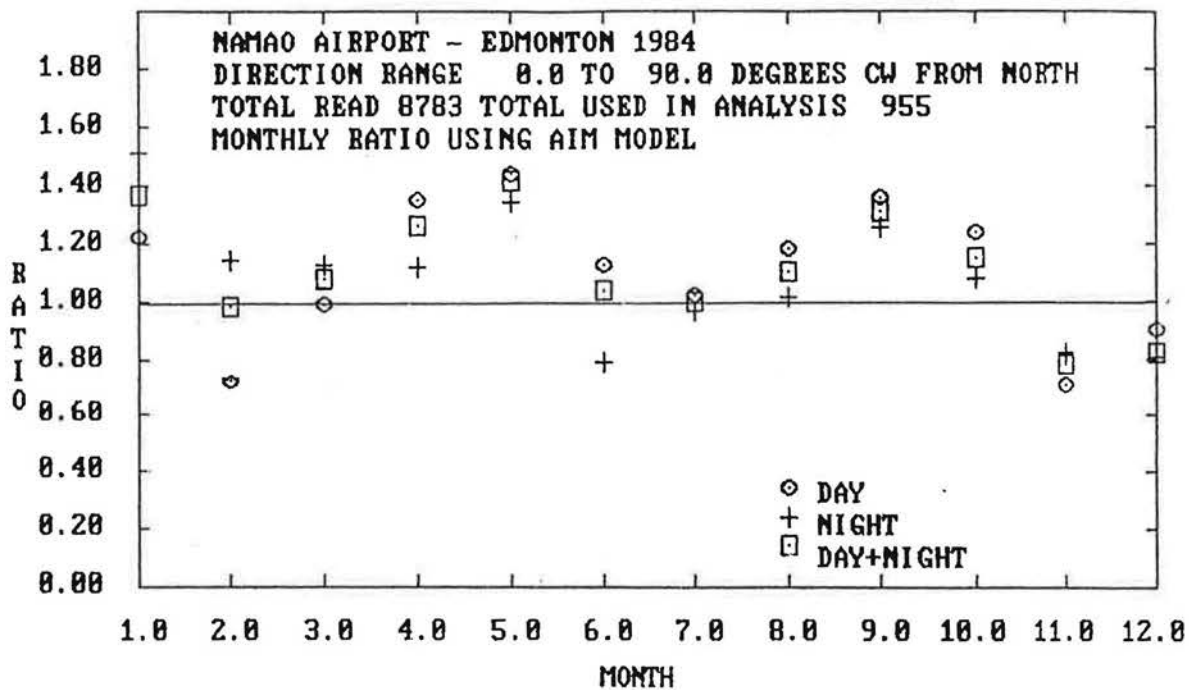


Figure A77

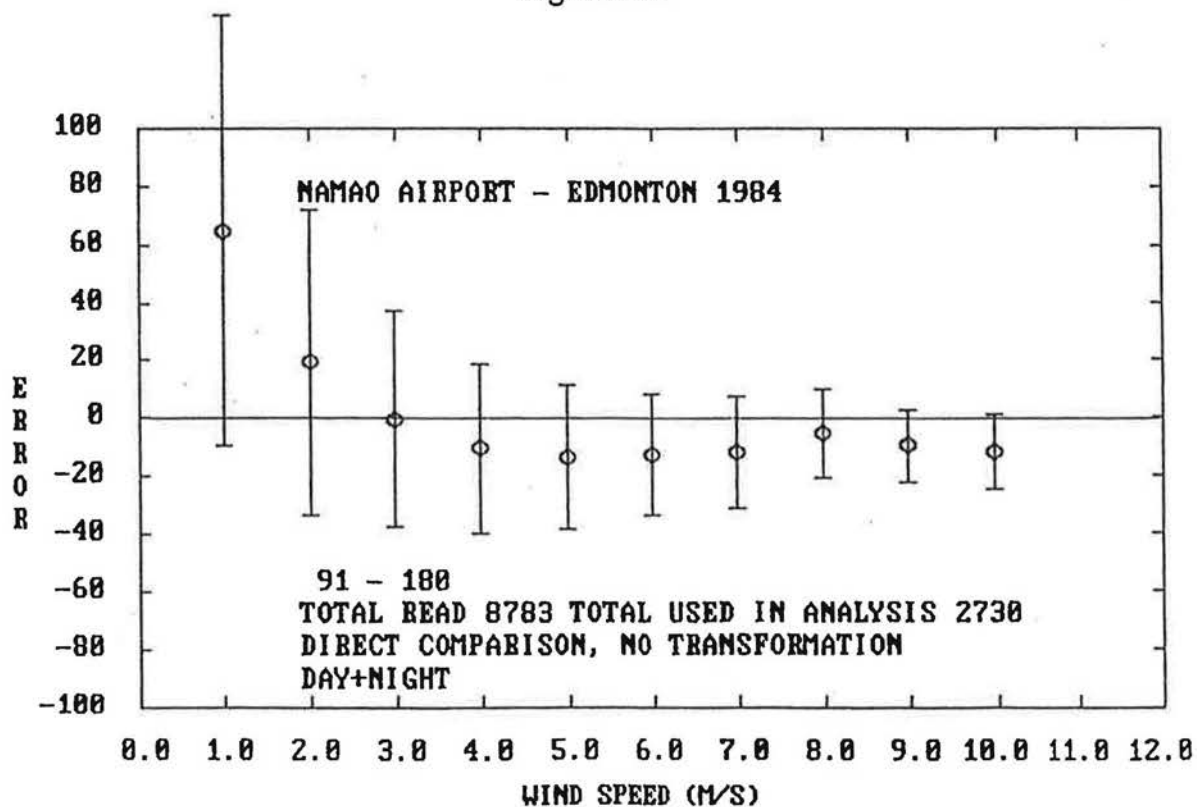


Figure A78

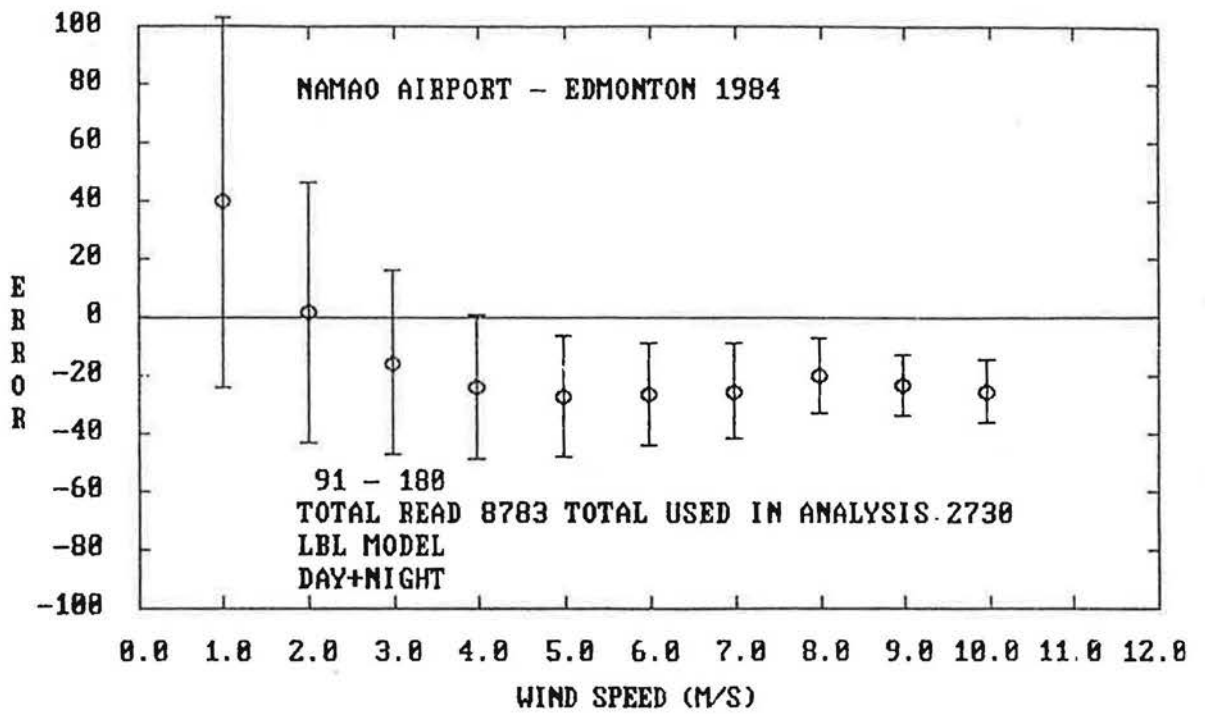


Figure A79

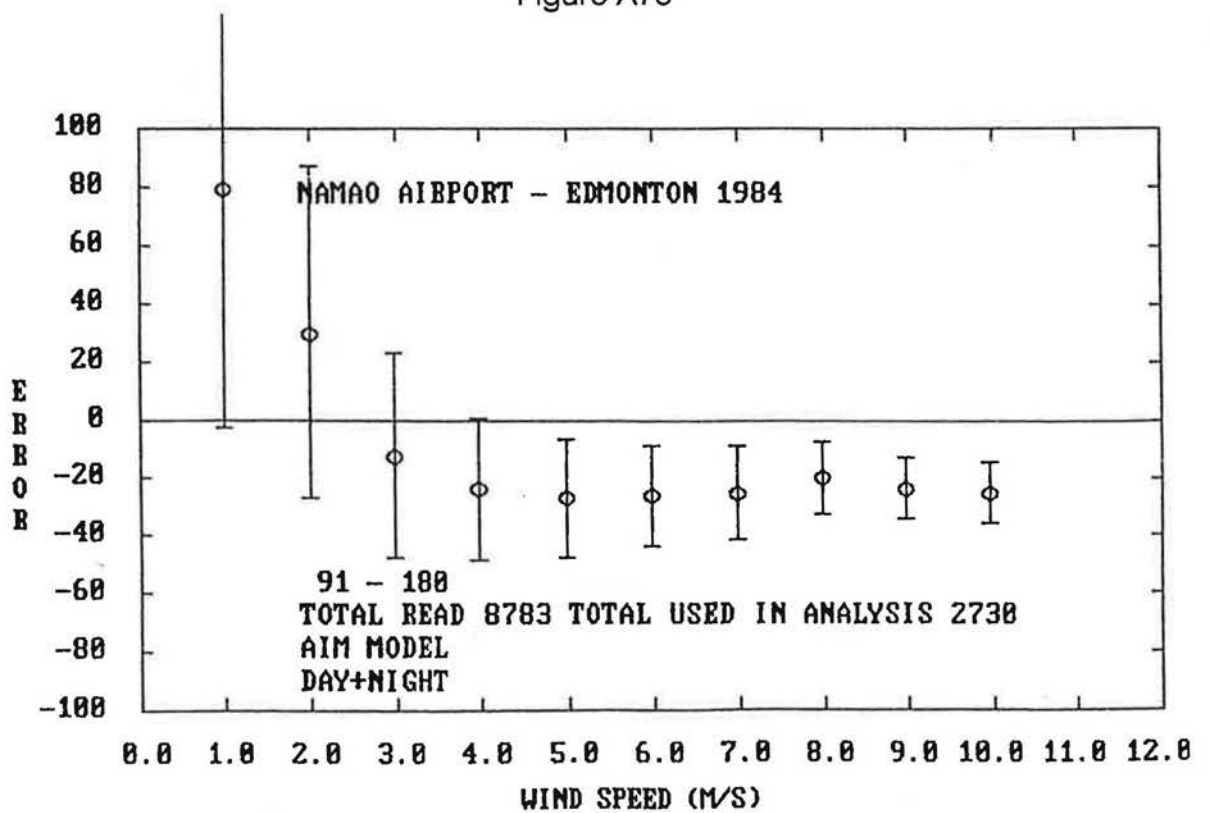


Figure A80

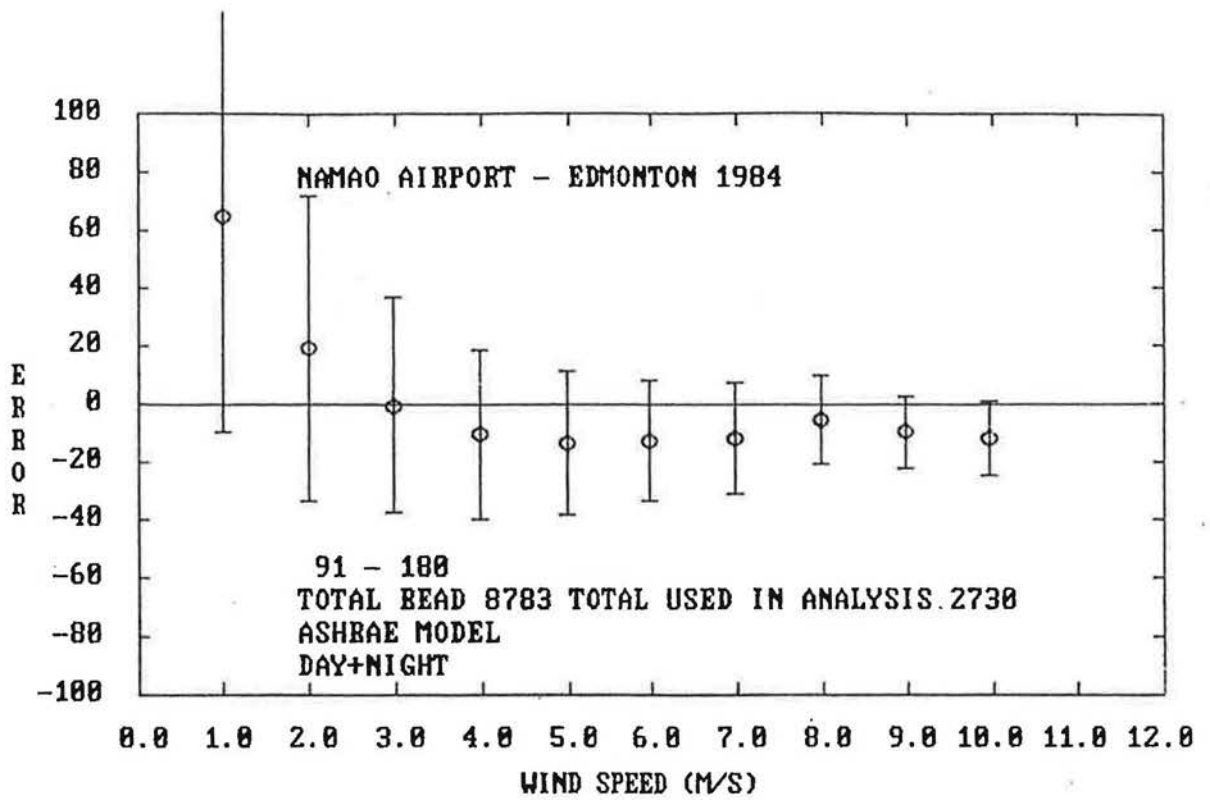


Figure A81

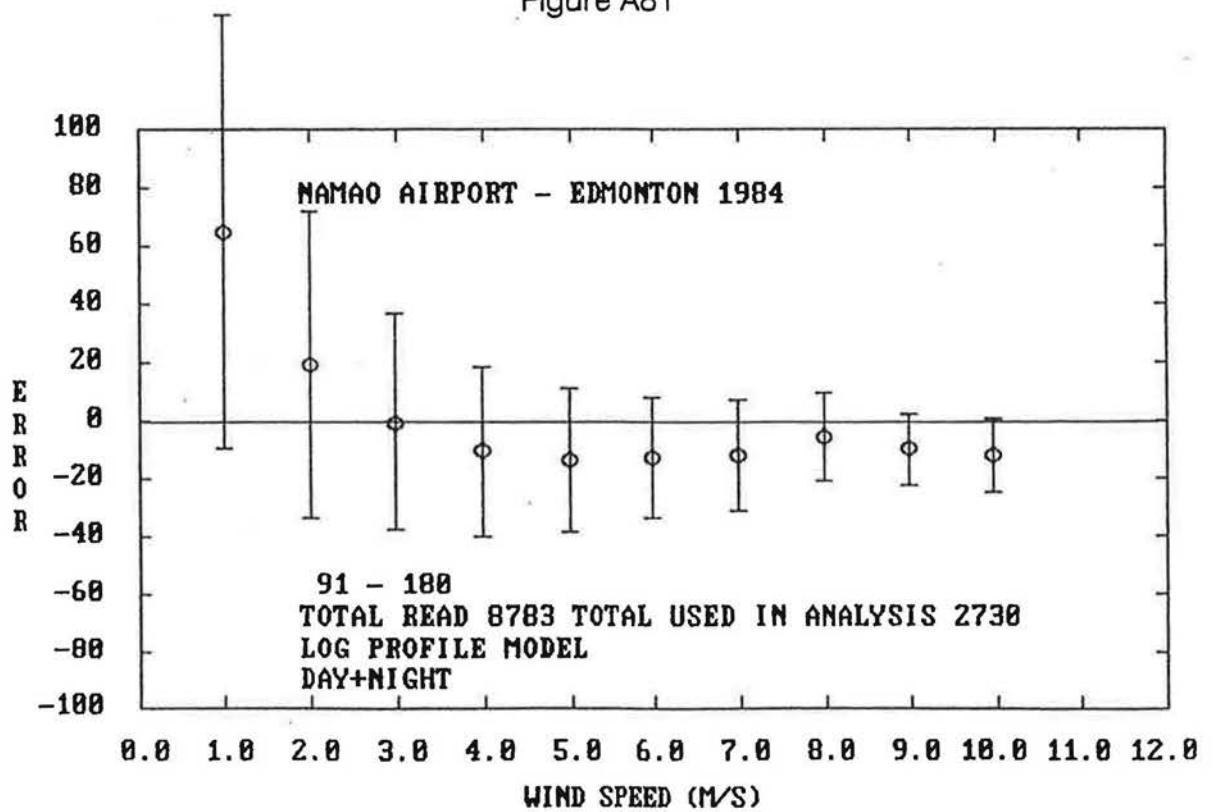


Figure A82

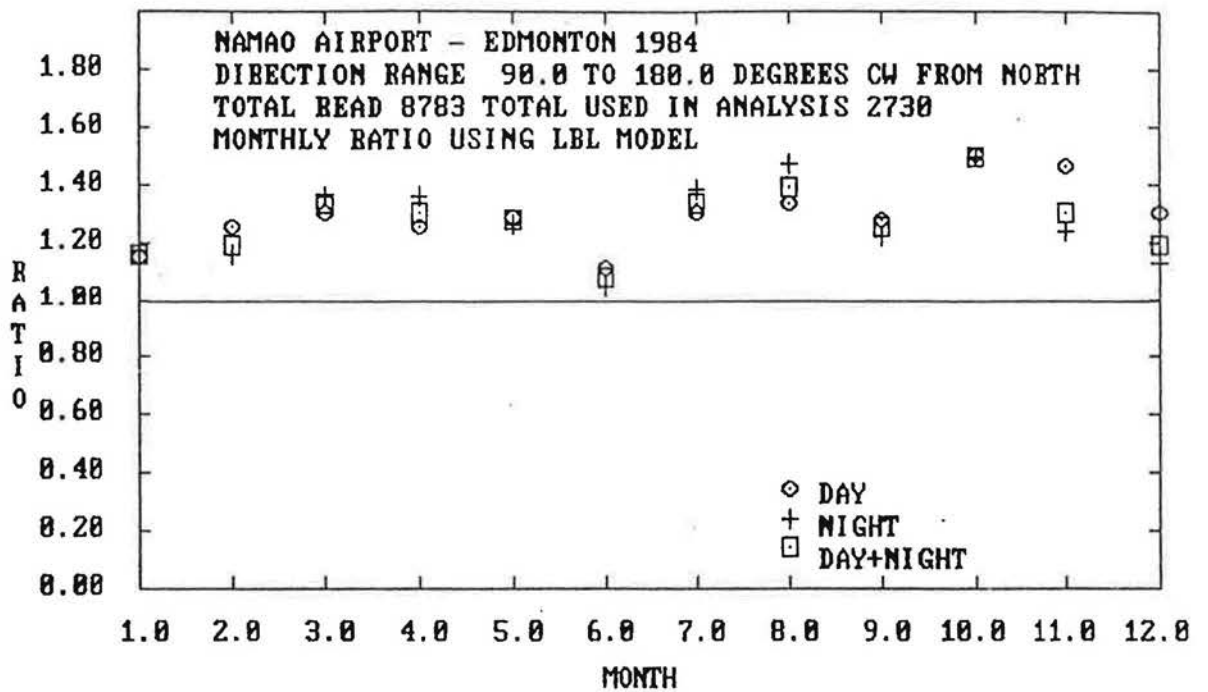


Figure A83

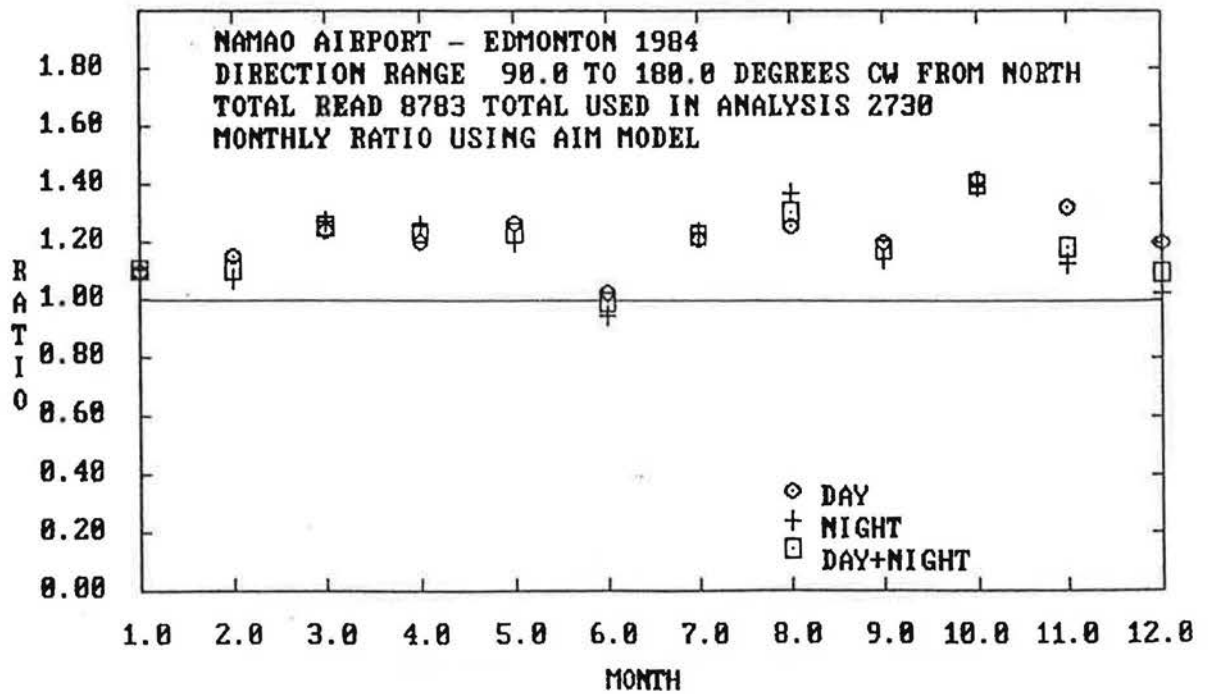


Figure A84

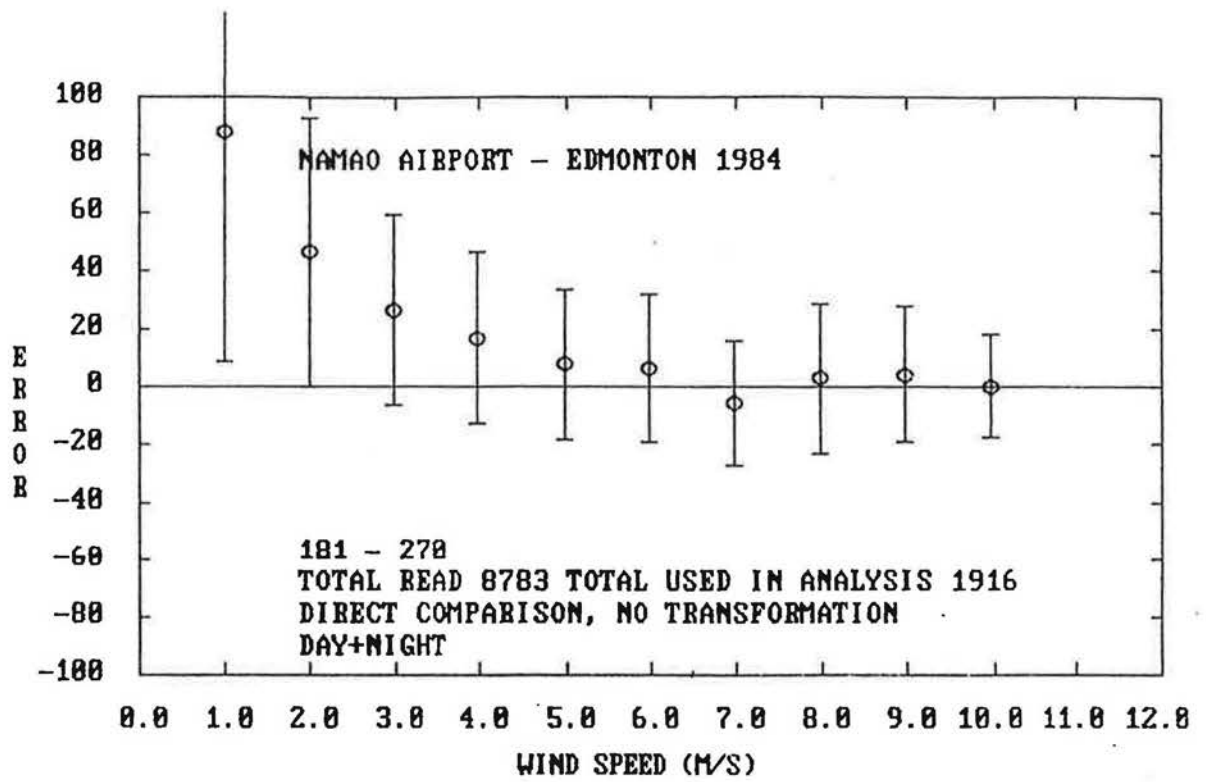


Figure A85

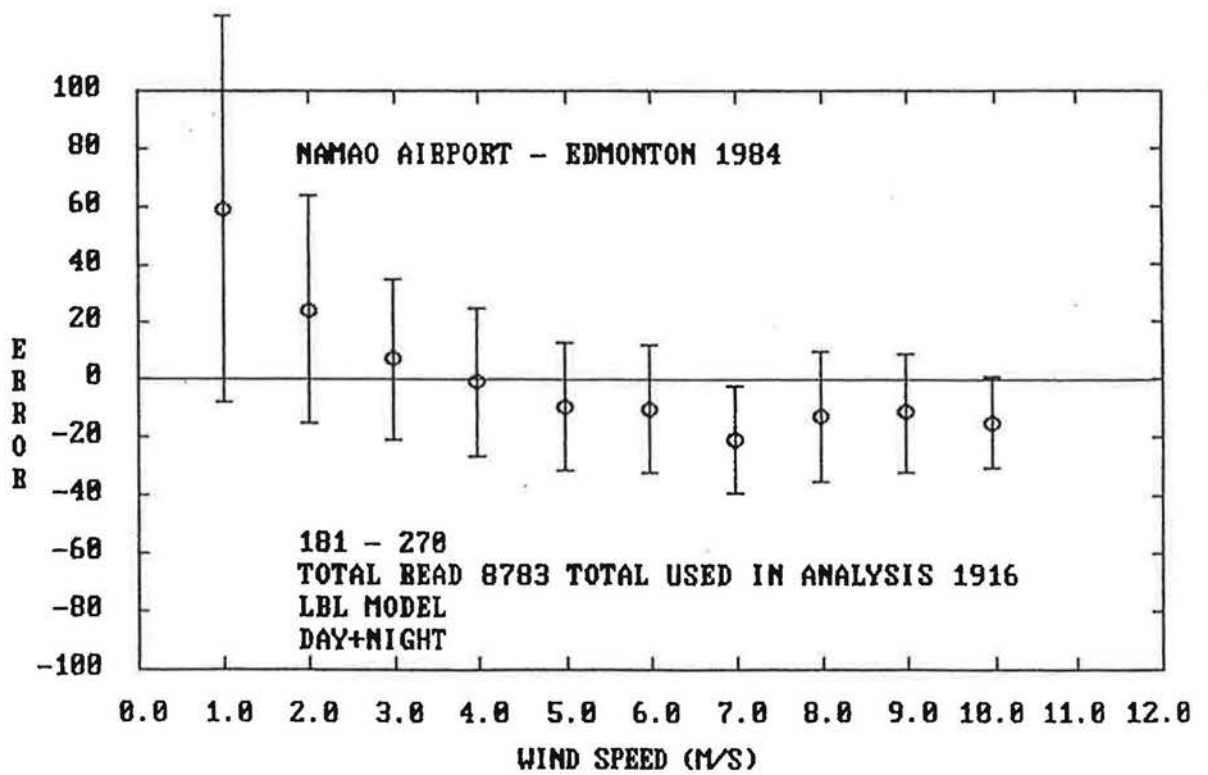


Figure A86

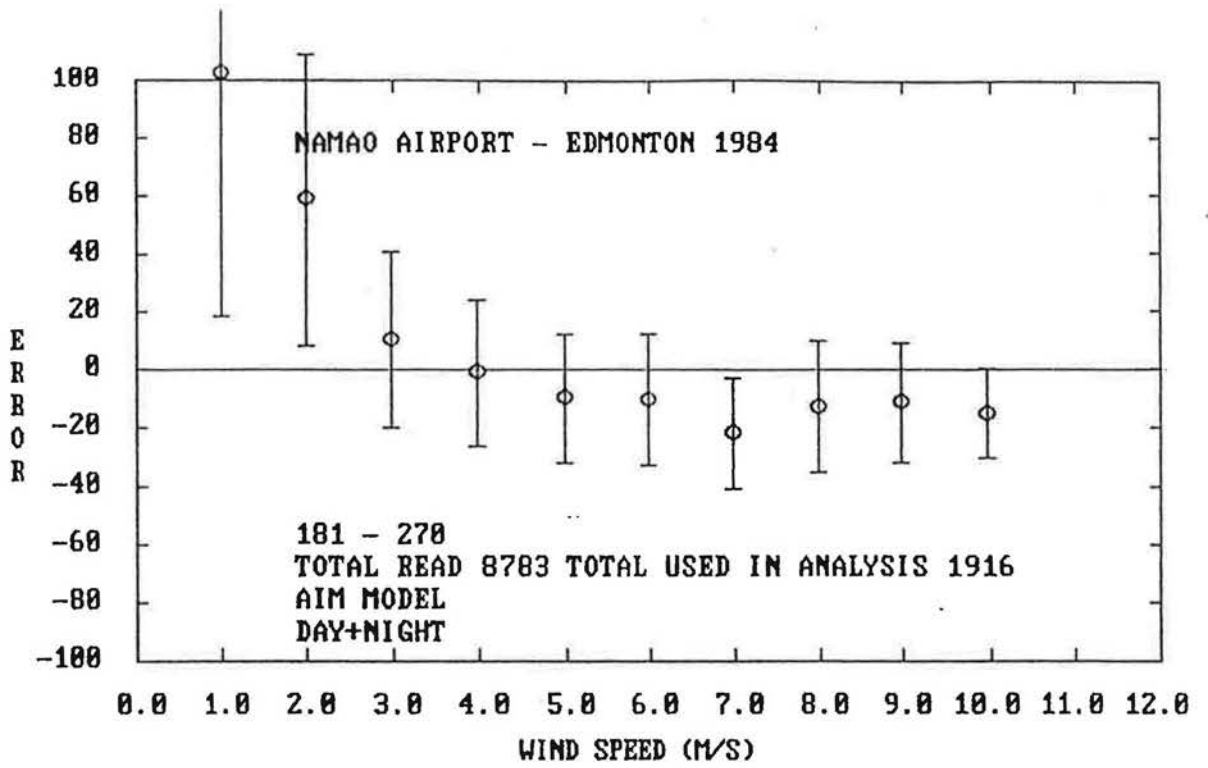


Figure A87

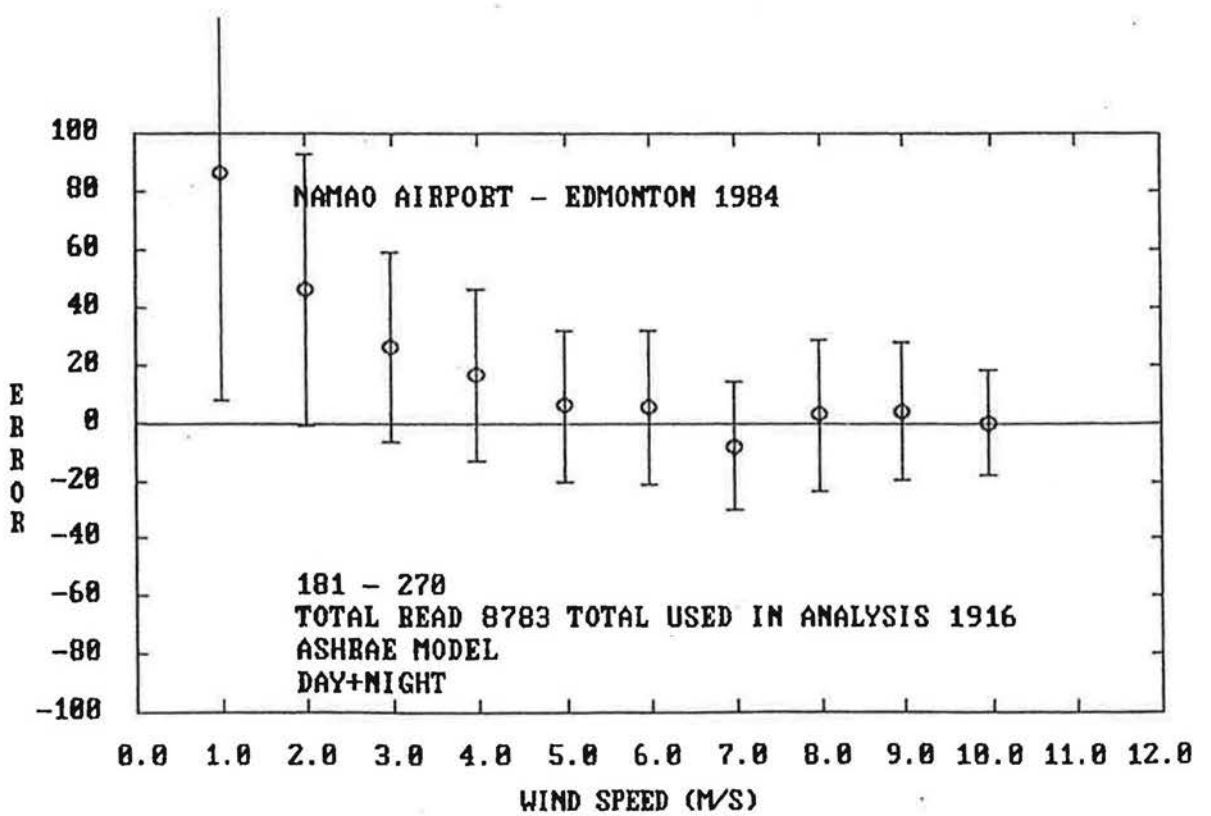


Figure A88

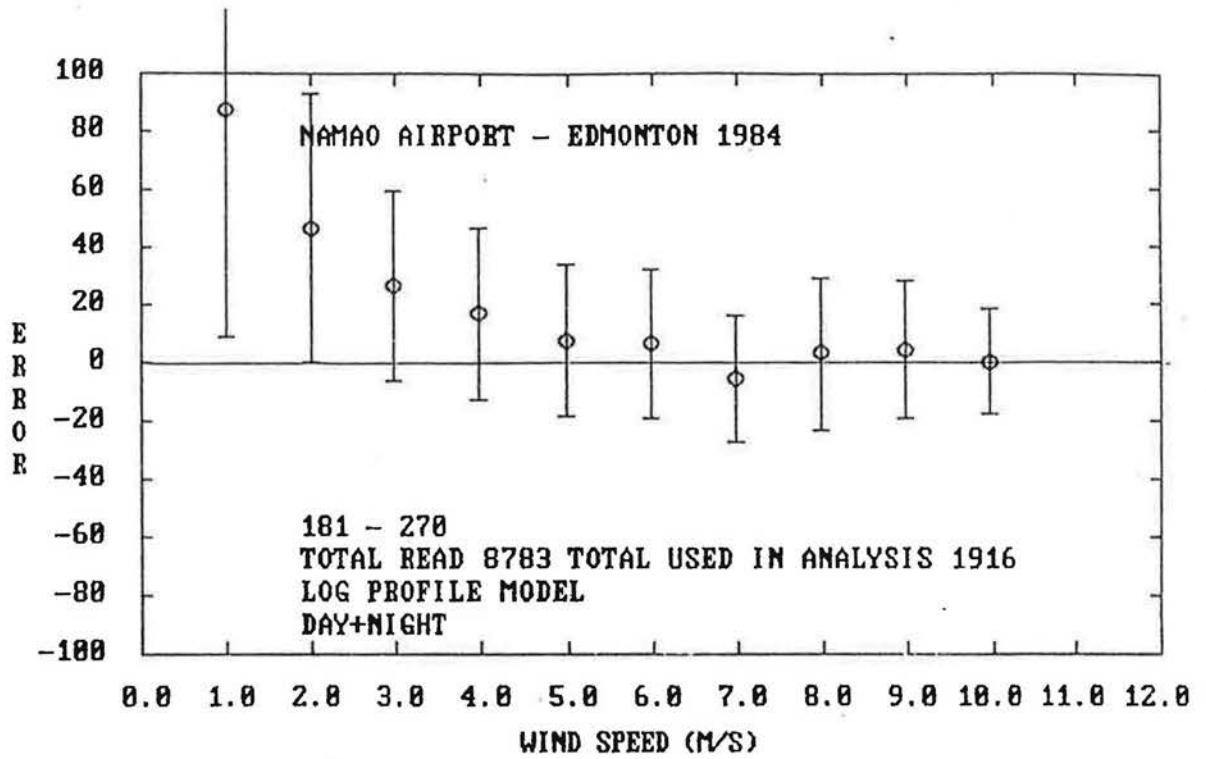


Figure A89

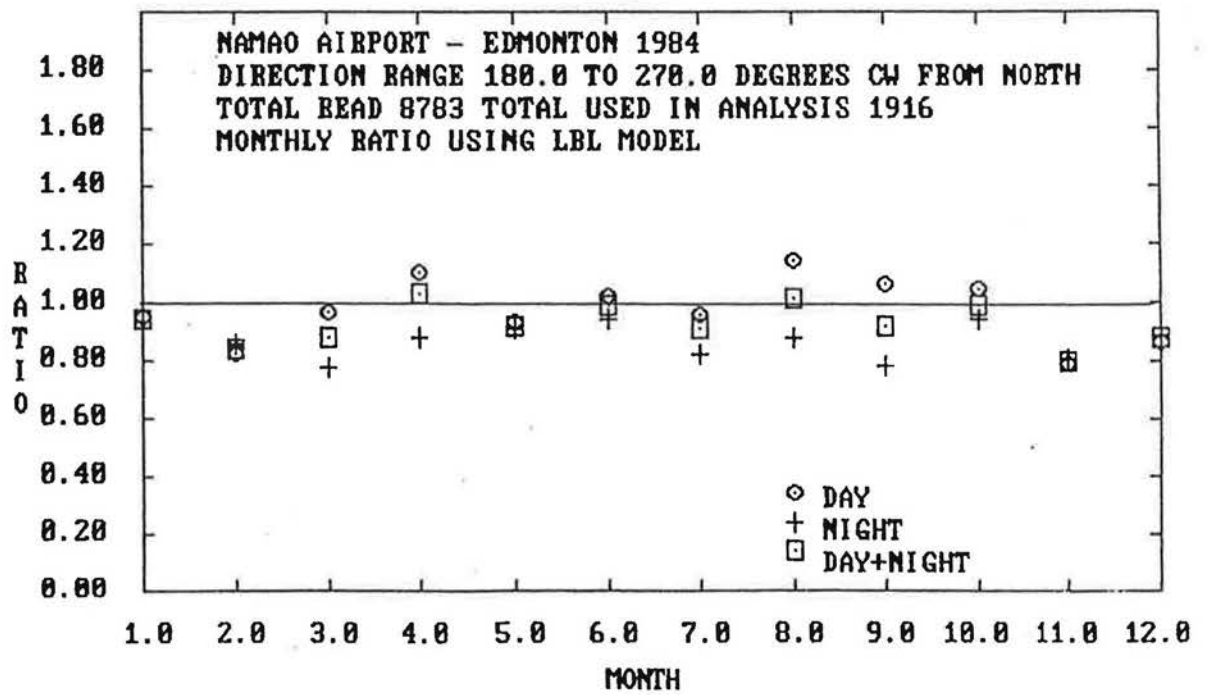


Figure A90

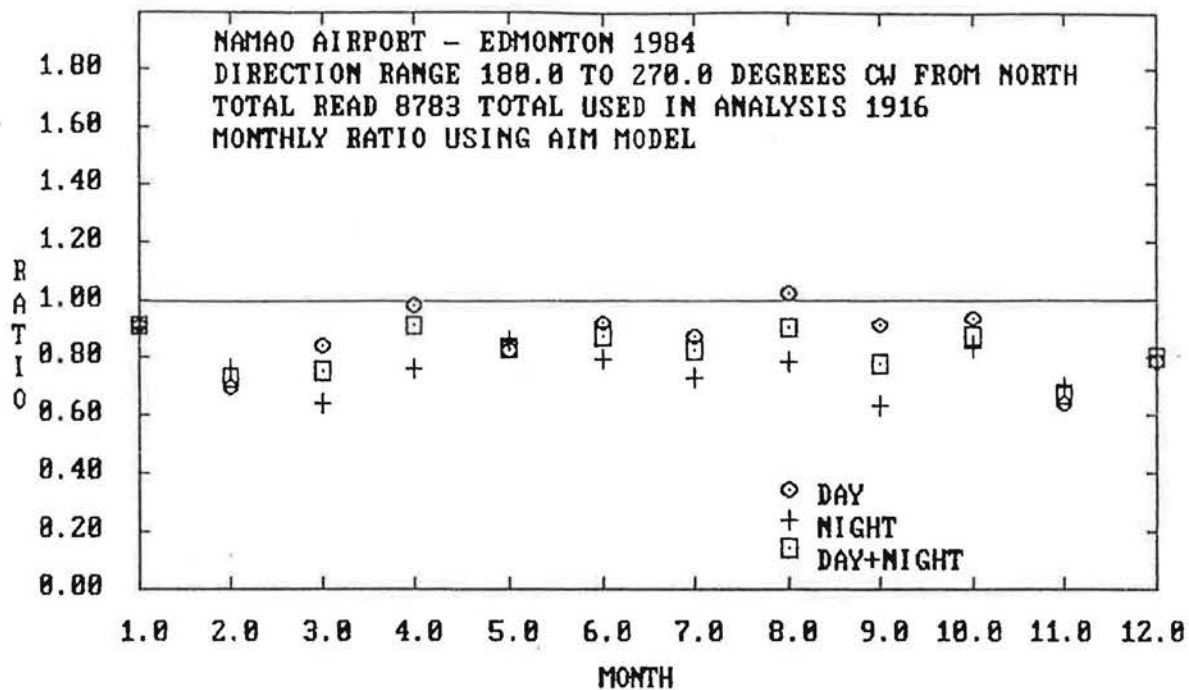


Figure A91

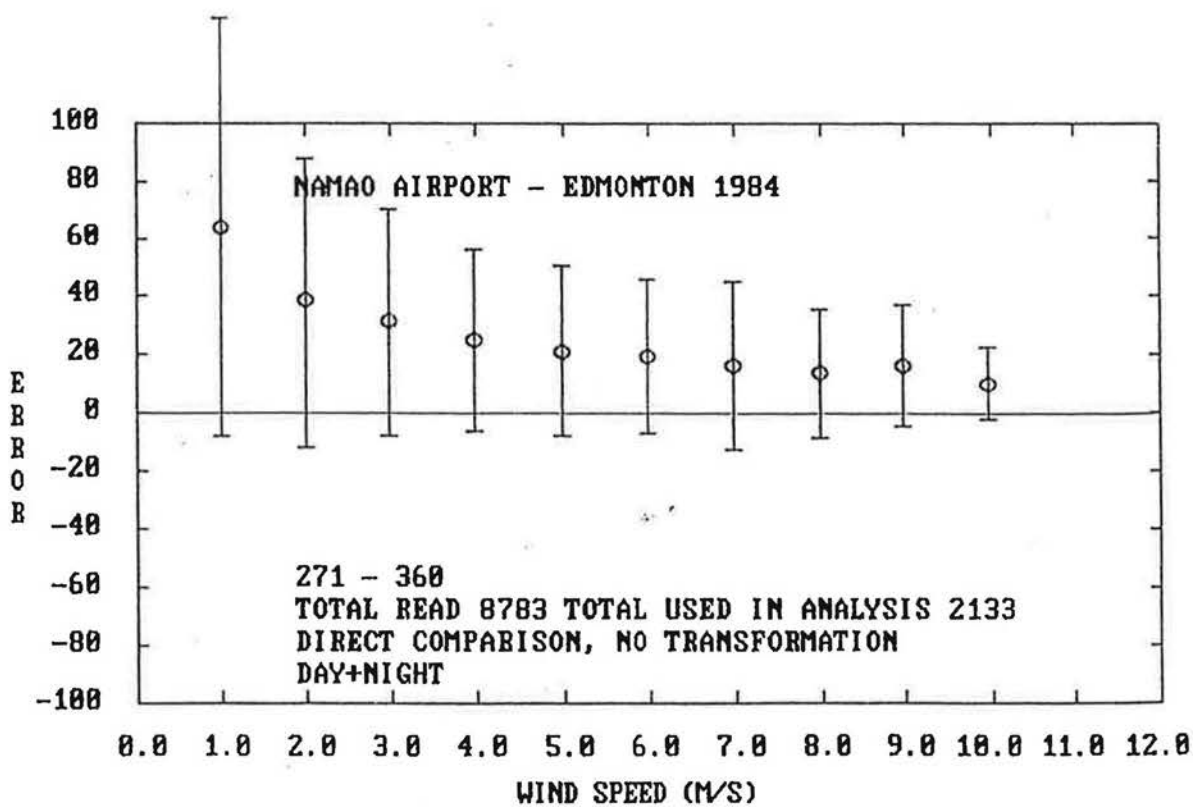


Figure A92

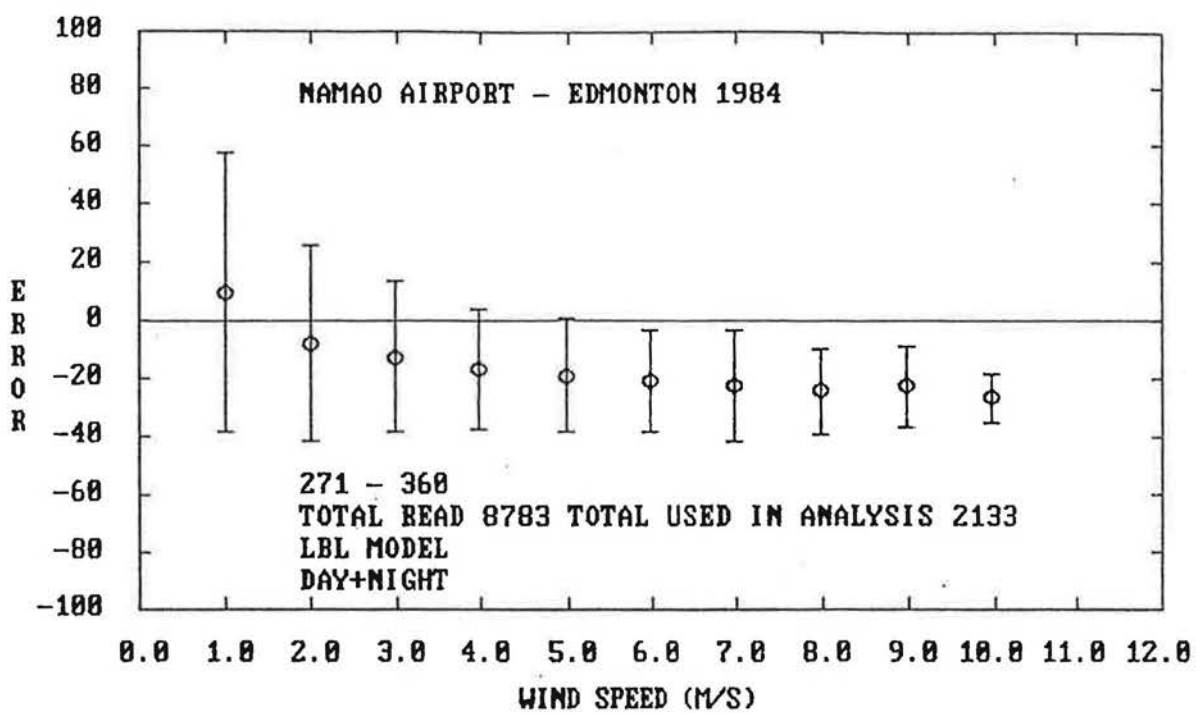


Figure A93

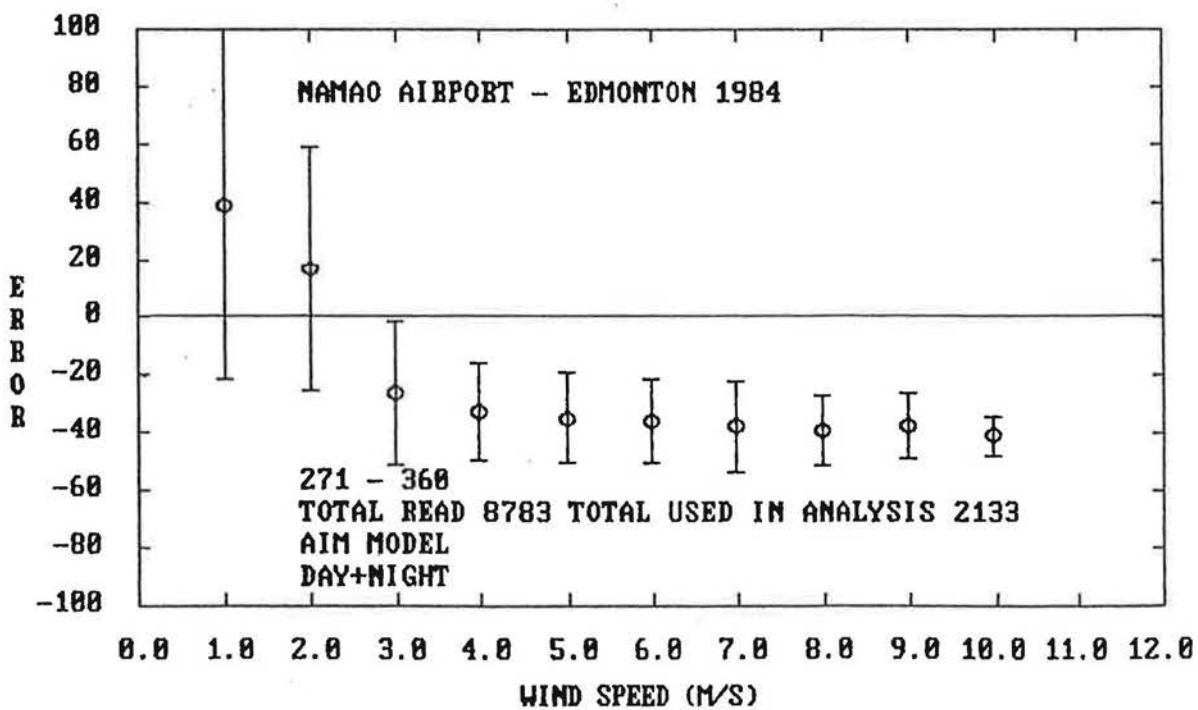


Figure A94

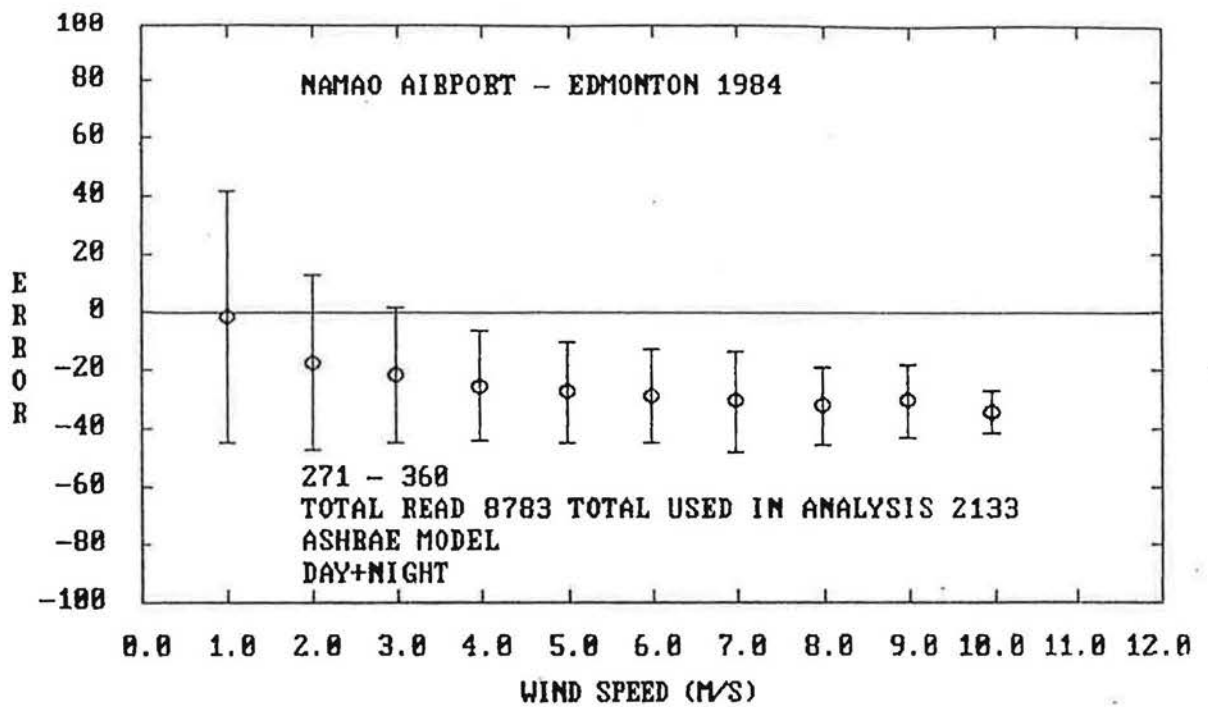


Figure A95

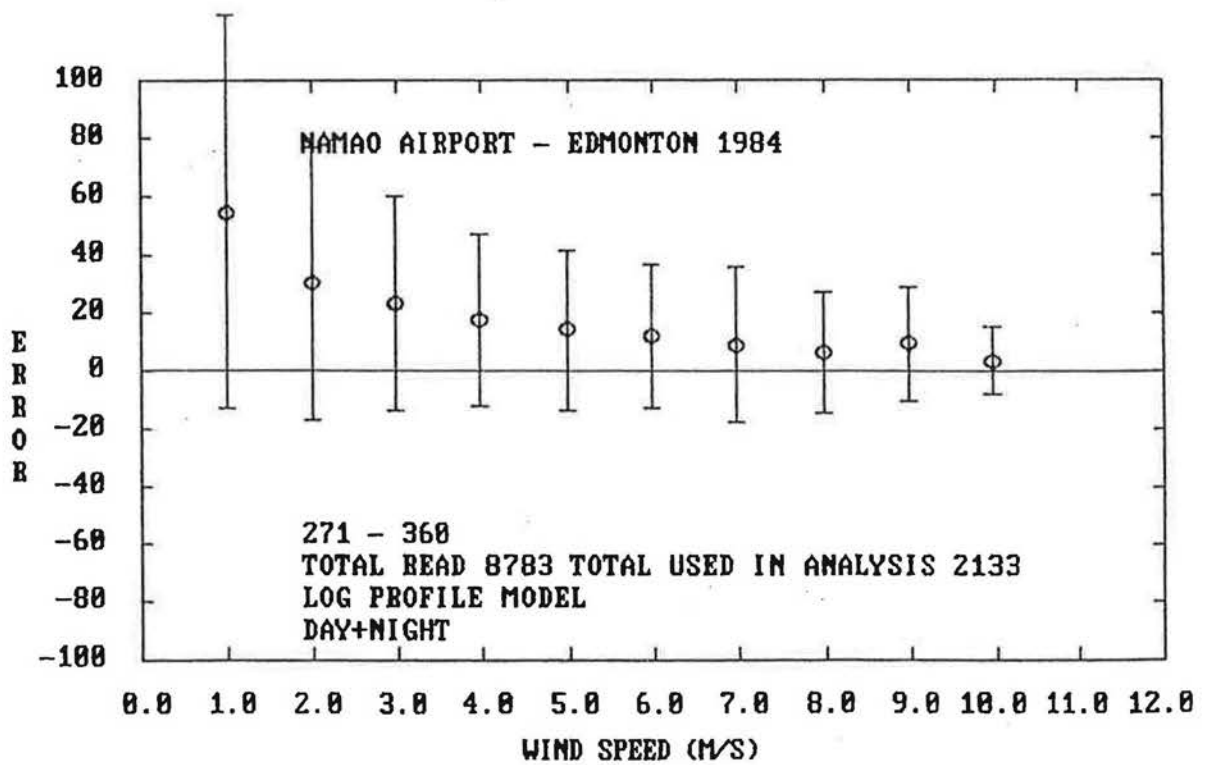


Figure A96

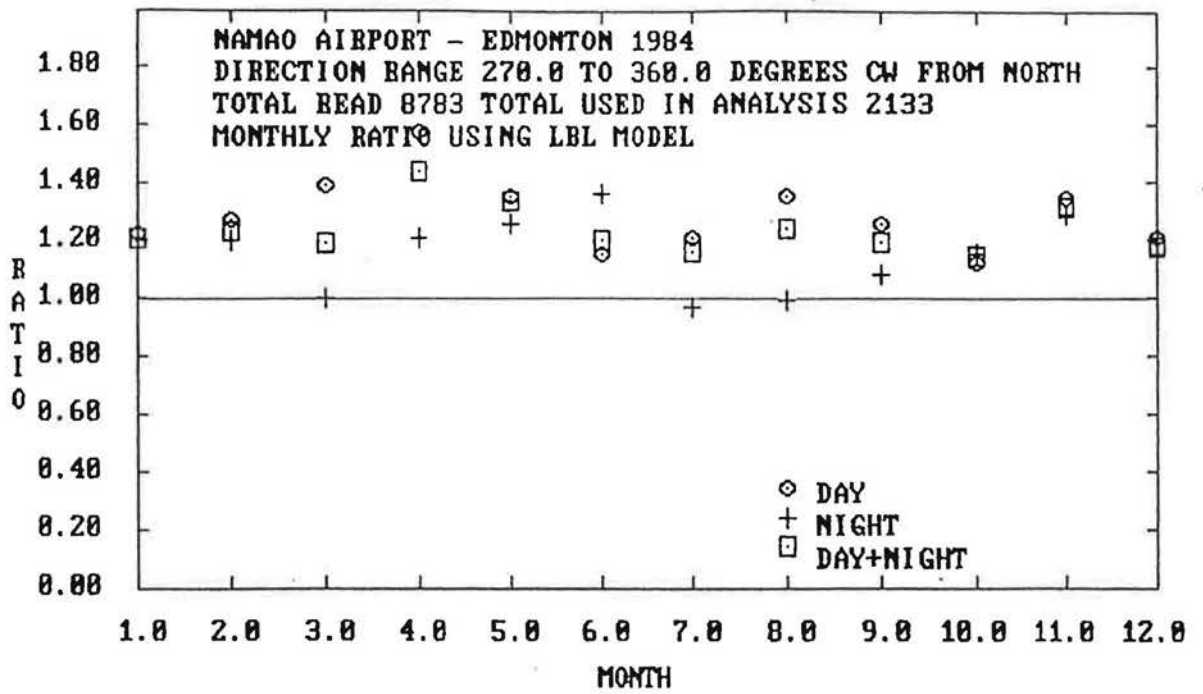


Figure A97

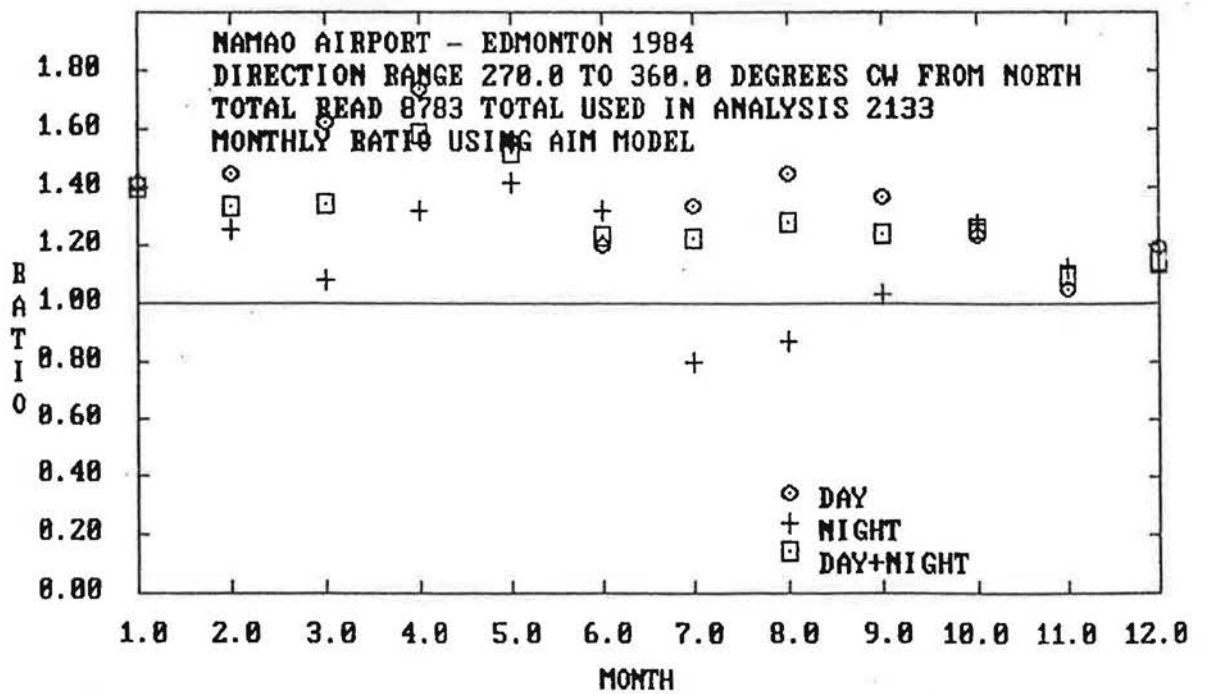


Figure A98

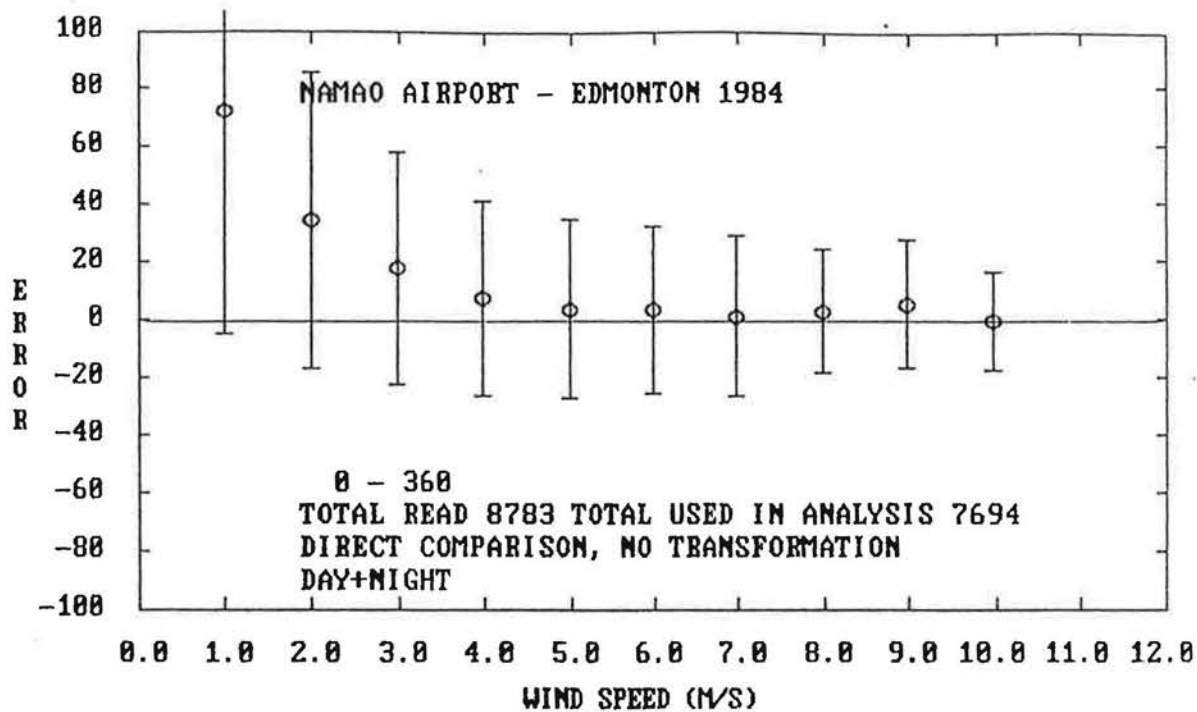


Figure A99

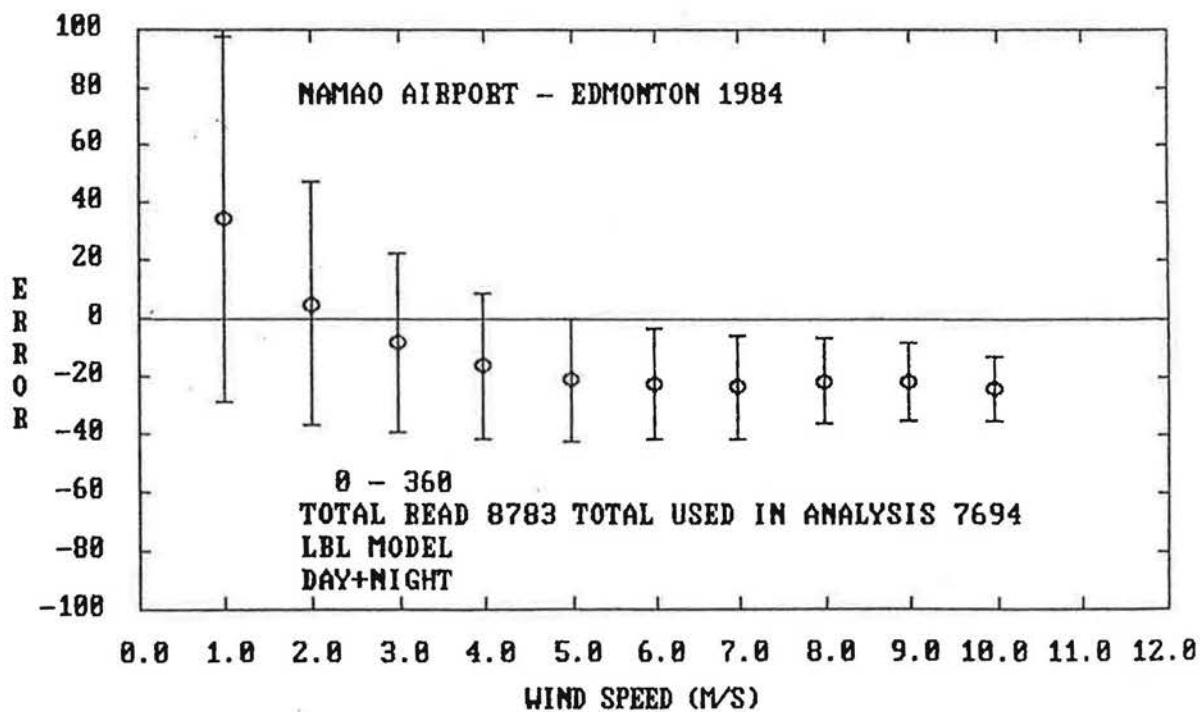


Figure A100

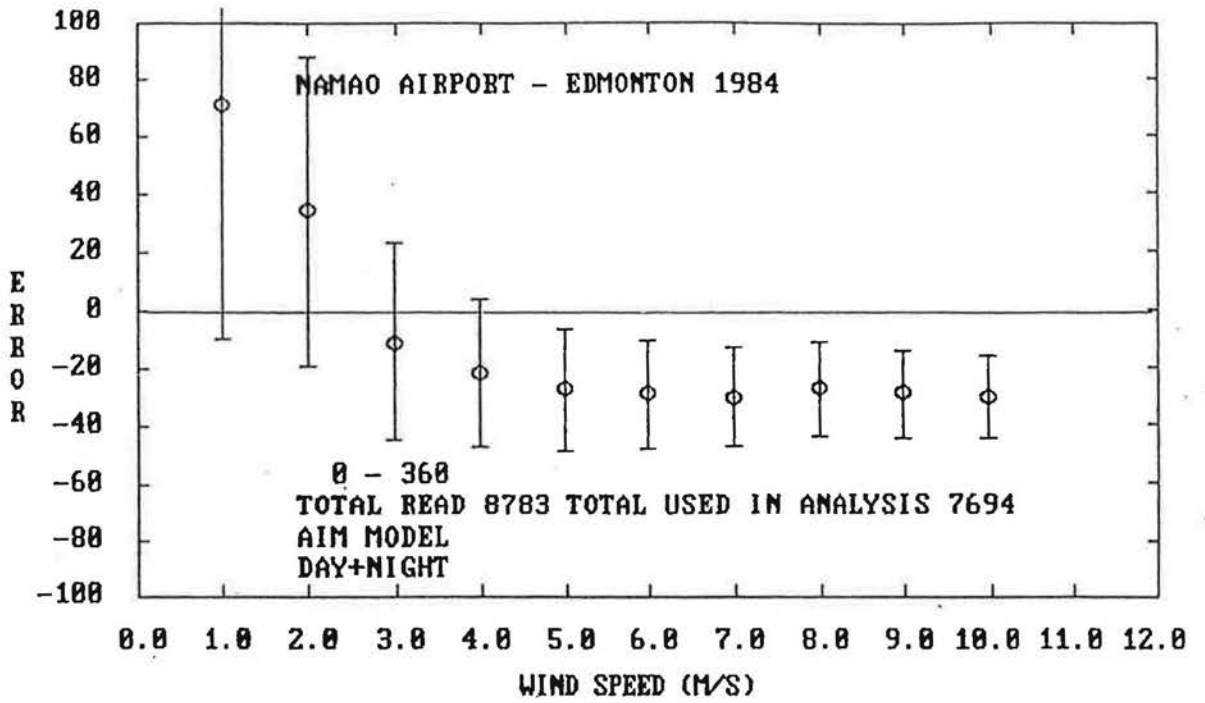


Figure A101

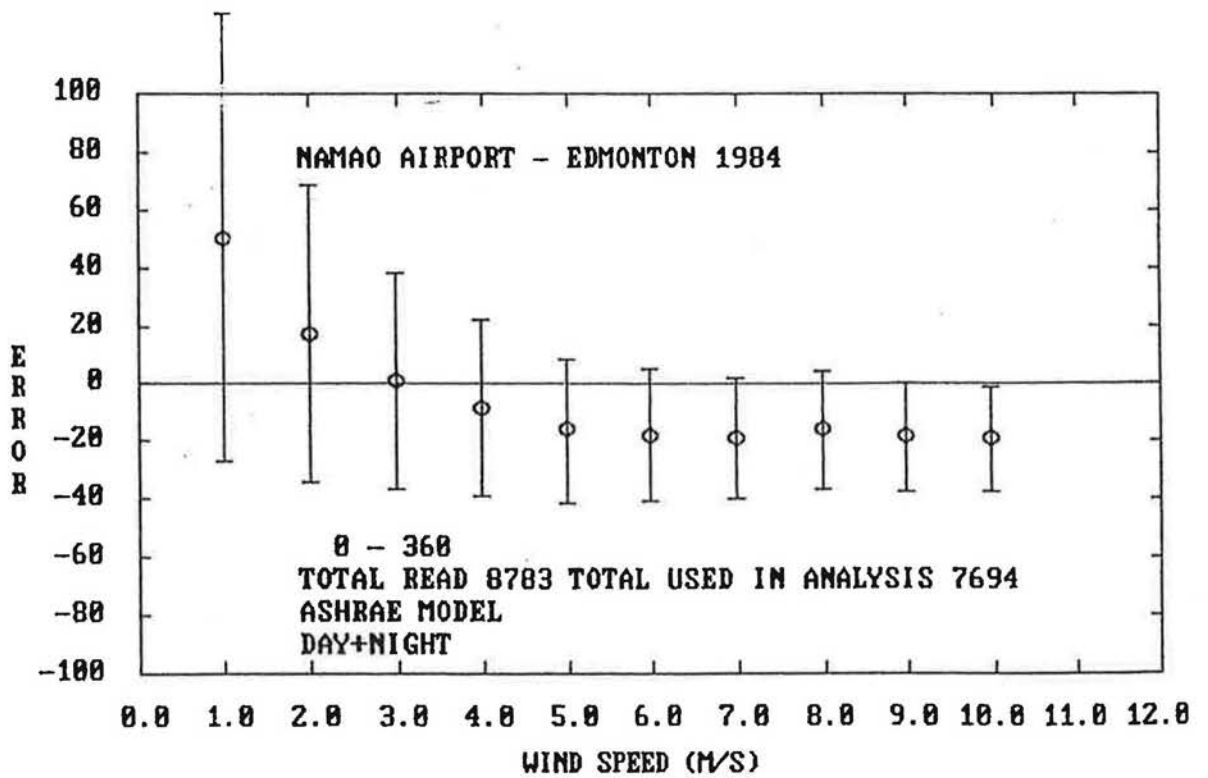


Figure A102

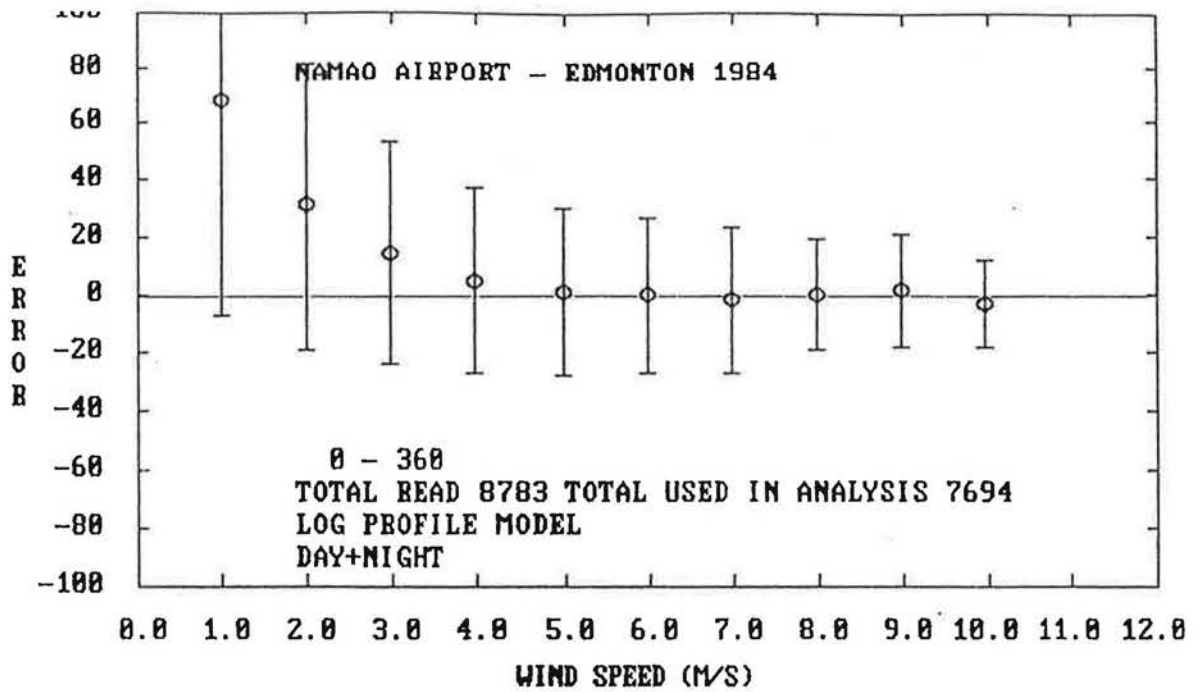


Figure A103

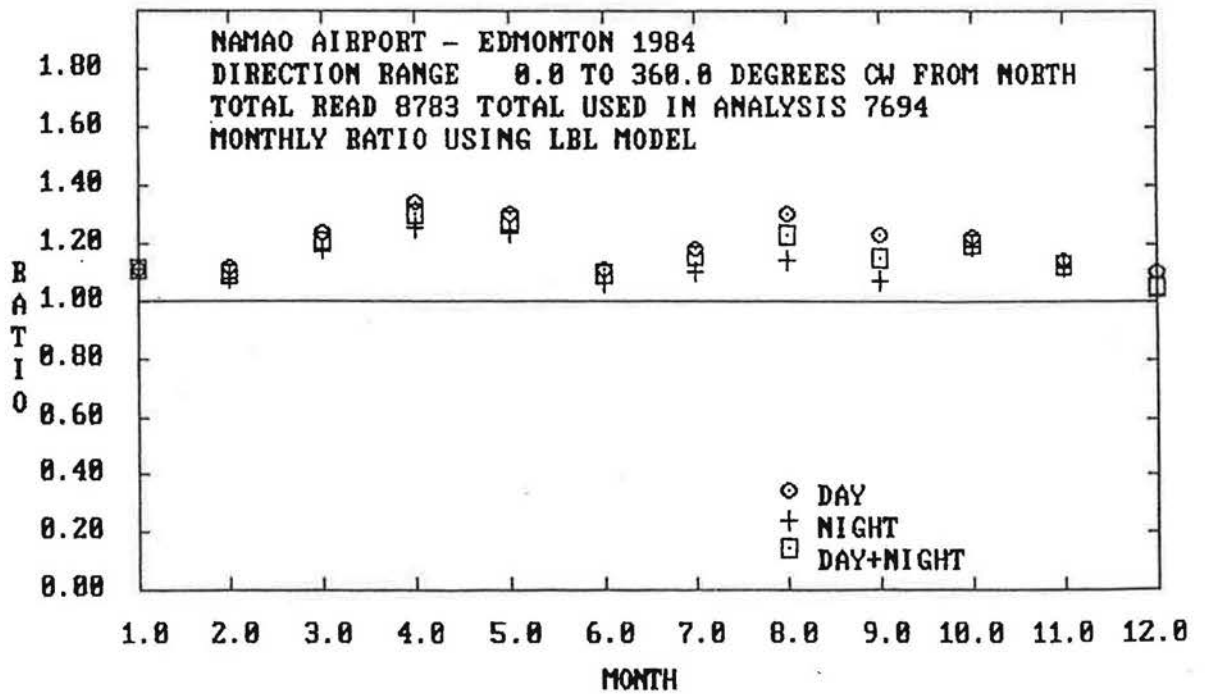


Figure A104

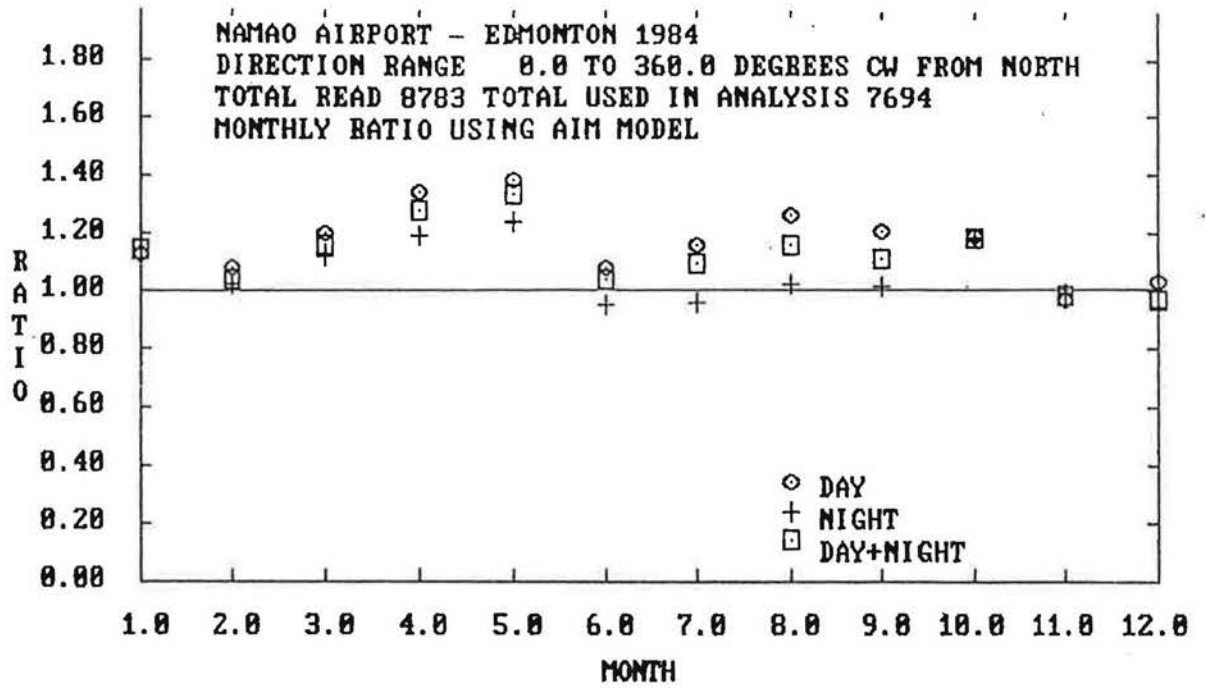


Figure A105

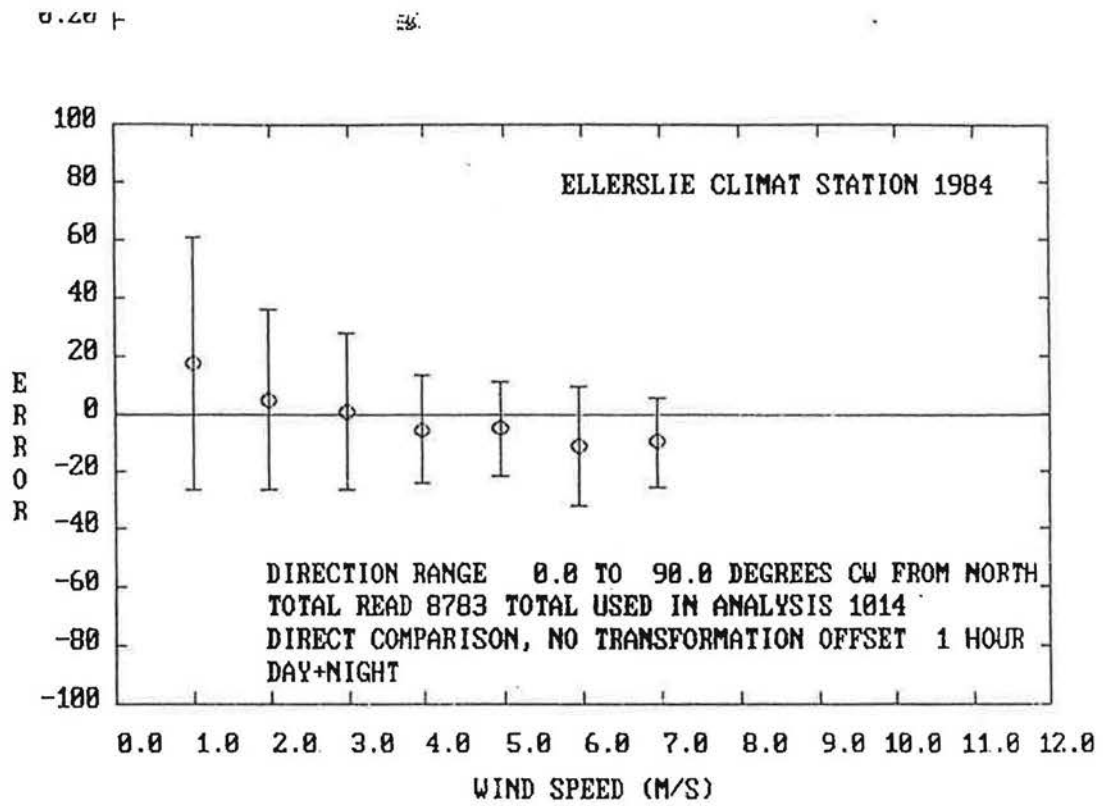


Figure A106

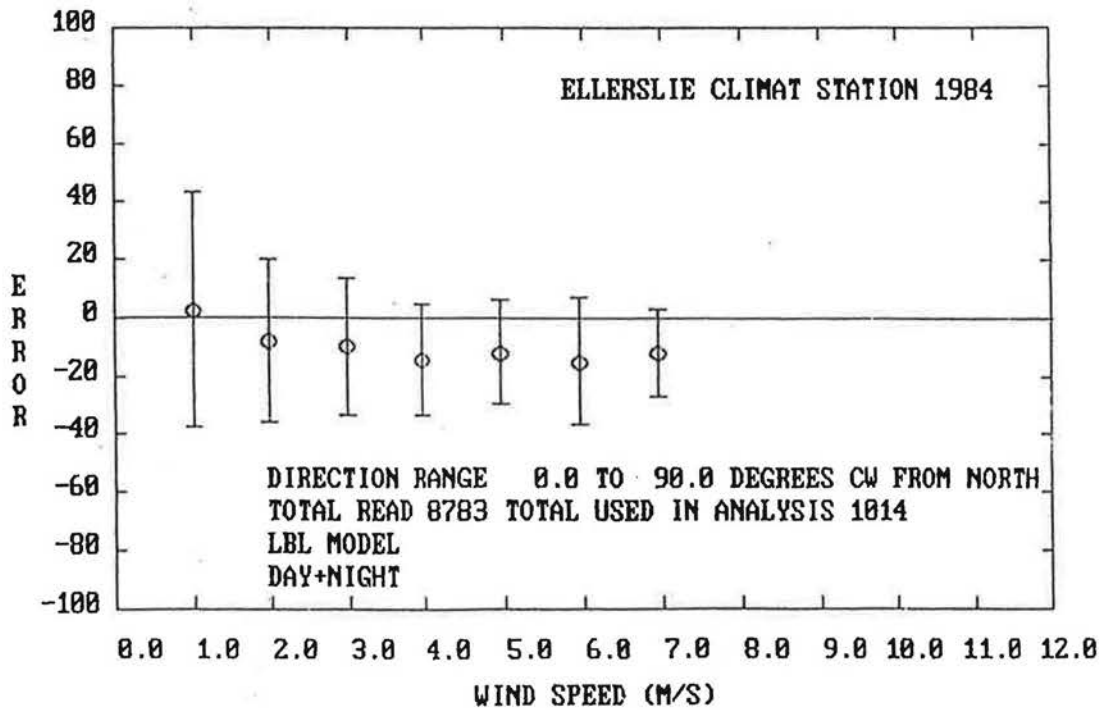


Figure A107

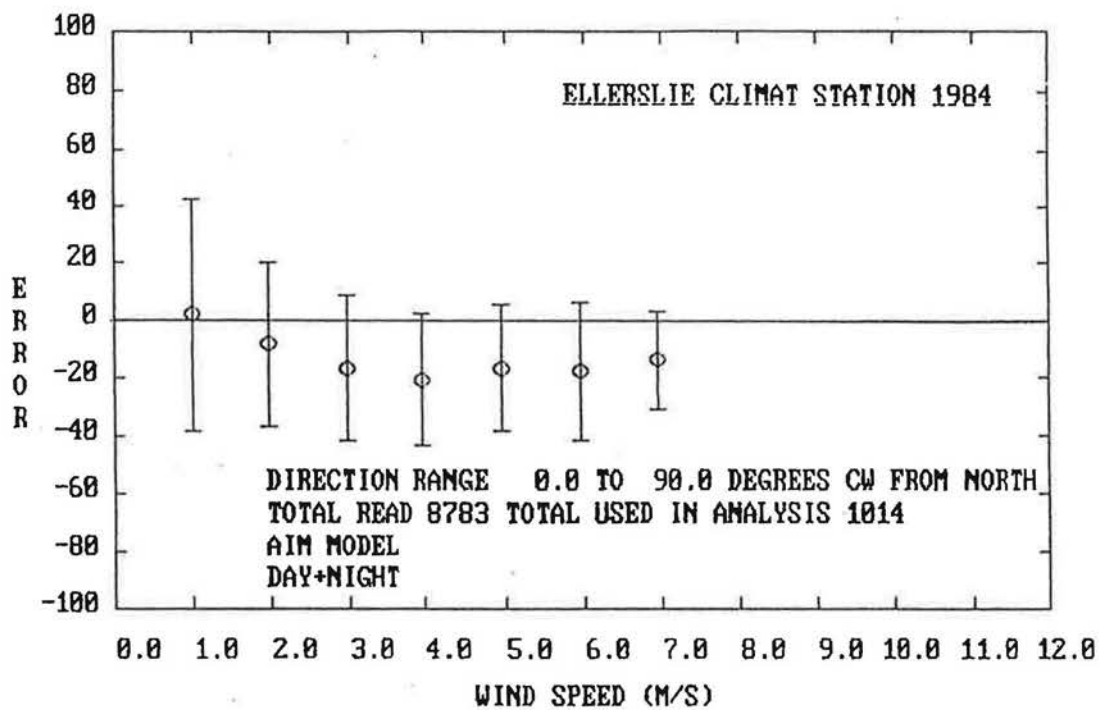


Figure A108

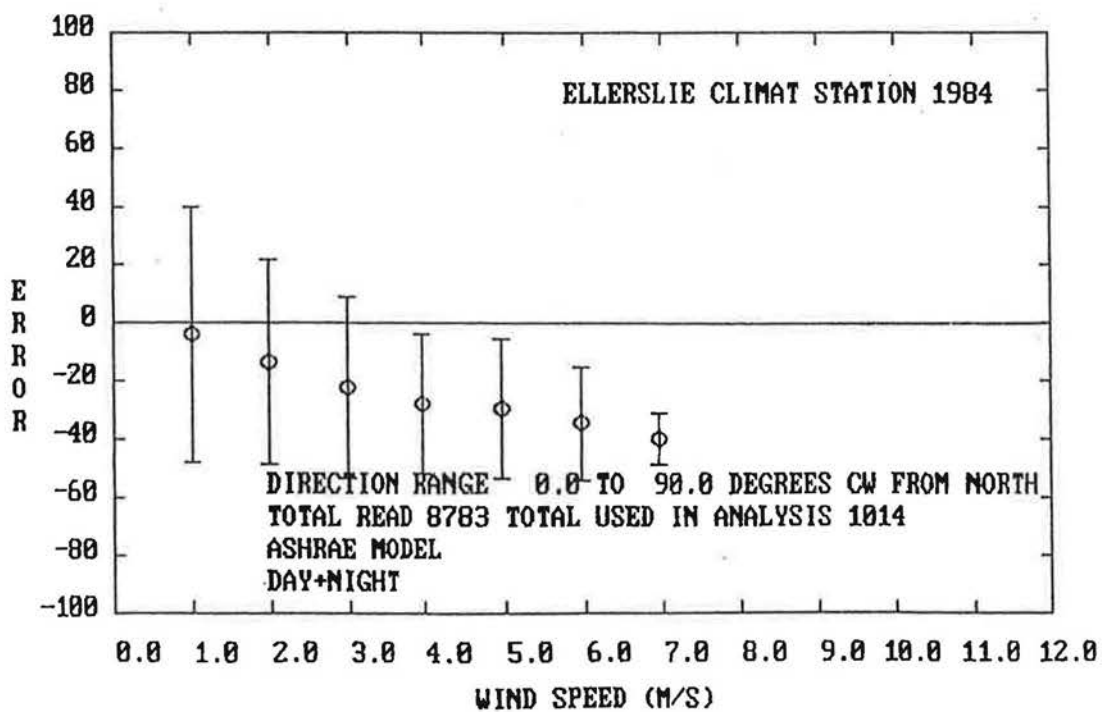


Figure A109

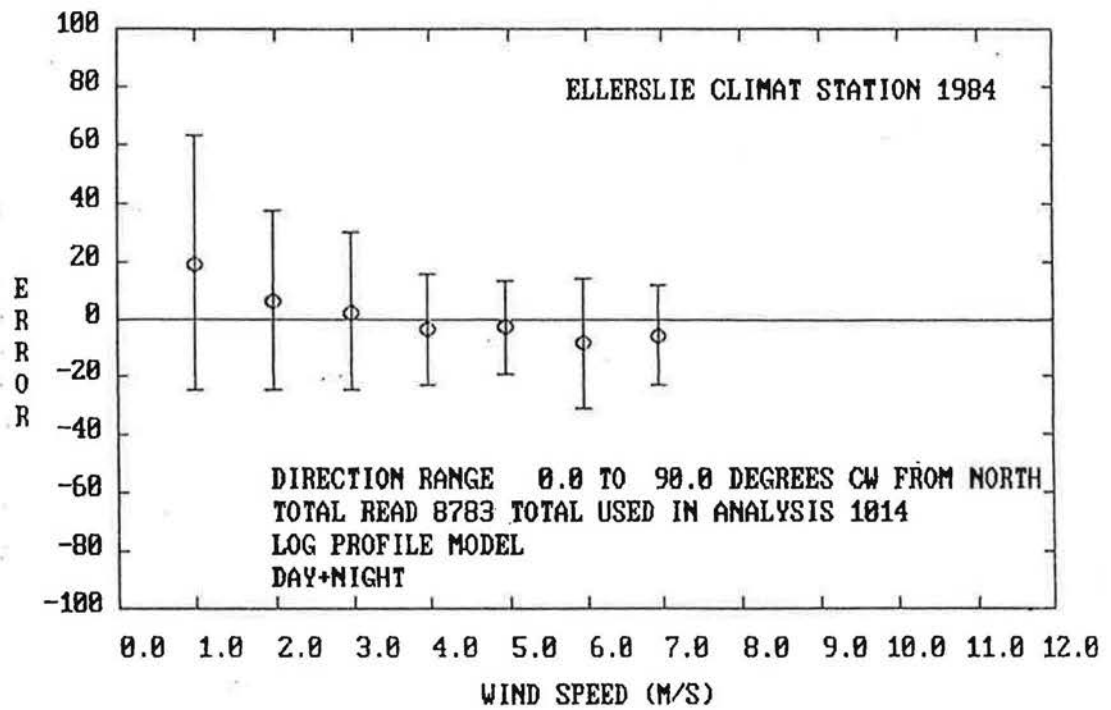


Figure A110

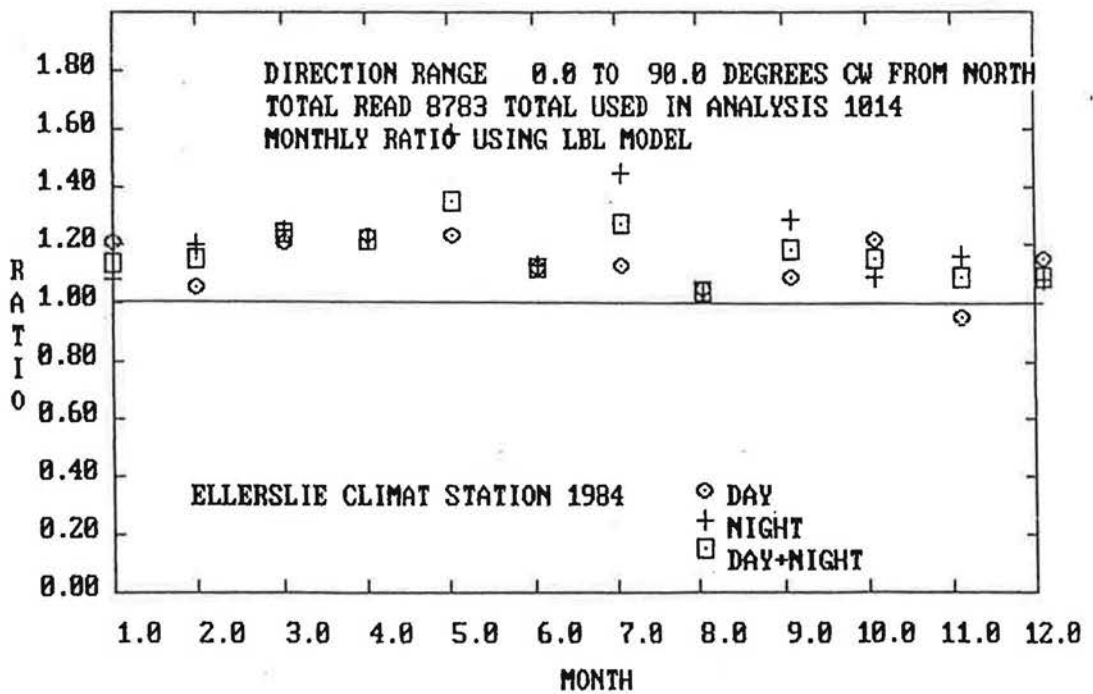


Figure A111

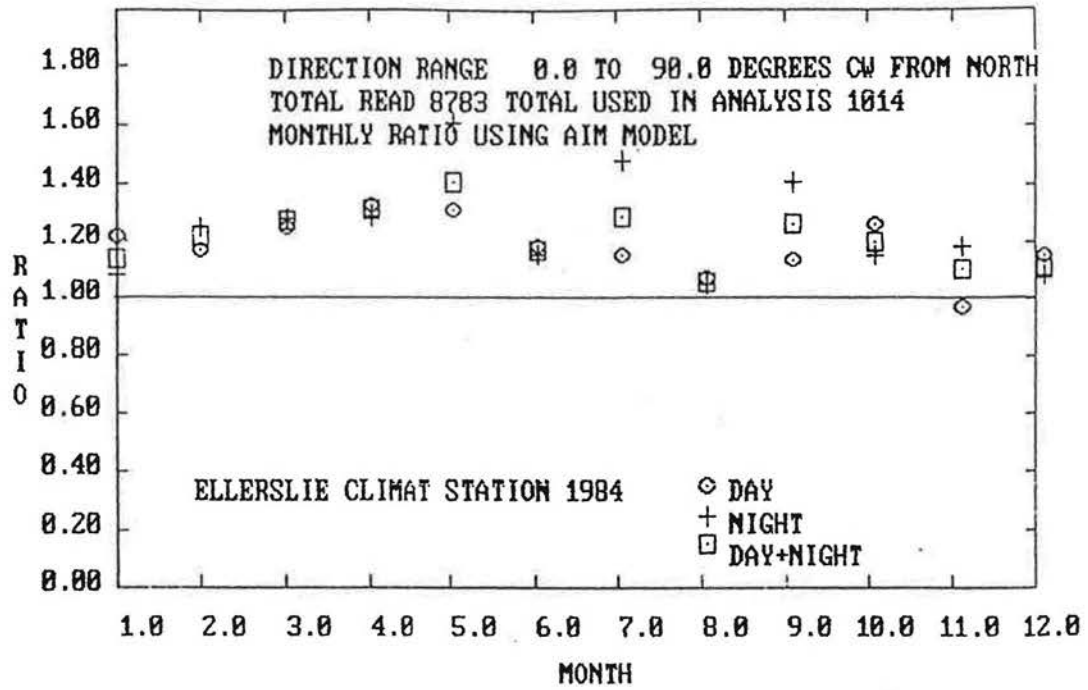


Figure A112

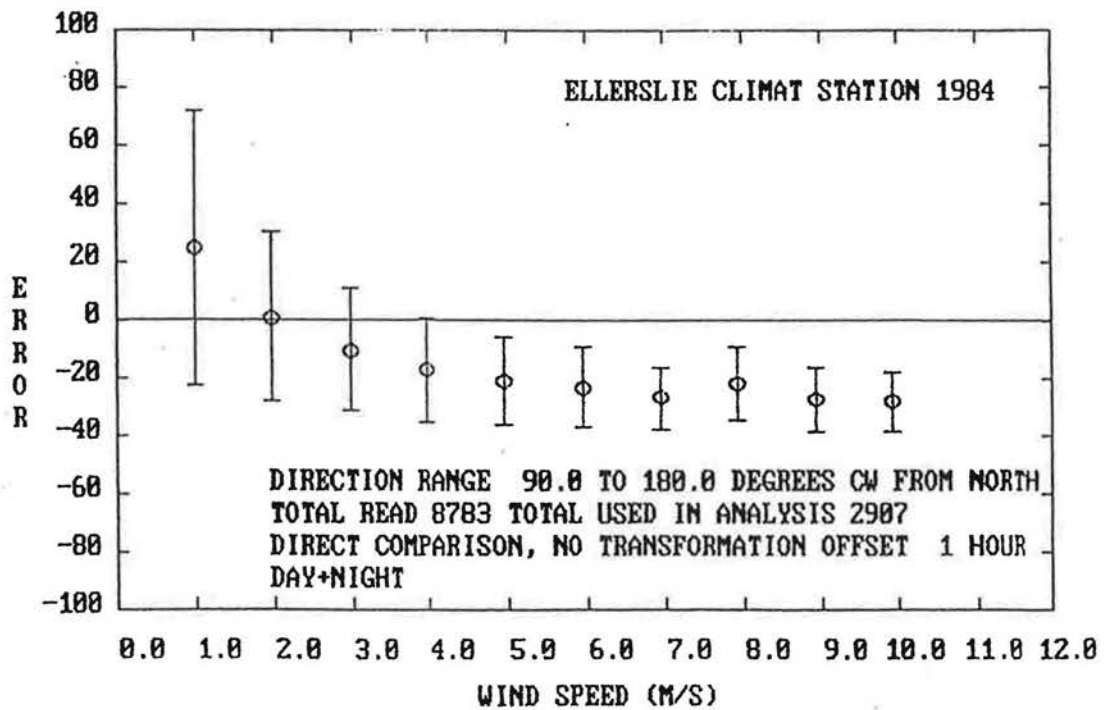


Figure A113

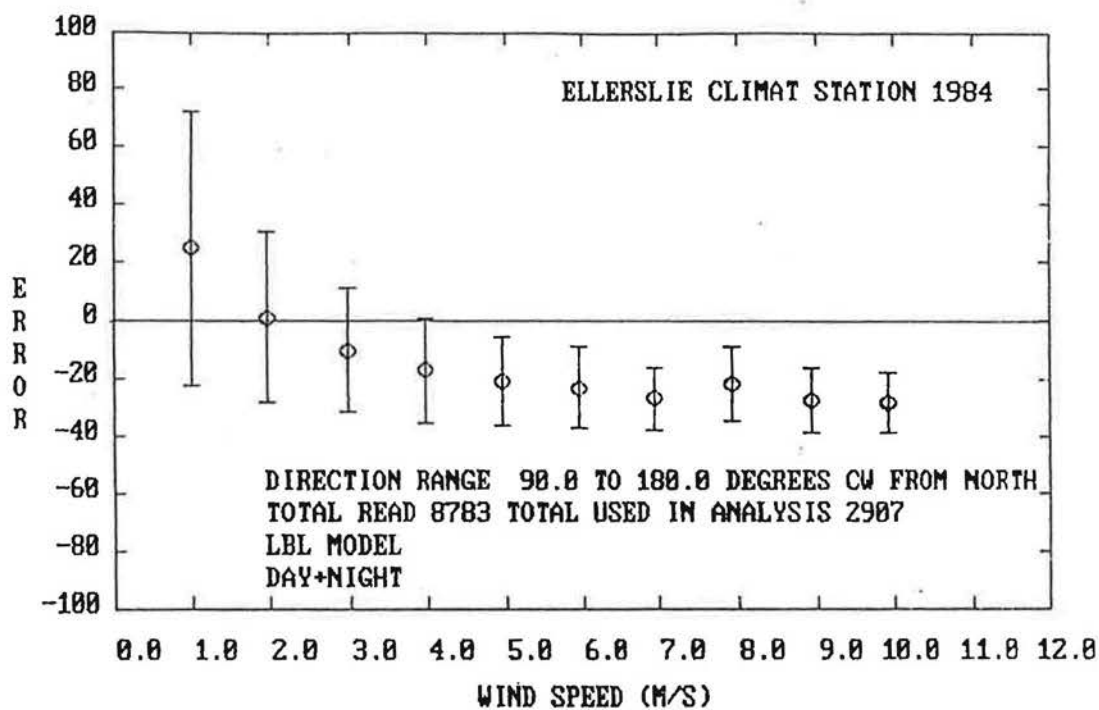


Figure A114

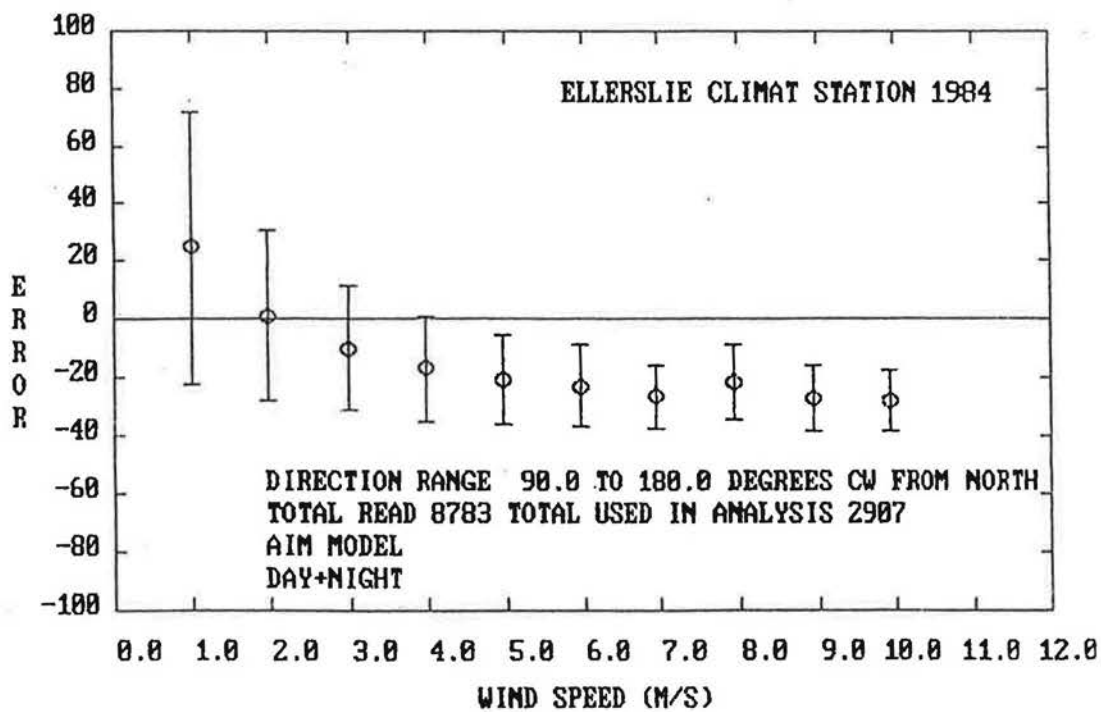


Figure A115

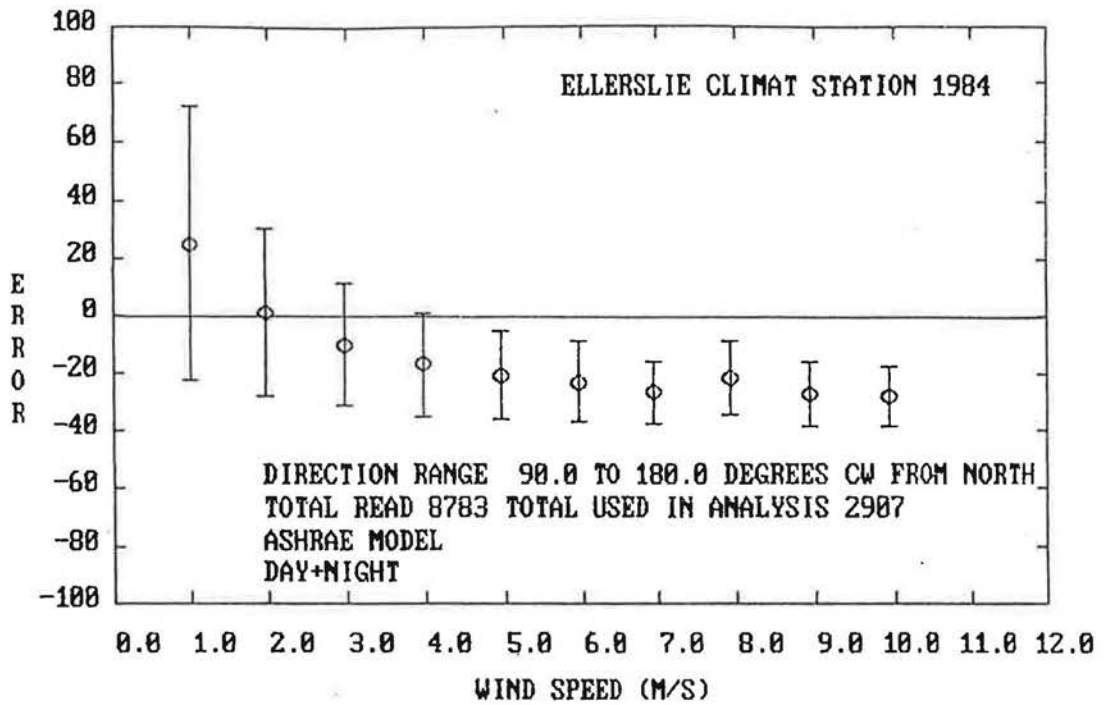


Figure A116

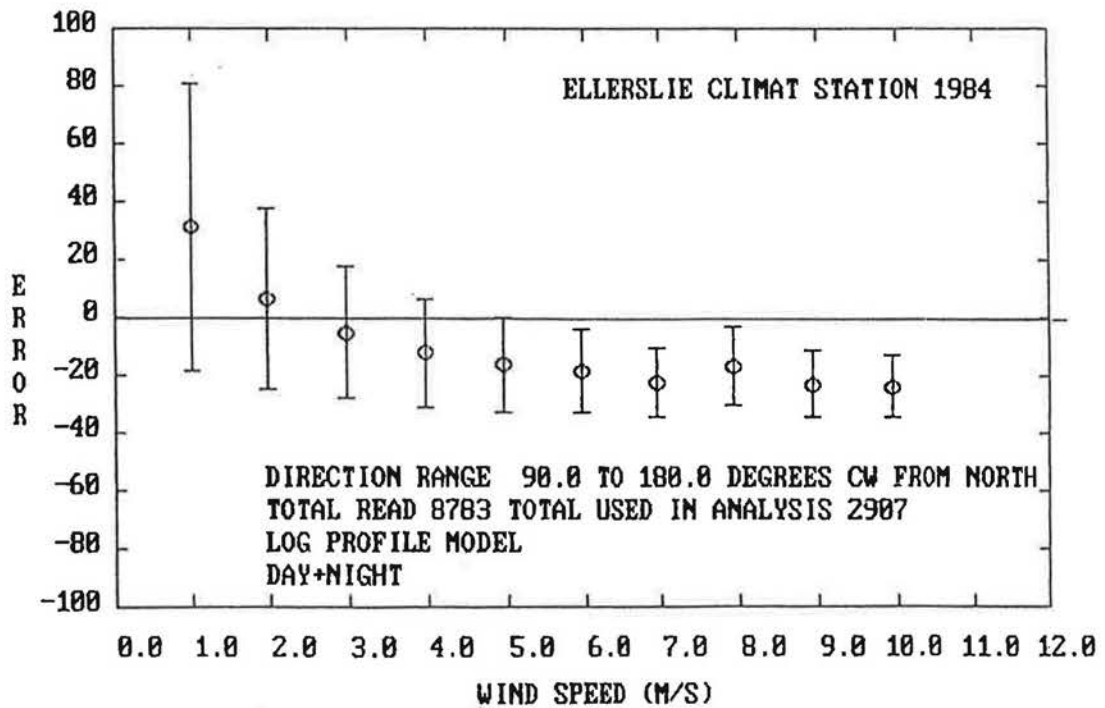


Figure A117

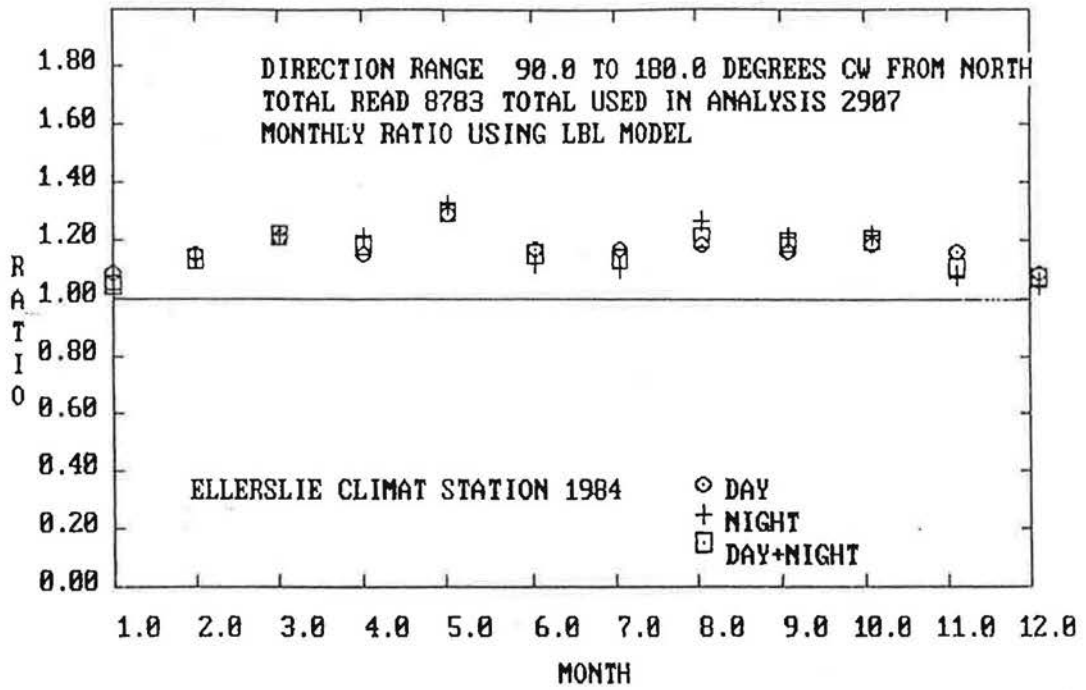


Figure A118

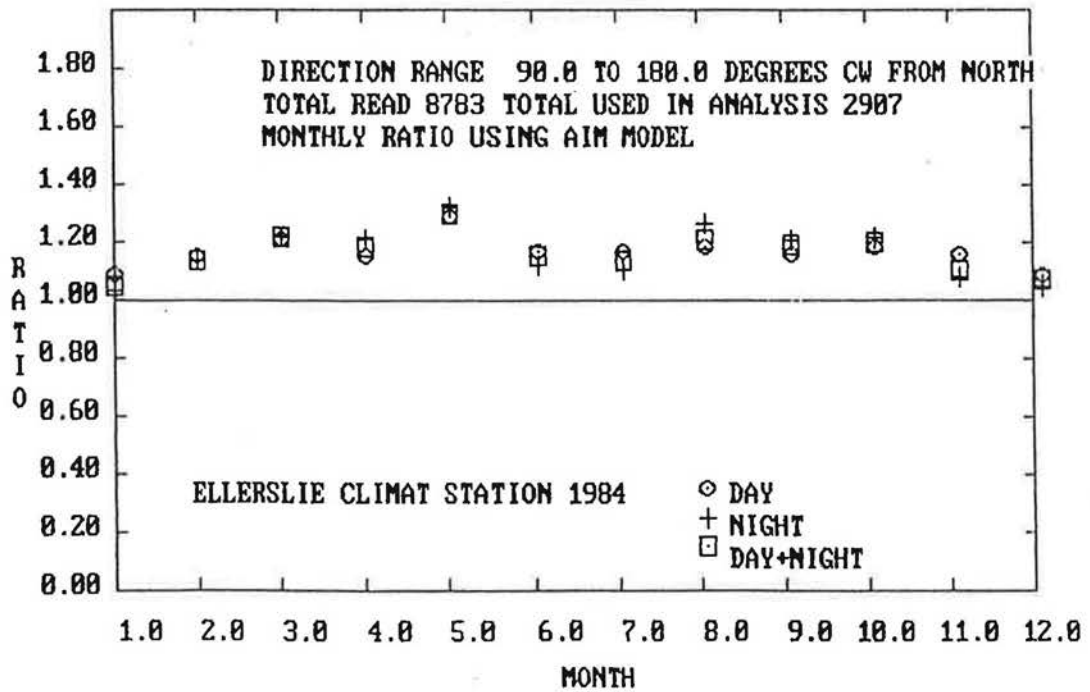


Figure A119

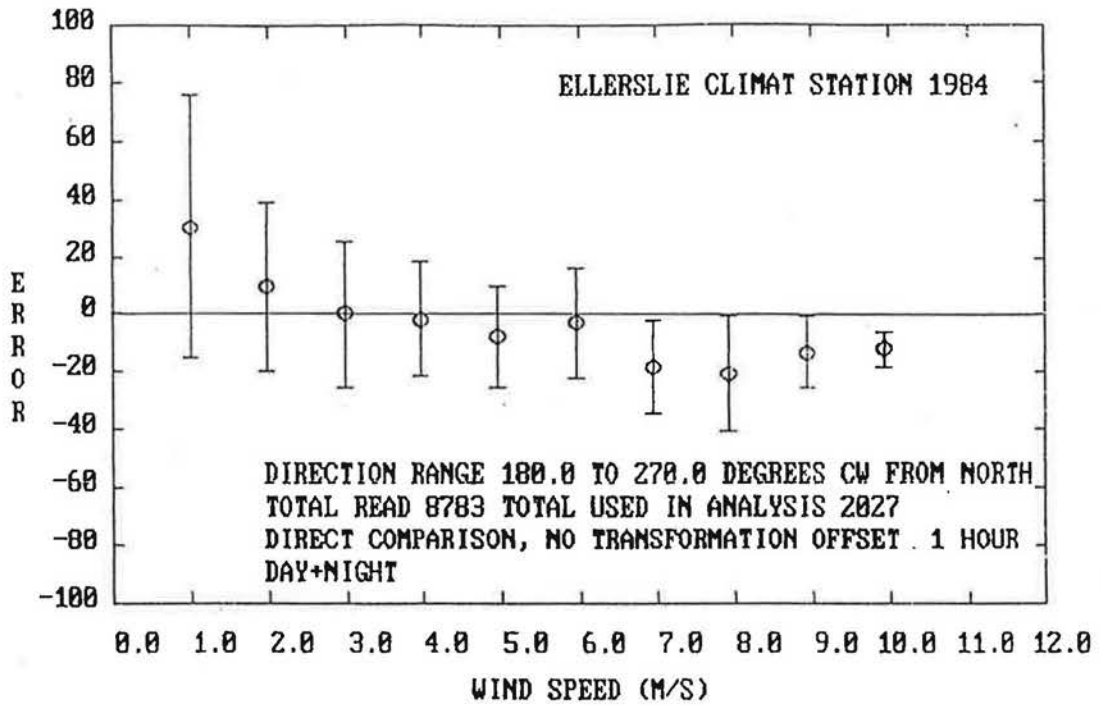


Figure A120

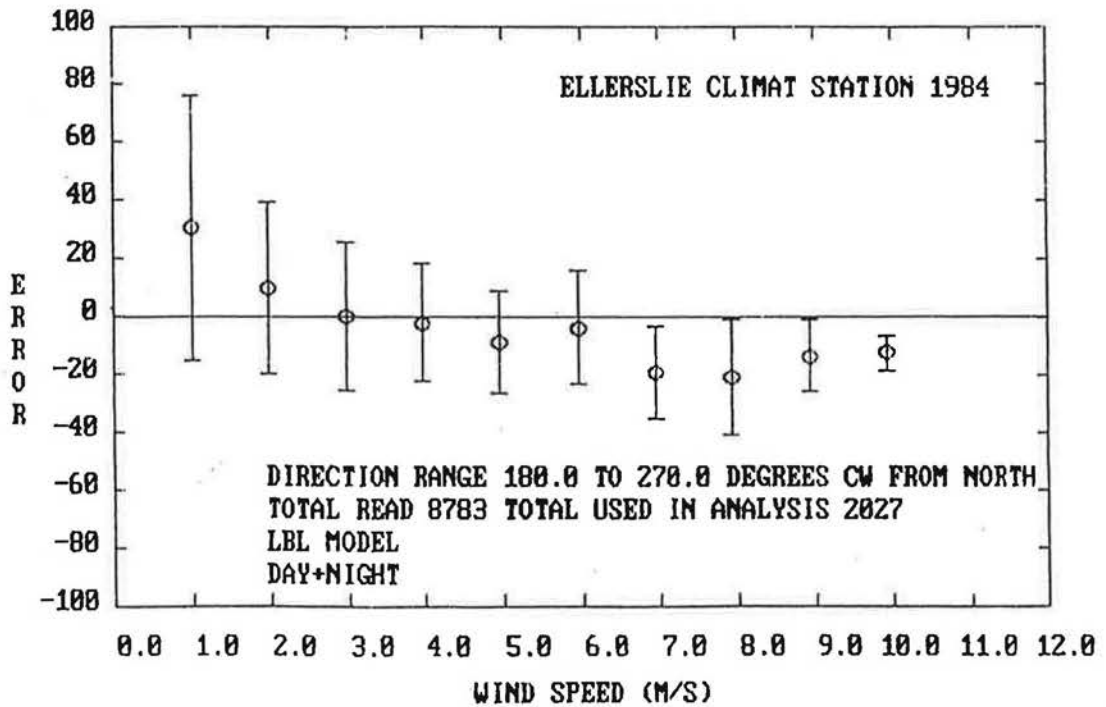


Figure A121

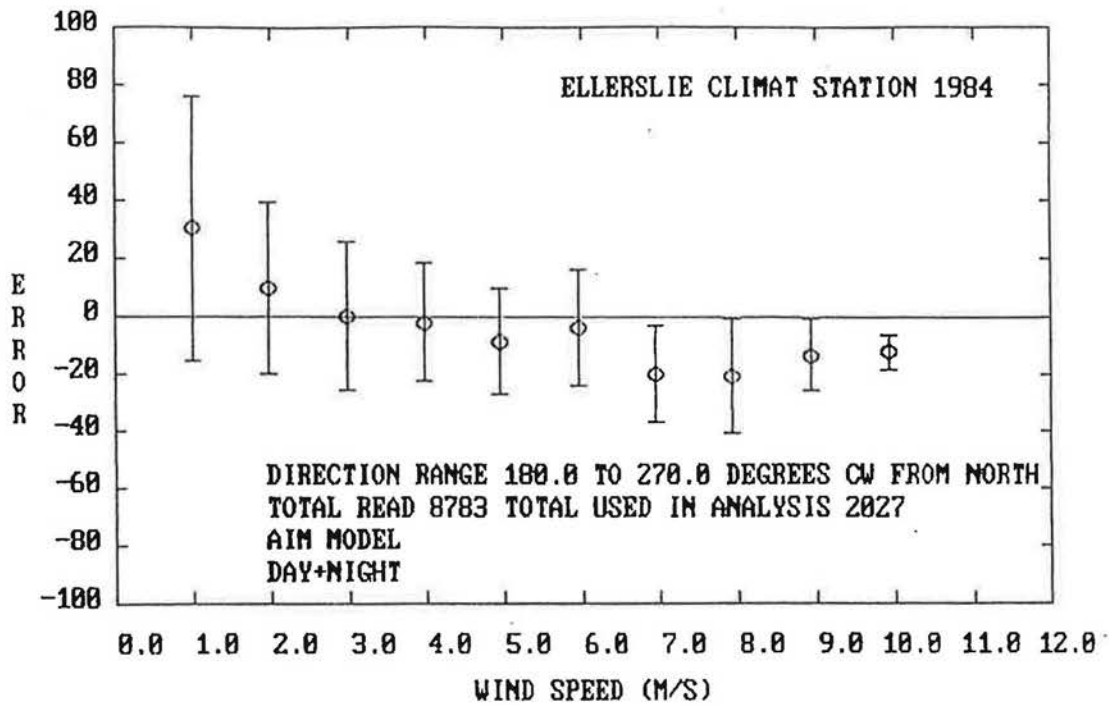


Figure A122

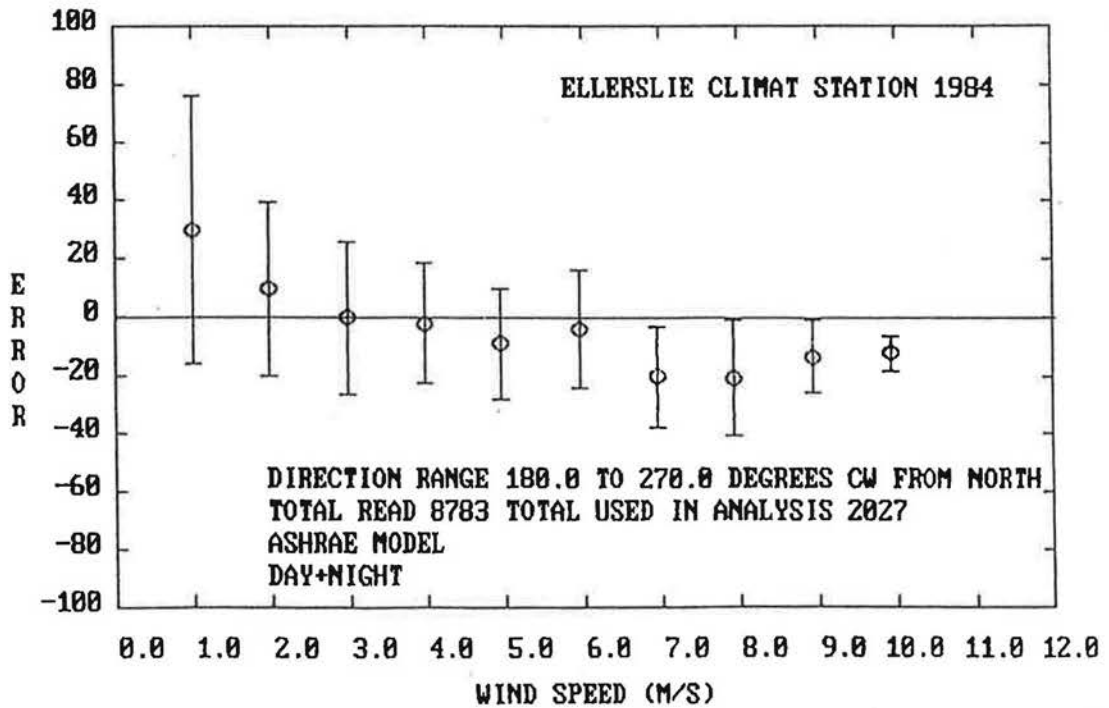


Figure A123

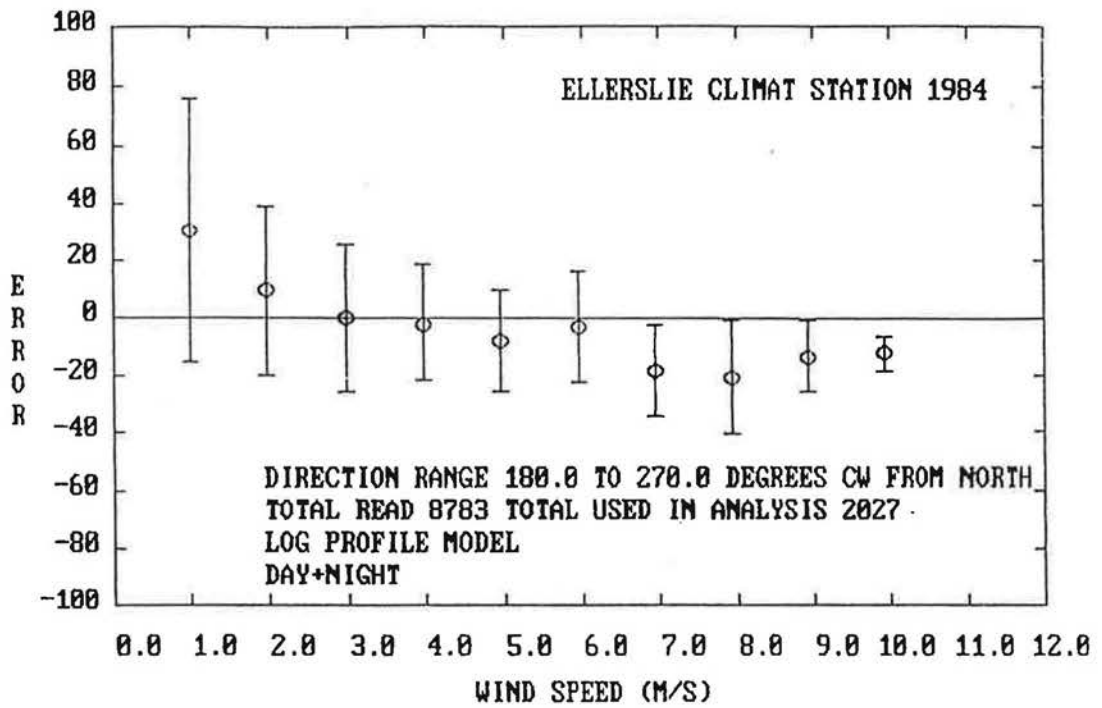


Figure A124

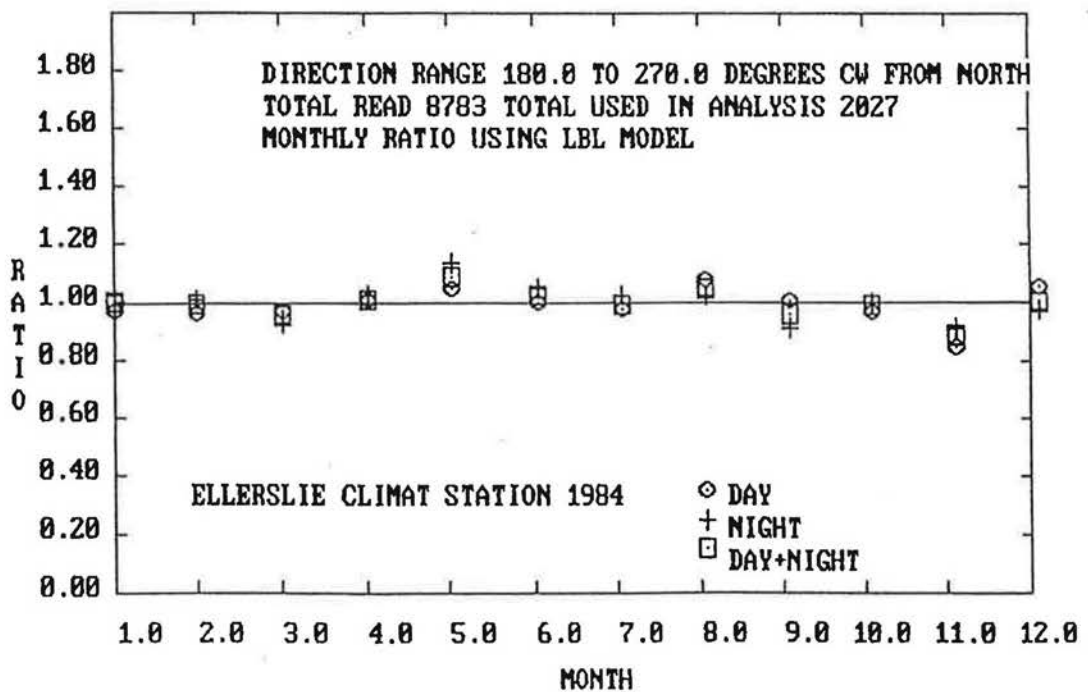


Figure A125

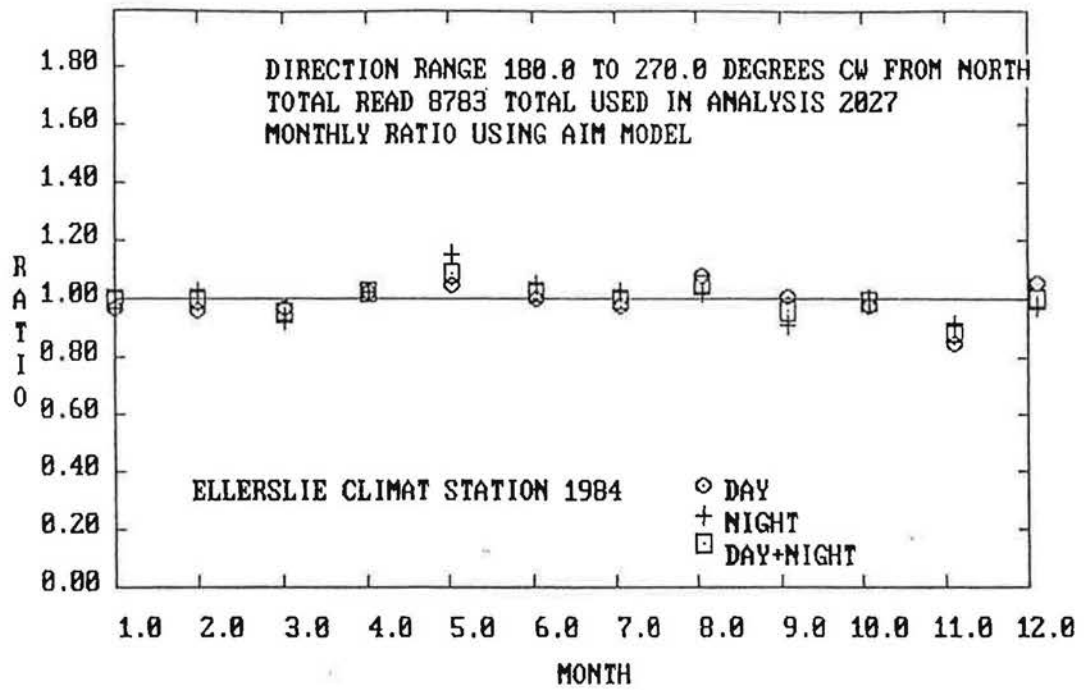


Figure A126

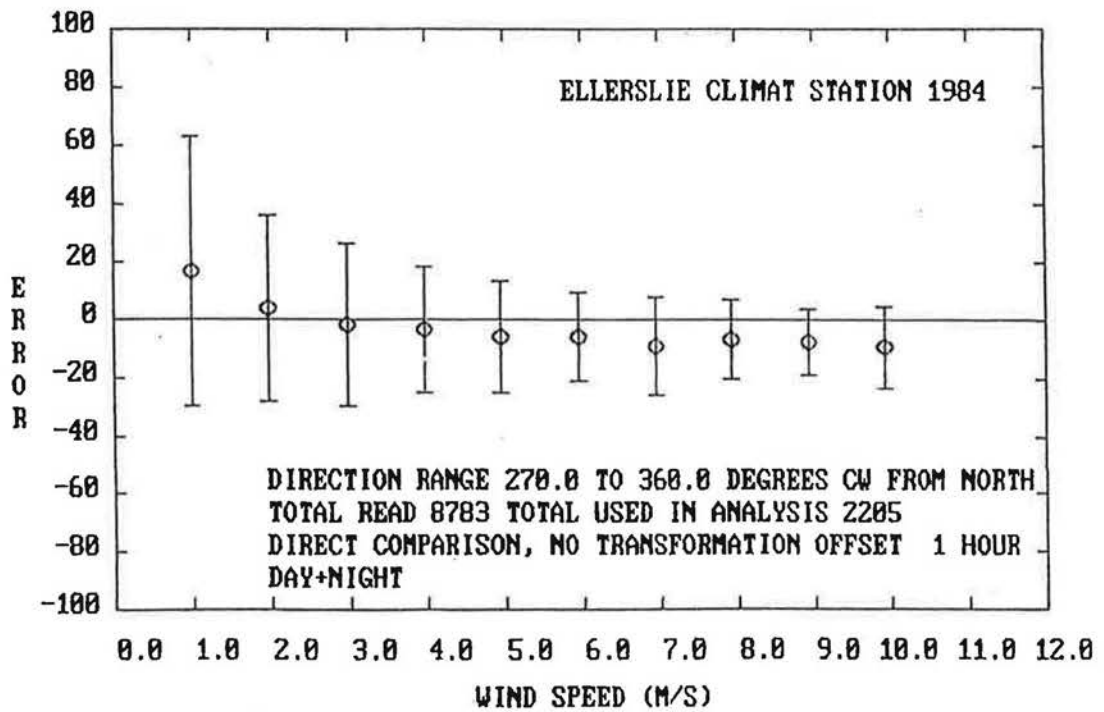


Figure A127

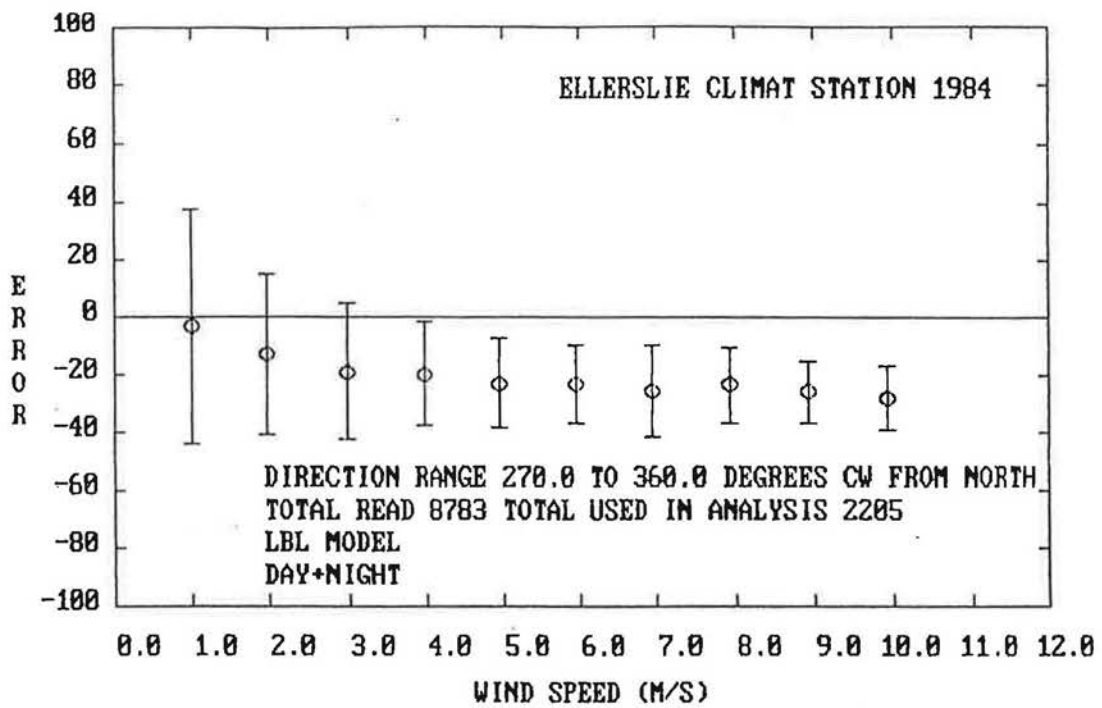


Figure A128

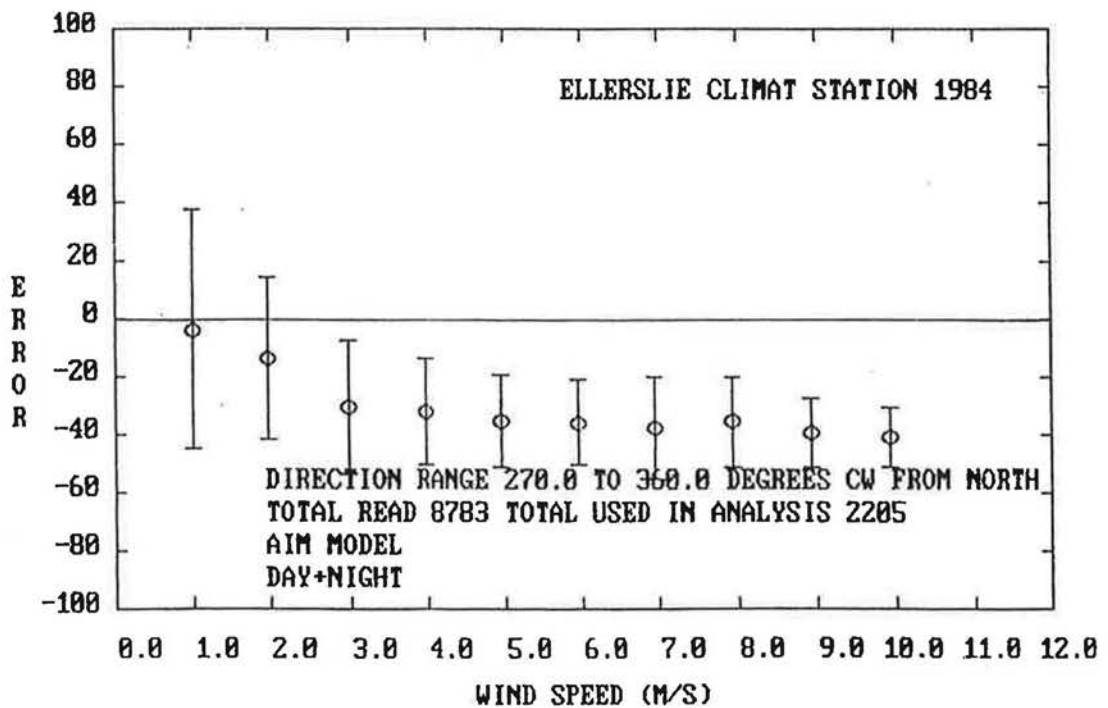


Figure A129

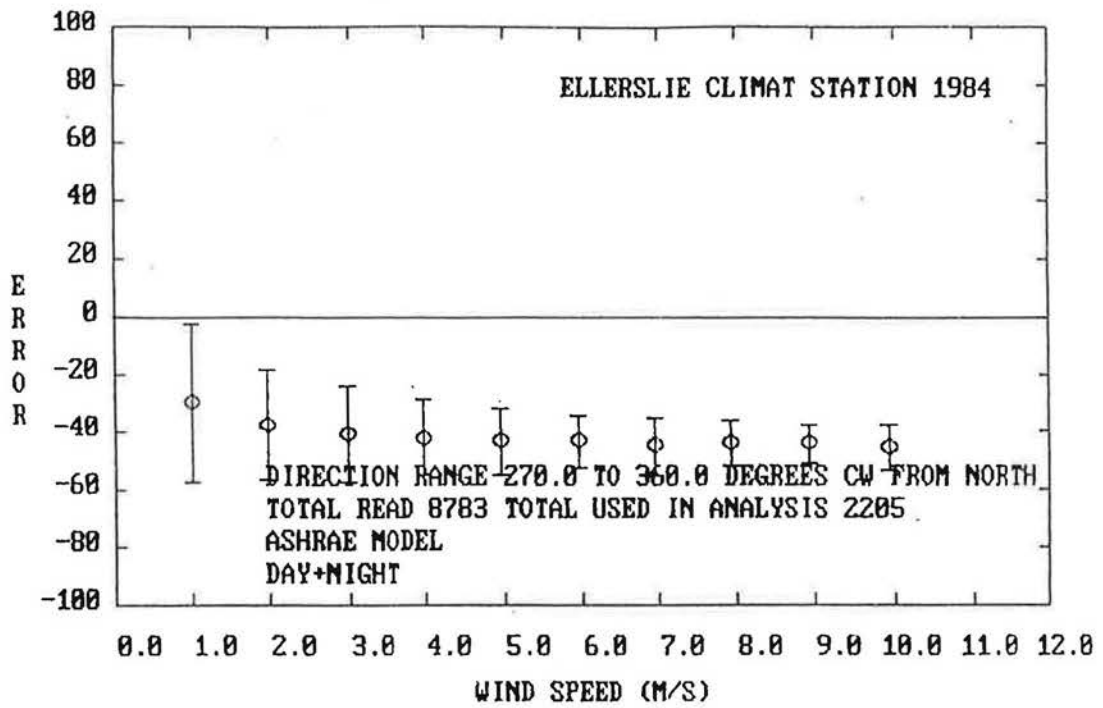


Figure A130

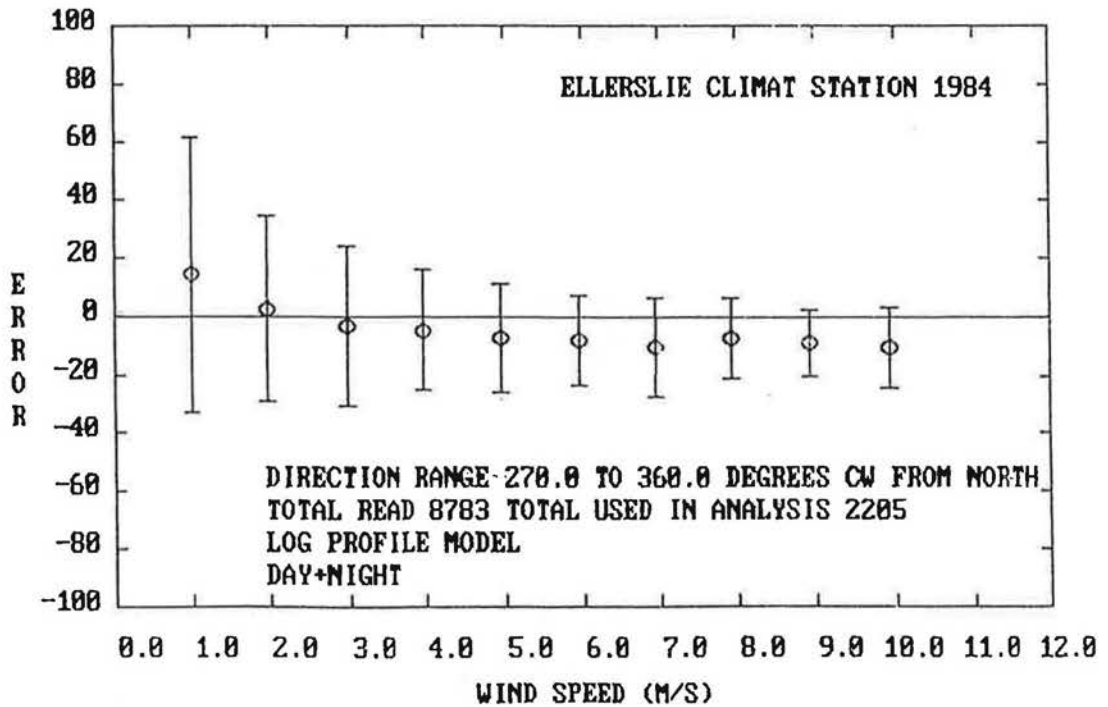


Figure A131

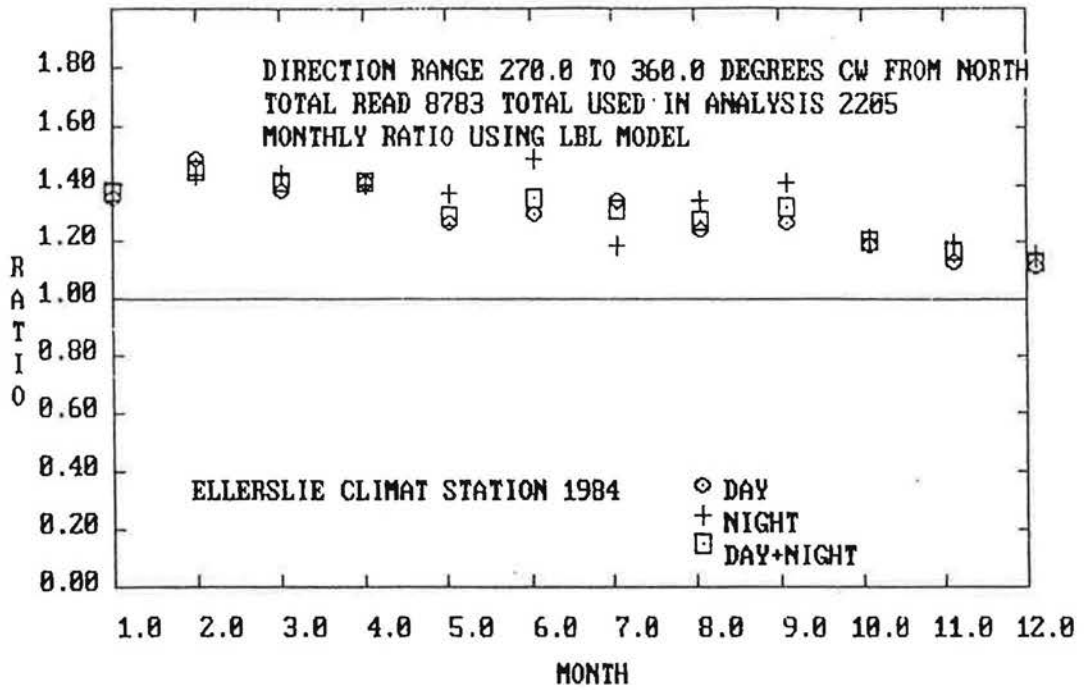


Figure A132

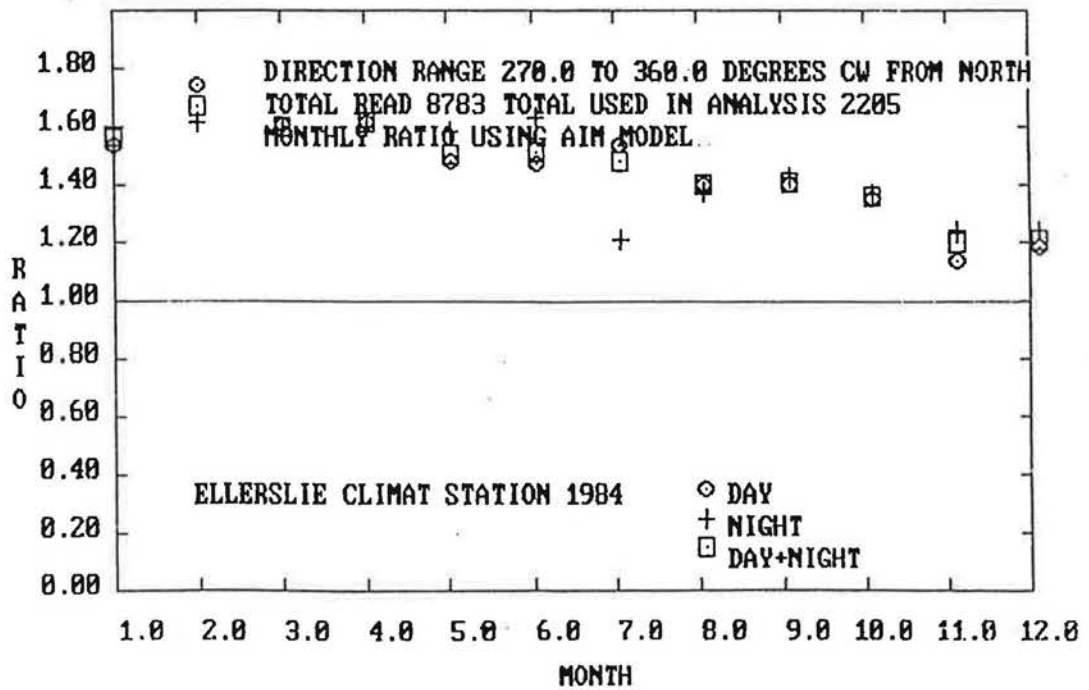


Figure A133

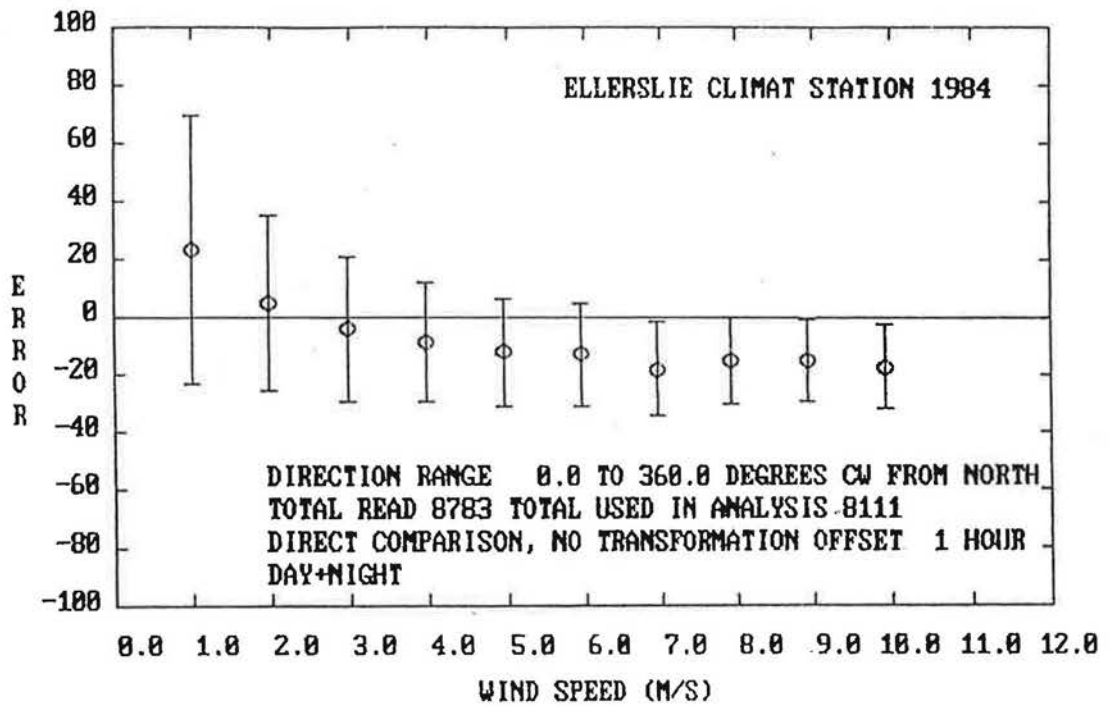


Figure A134

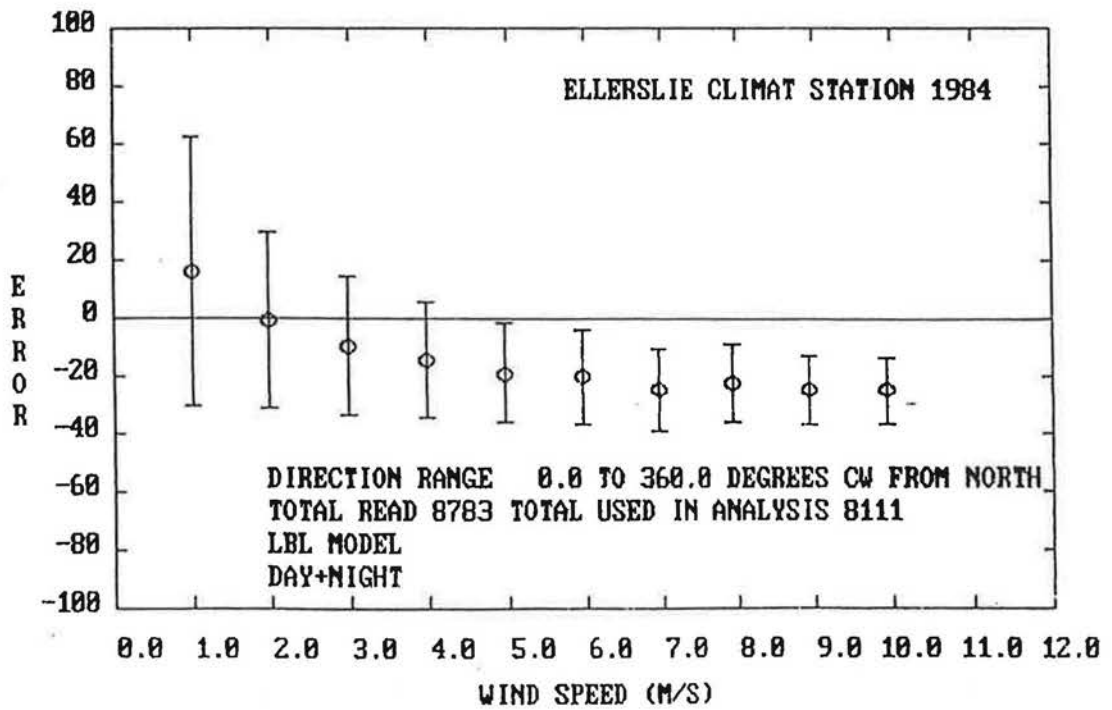


Figure A135

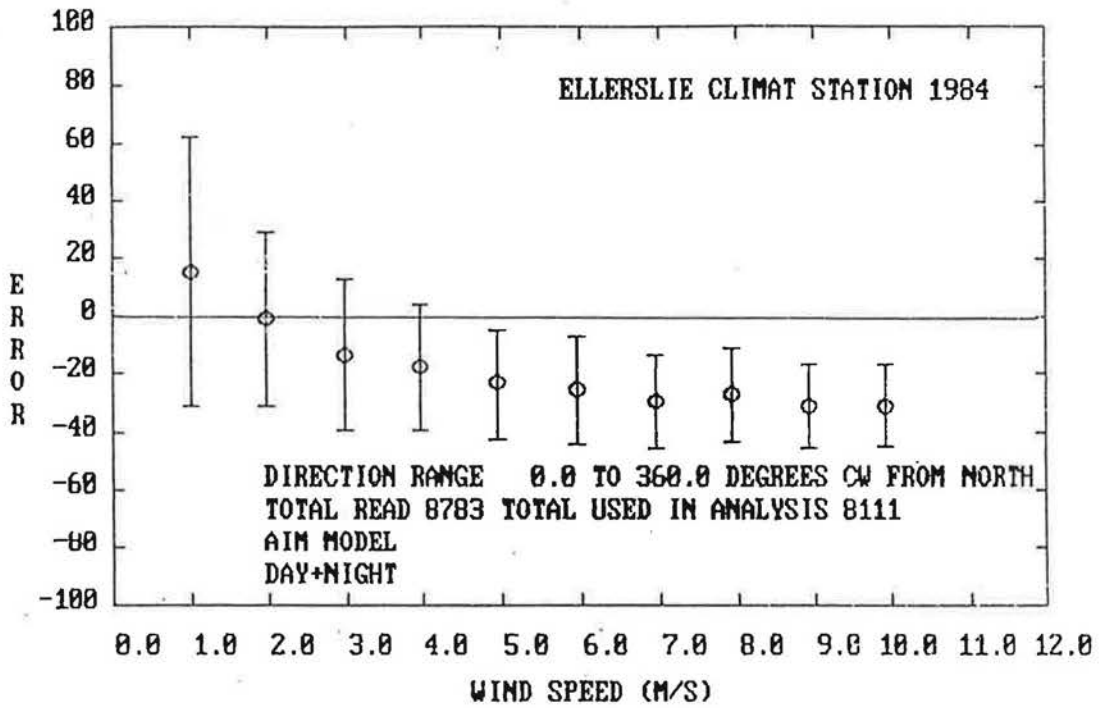


Figure A136

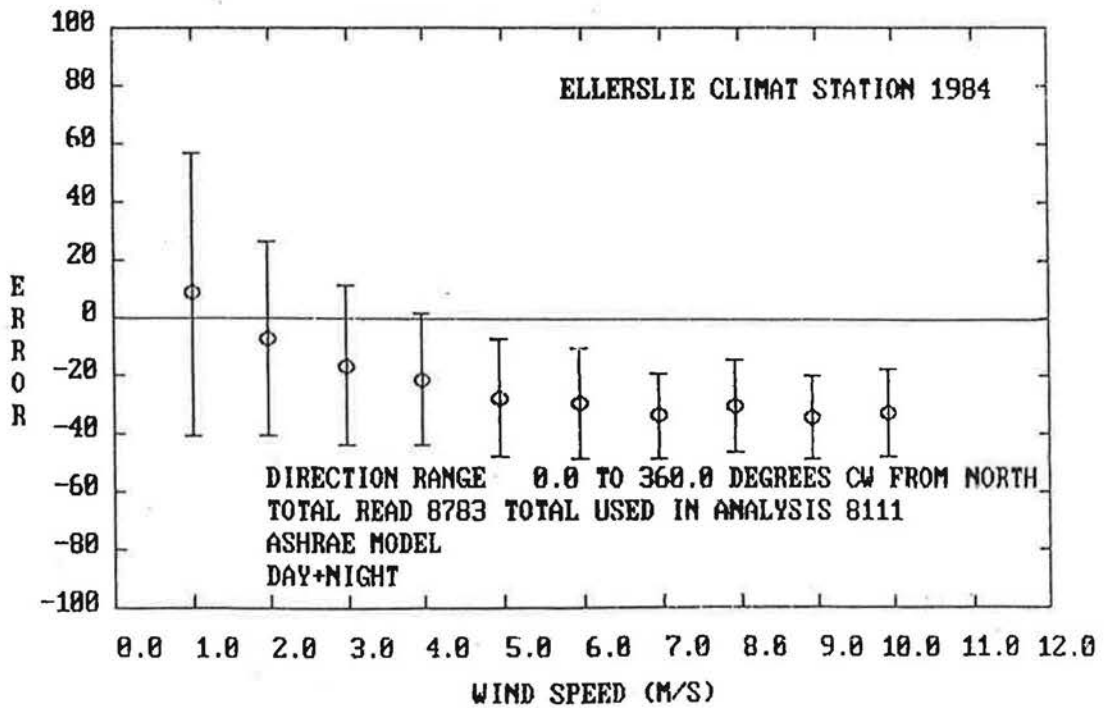


Figure A137

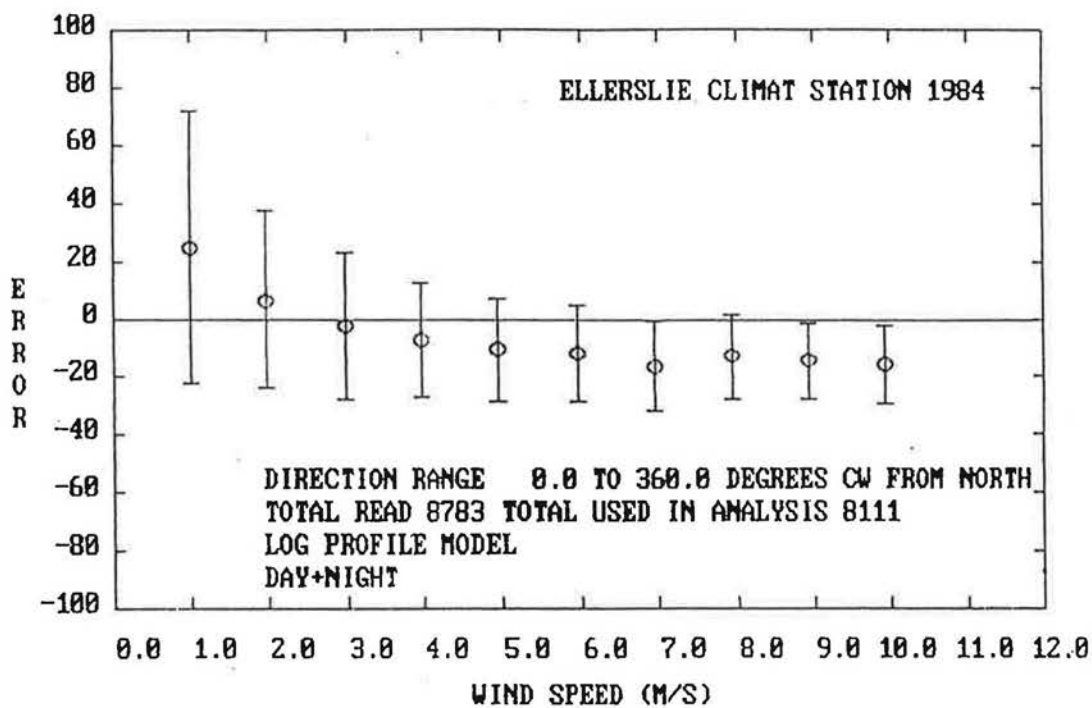


Figure A138

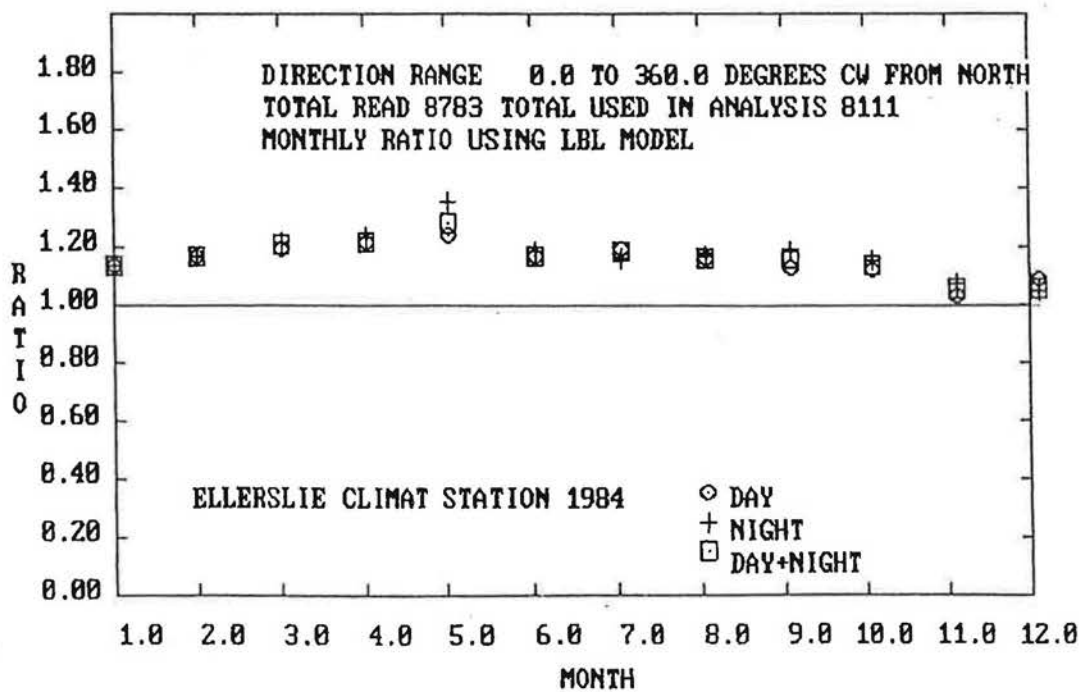


Figure A139

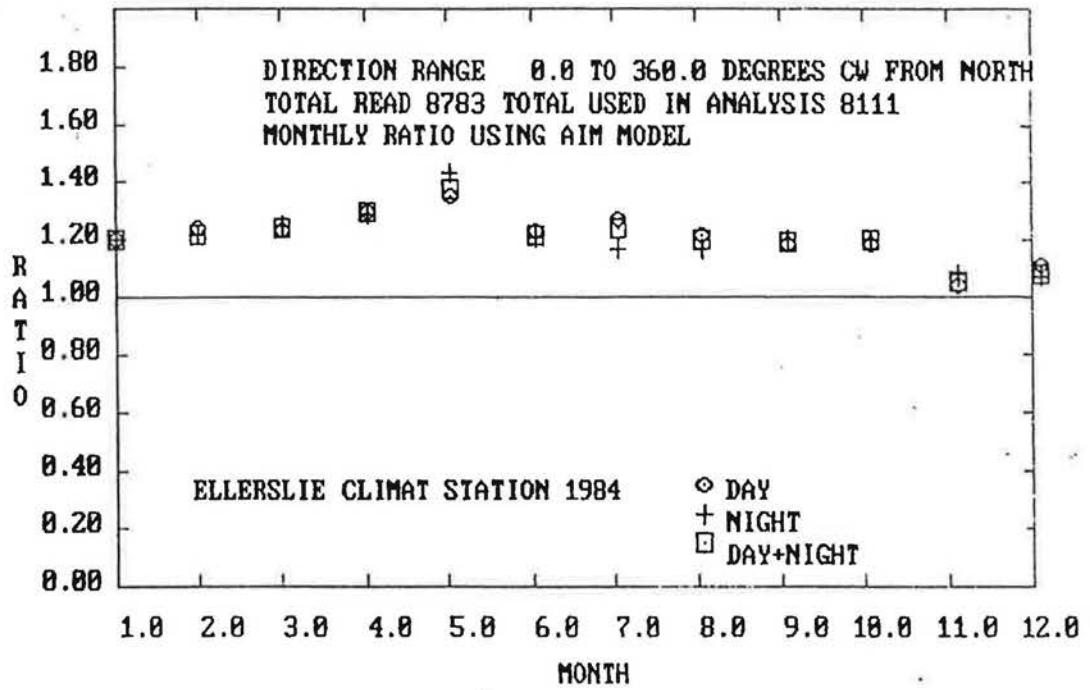


Figure A140

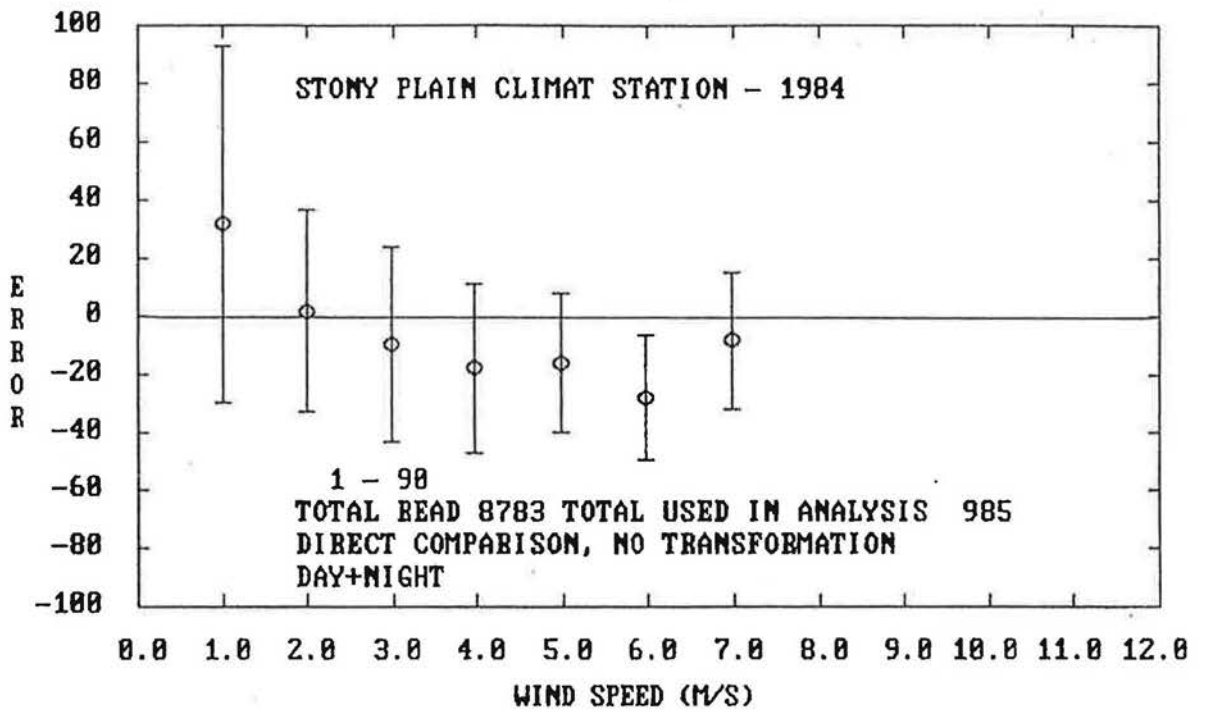


Figure A141

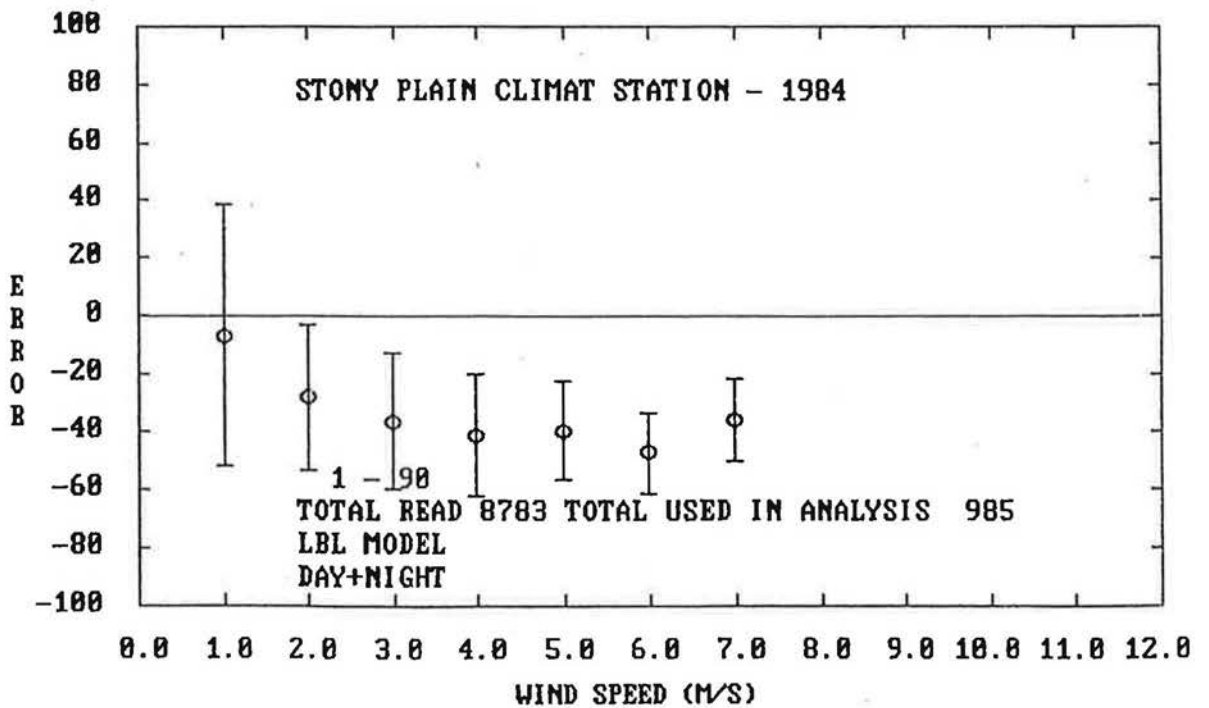


Figure A142

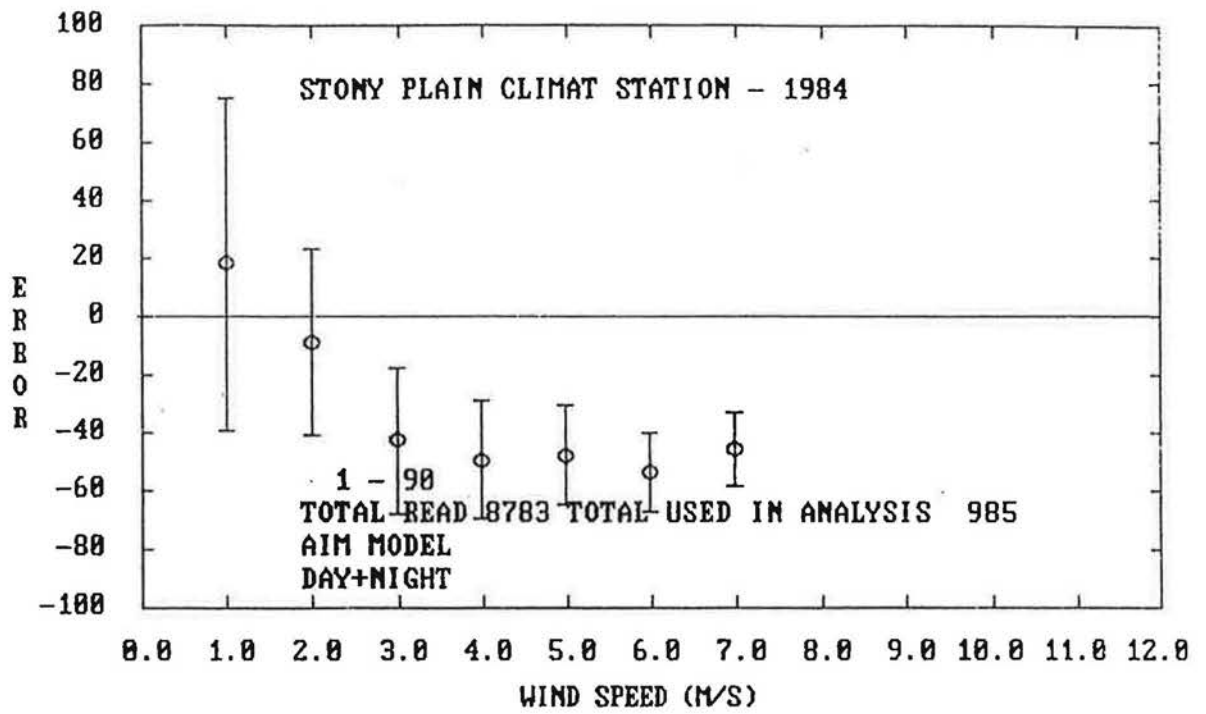


Figure A143

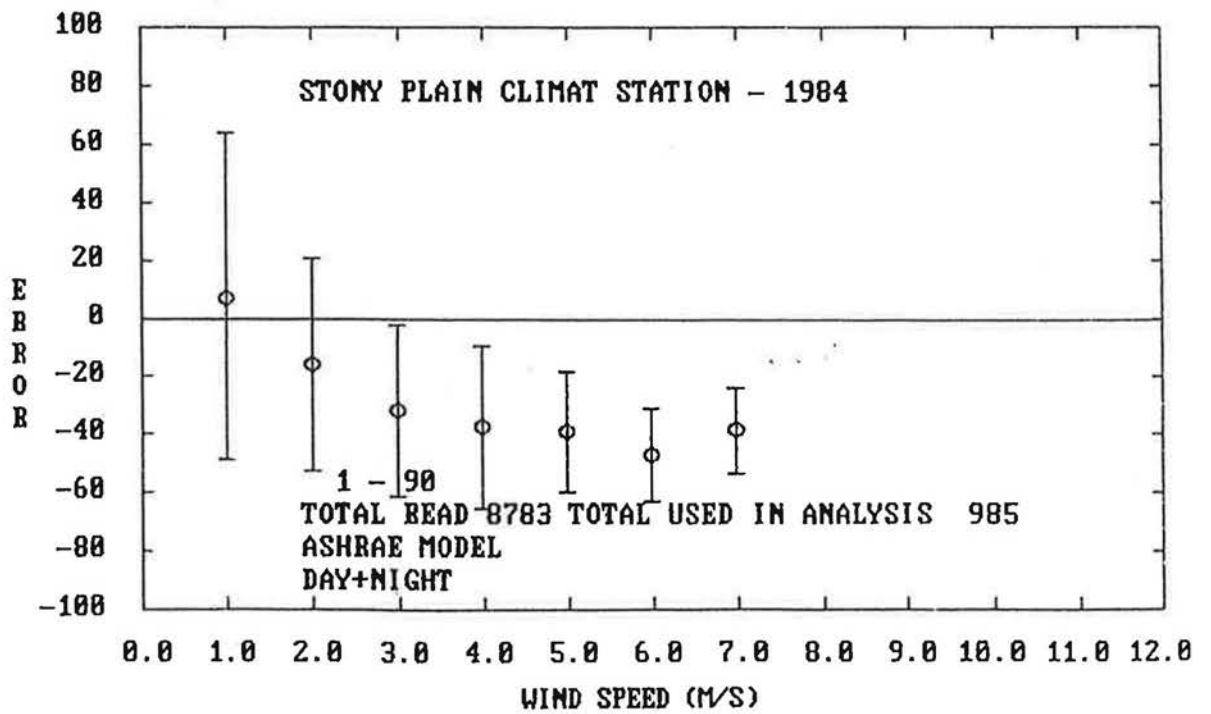


Figure A144

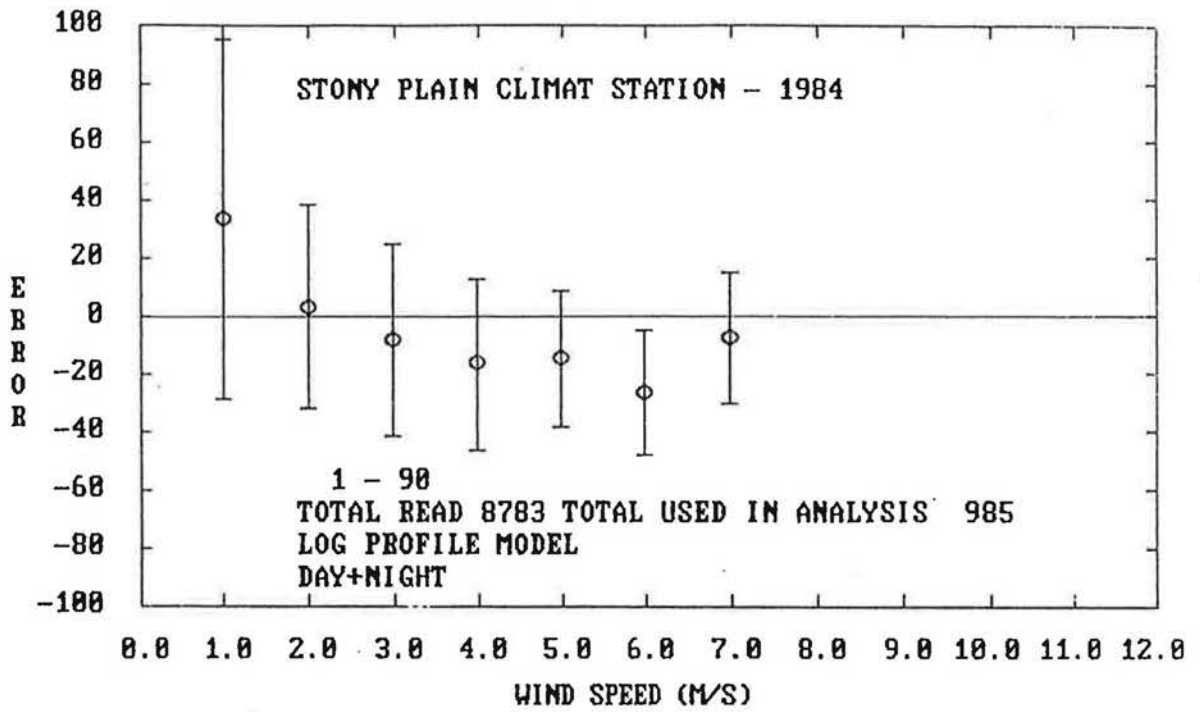


Figure A145

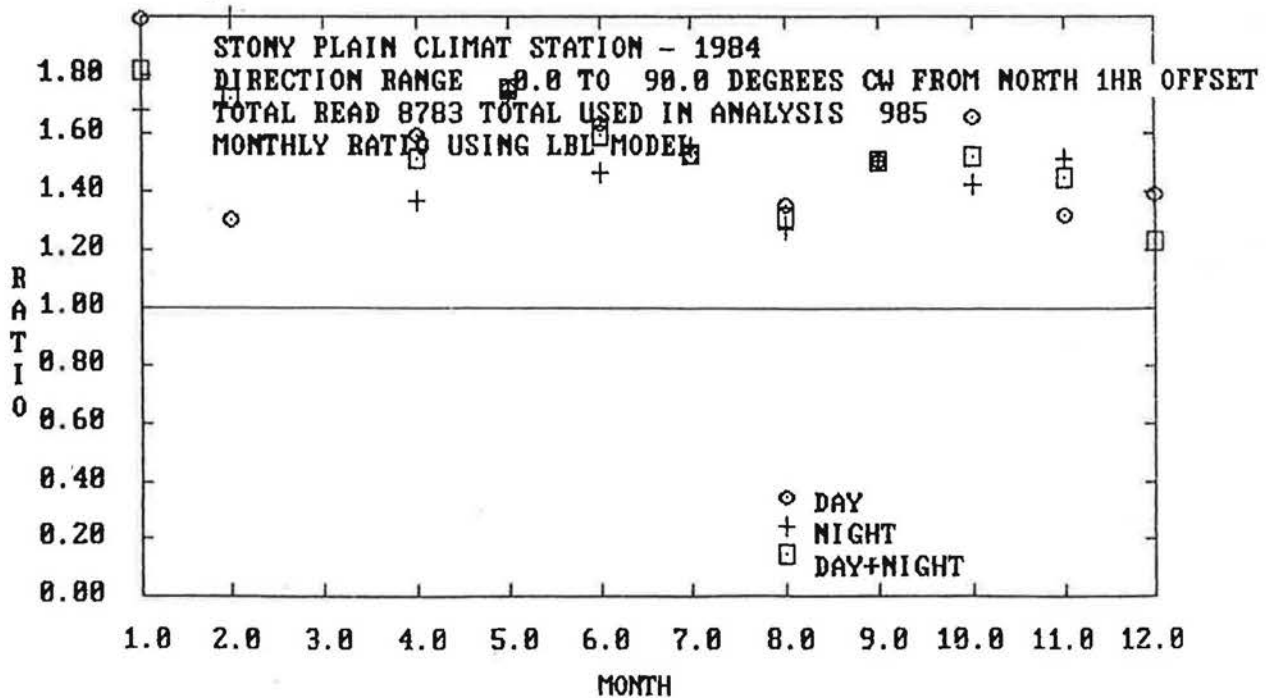


Figure A146

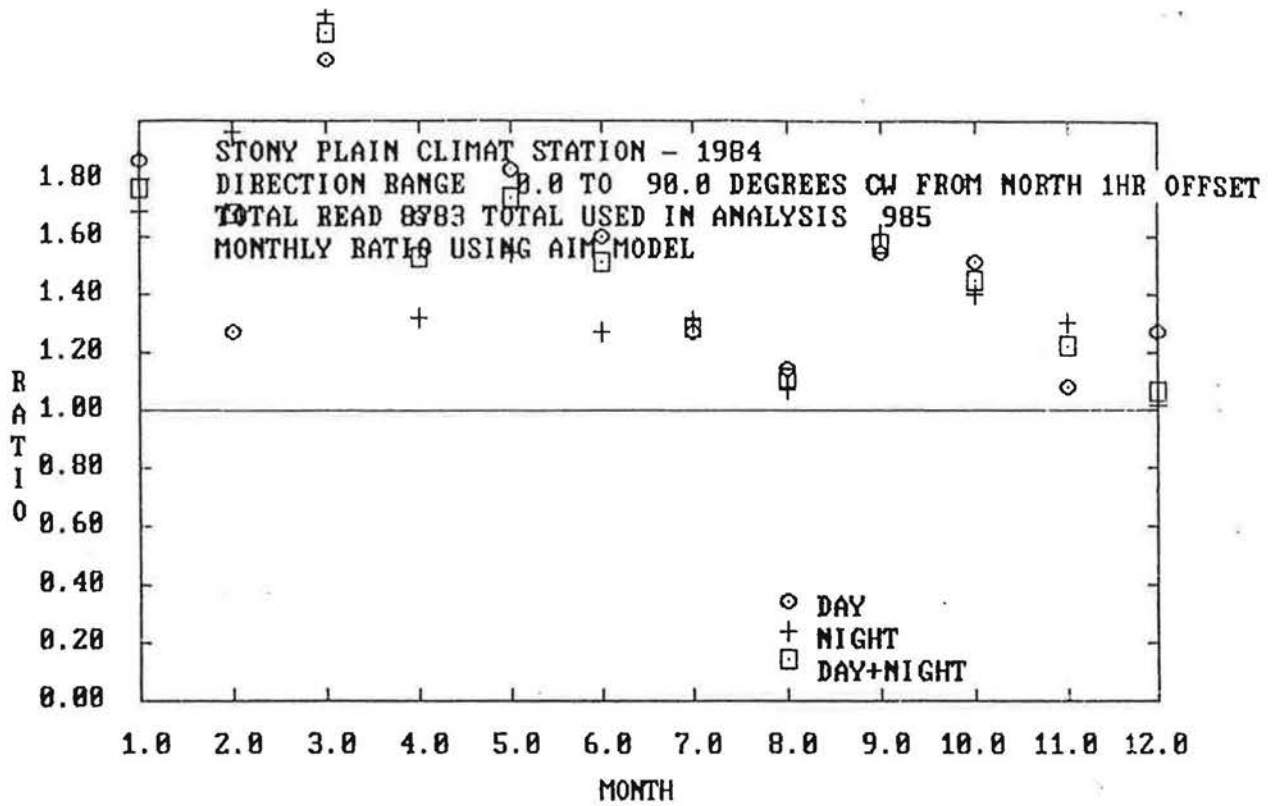


Figure A147

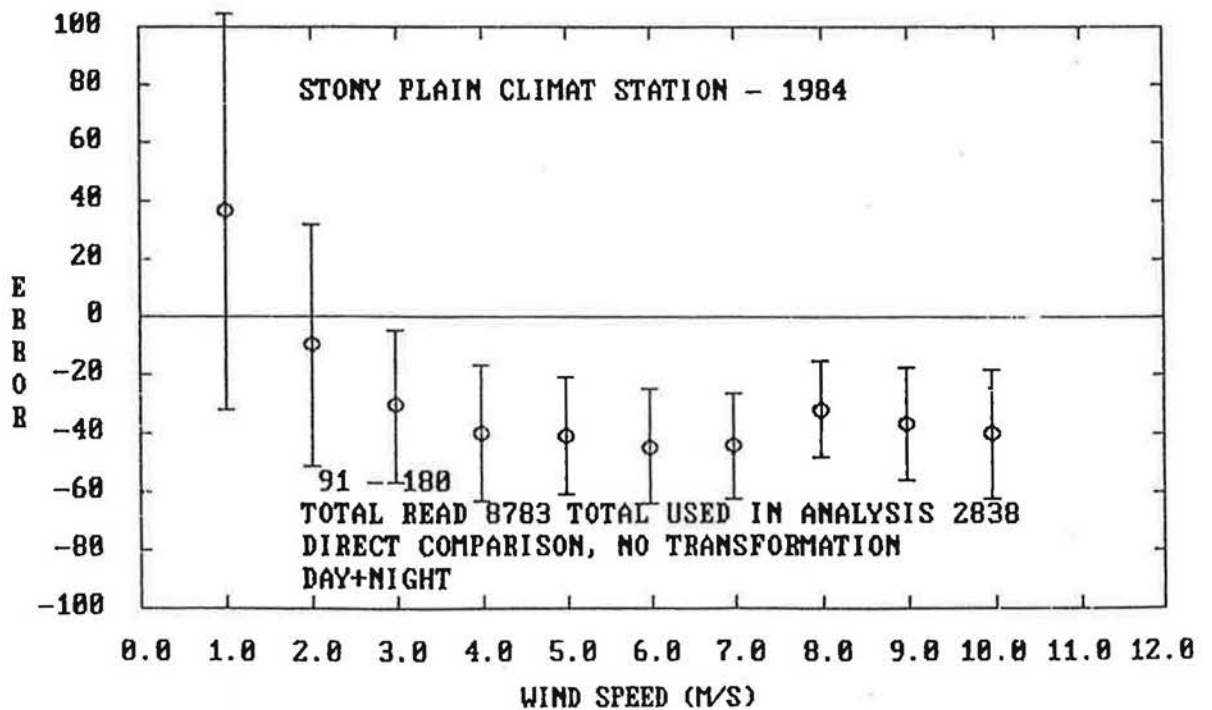


Figure A148

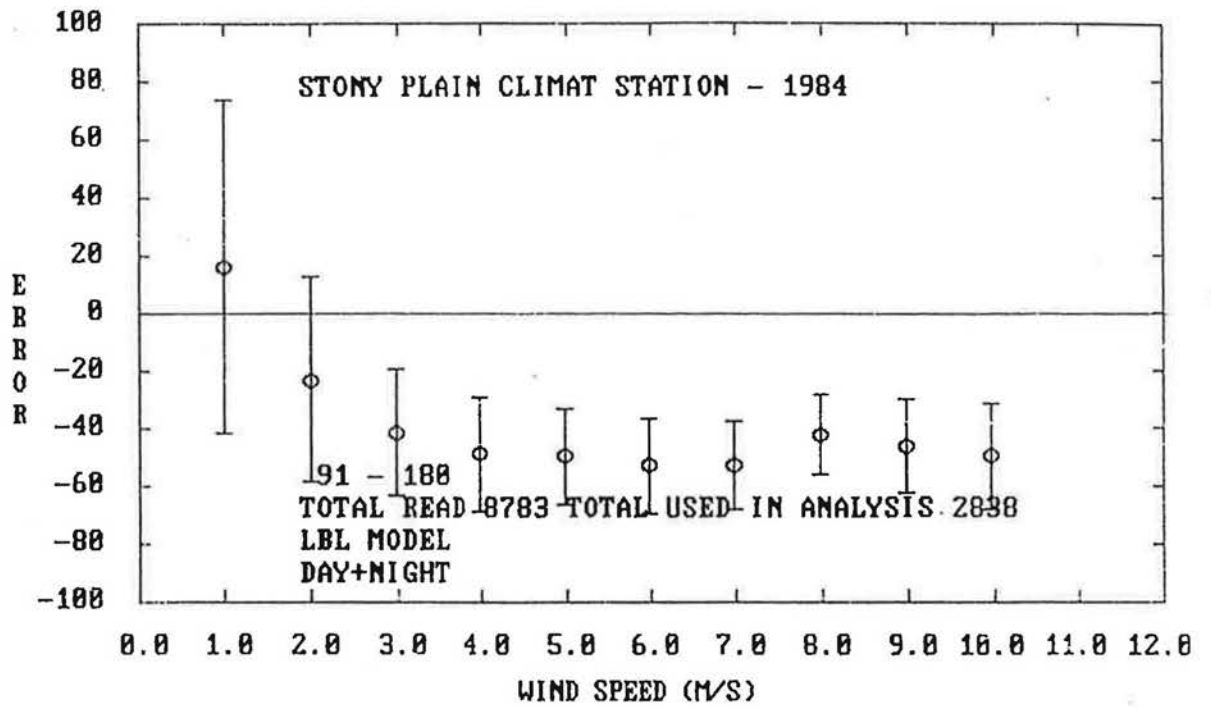


Figure A149

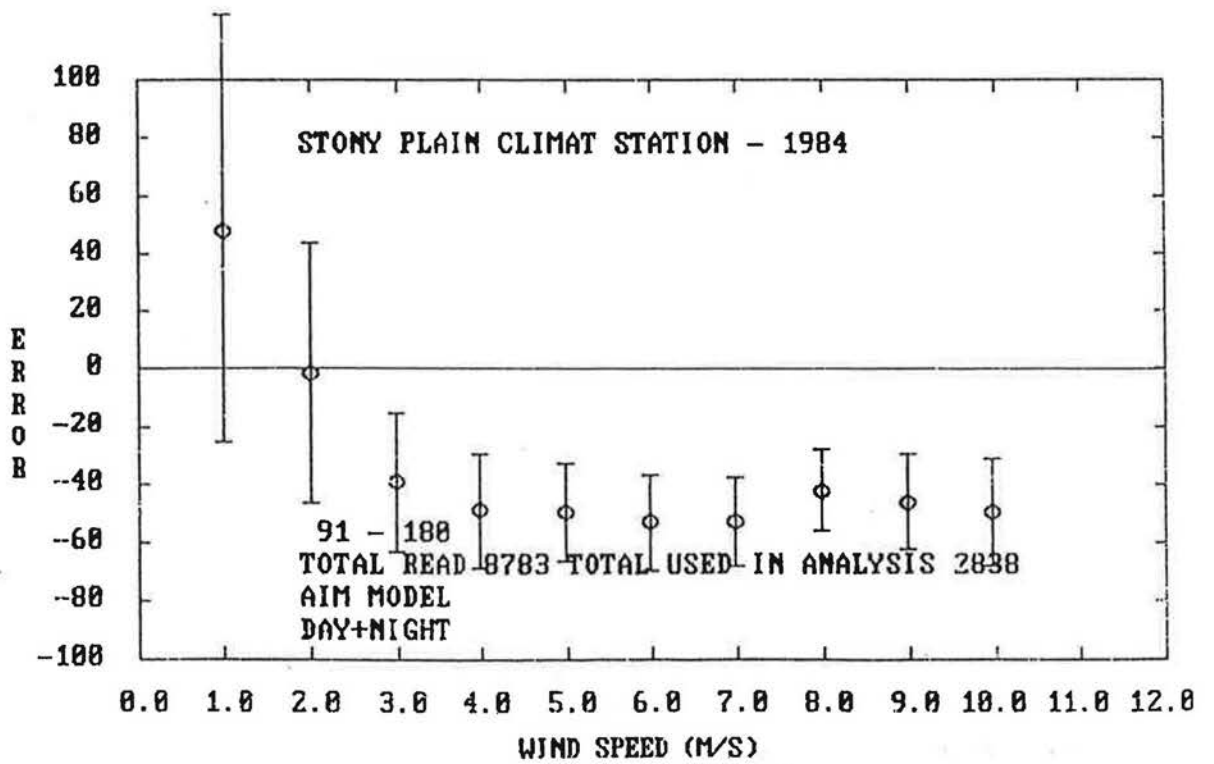


Figure A150

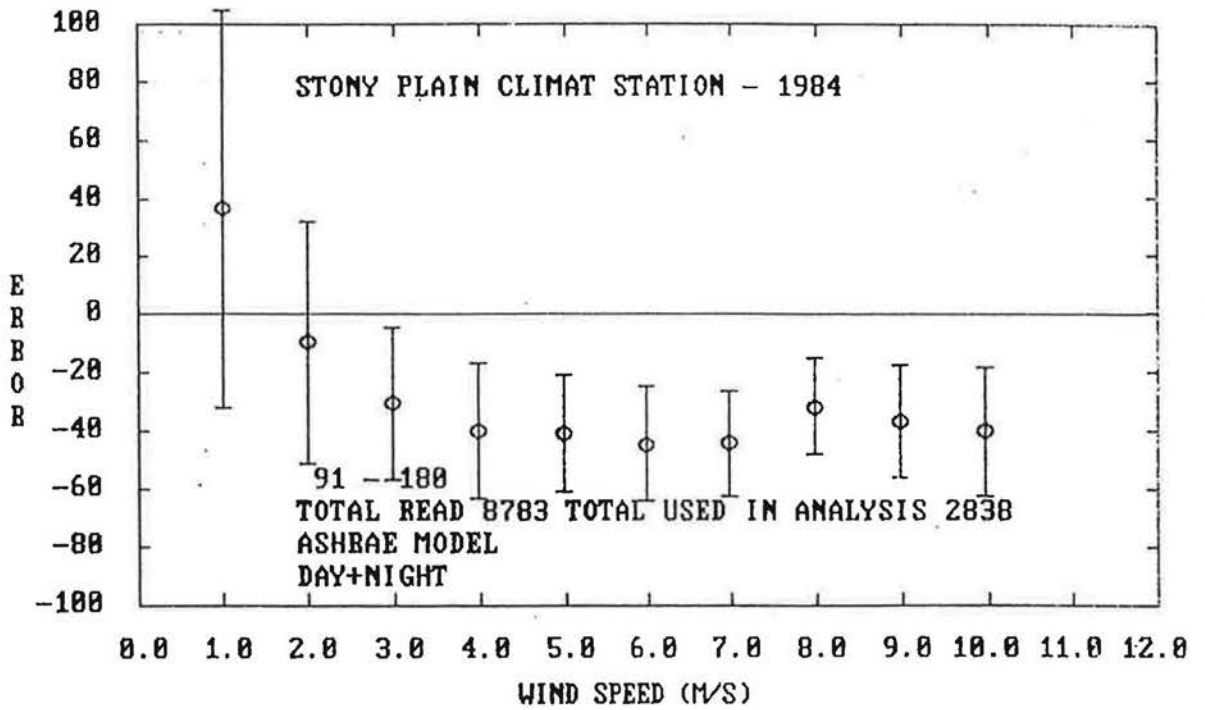


Figure A151

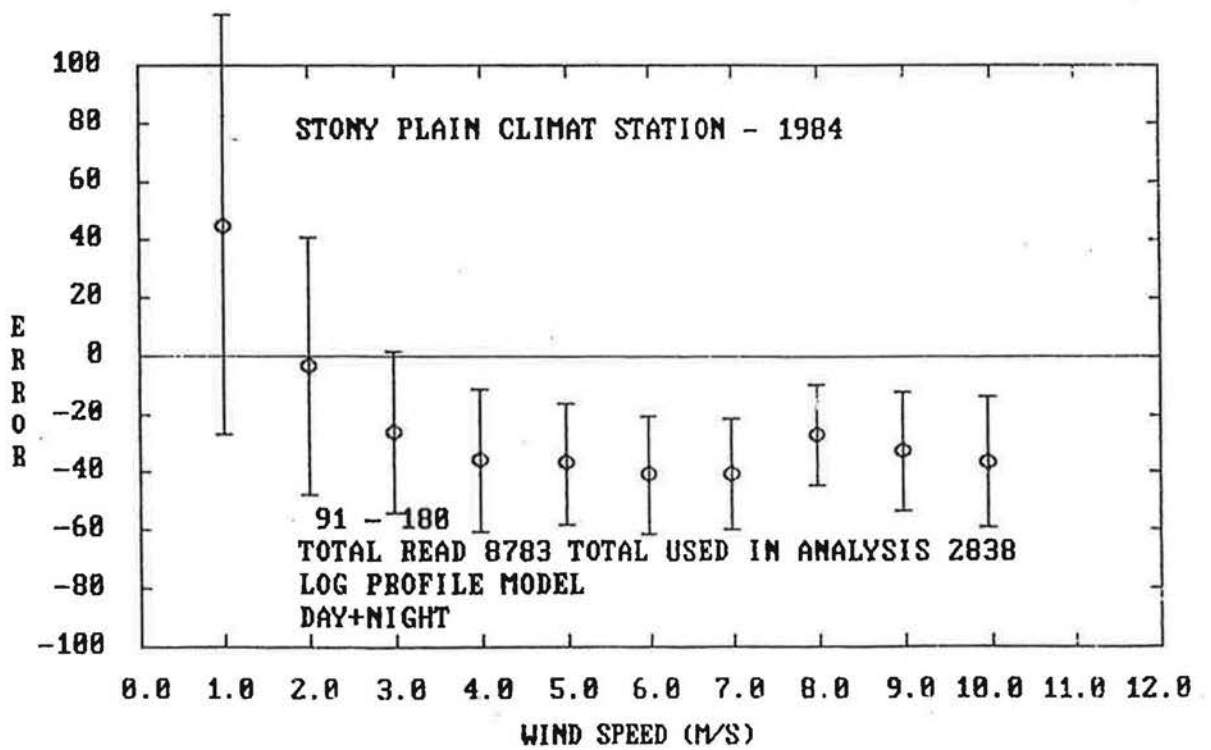


Figure A152

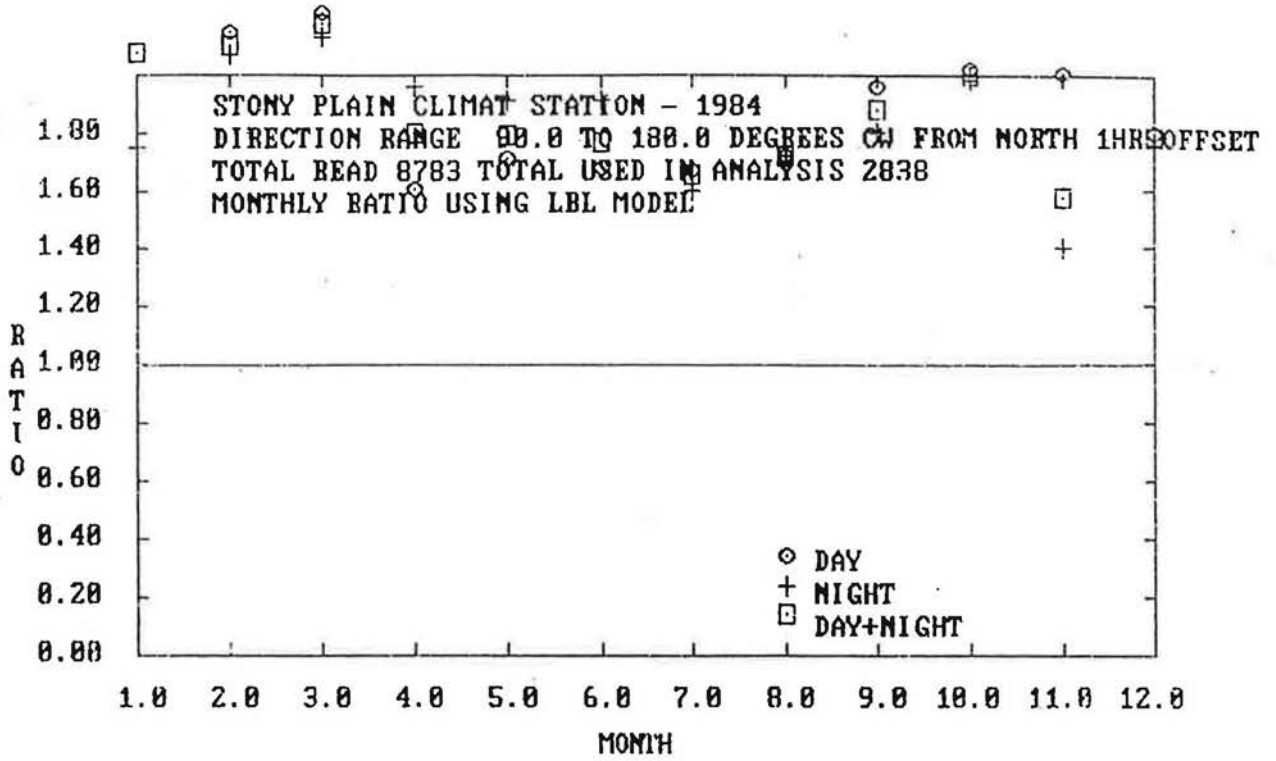


Figure A153

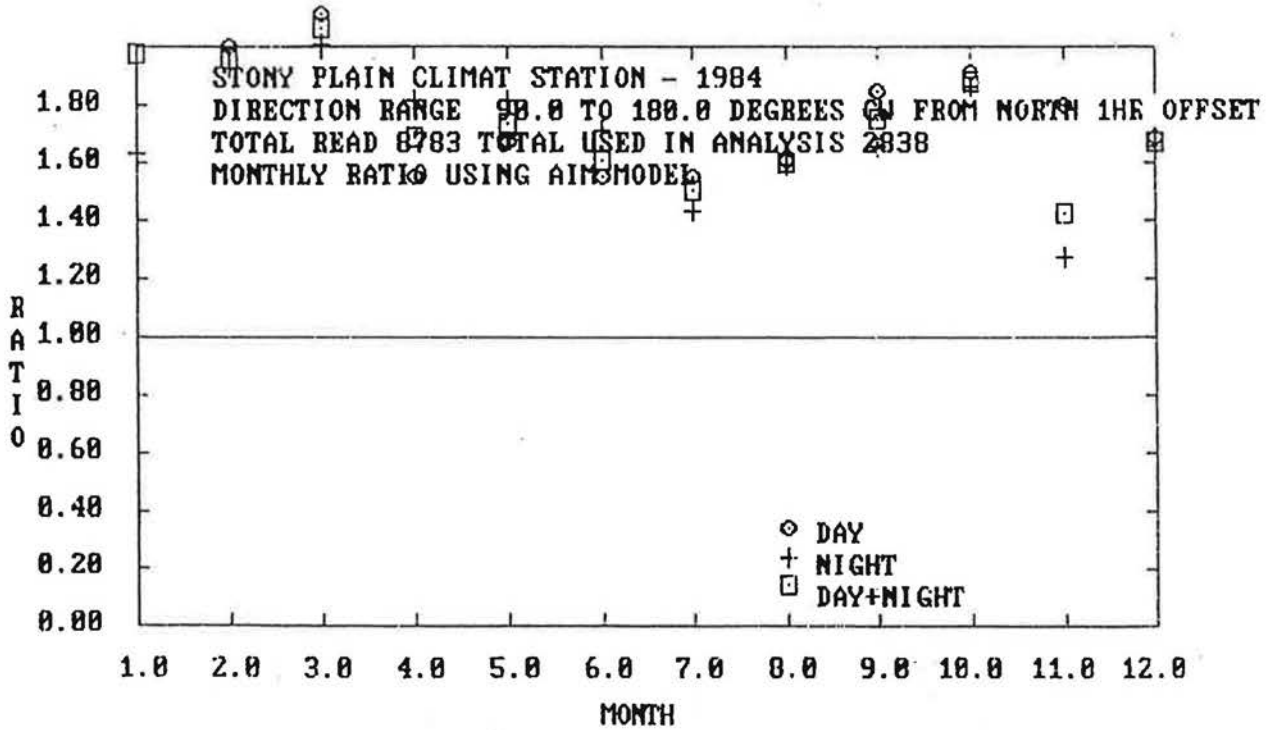


Figure A154

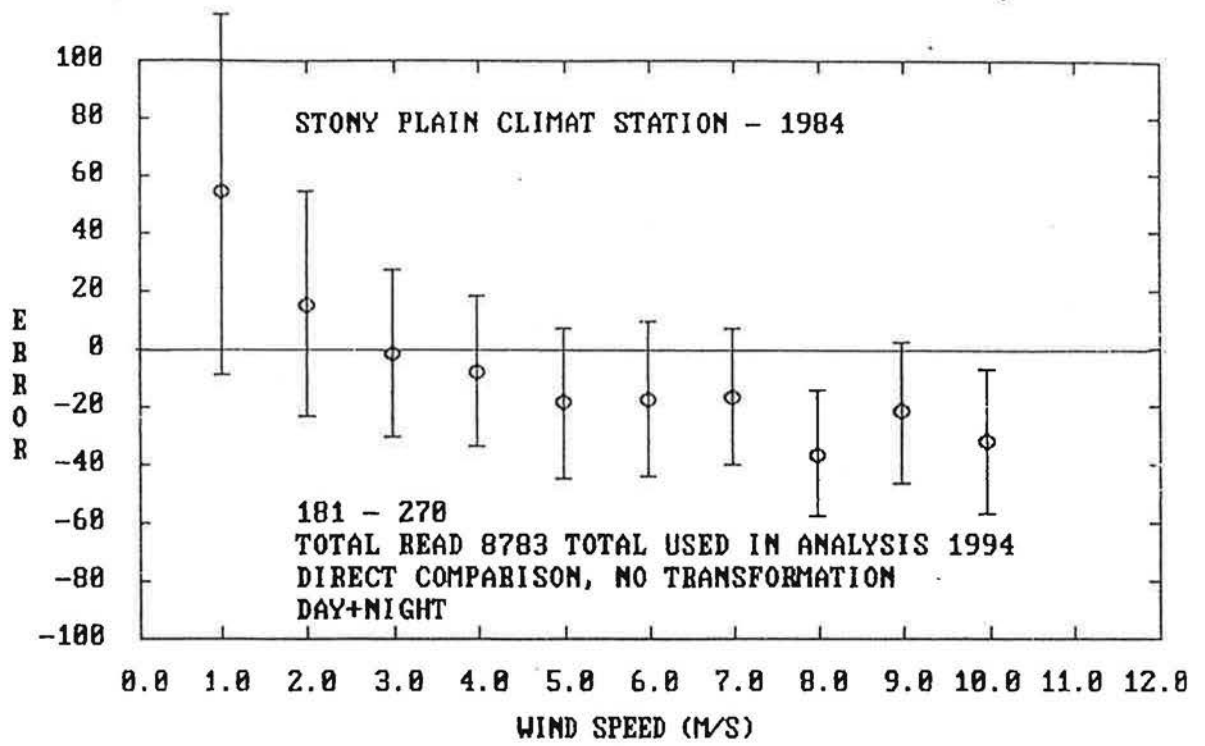


Figure A155

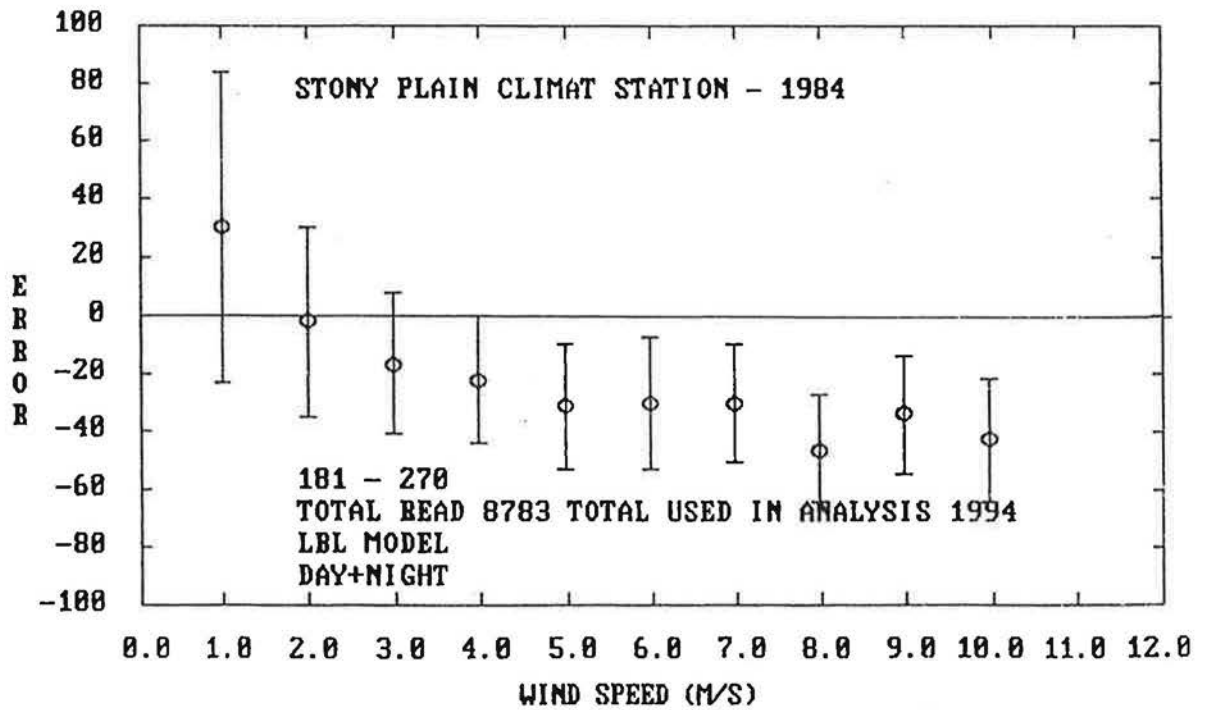


Figure A156

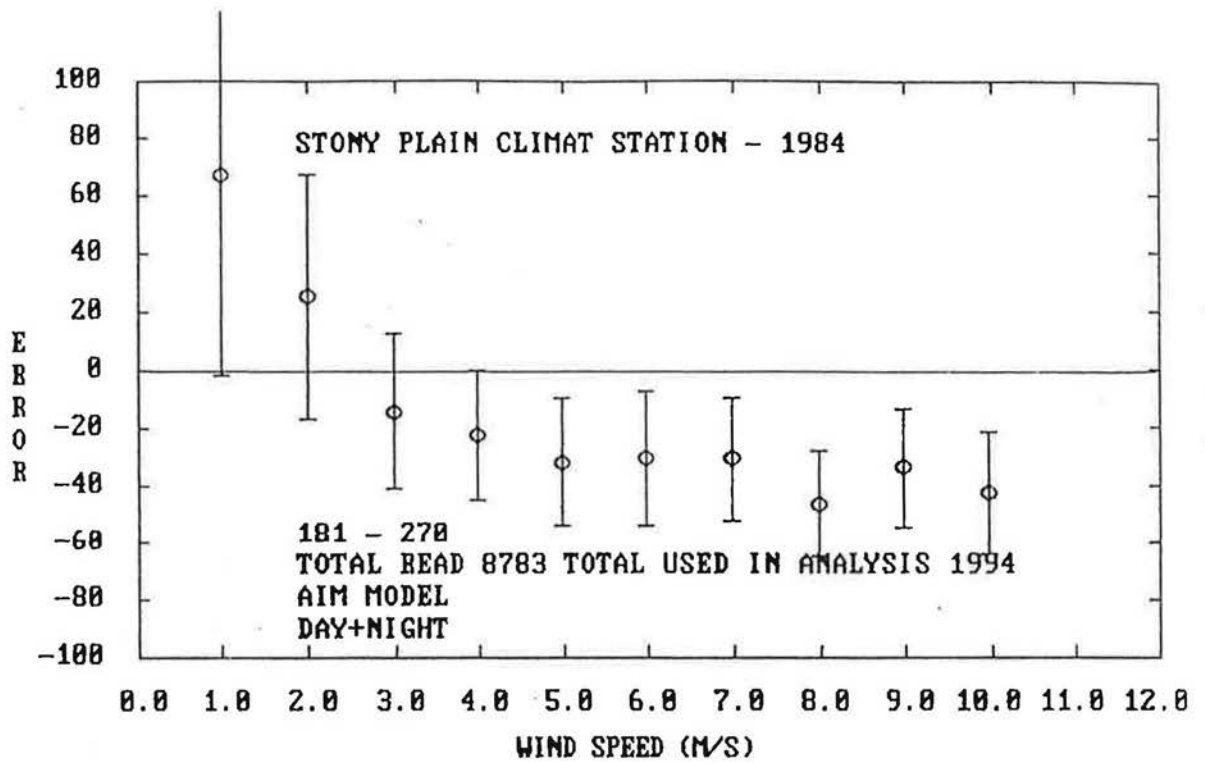


Figure A157

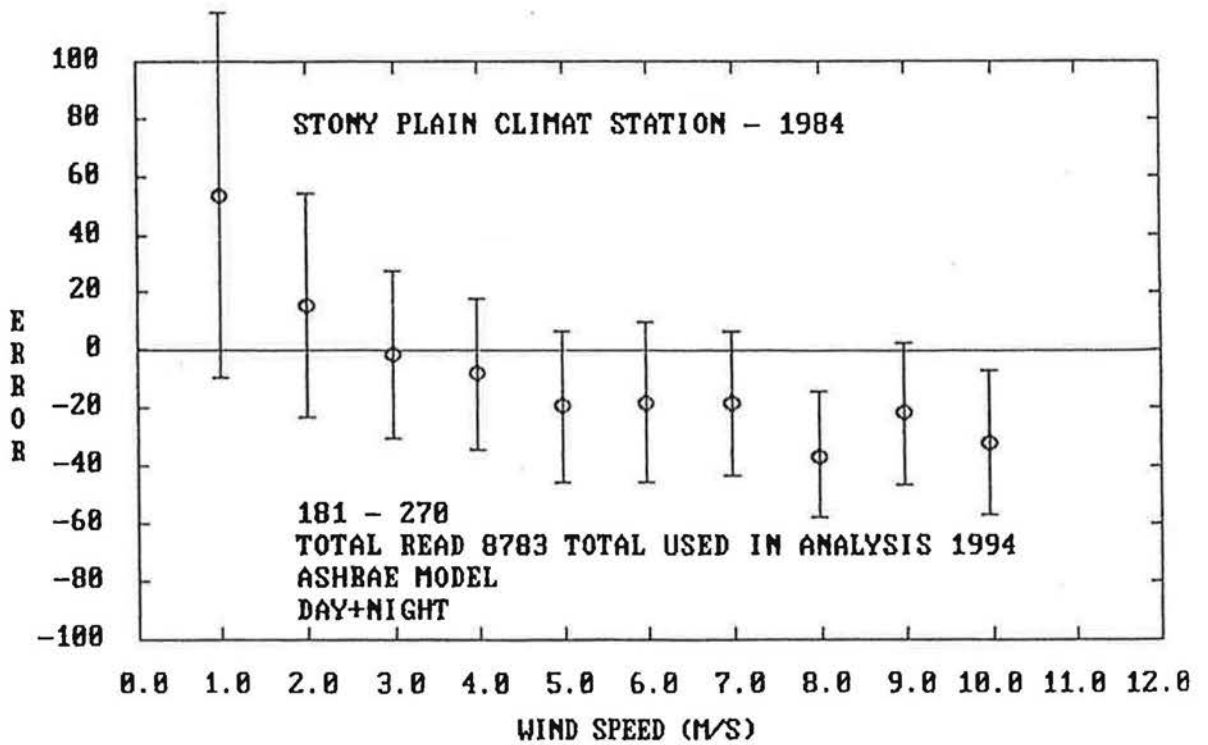


Figure A158

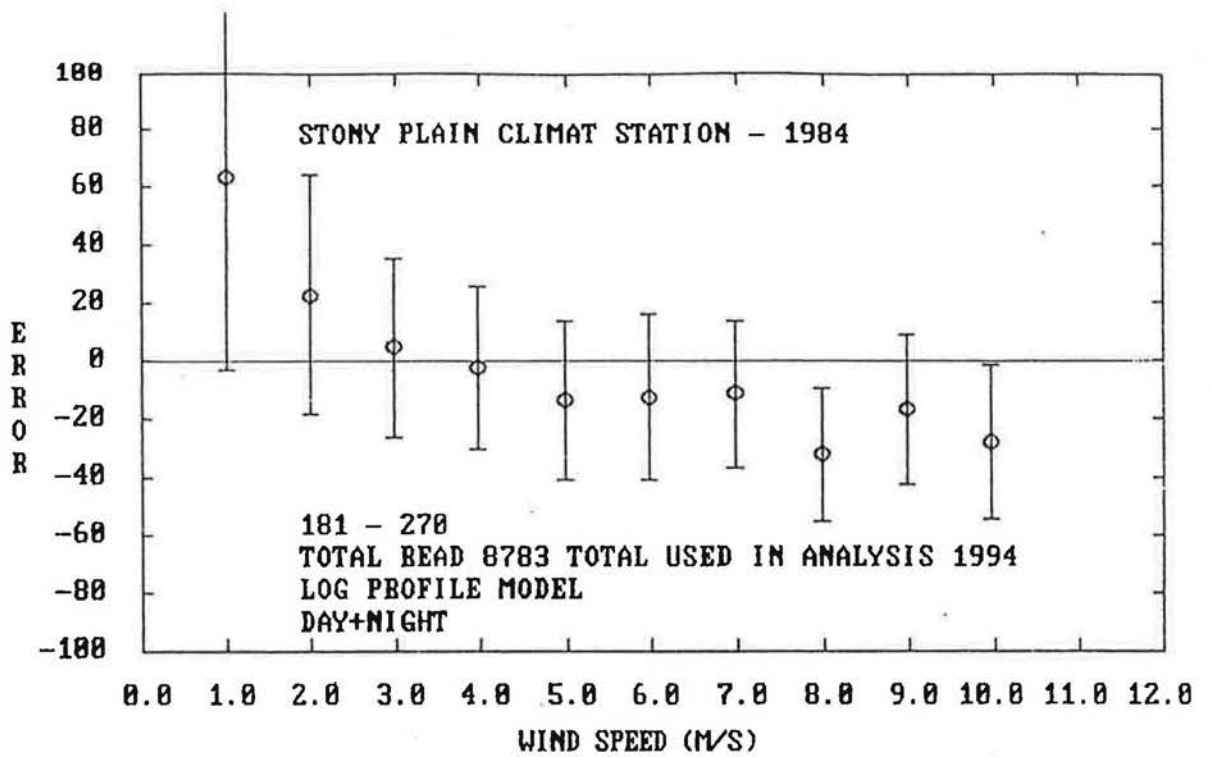


Figure A159

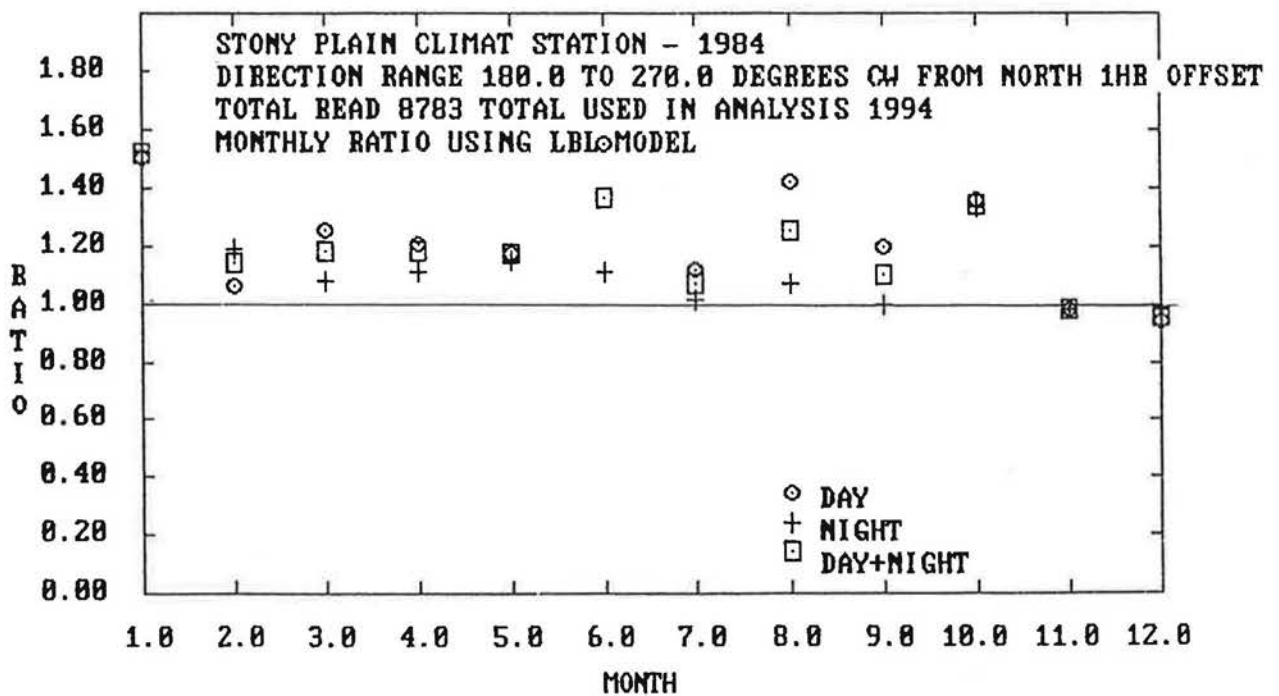


Figure A160

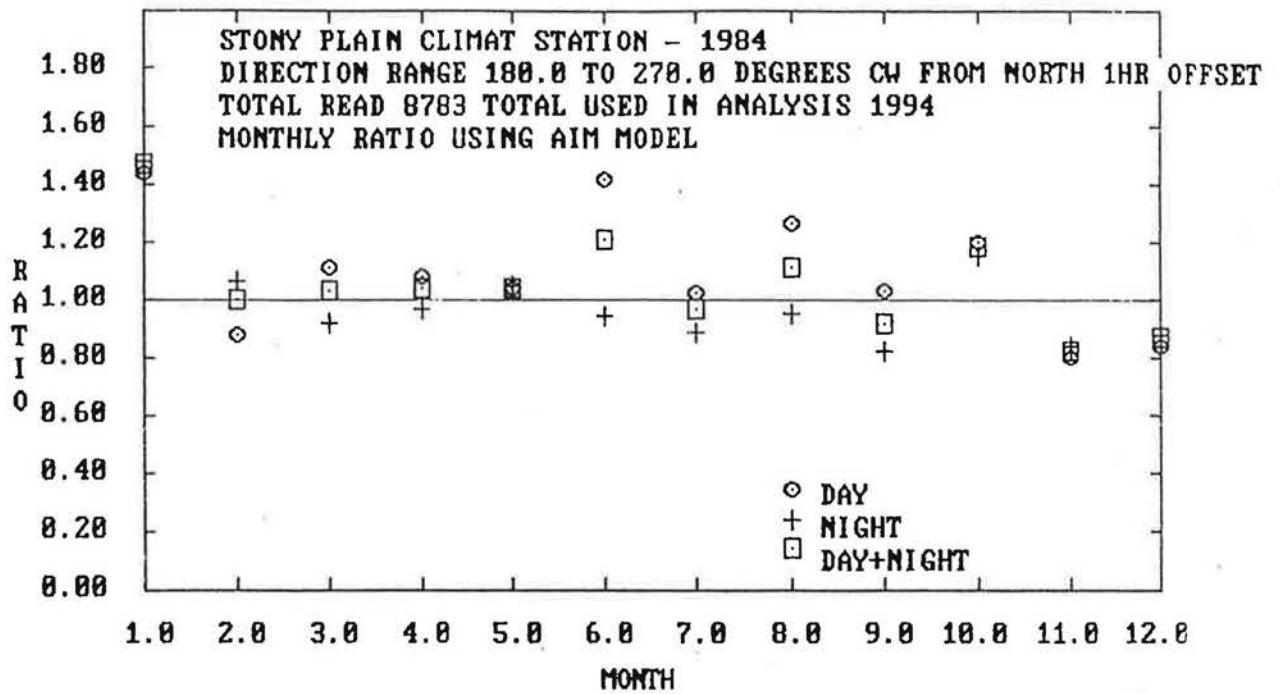


Figure A161

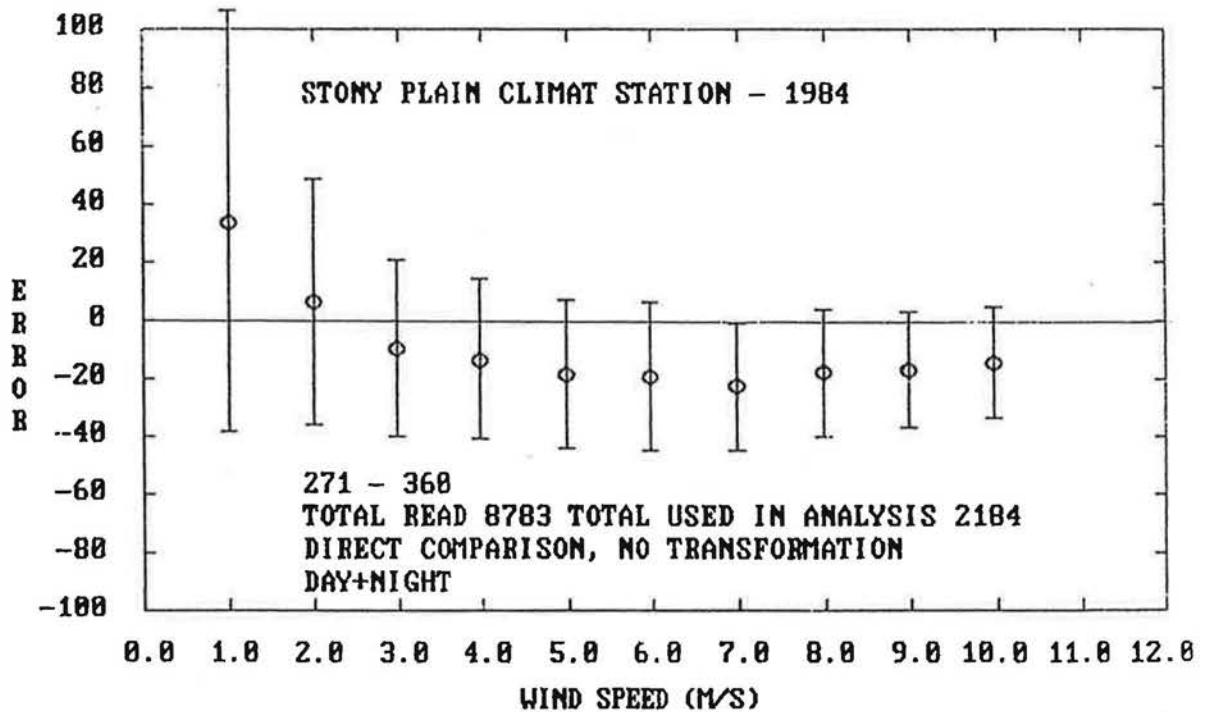


Figure A162

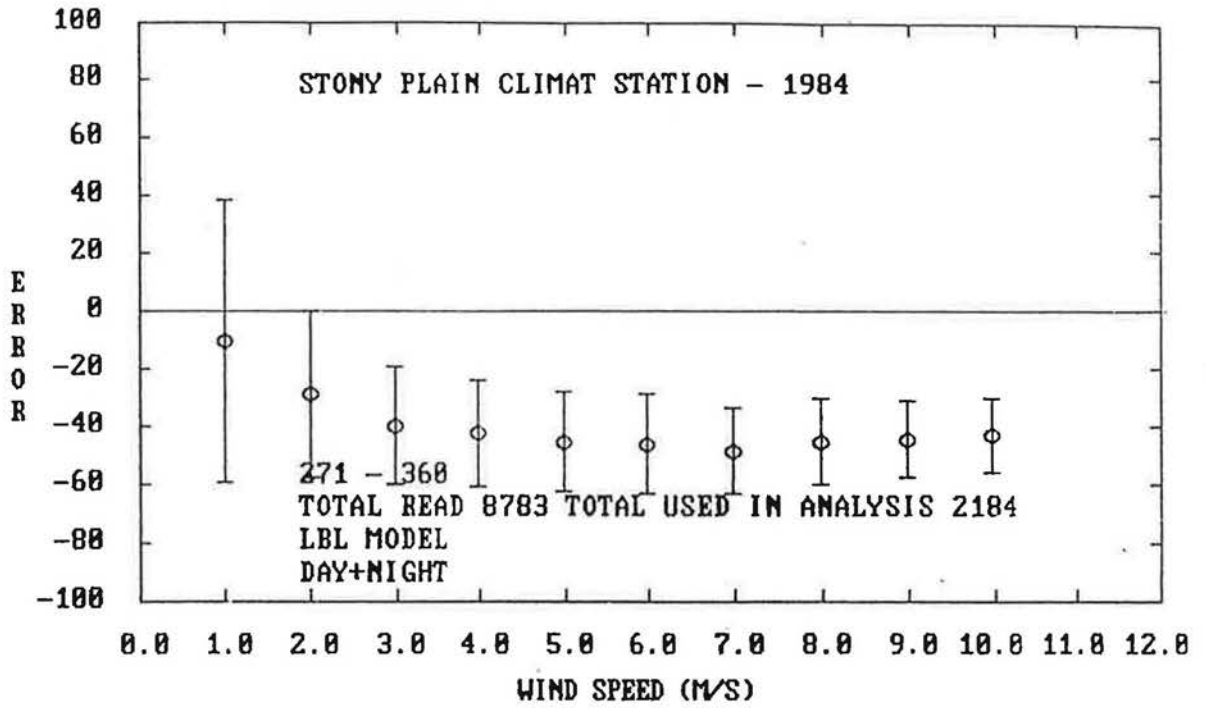


Figure A163

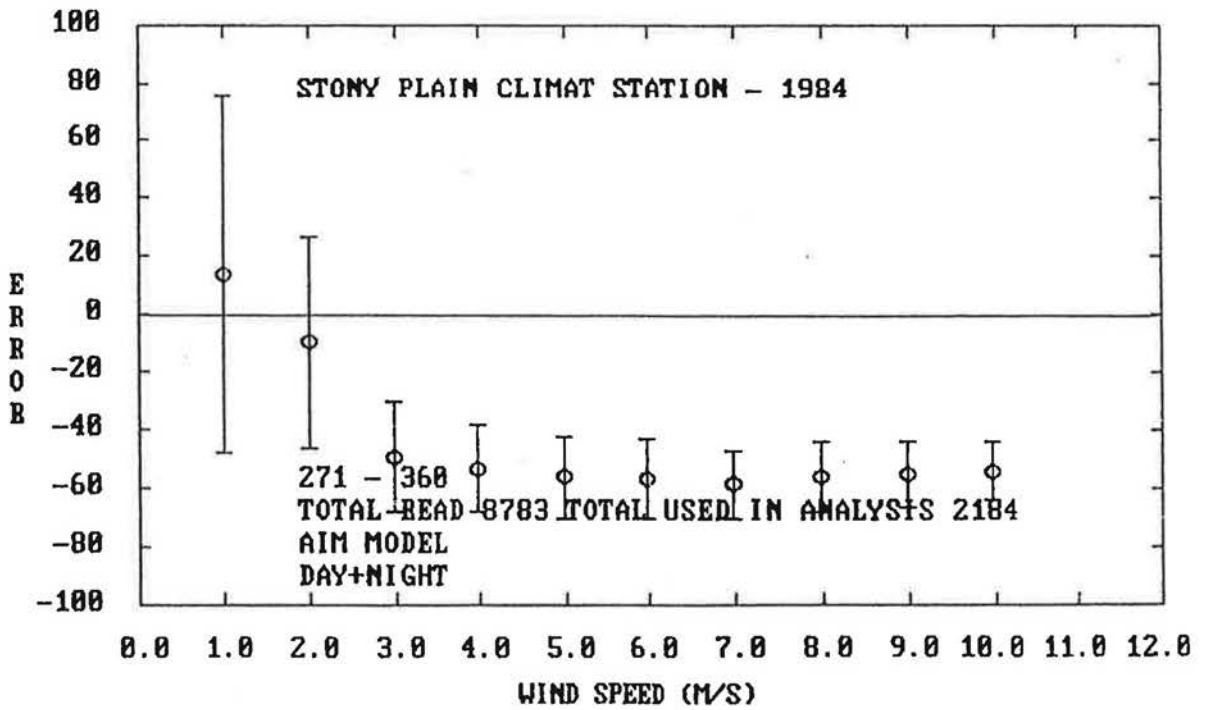


Figure A164

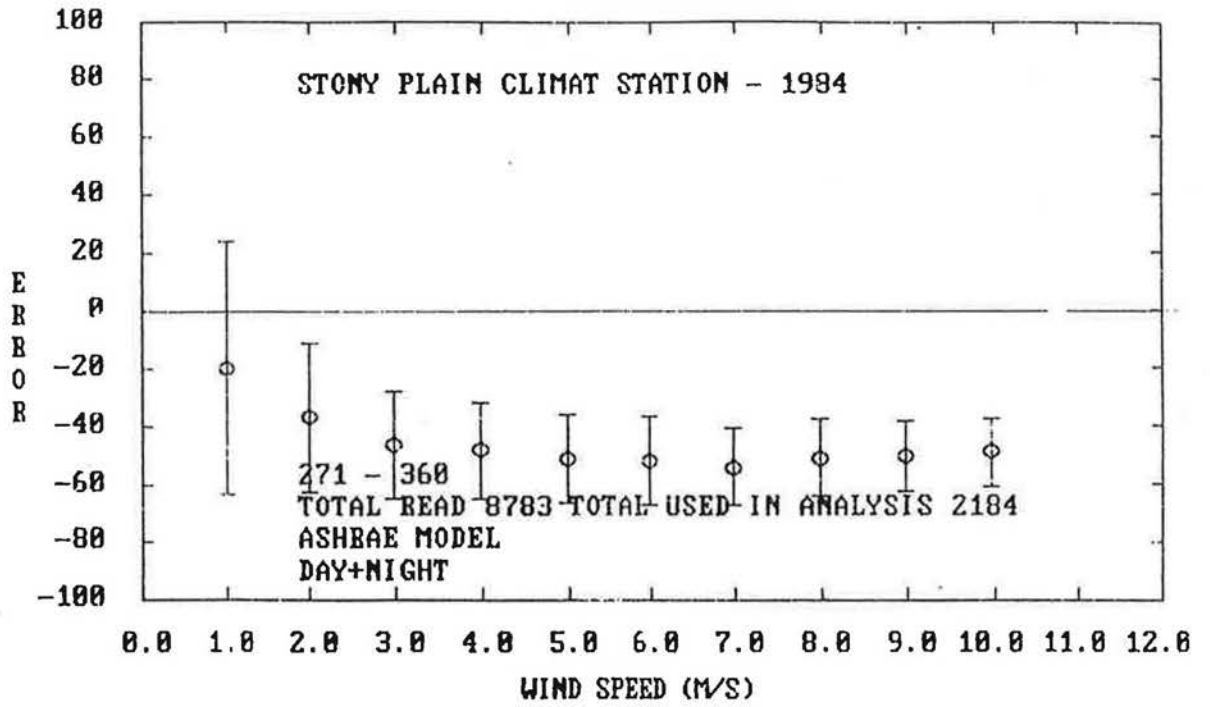


Figure A165

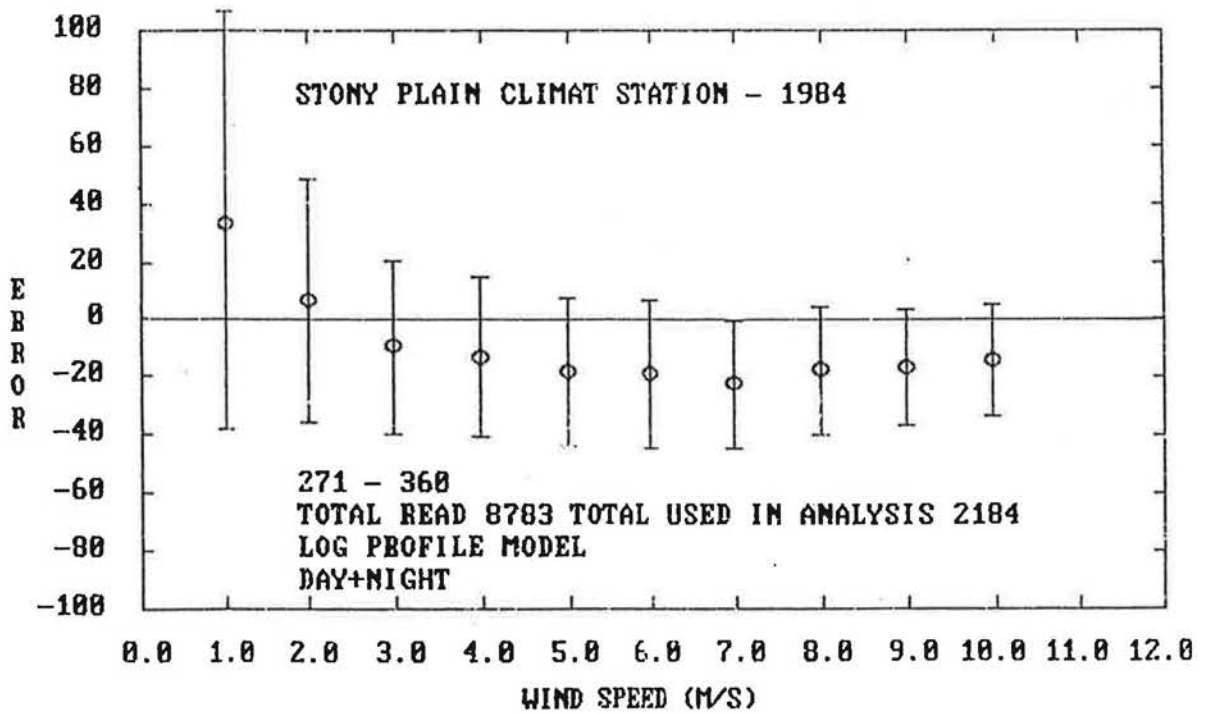


Figure A166

○ □ ◇

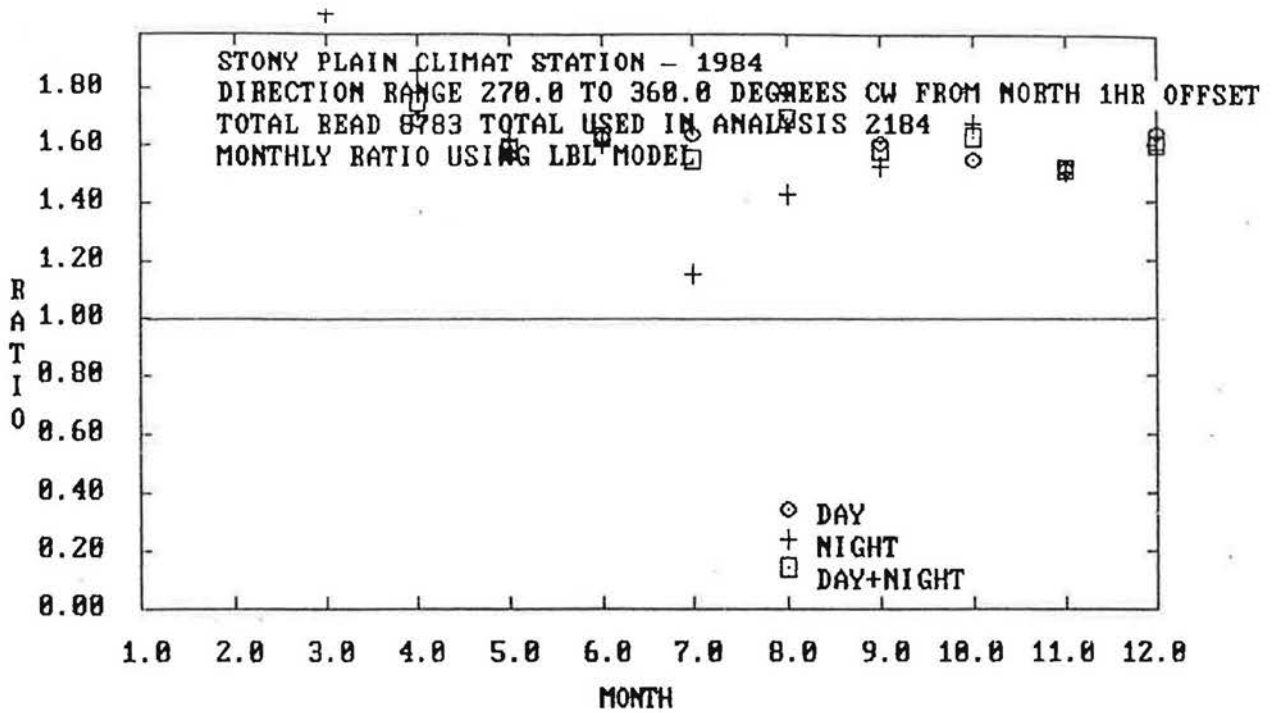


Figure A167

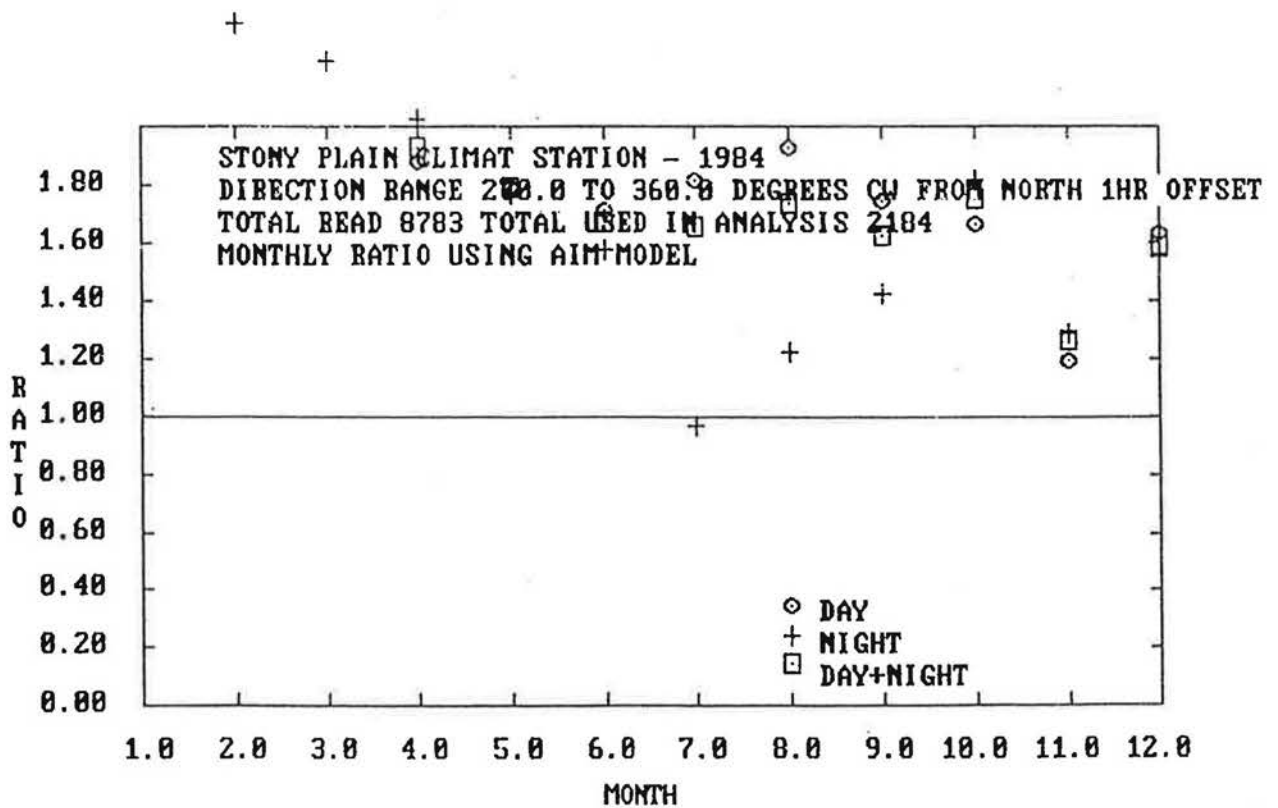


Figure A168

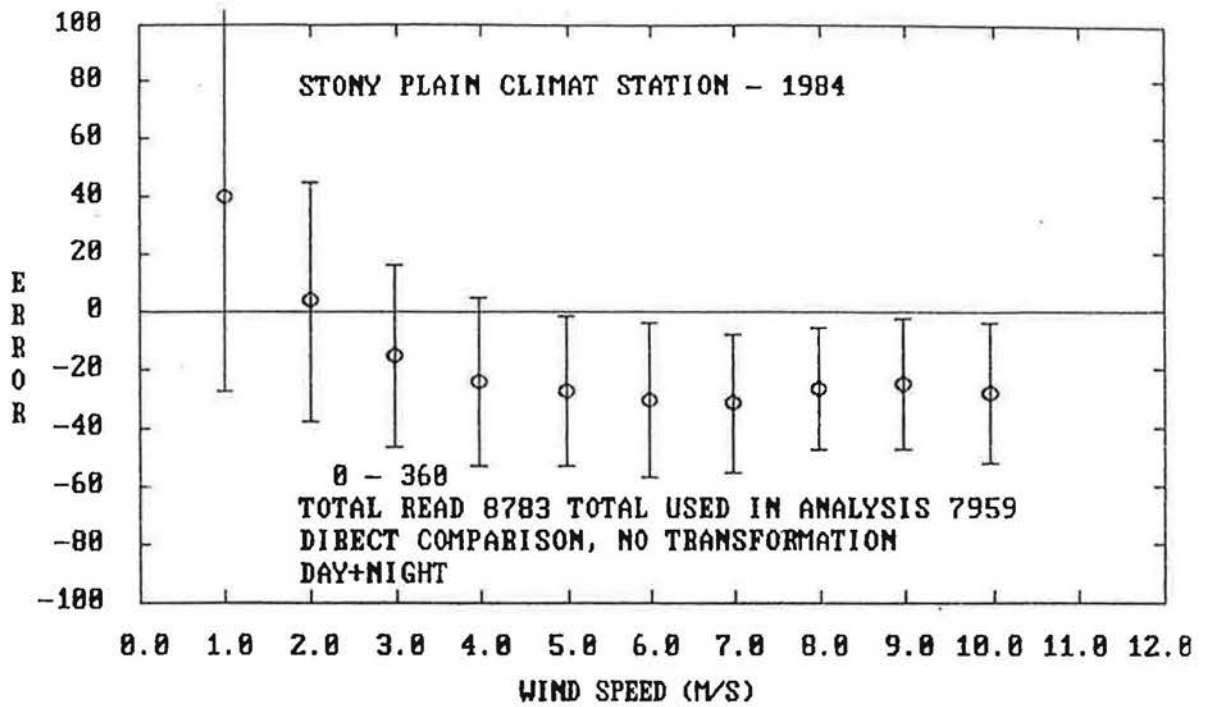


Figure A169

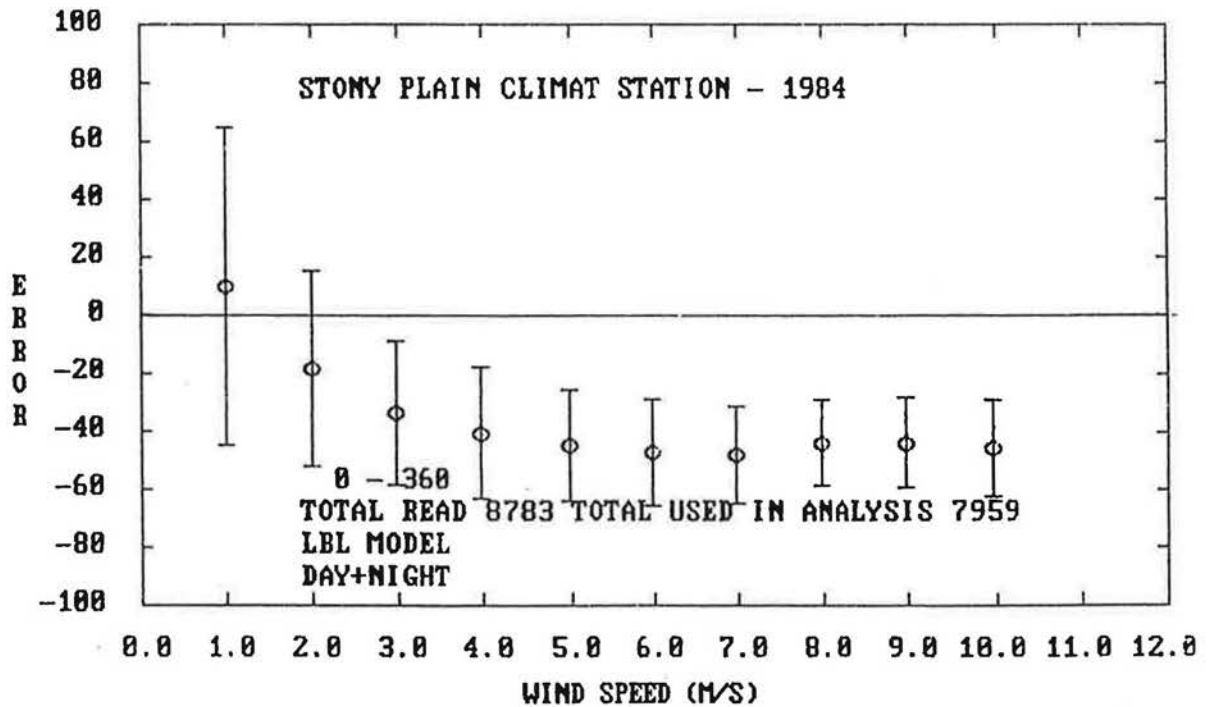


Figure A170

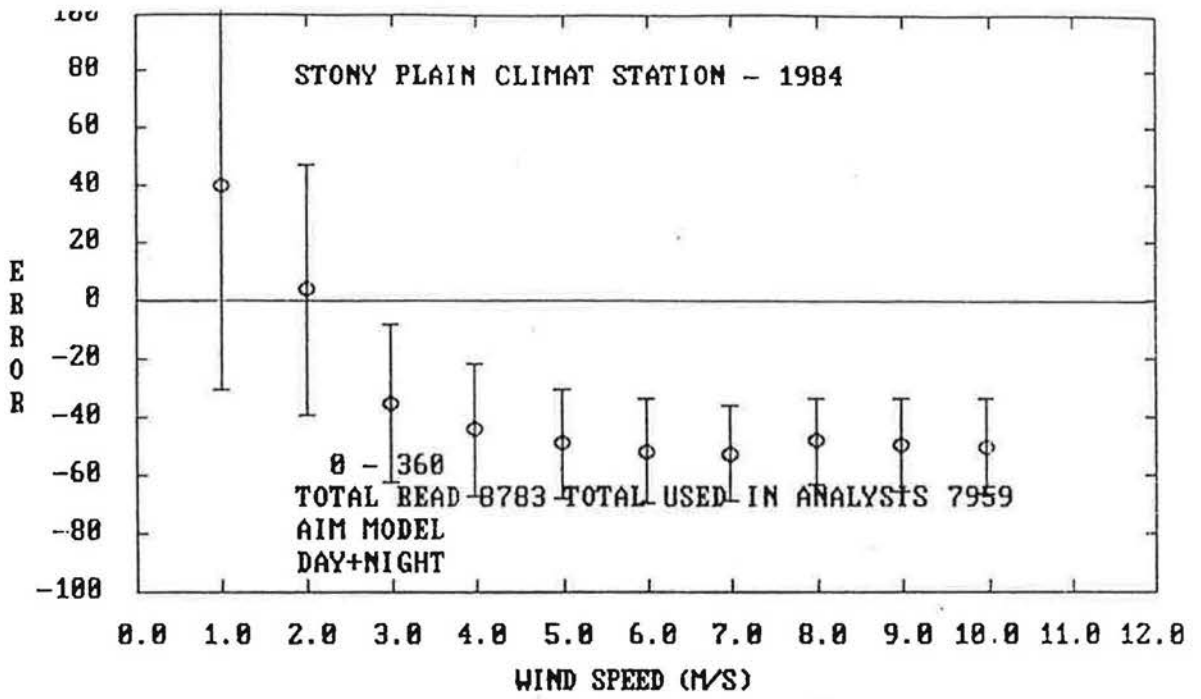


Figure A171

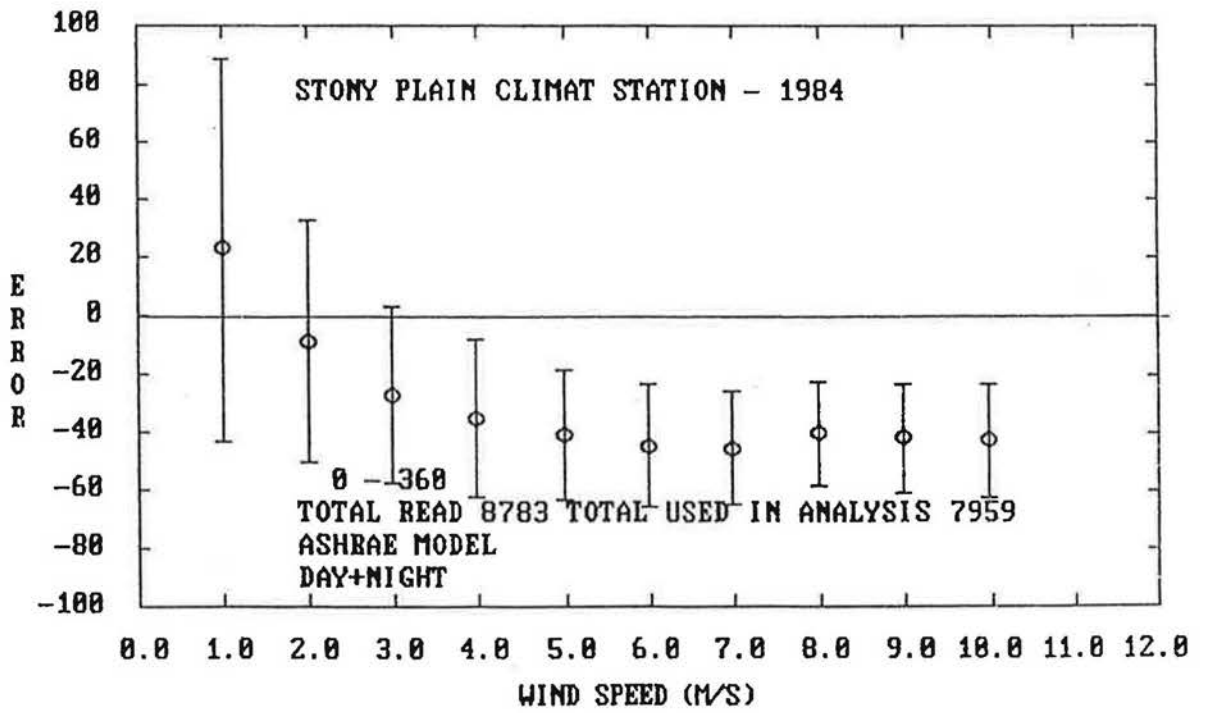


Figure A172

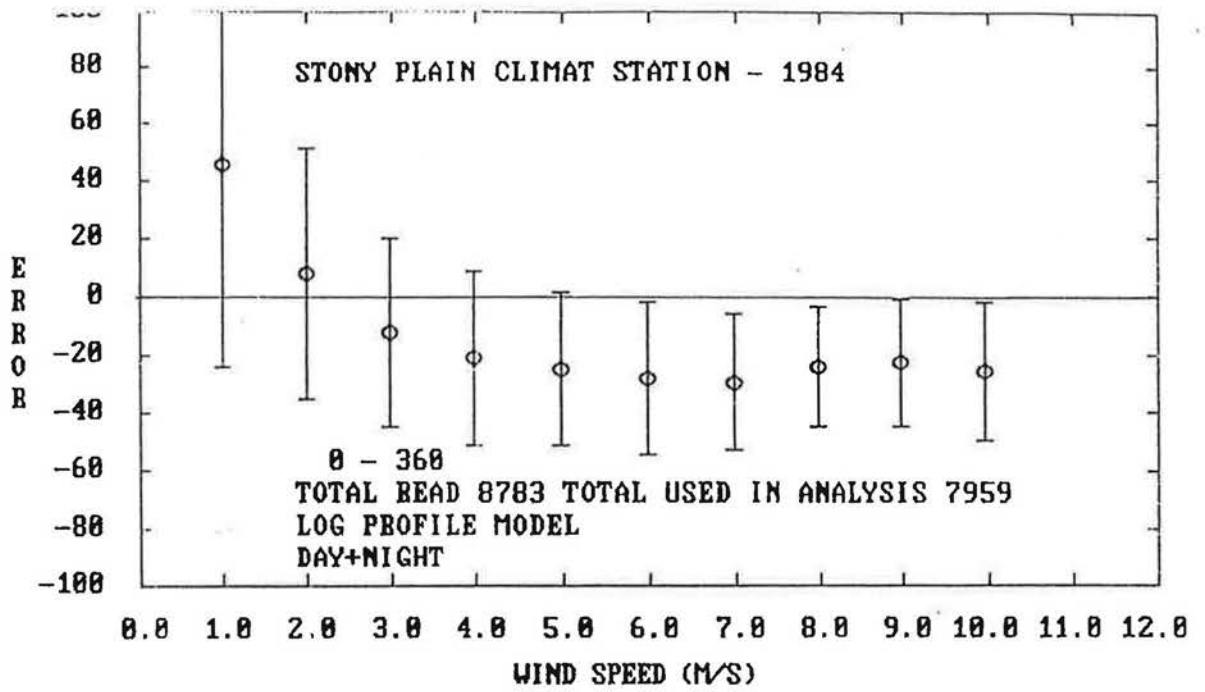


Figure A173

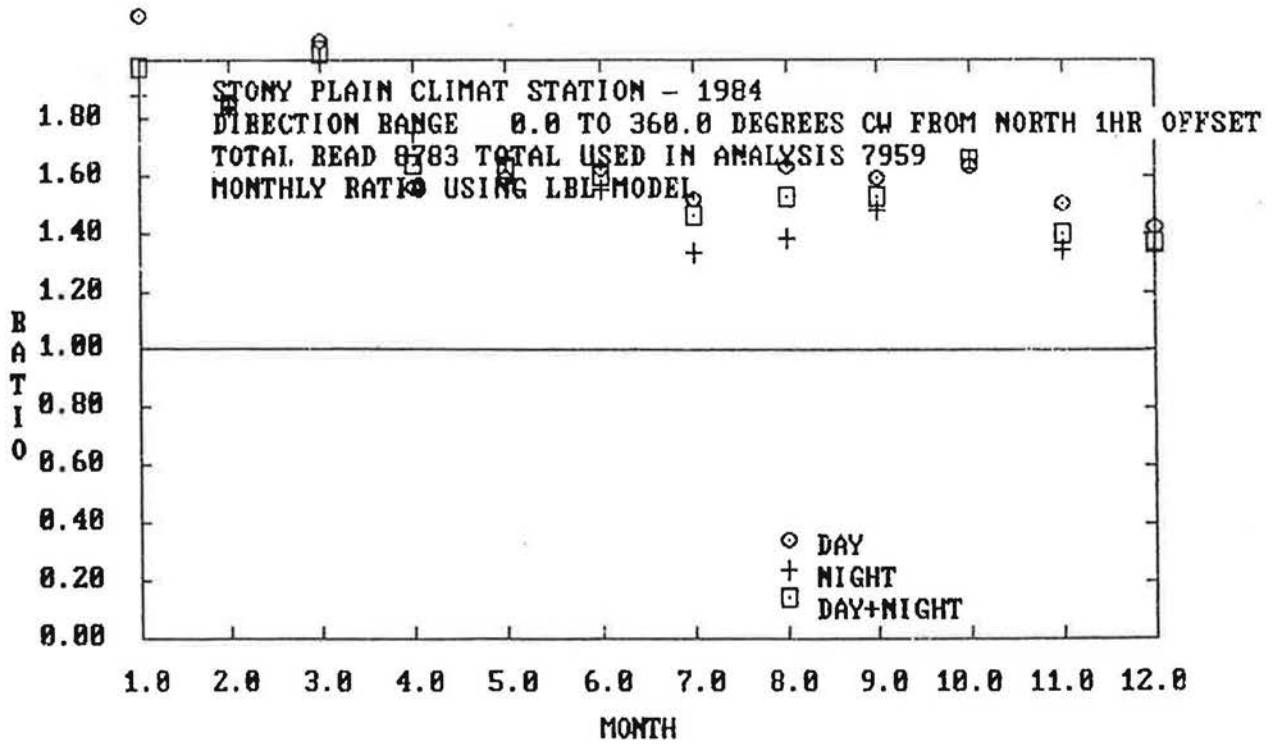


Figure A174

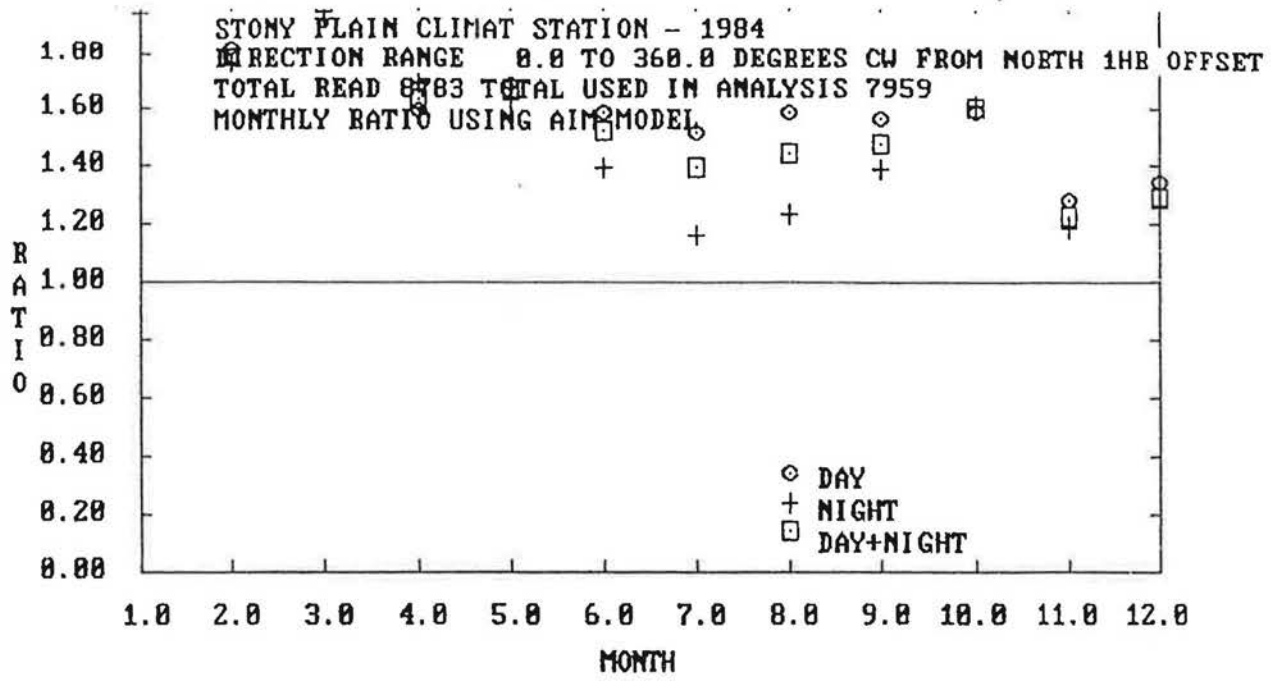


Figure A175

APPENDIX B

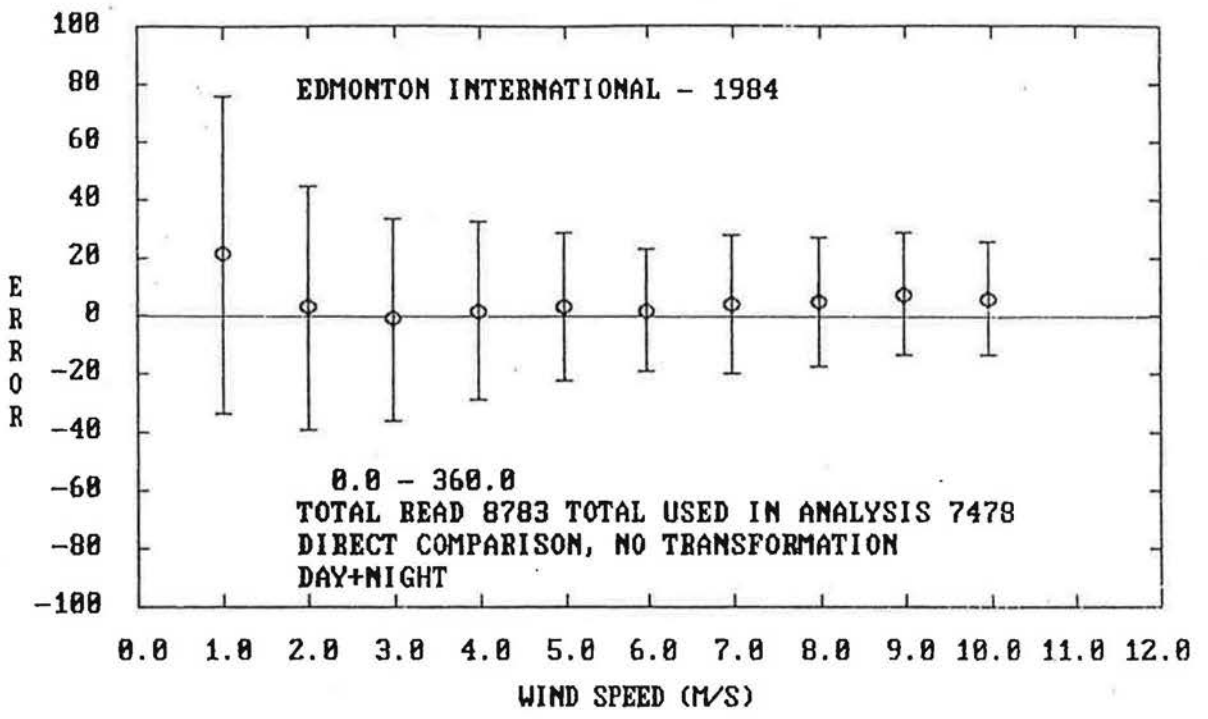


Figure B1

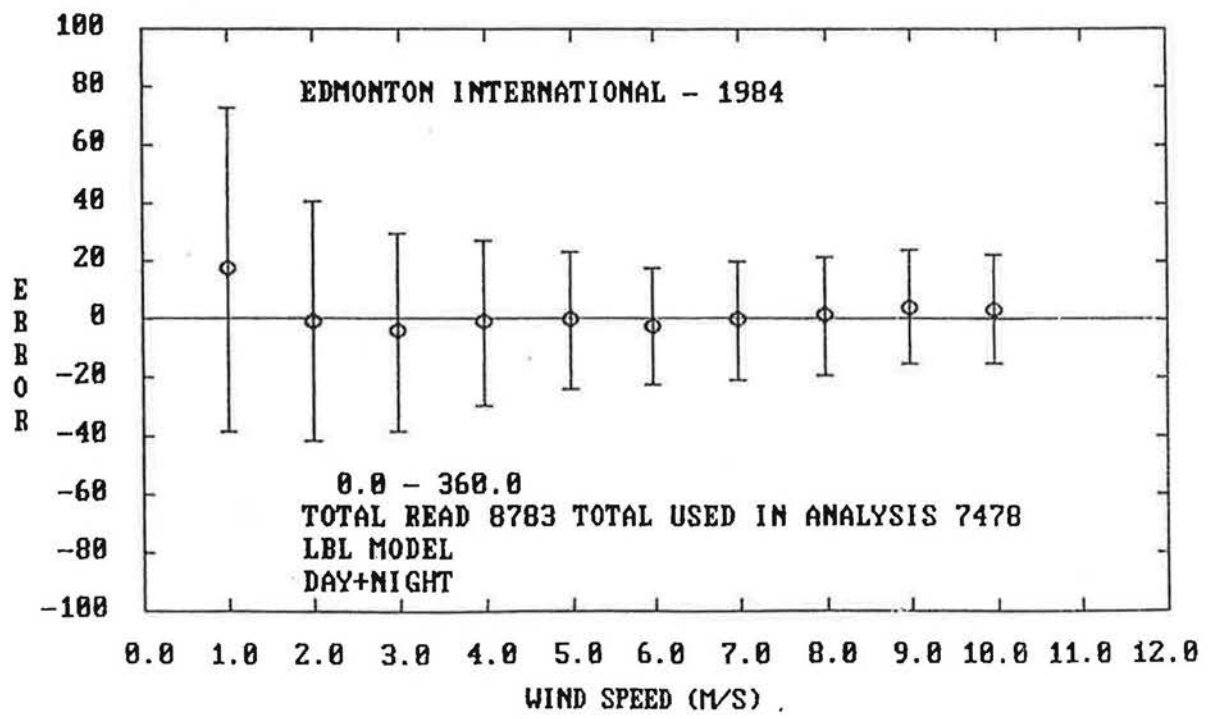


Figure B2

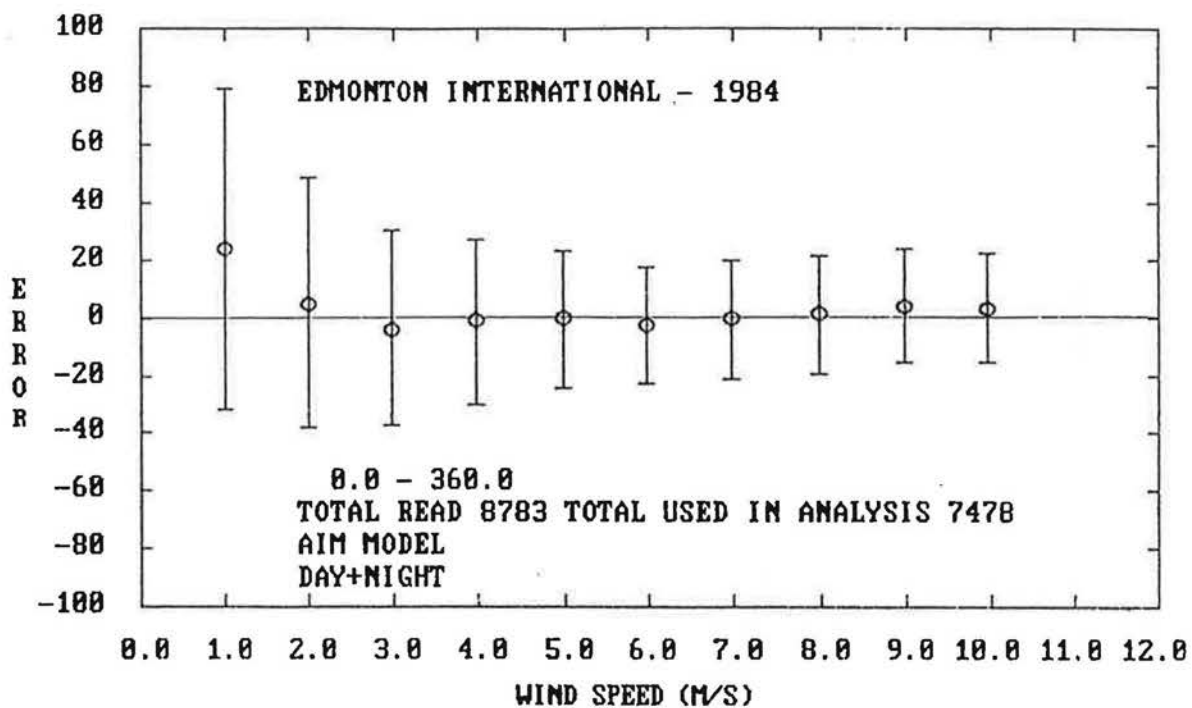


Figure B3

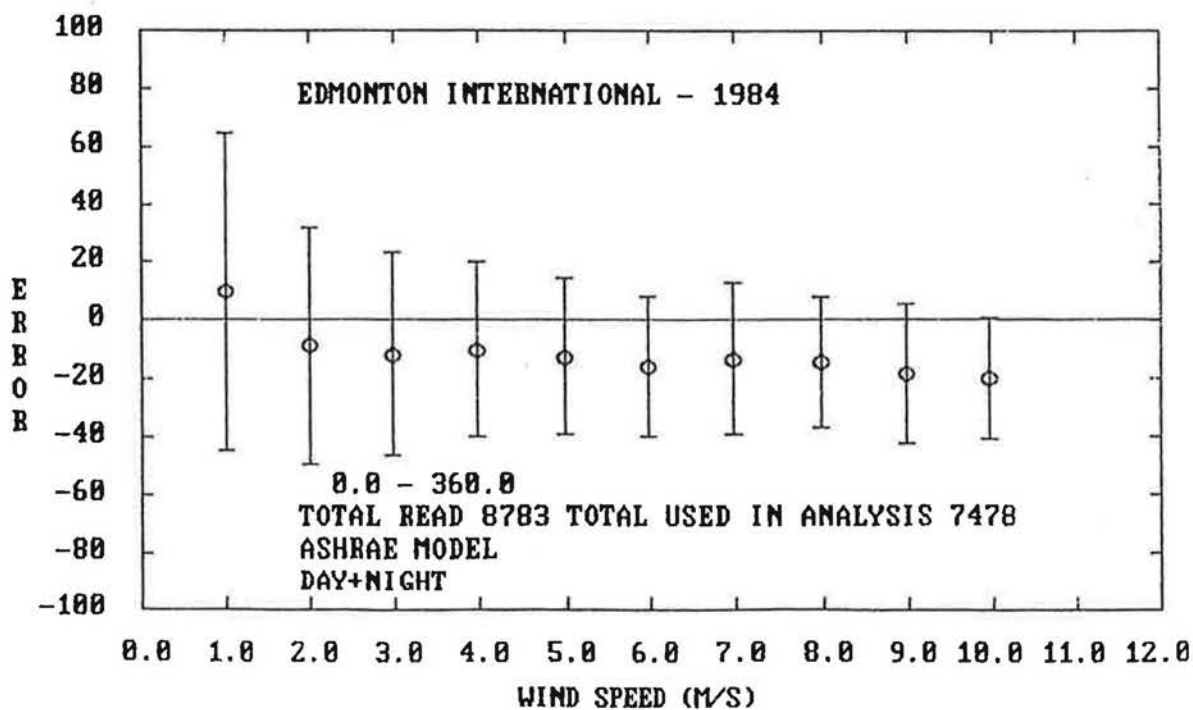


Figure B4

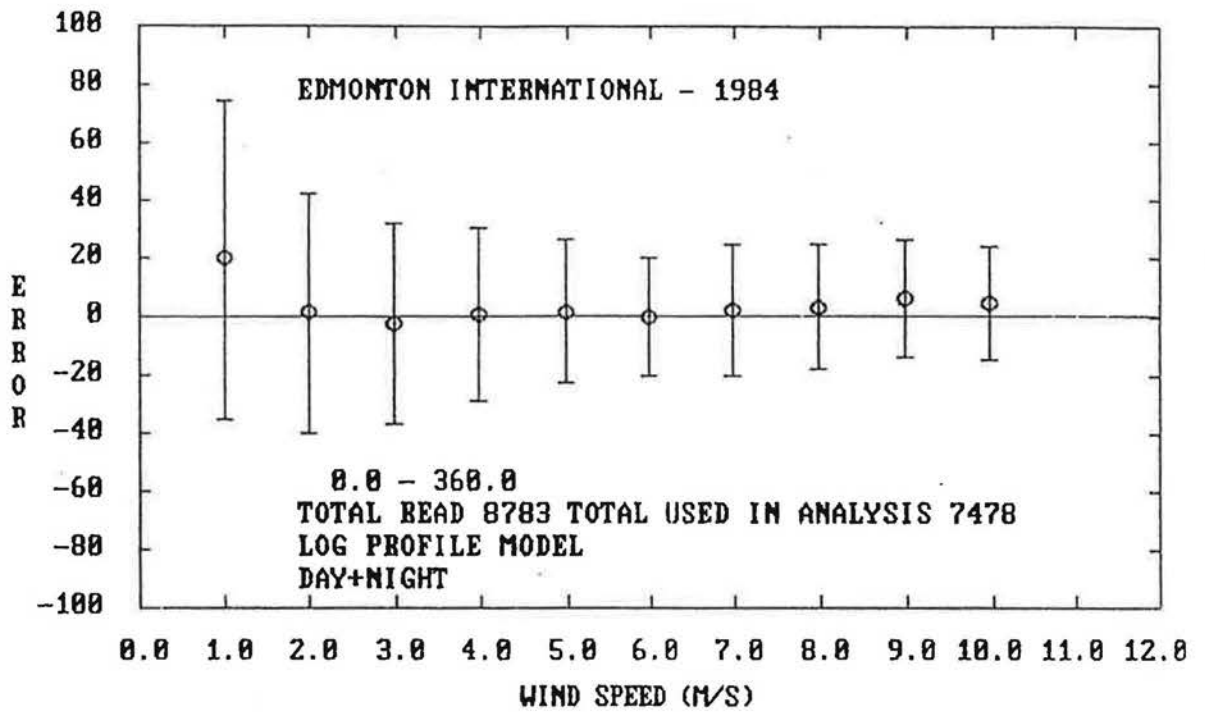


Figure B5

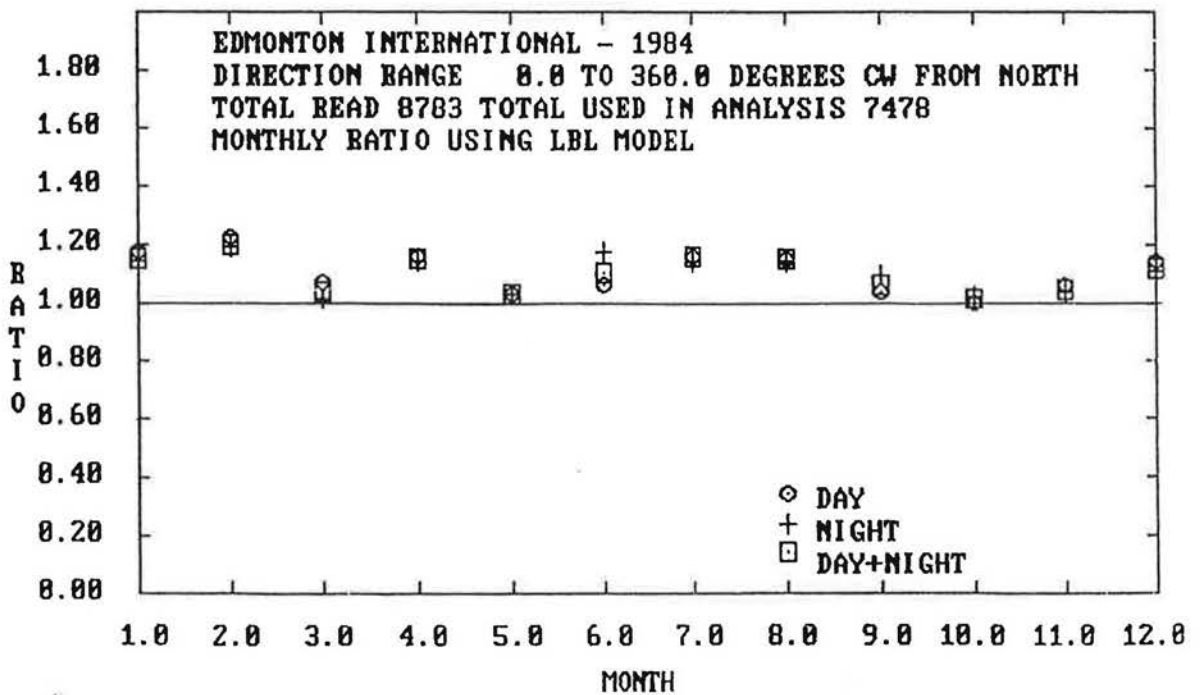


Figure B6

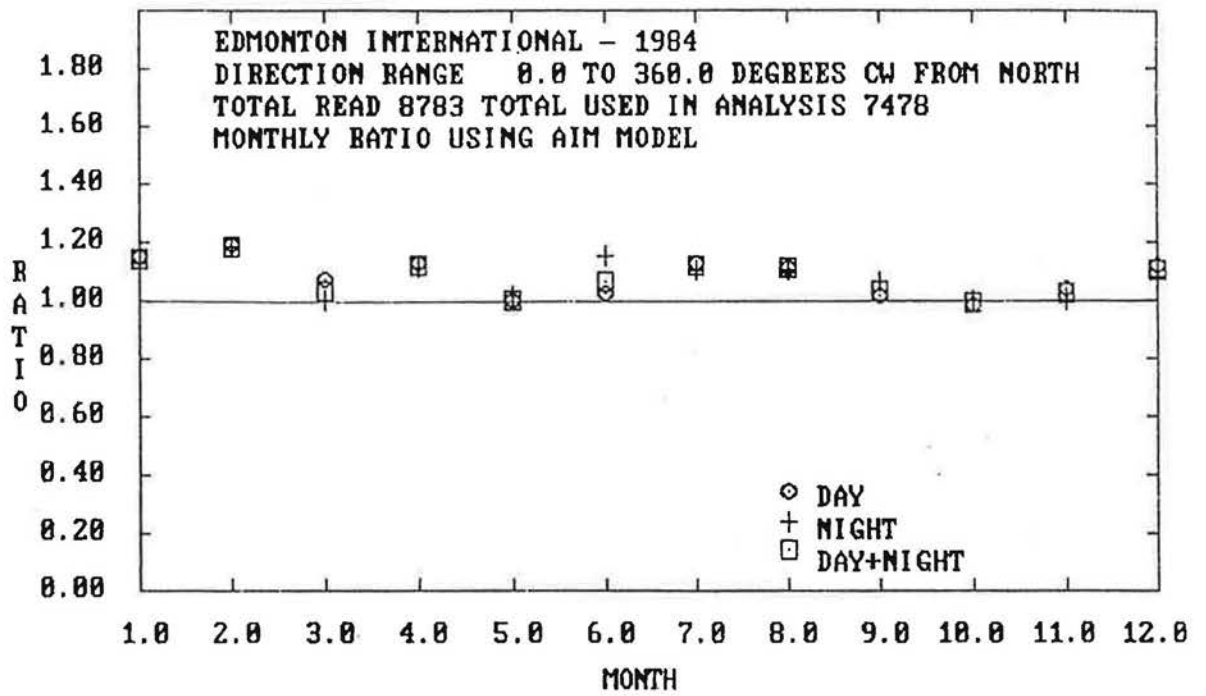


Figure B7

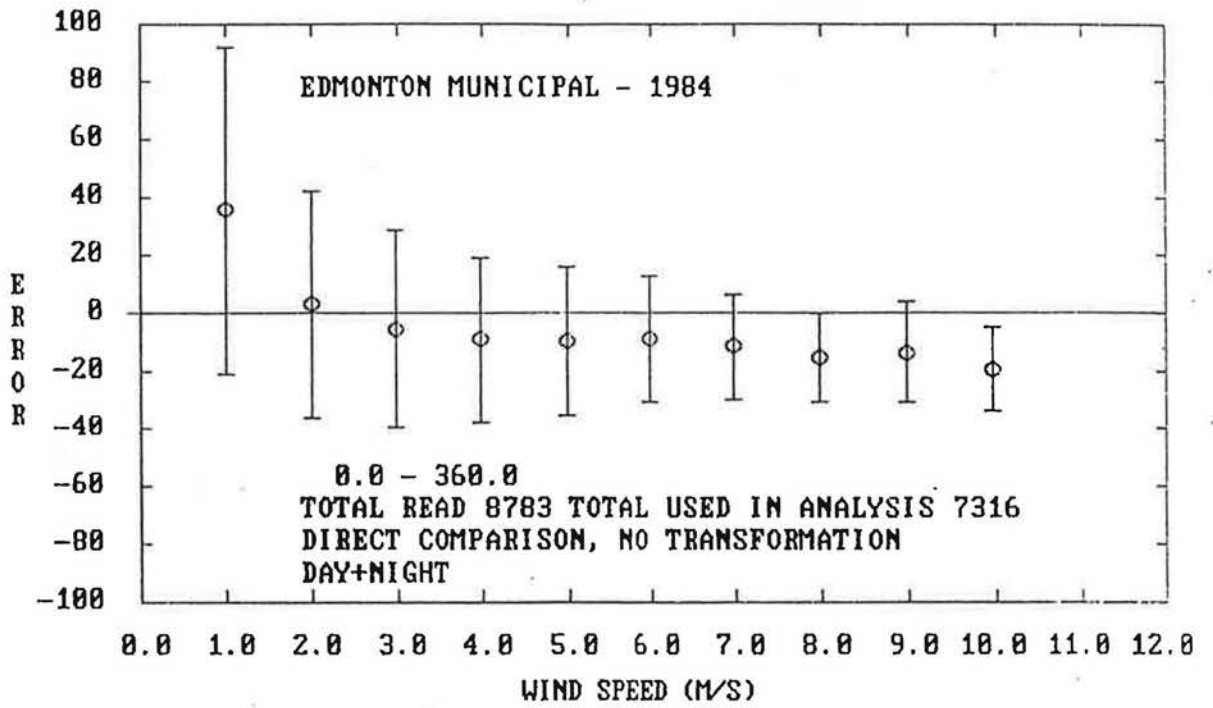


Figure B8

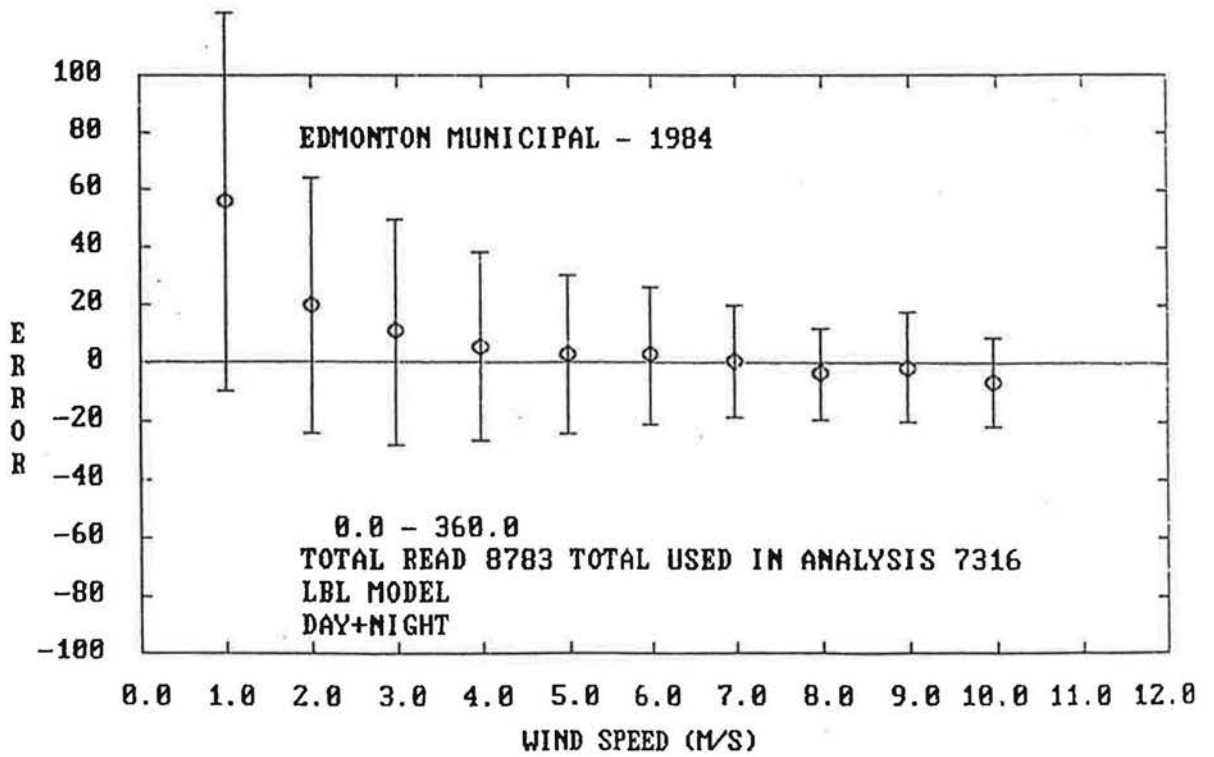


Figure B9

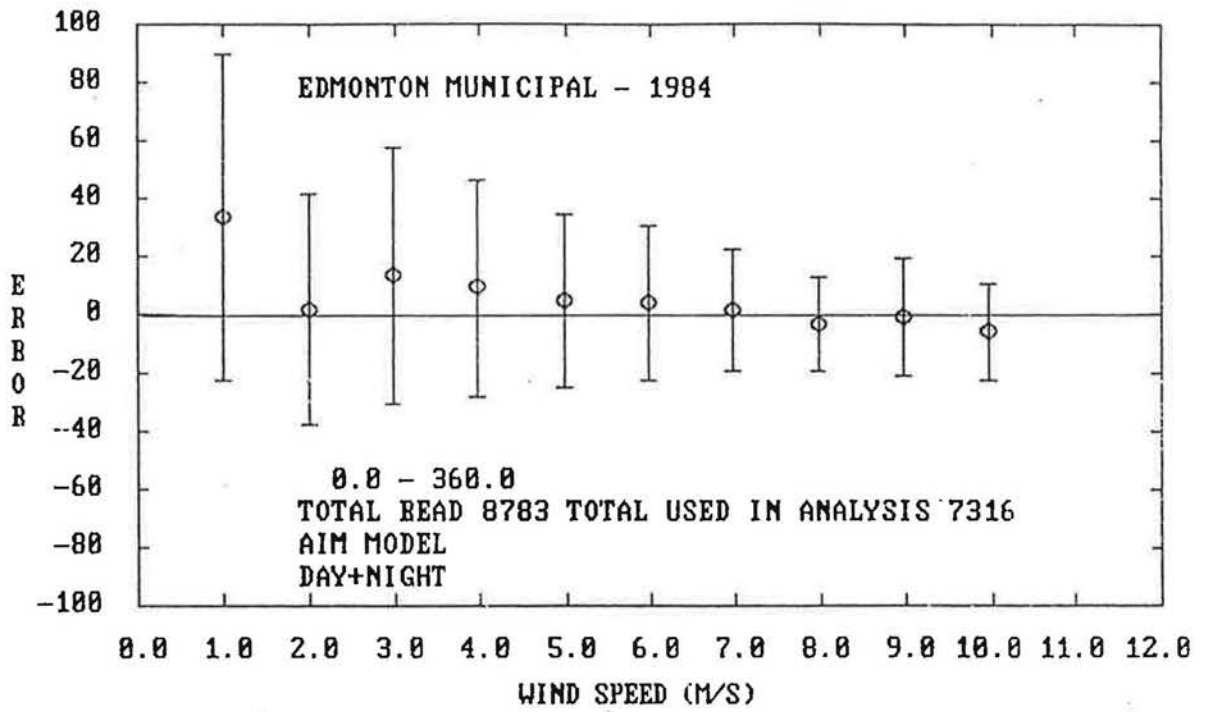


Figure B10

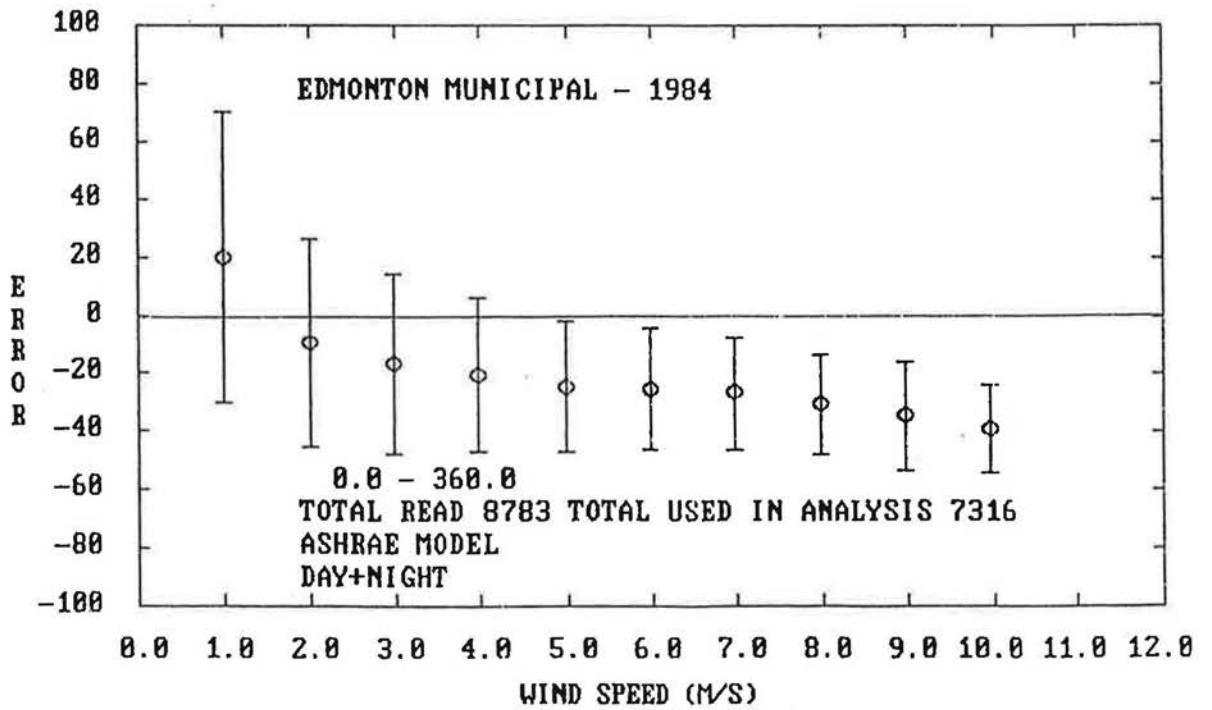


Figure B11

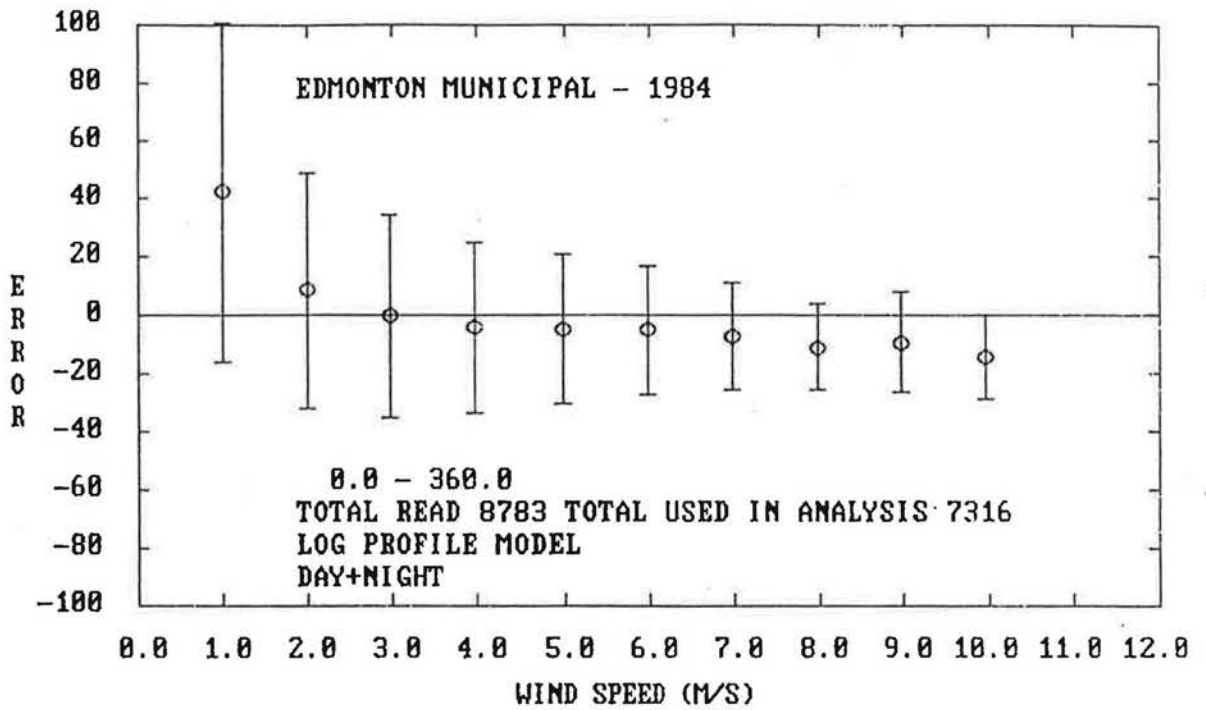


Figure B12

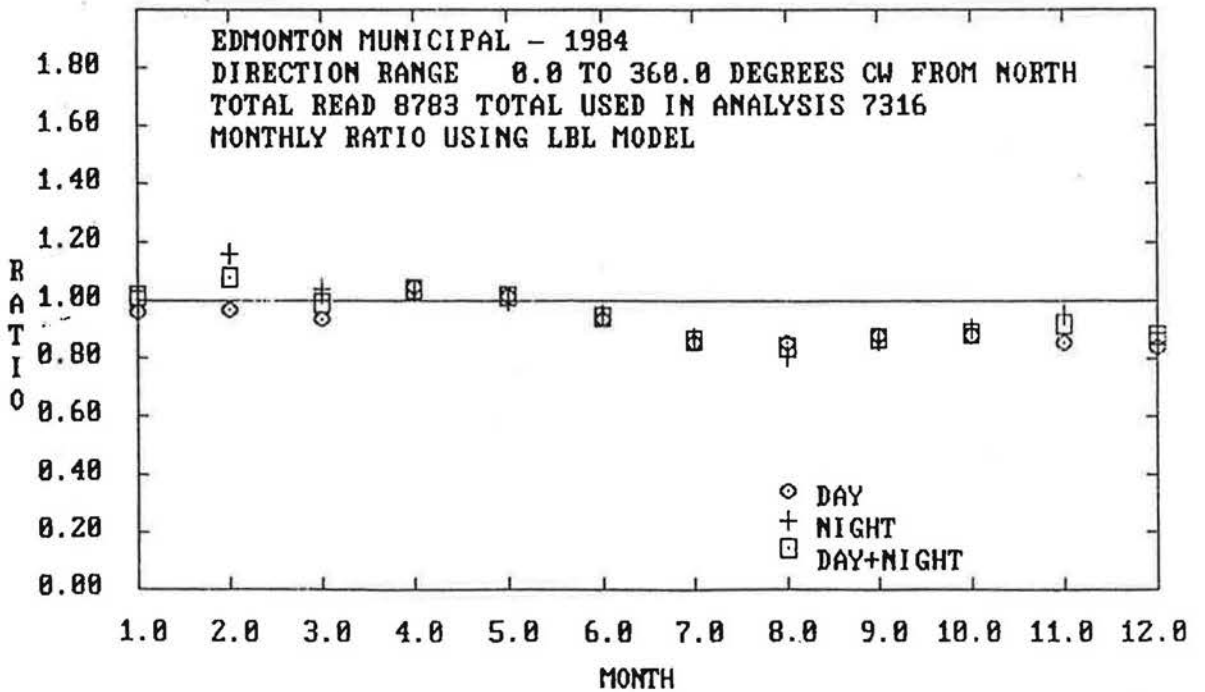


Figure B13

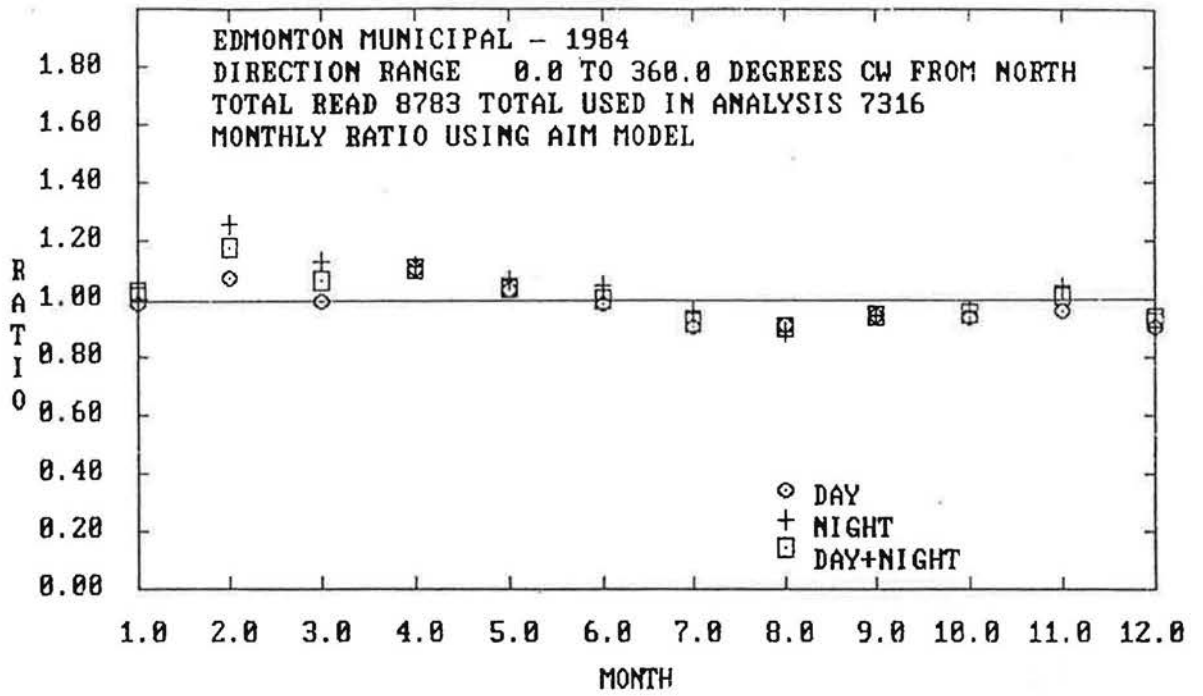


Figure B14

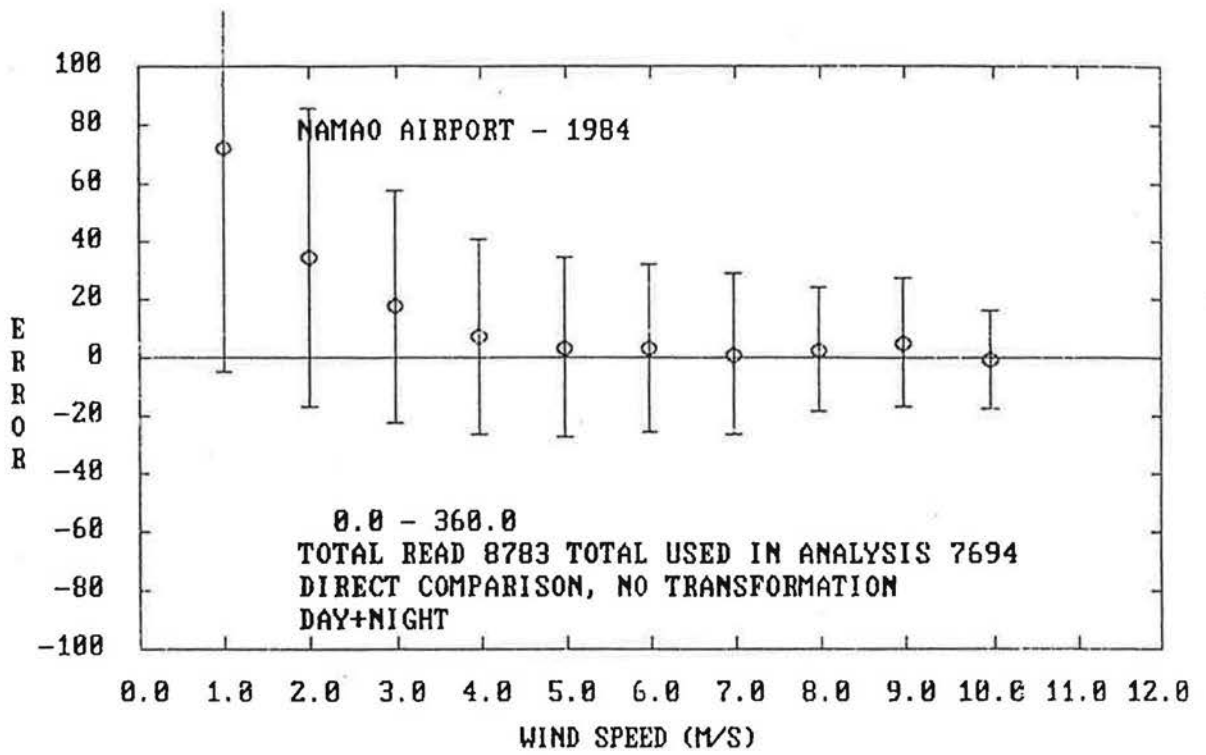


Figure B15

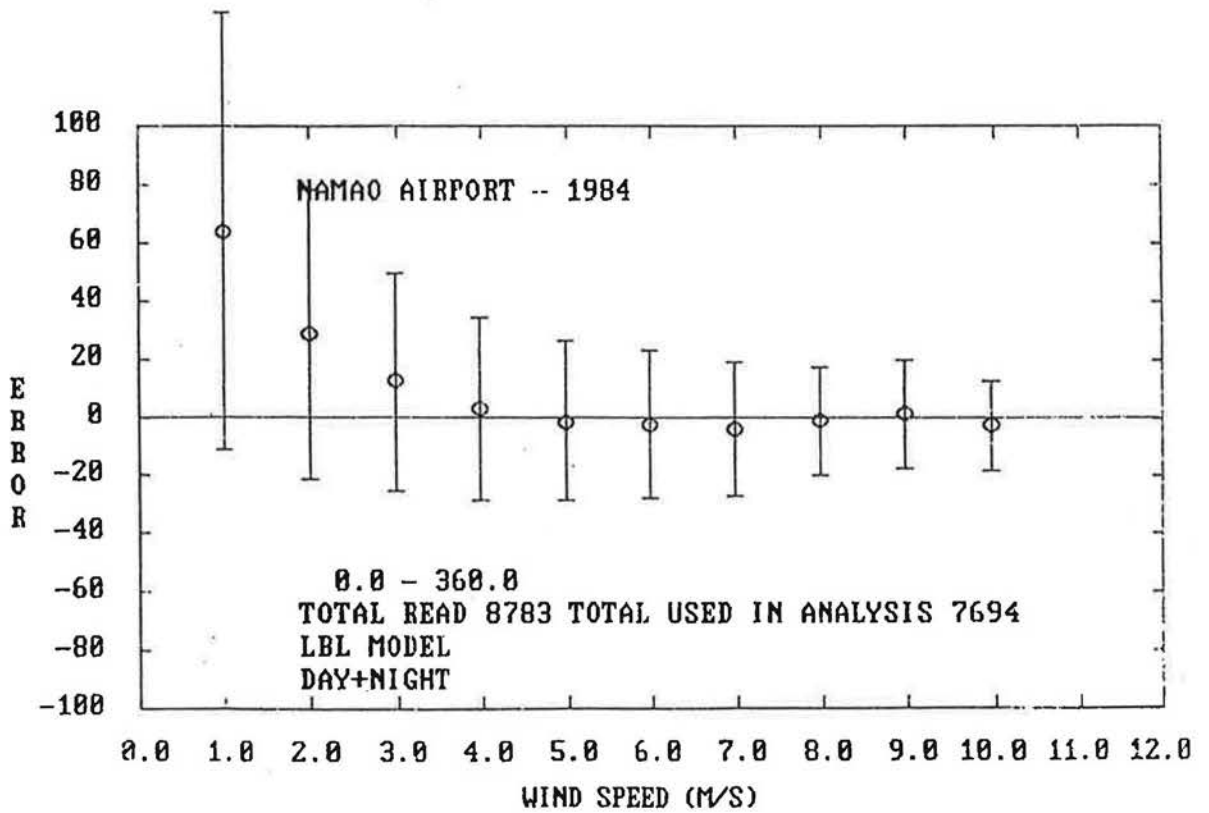


Figure B16

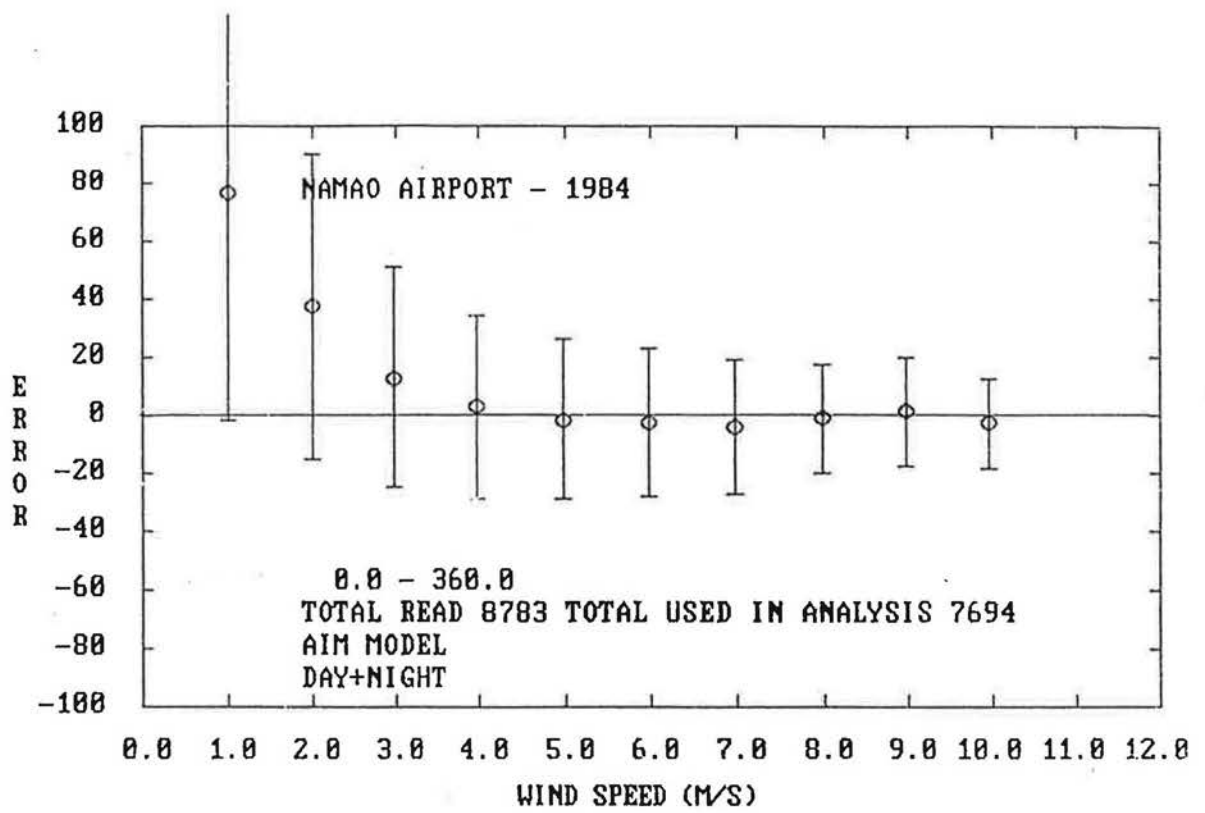


Figure B17

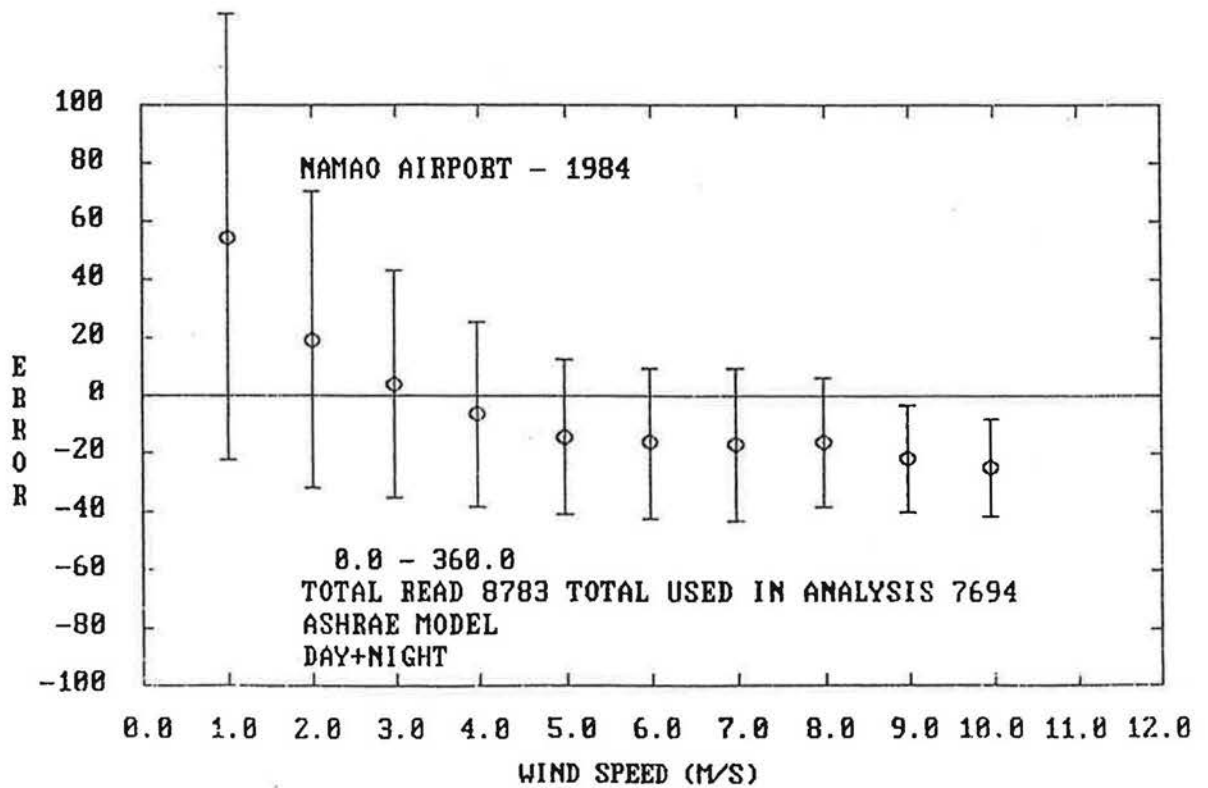


Figure B18

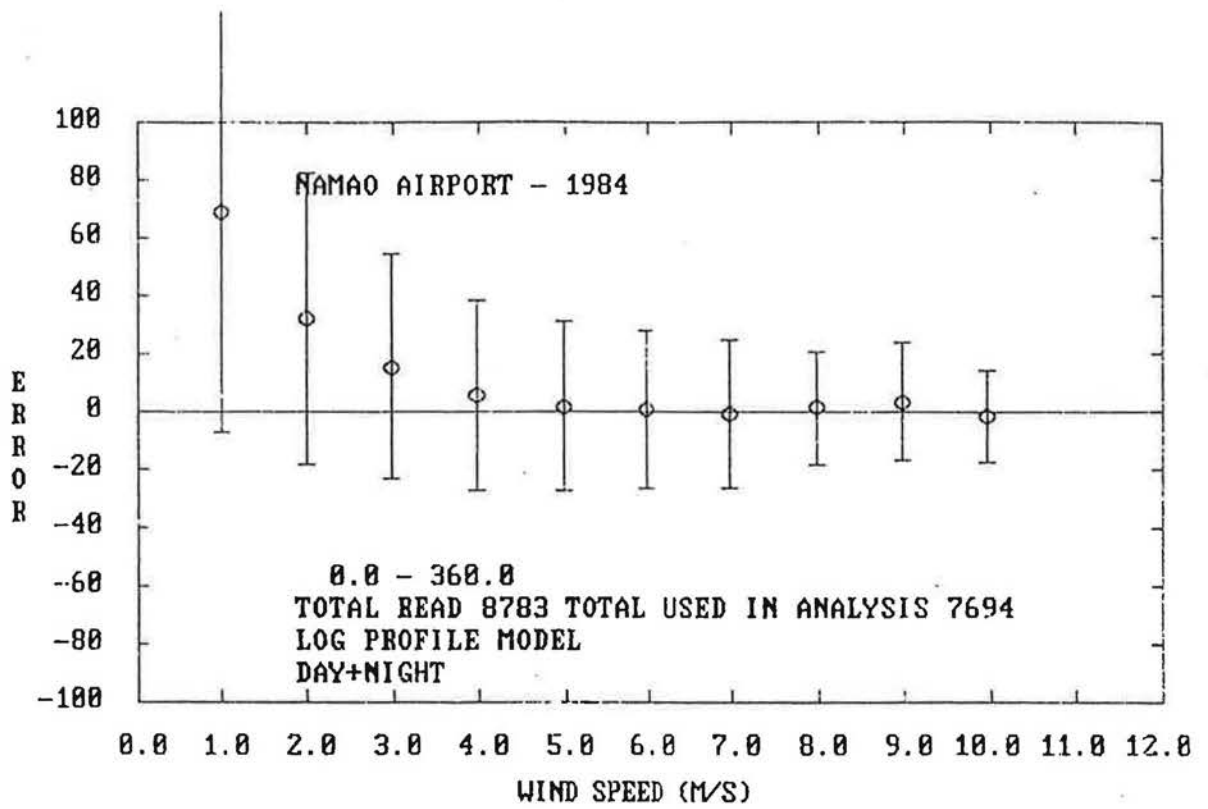


Figure B19

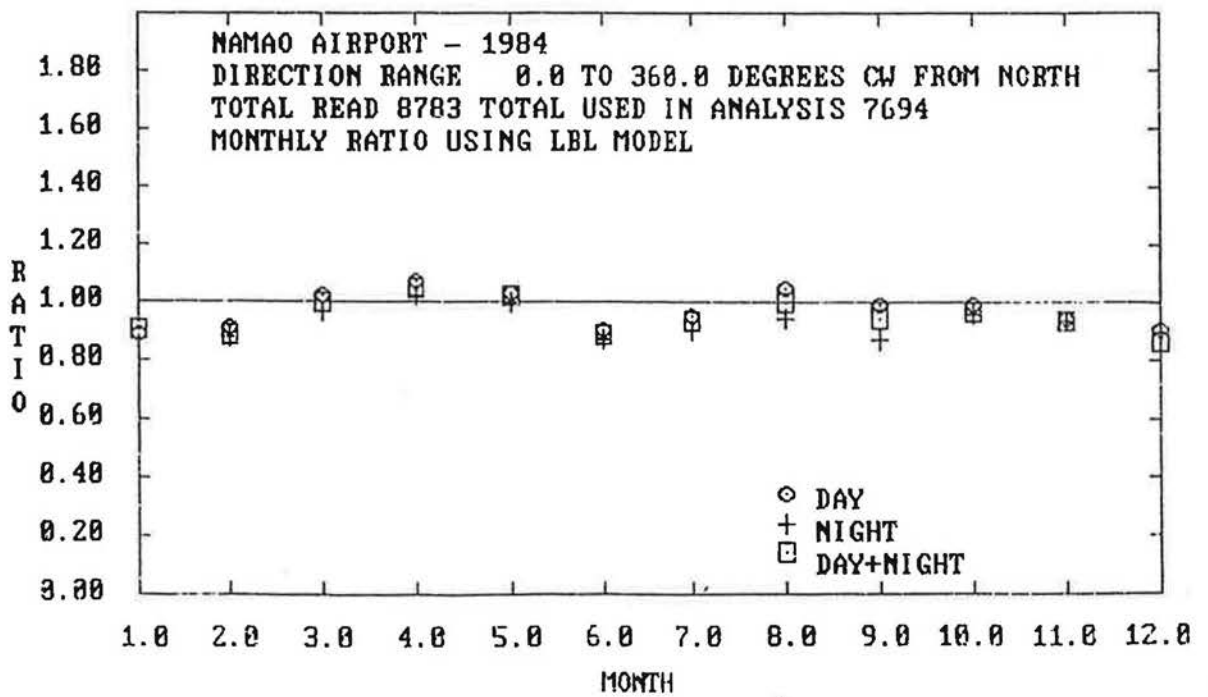


Figure B20

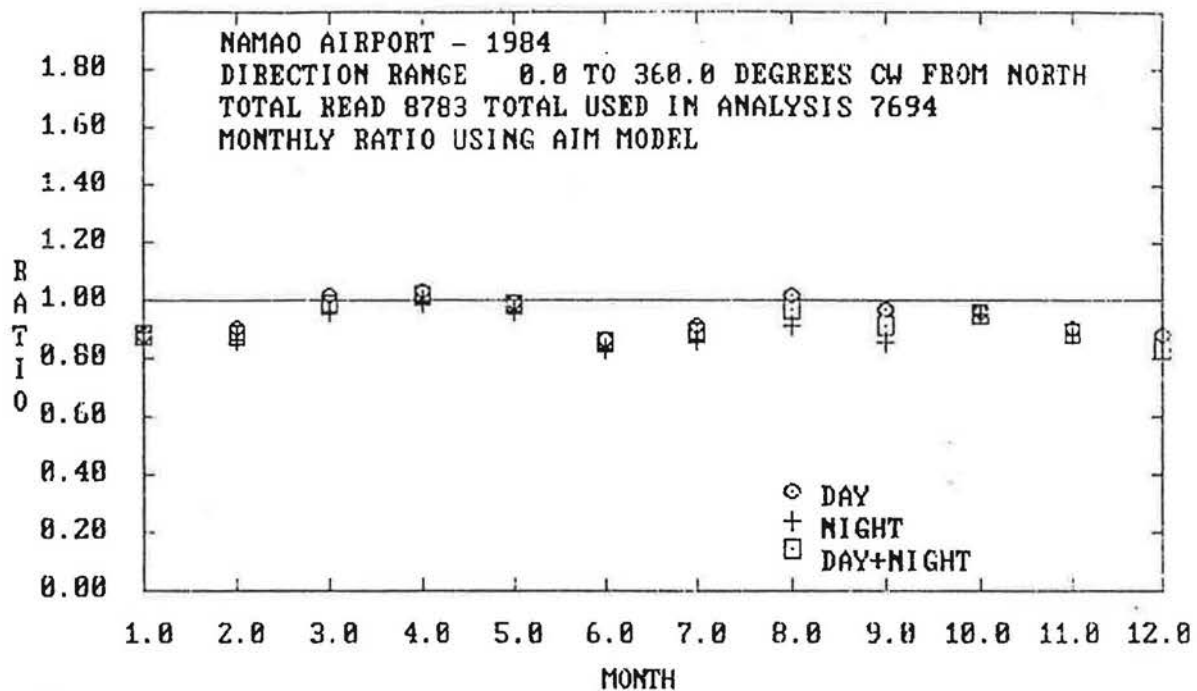


Figure B21